

Study of Trace Gases in the Tropical Troposphere

A THESIS

Submitted for the Award of Ph. D degree of

Mohan Lal Sukhadia University, Udaipur, India

In the Faculty of Science

By

Duli Chand



Under the Supervision of

**Prof. Shyam Lal
Physical Research Laboratory**

Space and Atmospheric Sciences Division
Physical Research Laboratory, Navrangpura, Ahmedabad, India-380 009.

Mohan Lal Sukhadia University, Udaipur

Year of submission: 2002

Dedicated to my Parents

and

Elder Brother

CERTIFICATE

This is to certify that the thesis entitled “Study of Trace Gases in the Tropical Troposphere” submitted for the award of the degree of *Doctor of Philosophy* of Mohan Lal Sukhadia University in the Faculty of Science is a record of bonafide investigations carried out by Shri Duli Chand under my supervision and guidance.

This is an original piece of work on which no one has been awarded a degree in this university or in any other university.

The literary presentation of the thesis is satisfactory and it is in a form suitable for publication. The work presented in this thesis has been done after registration in this University.

Further, the candidate has put in attendance of more than 200 days in my institution as required under rule 7(b) and thus completed the residential requirement.

Prof. Shyam Lal
(SUPERVISOR)

CONTENTS

Acknowledgement	v-vi
1 Introduction	1
1.1 Structure of the atmosphere	2
1.2 Composition of the atmosphere	3
1.3 Importance of the tropospheric ozone	4
1.3.1 Role in atmospheric chemistry	4
1.3.2 Radiative forcing (greenhouse warming)	5
1.3.3 Impact on the biological system	7
1.4 Budget of the tropospheric ozone and its precursors	8
1.4.1 Ozone (O ₃)	8
1.4.2 Nitrogen oxides (NO _x)	12
1.4.3 Non-methane hydrocarbons (NMHCs)	14
1.4.4 Carbon monoxide (CO)	14
1.4.5 Methane (CH ₄)	15
1.5 Physical processes affecting the tropospheric ozone	16
1.5.1 Stratospheric-tropospheric exchange (STE)	16
1.5.2 Surface deposition of ozone	18
1.5.3 Transport	19
1.6 Objectives of this study	20
1.6.1 Indian scenario	20
1.6.2 Focus of this thesis	20
2 Experimental techniques	23
2.1 Ozone measurements	24

2.2 Carbon monoxide measurements	27
2.3 Nitric oxide measurements	29
2.4 Measurements of trace gases using GC techniques	31
3 Ozone and other trace gases over the Indian Ocean and Arabian Sea	35
3.1 Introduction	36
3.2 Meteorological conditions	37
3.3 Experimental details	39
3.4 Variations in ozone	41
3.4.1 Ozone levels during INDOEX 1998	41
3.4.2 Ozone levels during INDOEX 1999	43
3.4.3 Latitudinal variations in ozone during INDOEX 1998 and 1999	47
3.4.4 Latitudinal gradients in ozone during INDOEX 1998 and 1999	50
3.4.5 Diurnal variations in ozone during INDOEX 1998 and 1999	52
3.5 Diurnal variations in nitric oxide (NO)	57
3.6 Variations in carbon monoxide (CO)	58
3.7 Variations in methane (CH ₄)	61
3.8 Variations in sulfur hexafluoride (SF ₆)	62
4 Ozone and other trace gases over the Bay of Bengal	65
4.1 Introduction	66
4.2 Experimental details	66
4.3 Meteorological conditions	67
4.4 Ozone and other trace gases	68
4.4.1 Variations in ozone	68
4.4.2 Variations in other trace gases	71

4.5 Correlations of ozone with other trace gases	72
4.6 Variabilities in UVB and total solar flux	74
4.7 Diurnal variations in NO and O ₃	75
4.8 Comparison with INDOEX results	77
5 Surface ozone in downwind of urban Gujarat in India	80
5.1 Introduction	81
5.2 Experimental details	82
5.3 Ozone at urban and its surrounding regions	83
5.4 Ozone at other continental stations	86
6 Trace Gases at remote site: Mt Abu	91
6.1 Introduction	92
6.2 Experimental site and general meteorology	94
6.3 Diurnal variations in ozone	96
6.3.1 Low ozone levels daytime	100
6.3.2 Background ozone levels	102
6.4 Seasonal variations in ozone	104
6.5 Variations in O ₃ and CO	105
6.6 Mobile lab experiments: O ₃ and CO in BL and FT	107
7 Summary and future directions	112
7.1 Trace gases over the Indian Ocean and Arabians Sea	112
7.2 Trace gases over the Bay of Bengal	114
7.3 Ozone in downwind of urban Gujarat	115
7.4 Ozone and related gases over remote site: Mt Abu	116
7.5 Future directions	118

Bibliography	119-138
List of abbreviations	139
Appendix	140
Field campaign photographs	141-144
Publications	145-146

ACKNOWLEDGEMENT

I express, with deep gratitude my indebtedness to Prof. Shyam Lal, my supervisor, who has introduced me to this field. Throughout the course of my work, his everlasting enthusiasm, critical insight and friendly nature have left a deep impression on me. His valuable guidance and discussions have benefited me throughout my research work at PRL. It is, indeed, a great pleasure and privilege to have worked with him.

I am deeply grateful to Prof B.H. Subbaraya and Prof G. S. Agarwal for their encouragement and personal interest in the progress of my work,

I am indebted to Mr. S. Venkataramani for his invaluable help in instrumentation, cruise and field campaigns, discussions and data analysis. He always stood besides me during my hard times without any invitation. His friendly nature and cheerful company make my stay pleasant at PRL. I am grateful to Mr. K. S. Modh and T. K. Sunil for their help during the field trips, in running the instruments in perfect condition and cheerful company throughout my stay at PRL. Thanks to Mrs. Suchita Desai for helping in data analysis. My sincere thanks to Drs Manish Naja, Prabir K. Patra and Varun Sheel for their wonderful company, useful comments and discussions. I thank all of these team members for their sincere help and support.

I accord my sincere thanks to Prof. A. Jayaraman, Prof. M. M. Sarin, Prof. R. Ramesh and Dr. S. Ramachandran for fruitful discussions. I would like to express my sincere thanks to Prof H. Chandra, Prof. H.S.S. Sinha, Dr. Y. B. Acharya, Dr. K. P. Subramanian, Dr. S. A. Haider, Dr. R. Sekar for their encouragements and helpful comments during my Ph. D. tenure.

My sincere thanks to Prof. R. Sridharan, Dr. K. Krishnamoorthy, Dr. P. Nair (SPL, Trivandrum); Dr. S. K. Satheesh (IISc Bangalore); Prof M.O. Andrae, Prof. J. Lelieveld, Dr. M. Lawrence (MPI, Mainz) for useful discussion and comments. Thanks to Prof. P. Kasibhata (Duke, USA) for helping and guiding me for developing the box model at ICTP, Trieste Italy.

I am thankful to the people associated with various supporting facilities at PRL, which have been extensively utilized during this work. To mention a few, workshops, glass blowing facility, Liquid nitrogen plant, photography and documentation etc. Special thanks are due to the staff members of library and computer center for their sincere support. I am grateful to all the PRL staff members of Mt Abu for providing me the necessary help for the mobile lab experiments and other measurements at PRL observatory, Gurushikhar. I thank Prof. B. L. K. Somayajulu, P. C. Pandey and M. Sudhakar for providing us the cruise.

Crew members of ORV Sagar Kanya are acknowledged for their co-operation and help. I thank Brahamakumari members for providing me facilities for observations at Abu Road.

I express my sincere thanks to my colleagues and friends, Watson, Poulouse, Siva, Biju, Ratan, Joyti, Bhusi, Prashant, Ghosh, Santhanam, Tarun, Ban; Alok, Alam, Anils, Koushik, Shikha, Aparna, Kunu, Jitti, Rajneesh, Sunish, Dipu, Rajesh, Vinay, Sudhir, Sankar, Som; Sai, Shajesh, Rishi, Tarun, Mondal, Subarto; Lokesh and his gang. I am deeply thankful to all those who made my stay in PRL pleasant.

Family members of Prof. Shyam Lal, S. Venkataramani, K. S. Modh T.K. Sunil and Suchita Desai have been kind and affectionate to me. I express my sincere thanks to all of them.

I express my heartiest regards to my parents and great uncle (Baba) for their encouragement and ceaseless worry about my well-being. I am grateful to my elder brother who has been a constant source of moral support, encouragement and inspiration. I am thankful to my elder sister, younger brother, sister-in-laws, brother-in-laws and all the relatives and friends for their moral support and care. My love to all my nephews and nieces for providing me joyful moments. I thank my relatives and family friends for their moral support.

My appreciation to my wife, Vinita, for her profound understanding and moral support during the course of this work. Finally I express my lovely blessings to my daughter, Bila, for providing refreshing moments.

*Ahmedabad
India-380009*

Duli Chand

Chapter 1

Introduction

The earth is surrounded by a life-supporting gaseous envelope called atmosphere. It is a mixture of a multitude of chemical constituents. The composition of the atmosphere is categorized in major and minor constituents. Most abundant of them (*major constituents*) are nitrogen N_2 (78%), oxygen O_2 (21%) and argon Ar (0.93%). About 99.9% of the mass of the atmosphere is concentrated in the homosphere (below approximately 100 km altitude), while the rest is distributed above it called heterosphere. Also 99.9% of the atmospheric gases belong to the major constituents where as the minor constituents are in trace amounts (ppmv^a to pptv^b ranges) (see *Table 1.1*). The major constituents as well as the noble gases (helium, neon, argon, krypton and xenon) have very long lifetime and hence, are relatively well mixed throughout the entire homosphere. The mixing ratios^c of the major constituents are almost constant in the homosphere. The boundary, which divides the homosphere and heterosphere, is called turbopause. The turbulent and random motions of air molecules in the homosphere control the mixing of atmospheric constituents, while molecular diffusion dominates the heterosphere.

^a Parts per million by volume

^b Parts per trillion by volume

^c Volume mixing ratio of a species is defined as the number of molecules of the species divided by the number of molecules of the air in a unit volume

1.1 Structure of the atmosphere

The atmosphere is generally described in terms of layers characterized by specific vertical temperature gradients. The region with negative temperature gradient nearest to the earth is called troposphere. The boundary with the minimum temperature at the upper troposphere is called the tropopause. The troposphere, which extends from the surface to the tropopause at about 18 km in the tropics, 12 km in mid latitude and 6-8 km near the poles, is characterized by a decrease of the mean temperature (~ 6.5 °C per kilometer) with increasing altitude (*Figure 1.1*). The tropopause temperature is about 200 K in the tropical region. This layer,

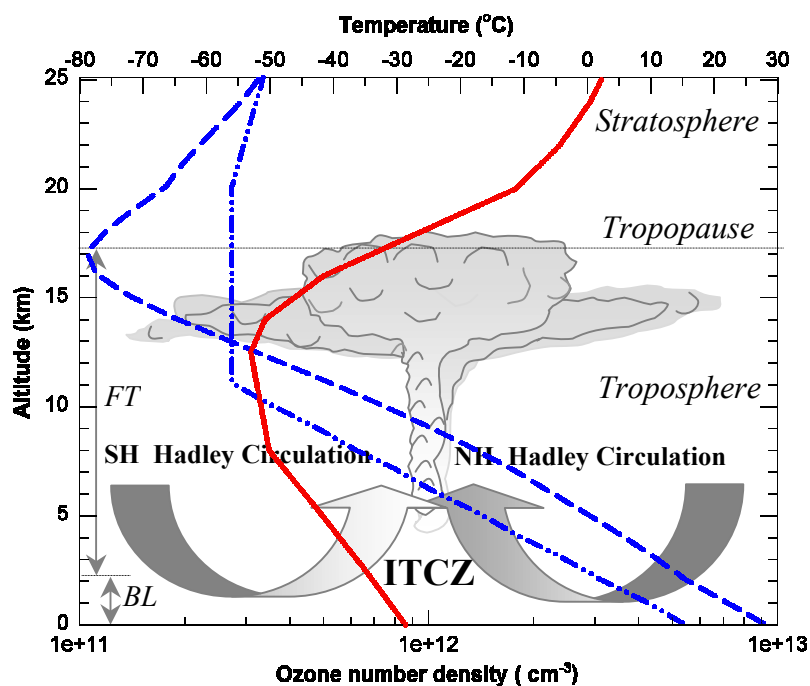


Figure 1.1 Convective activity and vertical structure of the lower atmosphere in tropics. Continuous line represents ozone number density (lower scale) and dashed line shows temperature (upper scale) at Thumba (8.5°N, 76.6°E, 5m) [Sasi and Sen Gupta, 1986]. Dotted-dashed line is the US standard atmospheric temperature, 1976. BL and FT represent the boundary layer and free troposphere respectively.

which contains about 85-90% of the atmospheric mass, is often dynamically unstable with rapid vertical exchanges of energy and mass being associated with convective activity. In the tropics, the convergence of Hadley cells from northern hemisphere (NH) and southern hemisphere (SH) result in fast convective motions at the region called Inter Tropical Convergence Zone, ITCZ (*Figure 1.1*). The ITCZ is dynamically most unstable part of the atmosphere where the air mass from troposphere can reach the stratosphere in few hours. Most of the mass exchange from troposphere to the stratosphere is driven by ITCZ. Much of the variability observed in the atmosphere occurs in this layer, including the associated

weather pattern such as, formation of the thunderstorms. Above troposphere, the upper layers of the atmosphere are stratosphere, mesosphere, thermosphere and exosphere. The boundaries separating the stratosphere-mesosphere, mesosphere-thermosphere and thermosphere-exosphere are called stratopause, mesopause and thermopause or exobase respectively.

The planetary boundary layer is the lowest region of the troposphere where the surface effects are dominant. Its thickness is of the order of 1-2 km and varies significantly with the time of the day, season, and with the meteorological conditions. The exchange between the surface and the free troposphere is directly dependent on the stability of the boundary layer.

1.2 Composition of the atmosphere

The atmosphere is composed primarily of N_2 , O_2 and noble gases, called the major constituent whose concentrations have remained remarkably unchanged over long time. There are some gases at relatively much smaller levels, whose concentrations are highly variable in space and time, known as minor constituents. Despite their low concentrations, the minor constituents such as water vapor, carbon dioxide, methane, carbon monoxide, ozone, oxides of nitrogen (NO_x), chlorofluorocarbons (CFCs) and many others, play important role in atmospheric chemistry and dynamics. *Table 1.1* provides information on the constituents of the atmosphere. Most of these gases affect the transmission of the solar as well as the terrestrial radiation in the atmosphere and are therefore linked with the physical climate system. Also, these gases are key components of the biogeochemical cycles. In addition, they determine the oxidizing capacity of the atmosphere and, hence control the atmospheric lifetimes of biogenic and anthropogenic trace gases. Many of the global environmental changes forced by human activities are mediated through the chemistry of the atmosphere. Important changes include the global spread of air pollution, increase in the concentration of tropospheric oxidants (including tropospheric ozone), stratospheric ozone depletion, and global warming (the so called greenhouse effect). Since the agricultural and industrial revolutions, the delicate balance among the physical, chemical and biological processes in the earth system have been perturbed. These perturbations are as a result of, for example, the quasi-exponential growth in world's population, the use of increasing amount of the fossil fuel and its related emissions, and the intensification of the agricultural practices including the more frequent use of fertilizers. Due to such anthropogenic activities, concentration of some of the trace gases like ozone, CH_4 etc., which have climatic and environmental implications, are increasing since pre-industrial time.

Table 1.1: Chemical composition of the atmosphere.

Gaseous Constituents of the Atmosphere	Chemical formula	Volume mixing ratio	Source(s)
Major constituents^a			
Nitrogen	N ₂	78.084%	Biological
Oxygen	O ₂	20.948%	Biological
Argon	Ar	0.934%	Inert
Minor/trace constituents			
Carbon dioxide	CO ₂	360 ppmv	Combustion, ocean, biosphere
Neon	Ne	18.18 ppmv	Inert
Helium	He	5.24 ppmv	Inert
Methane ^b	CH ₄	1.7 ppmv	Biogenic, anthropogenic
Carbon monoxide ^b	CO	50 – 200 ppbv	Photochemical, anthropogenic
Ozone (stratospheric)	O ₃	0.5 - 10 ppmv	Photochemical
Ozone (tropospheric) ^b	O ₃	5 - 500 ppbv	Photochemical
Nitrous oxide ^b	N ₂ O	310 ppbv	Biogenic and anthropogenic
Nonmethane hydrocarbons ^b	C _n H _n [*]	5 - 20 ppbv	Biogenic and anthropogenic
Halocarbons ^b	C _n H _m X _k [*]	3.8 ppbv	85% Anthropogenic
Oxides of nitrogen ^b	NO _y	5 pptv - 1 ppmv	Soil, lightning, anthropogenic
Hydroxyl ^b	OH	0.1 - 10 pptv	Photochemical
Peroxy ^b	HO ₂	0.1 - 10 pptv	Photochemical
Hydrogen peroxide ^b	H ₂ O ₂	0.1 - 10 ppbv	Photochemical
Particulate sulfate ^b	SO ₄ ⁻²	10 pptv - 10 ppbv	Photochemical, anthropogenic

^a After US Standard Atmosphere 1976.

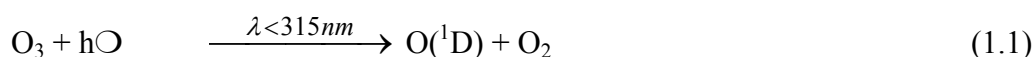
^b Concentration near the earth's surface

* Here X is halogen radical m≥0, n>2, k>1

1.3 Importance of tropospheric ozone

1.3.1 Role in atmospheric chemistry

The earth's troposphere acts like a chemical reactor in which huge quantities of the trace species are transformed from one form to another where ozone can be considered as the principal product of this reactor. Most of the OH radicals are produced by ozone in daytime by the following reactions:



The photodissociation of ozone in the wavelength range 290-315nm (UVB radiation) gives rise to the electronically excited O [i.e. O(¹D)], which further reacts with the water vapor to produce the most reactive radical (OH) in the atmosphere [Levy, 1971]. The hydroxyl radical is the dominant oxidizing agent in the atmosphere and thus acts as a tropospheric detergent. It controls the budget and lifetimes of various anthropogenic and natural trace gases such as

CO, CH₄, NMHC, HFCs, HCFCs, NO, NO₂ etc. In the reactions involving these gases, OH is regenerated in the catalytic cycles, sustaining its concentration in the order of 10⁶ molecules cm⁻³ during day time hours. The OH level is predicted to be 20% higher in the southern hemisphere (SH) as a result of large amounts of CO and HCs produced by human activity in the northern hemisphere (NH) that reduce OH concentrations. Due to large solar flux and water vapor, OH concentrations are found to be higher in the tropics than in the mid and higher latitudes. The variability in its concentration from tropics to mid latitude is approximately from 1.5×10⁶ to 0.5×10⁶ molecules cm⁻³ [Crutzen, 1995].

1.3.2 Radiative forcing (greenhouse warming)

The physical, chemical and optical properties of the atmosphere and the surface are being perturbed by human activity. These changes may lead to changes in the earth's energy balance and climate. In recent years, an increasing number of possible human-related climatic changes are being quantified. Climate can be directly affected by increasing amounts of greenhouse gases such as carbon dioxide (CO₂), ozone (O₃), methane (CH₄), nitrous oxide (N₂O), chlorofluorocarbons (CFCs) etc released into the atmosphere through anthropogenic activities [IPCC, 2001]. Perturbation of earth's energy balance by adding the above greenhouse gases in the atmosphere is called radiative forcing.

Tropospheric ozone is a potential greenhouse gas and contributes to global warming* by absorbing the terrestrial radiation at 9.6 μm. However, there are some uncertainties in knowledge of its contribution to the global warming due to its observed large variability in its growth rates in different environments. Each additional molecule of ozone produced in the atmosphere is about 1200-2000 times more effective in global warming than an additional CO₂ molecule. Also, an additional molecule of O₃ results in 22 and 217 times higher global warming compared to CH₄ and N₂O [Ramanathan *et al.*, 1985; IPCC 1990; Schwarzkopf and Ramaswamy, 1993; Myhre *et al.*, 2001]. The contribution of tropospheric ozone in radiative forcing was not considered until last decade. But most recent studies indicate that it can be the second largest contributor to net heating after CO₂. The observations show that surface concentrations of O₃ at some places have increased by a factor of 5 since the beginning of the twentieth century, corresponding to an increase of 1.6% per year and even higher (2.4%) since last few decades (Figure 1.2). Ozone concentrations are observed to be increasing at the rate of 1-2% in many parts of the globe in northern hemisphere [Volz and Kley, 1988;

* Anthropogenically enhanced greenhouse effect increases the atmospheric temperature and results in 'global warming'

Logan, 1994; Marenco *et al.*, 1994; Oltmans and Levy, 1994; Schmidt, 1994; Naja and Lal, 1996]. Increase in tropospheric ozone since the pre-industrial time is 20-200 % depending on the region and season [Mickley *et al.*, 1999]. However, in Canada, a decreasing trend in ozone concentration is observed for the time period of 1980 to 1993 at many observational sites [Logan, 1994; 1999]. Measurements at South Pole also show a decreasing trend in ozone concentrations [Oltmans and Levy, 1994].

Figure 1.3 shows the contribution of global ozone to the radiative forcing changes from the year 1750 to 2000 along with other radiative species [IPCC, 2001]. Ozone is the third most important trace species in this respect. Comparison of the regional and global

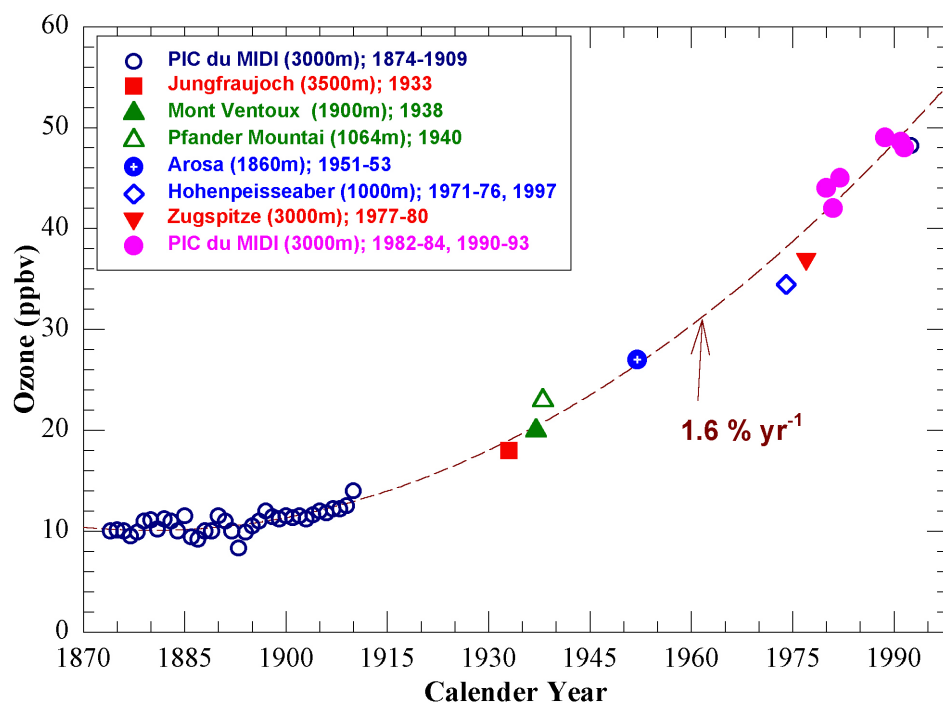


Figure 1.2 Ozone evolution in the free troposphere, based on O_3 measurements from high altitude stations in Europe [Marenco *et al.*, 1994].

forcing due to tropical ozone changes to the forcing by carbon dioxide and other trace gases since pre-industrial time (about 2.45 Wm^{-2}) suggest that this effect of the tropical ozone changes can lead to significant elevation of both regional and global anthropogenic radiative forcing and thus may result in significant climate change [IPCC, 1995; 2001]. A tentative evaluation of the impact of tropospheric ozone on radiative forcing confirms that ozone is currently the second most significant greenhouse gas, responsible for 22% and 13% of the radiative forcing changes since 1800, in the northern and southern hemispheres respectively [Marenco *et al.*, 1994]. In addition, recent observations over the tropical troposphere show substantial radiative forcing of $0.5\text{-}1.0 \text{ Wm}^{-2}$ and globally averaged radiative forcing of $0.1\text{-}0.4 \text{ Wm}^{-2}$ for most of the times of the year [Portmann *et al.*, 1997]. The mid latitude ozone

increase account for an additional 0.3 Wm^{-2} as estimated by *Marenco et al.* [1994]. Thus the total radiative forcing due to tropospheric ozone changes worldwide as suggested by *Portmann et al.* [1997] could be as large as 0.7 Wm^{-2} .

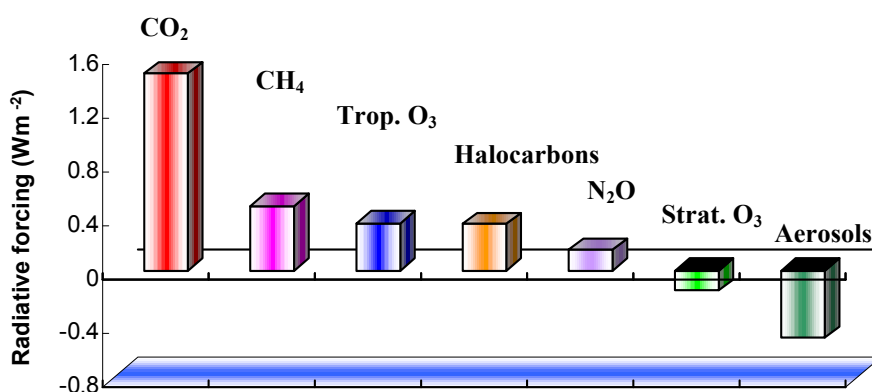


Figure 1.3 Annual mean global radiative forcing (Wm^{-2}) due to the greenhouse gases for the period from pre-industrial (1750) to 2000. For comparison, the net radiative forcing due to all types of aerosols is also shown [IPCC 2001].

1.3.3 Impact on the biological system

Elevated concentrations of ozone at ground-level are known to cause adverse effects on the human health, ecosystems and materials. Due to its deleterious effects, photochemical air pollution is given a high priority in scientific investigations and environmental policies. High ozone concentrations are not confined to the urban environments but is also spreading to the relatively cleaner areas in remote locations. Most of these pollution spreads are observed in the downwind side of the urban/industrial areas [*White et al.*, 1983; *Xiude et al.*, 1996; *Trainer et al.*, 1995; *Aneja et al.*, 1999; *Syri et al.*, 2001; *Chand et al.*, 2002; *Lal et al.*, 2002]. In addition, decline in growth rate in forest vegetation was observed on extreme ozone exposure sites such as mountaintops [*Vogelmann*, 1982].

In Europe, the abatement of air pollution is based on the concept of critical loads and levels of adverse environmental effects [*Bull*, 1991]. For ozone the critical levels are currently expressed as the accumulative exposure in hours above a threshold concentration of 40 ppbv, abbreviated as AOT40 [*Fuhrer et al.*, 1997]. The values of the AOT (accumulated ozone threshold is an index for describing adverse environmental effects) indices have been shown to have a statistical relationship with the negative growth response in plants observed in the controlled exposures. *Figure 1.4* shows spring time relative wheat yield dropping to

50% if AOT70 is more than 10 thousand ppb-hours and the impact may be much severe for AOT70 beyond 10-20 thousand ppb-hour levels. *Reich and Amundson* [1995] conducted similar experiments at different exposures of ozone for different species of plants and observed drastic drops in their growth rates (up to 60%). In the well known project called 'China Map', *Chameides et al.* [1999] have shown that elevated ozone in a developing

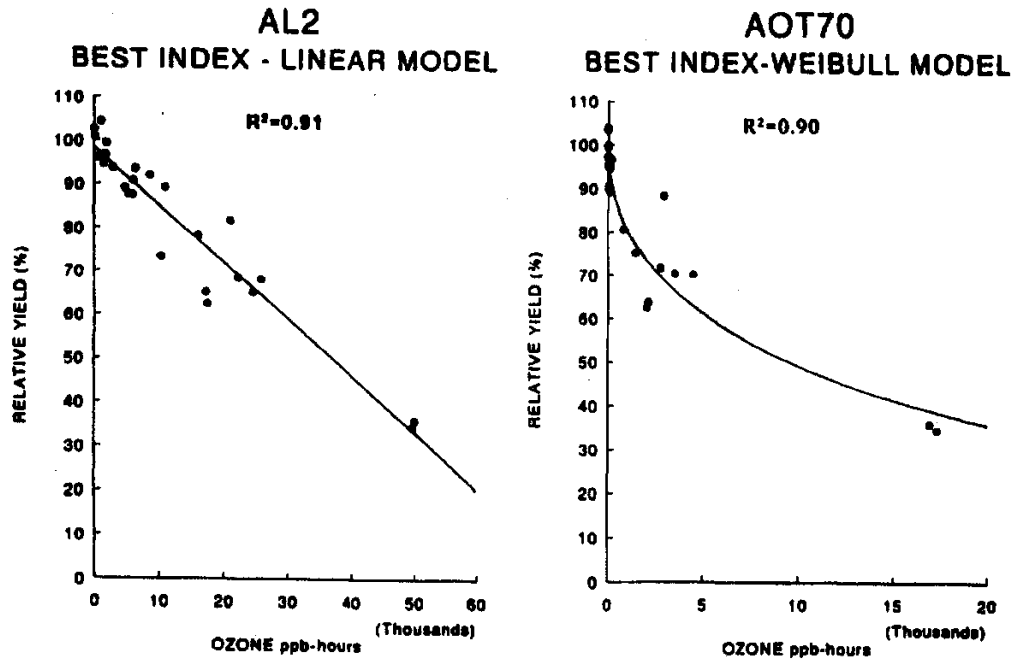


Figure 1.4 Relative yield of wheat as a function of ozone exposure time. X axis is the accumulated ozone exposure time [Finnan et al., 1997].

country like China can significantly reduce the crop yield of winter wheat and thus can affect the economy of China. Experiments under controlled conditions confirm that O_3 is a pollutant and is affecting the health of both humans and plants [Reich, 1995; Bascom et al., 1996].

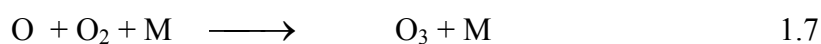
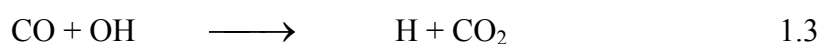
1.4 Budget of the tropospheric ozone and its precursors

1.4.1 Ozone (O_3)

About 90% of the atmospheric ozone is present in the stratosphere and only 10% resides in the troposphere. Despite this relatively small fraction, tropospheric ozone governs the chemistry of the atmosphere, as mentioned in section 1.2. Traditionally, it was assumed that tropospheric ozone is controlled by Stratospheric-Tropospheric Exchange (STE) across the extratropical tropopause [Regener, 1957; Junge, 1962]. This first analysis was based on the observed O_3 gradient with altitude and suggested a source at the tropopause and a sink at the surface. In 1960s, *in situ* photochemical ozone formation in the troposphere drew the attention by showing that the breakdown of the hydrocarbons in presence of sunlight and

NO_x^* can cause O_3 episodes in urban environment during summer [Haagen-Smit and Fox, 1956; Leighton, 1961]. The *in situ* O_3 formation is catalyzed by nitrogen oxides which are often emitted simultaneously with hydrocarbons (RH) and carbon monoxide (CO), in particular by man made sources [Crutzen, 1974]. In daytime, oxidation of CO, CH_4 and RH leads to ozone production or loss depending upon the critical concentration of NO. A simple example of ozone production by CO oxidation is as follows:

NO_x rich air:



NO_x poor environment:



In general, reaction 1.5 predominates in NO rich air plumes such as urban and/or its downwind environments and reaction 1.9 prevails in NO poor air plumes like remote marine environments. Similarly, oxidation of CH_4 and NMHC leads to ozone production or loss depending upon the concentration of NO. However, the reaction mechanisms in oxidation of CH_4 and NMHC are more complex, and leads to production of many other trace gases including ozone precursors. The critical limit or threshold of NO which leads to ozone production or loss can be obtained by simple calculation as follows:

The decisive reaction which leads to ozone production, is given by reaction 1.5, i.e.,



And the reaction which leads to ozone loss, is given by 1.9, i.e.,

* NO_x is the group of the two species, NO and NO_2 i.e. ($\text{NO}_x = \text{NO} + \text{NO}_2$)



$$\text{Production rate of O}_3 = k_2 \times \text{HO}_2 \times \text{NO}$$

$$\text{Loss rate of O}_3 = k_6 \times \text{HO}_2 \times \text{O}_3$$

Here k_2 and k_6 are the rate constants of the reactions 1.5 and 1.9 respectively. For net O_3 production, production rate should be more than the loss rate of ozone,

$$\begin{aligned} \text{i.e.} \quad k_2 \times \text{HO}_2 \times \text{NO} &> k_6 \times \text{HO}_2 \times \text{O}_3 \\ \Rightarrow \text{NO}/\text{O}_3 &> [k_6/k_2]; \quad (k_6/k_2 = 0.23 \times 10^{-3}) \end{aligned}$$

If we take $\text{O}_3 = 40$ ppbv

$$\Rightarrow \text{NO} \approx 9 \text{ pptv}$$

This implies that for 40 ppbv of ambient O_3 , there will be a net ozone production if NO is more than 9 pptv else there will be a net ozone loss. Here it should be noted that the above threshold calculation of NO gives its lower limit and it may be different if we include all the chemical processes like oxidation of CH_4 and NMHC along with oxidation of CO. The ratio of NO/O_3 to cross the threshold of NO for ozone production is in range of 0.23×10^{-3} to 4.0×10^{-3} depending upon the environment [Crutzen, 1995]. The hydroxyl radicals from reactions 1.1 and 1.2 initiate the reaction sequence from reaction 1.3 to 1.8 in which O_3 is produced through NO-to- NO_2 conversion and finally OH is regenerated.

To some extent the above radical reaction chain can be compared with a combustion process for which $\text{R}^\diamond\text{H}$ and [CO] emissions supply the ‘fuel’ [Johnston and Kinnison, 1998]. The difference in these two systems is that in combustion the energy is supplied from combustion itself whereas in the photochemical reactions above, the ignition is supplied by solar photons (Figure 1.5). At night, reaction sequence ceases and there is no ozone formation. Furthermore, emission of NO_x plays a key role. If the only fuel substances RH and CO are added to the tropospheric reaction mixture without NO_x , the HO_2 radicals formed will destroy O_3 , or they combine to form peroxides. Hence, without NO_x , the reaction chain (1.3, 1.4, 1.10) resembles decaying of the combustion process and there is no production of ozone. If this mechanism prevails in the troposphere, removal of RH, CO and other pollutants through OH attack would be fully dependent on O_3 transport from the stratosphere.

$^\diamond$ R may be alkyl or group of alkyl radicals

In the early 1970s it was suggested that photo-oxidation of CH_4 , the simplest and most abundant of all the hydrocarbons and carbon monoxide cause O_3 formation in large areas of the troposphere. It was predicted that tropospheric ozone predominates in the NO_x rich air, in particular, over much of the continental northern hemisphere (NH), while destruction prevails in NO_x deficient air [Crutzen, 1973]. In subsequent years, two schools of thoughts evolved about the origin of tropospheric ozone: one emphasized the role of *in situ* O_3 production by photochemical reactions in the troposphere itself [Crutzen, 1974; Chameides and Walker, 1976; Fishman *et al.*, 1979], and the other emphasized on the ozone

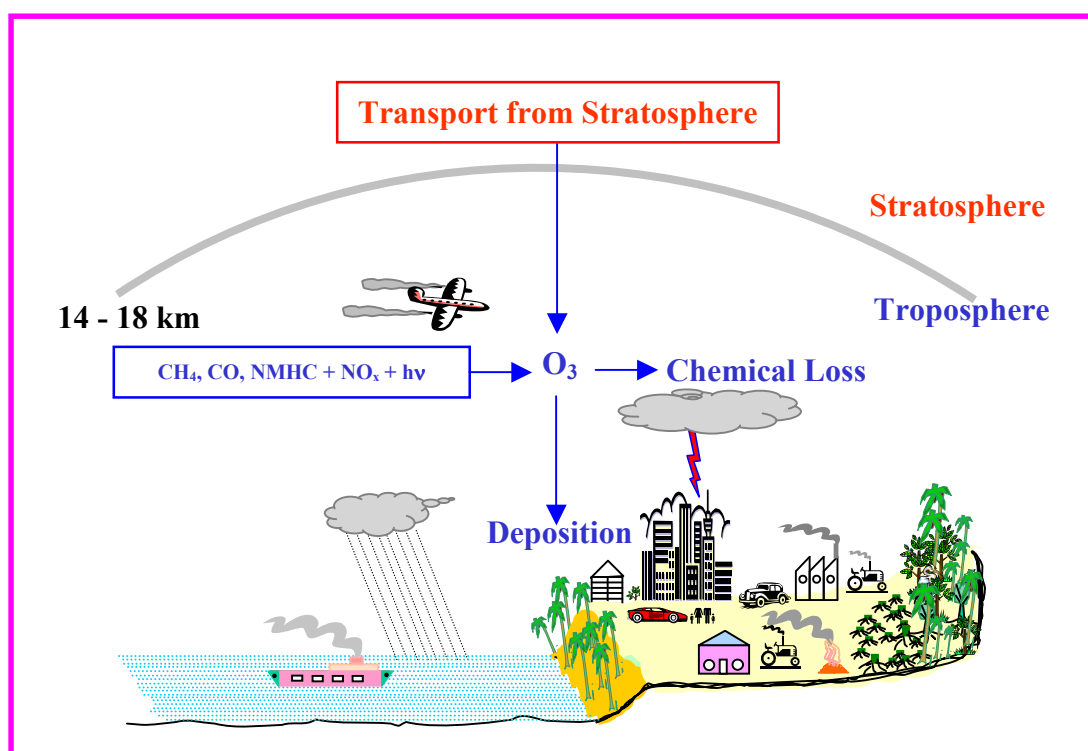


Figure 1.5 Main processes affecting the tropospheric ozone budget.

transport from the stratosphere [Chatfield and Harrison, 1976; Fabian and Pruchniewicz, 1977; Levy *et al.*, 1985]. The budgets of the tropospheric ozone calculated in different models are given in Table 1.2. The large variability in the two main sources of ozone *viz* the intrusion from the stratosphere and *in situ* photochemical production is due to poor understanding of the dynamical parameters like advection, en route transport and transformations of ozone and other short lived trace species, boundary layer process and also lack of complete knowledge of the budget of ozone precursors.

Table 1.2: Budgets of various processes contributing to the tropospheric ozone as given in some of the global chemistry-transport models ($\text{Tg O}_3 \text{ yr}^{-1}$)* [WMO 1998].

Model References	Stratospheric Input	Dry Deposition	Photochemical Production	Photochemical Loss	Net Photochemistry
Müller and Brasseur (1995)	550	1100	4550	4000	550
Berstsens and Isaksen (1997)	846	1178	--	--	295
Levy et al. (1997)	696	825	--	--	125
Roelofs et al. (1997)	459	534	3425	3349	75
Houweling et al. (1998)	768	681	3979	4065	-86
Wang et al. (1998)	400	820	4100	3680	420
Range	400-846	534-1178	3425-4550	3349-4065	-86-550

Ozone precursors are the trace gases such as NO_x , NMHCs, CO and CH_4 , which are responsible for ozone formation through photochemical reactions as shown by reactions 1.3 to 1.7. Ozone precursors have both anthropogenic as well as natural sources though there are large uncertainties in their budgets (see Table 1.3). The main common anthropogenic sources for all these gases are fossil fuel combustion and biomass burning.

1.4.2 Nitrogen oxides (NO_x)

Nitrogen oxides play a central role in photochemical production of ozone in the troposphere, as mentioned earlier. In the troposphere, NO_x can have both anthropogenic as well as natural sources but the major contribution is from the anthropogenic sources. The dominant source of NO_x to the atmosphere is fossil fuel combustion for energy production and it contributes about 22 Tg N yr^{-1} (see Table 1.3). Other major sources are biomass burning, emission from soils and production by lightning activity. Biomass burning constitutes an important anthropogenic NO_x source in the tropics and subtropics of America, Africa and South Asia, contributing about $3\text{-}13 \text{ Tg N yr}^{-1}$ to the NO_x budget.

* $1 \text{ Tg} = 10^{12}$ grams

Table 1.3 Estimated emissions of ozone precursors. The dashed cells indicate no sources [Adapted from WMO, 1998].

Source	CH ₄ (Tg yr ⁻¹)	CO (Tg yr ⁻¹)	NMHC (Tg C yr ⁻¹)	NO _x (Tg N yr ⁻¹)
Anthropogenic				
Energy use	110 (65-155)	500 (300-900)	70 (60-100)	22 (20-24)
Aircraft	--	--	--	0.5 (0.2-1)
Biomass burning [†]	40 (10-70)	500(400-700)	40 (30-90)	8 (3-13)
Rice paddy	80 (30-120)	--	--	--
Ruminants	85 (60-105)	--	--	--
Animal wastes	30 (15-45)	--	--	--
Natural				
Vegetation	--	100 (60-160)	400 (230-1150)	--
Soils	--	--	--	7 (5-12)
Lightning	--	--	--	5 (2-20)
Animal wastes	30 (15-45)	--	--	--
NH ₃ oxidation	--	--	--	0.9 (0-1.6)
N ₂ O breakdown*	--	--	--	0.6 (0.4-1)
Domestic sewage	25 (20-30)	--	--	--
Wetlands	145 (115-145)	--	--	--
Others	45 (12-80)	50 (20-200)	50 (20-150)	--
Total sources	590 (342-795)	1150 (780-1960)	560 (340-1490)	44 (30-73)

[†] Biomass burning has both natural as well as anthropogenic sources

* NO_y produced in the stratosphere and transported to the troposphere.

Relatively large uncertainty in the budget of NO_x is mostly due to limited information available about the amount of biomass burning in forests as well as in rural areas and the nitrogen content of the fuel. In comparison to the fossil fuel combustion, biomass burning occurs at much lower temperature, and NO_x production from N₂ and O₂ conversion is much less efficient. In most of the biomass burnings, NO_x results from organic nitrogen transformation while a substantial part of the emissions occurs due to reduced nitrogen species [Lobert *et al.*, 1991]. Among the NO_x (NO₂ and NO), some of NO₂ is emitted directly into the atmosphere by combustion processes but most of NO₂ is formed by photo oxidation of NO (the major nitrogenous product of combustion). The conversion of NO to NO₂ occurs as a part of the oxidation of the organic compounds initiated by reactive species such as OH radicals as shown in reactions 1.3 to 1.7. The contribution of soil-biomass burning to NO and NO₂ is 97% and 3% respectively [Berntsen and Isaksen, 1997].

It is likely that the emission rates from Europe and North America are either decreasing or remaining constant due to decrease in fossil fuel combustion and improved technology. On

the other hand, due to larger population and higher economical growth rates, the emission growth rates have been increasing in Asia and more so in the central and South Asia [Lelieveld *et al.*, 2001]. The largest contribution to the Asian countries is from China where increase in NO_x growth rate is found to be about 7% per year from 1990 to 1994 [WMO 1998]. Due to scarce measurements in tropics, particularly from India, trend and even distribution of NO_x is not available in this region.

1.4.3 Non-methane hydrocarbons (NMHCs)

Most of the NMHCs are emitted from the natural sources and vegetation is the major source among them. The relative contribution of natural sources (vegetation and oceans) and anthropogenic sources (fossil fuel combustion and biomass burning) are about 80% and 20% respectively [WMO, 1998]. Measurements from the southeastern U.S. during summer show that isoprene contributes more than half of the hydrocarbon reactivity [Lawrimore *et al.*, 1995]. The release of natural gas and fuel evaporation are the major sources of light hydrocarbons in Europe [Solberg *et al.*, 1996]. A global source inventory of NMHCs included contribution from isoprene (44%), monotarpenes (11%) and other reactive (22.5%) and less reactive (22.5%) NMHCs [Guenther *et al.*, 1995]. The large uncertainty in the NMHCs concentrations, as shown in *Table 1.3*, is due to the poor knowledge in global distribution of OH radicals and the uncertainties in the net emissions by different sources unevenly distributed on the globe. Despite having large ozone production efficiency, measurements of NMHCs in India are not available.

1.4.4 Carbon monoxide (CO)

The major surface sources of CO are fossil fuel combustion and biomass burning. In addition to this, a significant amount of CO is produced through oxidation of methane and NMHCs. The relative anthropogenic contribution of atmospheric carbon monoxide is about 87% whereas the natural source contributes the rest 13% [WMO, 1998]. Northern hemispheric sources are estimated to be about twice as large as that in the southern hemisphere [Logan *et al.*, 1981]. Reaction 1.3 accounts for 80-90% loss of CO in troposphere and the remaining part is lost in the stratosphere and/or via biological processes in soil [Warneck, 1988]. CO mixing ratios at different sites around the globe show considerable inter-annual variability due to changes in the strengths of sources and sinks. Although the evaluation of the long term trends in CO are limited by the available measurements, comparison of CO made by solar

spectra during 1950-1951 above Switzerland to measurements made in the mid 1980s at the same site suggest a linear rate of increase of column CO of about 1% per year [Khalil and Rasmussen, 1988]. CO measurements from Greenland ice cores suggest that there has been an increase in the higher NH latitudes since 1850, whereas samples from Antarctica show no trend [Haan *et al.*, 1996]. But surface measurements since mid 1980s show decreasing trends in CO in both the hemispheres [Khalil and Rasmussen, 1994]. Observations of vertical abundance of CO also show a negative trend over Jungfraujoch in Europe for the period 1984 to 1997 [Mahieu *et al.*, 1997].

1.4.5 Methane (CH₄)

More than 50% of the atmospheric methane has anthropogenic sources (see *Table 1.3*). The burden of the tropospheric methane continues to increase, but the rate of growth of this burden is declining [Matsueda and Inoue, 1996; Matsueda *et al.*, 1996]. Recent measurements indicate a growth rate of about 3 to 4 ppb (parts per billion) per year in the 1996-1997 period [Dlugokencky *et al.*, 1998]. In their analysis, CH₄ data from Antarctic ice cores, Antarctic firn air, the Cape Grim (Tasmania) Air Archive (CGAA) dating back to 1978 and direct atmospheric measurements since 1984 have been combined to present a very high resolution record of atmospheric CH₄ from 1000 AD to the present. They concluded that “*unless the global CH₄ budget changes, the globally average CH₄ mole fraction will slowly increase to about 1800 ppbv, and contribution of CH₄ to the greenhouse effect will not increase significantly above its current levels.*”

The improvements in the knowledge of CH₄ budget have come from more accurate estimation of the lifetime of CH₄, which is mostly removed by OH [Prinn *et al.*, 1995]. The new total atmospheric lifetime value of 8.9 years is lower than the previous estimates of 10 years and is based on improved calibration scale of methyl chloroform (CH₃CCl₃) and a good knowledge of respective reaction rate constants with OH. But there is a large uncertainty in the lifetime of the short-lived trace species due to limited measurements. Since most of these species have both natural as well as anthropogenic sources, the seasonal variations of these species further depend on meridional and vertical changes in the strength of their sources. The main sink of tropospheric CH₄ is its removal by OH radicals and transport to the stratosphere. The following table gives the lifetimes of different trace gases in the troposphere.

Table 1.4: Atmospheric lifetimes of different trace gases and radicals [adapted from WMO 1994, 1998 and IPCC 1995,2001].

Gases	Lifetimes	Remarks
Ozone (O ₃)	Few hours to months	In CBL ~ few hours In MBL ~ 5 days
Nitric oxide (NO)	Few minutes to ~ days	
Nitrogen dioxide (NO ₂)	Few hours to several days	NO _x live for few days in FT
Methane (CH ₄)	8.9 years	
Carbon monoxide (CO)	1-2 Months	
Non methane hydrocarbons (NMHCs)	Hours to months	
Hydroxyl radicals (OH)	Few seconds	
Hydroperoxyl radical (HO ₂)	Few minutes	
Carbon dioxide (CO ₂)	~120 years	
Nitrous oxide (N ₂ O)	120 years	
Sulfur hexafluoride (SF ₆)	3200 years	

CBL : Continental Boundary Layer. CBL varies from 20-3000m, depending on day, night, season and latitude.
 MBL: Marine Boundary layer. MBL varies from 800-1600m, depending on season and latitude.
 FT : Free Troposphere. It starts from top of the boundary layer and ends at the tropopause level.

1.5 Physical processes affecting the tropospheric ozone

1.5.1 Stratospheric-tropospheric exchange (STE)

The exchange of mass between the stratosphere and troposphere is important to the chemistry of both the regions, e.g., CFCs are transported from troposphere to the stratosphere and ozone is transported from stratosphere to the troposphere. Both these regions are divided by a layer called tropopause, characterized by inversion of temperature, as shown in *Figures 1.1* and *1.6*. The positive gradient in temperature in the stratosphere makes it highly stable where as the negative temperature gradient makes the troposphere highly unstable. As the boundary layer is turbulent and well mixed compared to the troposphere at large, the troposphere is well mixed horizontally as well as vertically compared to the stratosphere. According to simplest qualitative plausible model of STE, there is a uniform rising motion in the tropics and sinking air at the poles across their respective tropopause. Such a circulation was proposed by *Brewer* [1949] to explain the observed low water vapor mixing ratios in the stratosphere. *Dobson* [1956] pointed out that poleward and downward advection of this type of mean circulation was qualitatively consistent with the observed high concentration of ozone in the lower polar stratosphere, far from the region of the photochemical production. The Brewer-Dobson circulation cell is now known to be primarily driven by wave disturbances that originate in the troposphere. These waves are excited by air-flow over mountains, synoptic weather systems and deep convections. While propagating into the

stratosphere, these waves get dissipated and exert a drag force on the stratospheric westerlies. By thermal wind balance, the wave forcing induces poleward motion and a downward mass flux toward the mid-latitude and high-latitude troposphere [Holton *et al.*, 1995]. The stratospheric mass balance is maintained by upward motion across the tropical tropopause as shown in *Figure 1.6*.

Nonetheless, Holton *et al.* [1995] suggested that, the chemical species whose source or sink lies entirely in the overworld (the region below 2 PVU potential vorticity surface in extratropics), STE can be evaluated most simply and effectively in terms of mass flux through the lower boundary of the underworld which is controlled by the wave driven

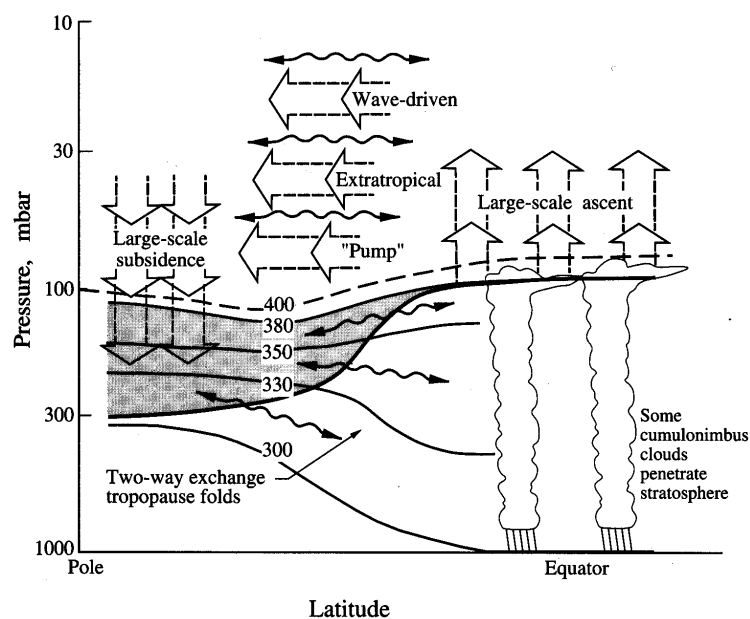


Figure 1.6 Dynamical aspect of stratospheric-tropospheric exchange [Holton *et al.*, 1995]. The tropopause is denoted by the thick solid line. Thin lines are surface of constant potential temperature in kelvin units. Tropopause folding occurs in the shaded region between tropopause and 380 K potential surface. The broad arrows indicate the transport by global scale circulations.

meridional circulation. Furthermore, seasonal changes in the mass of the lowermost stratosphere also cause STE. During spring the tropopause altitude increases, which entrains stratospheric air into the troposphere [Appenzeller *et al.*, 1997]. The combined effects of these processes lead to the downward O₃ transport, which is maximum in late winter and early spring. Since this almost coincides with a spring ozone maximum observed at several background monitoring stations, it is tempting to assume an important role for STE, even at the surface. However it should be noted that at many locations in NH mid-latitudes, the spring O₃ maximum is observed due to *in situ* photochemistry rather than STE.

1.5.2 Surface deposition of ozone

Wet and dry depositions are the ultimate paths by which trace gases and other particles are removed from the troposphere. Dry deposition, in general refers to the transport of gaseous and particulate species from the atmosphere onto the earth's surface in the absence of precipitation. The factors that govern the dry deposition of a gaseous species or particle are the atmospheric turbulence, the chemical property of the species, and the nature of the surface itself. For trace gases, the solubility and chemical reactivity may affect the uptake at the surface. The dry deposition flux is directly proportional to the local concentration (C) of the depositing species at some reference height above the surface (e.g. 10 m or less),

$$F = - V_d C \quad (1.11)$$

where F represents the vertical dry deposition flux, i.e., the amount of material deposited on a unit surface area per unit time. The proportionality constant, V_d , has the unit of length per unit time and is known as deposition velocity. Since C is a function of height 'z' above the ground, V_d is also a function of 'z' and must be related to a reference at which C is specified. By convention, the downward flux is negative so that v_d is positive for a depositing substance. There is a large uncertainty in the deposition velocities of these trace species at different surfaces (see *Table 1.5*) [*Liu et al.*, 1983; *Thompson and Zafiriou*, 1987; *Sillman et al.*, 1993].

Table 1.5: The dry deposition velocities of different trace species in cm s^{-1} at one meter height at different surfaces [adapted from *Berntsen and Isaksen*, 1997]

Species	Dry Deposition Velocities at 1.0 m height (cm s^{-1})		
	Land	Sea	Ice
O_3	0.6	0.1	0.05
NO_2	0.1	0.05	0.02
HNO_3	4.0	1.0	0.05
PAN	0.2	0	0
H_2O_2	1.0	1.0	0.05
CO	0.03	0	0

Even on land, there is large variability in dry surface deposition among the trace species at different vegetations, barren surface and other materials. Surface deposition is one among the major sinks of tropospheric ozone, as shown in *Figure 1.5* and *Table 1.2*. These large

variabilities in the deposition rates of trace species at different surfaces add to the uncertainty in the tropospheric ozone budget.

1.5.3 Transport

Air motions play key role in determining the distribution of chemical species in the atmosphere. Transport of air is decided by three principle forces *viz* gravity force, pressure-gradient force and coriolis force. Apart from these forces, horizontal and vertical mixing of air in the atmosphere is decided by the turbulent flow of the air and its diffusion. Time taken for mixing of the atmospheric air within the hemispheres, between hemispheres and in vertical direction are shown in *Figure 1.7*. West to east (zonal) mixing of the air around the globe takes about 2 weeks, inter-hemispheric exchange takes about 1.5 years [Geller *et al*, 1997; Chand *et al.*, 2001a] and mixing within a hemisphere takes about 1-2 months. Vertical

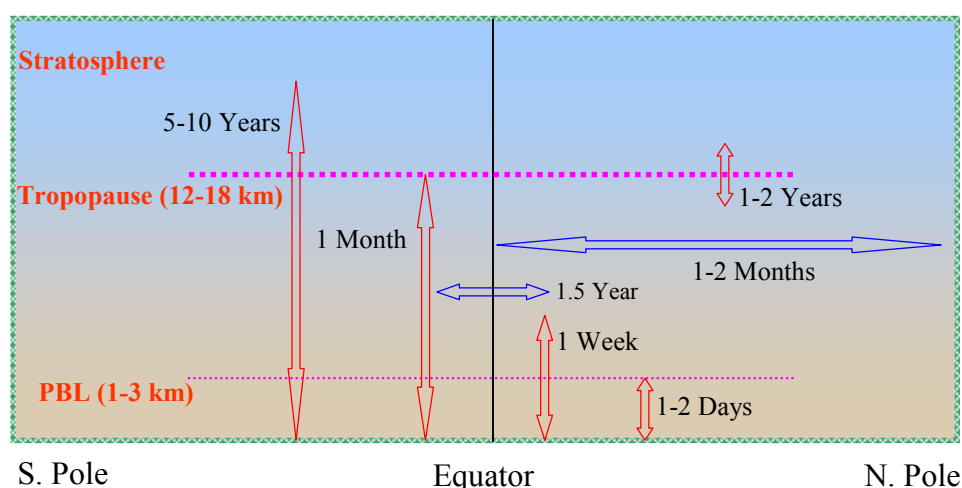


Figure 1.7 Approximate horizontal and vertical mixing and/or transport times of the trace species in planetary boundary layer (PBL), free troposphere (FT), and between PBL-FT, FT-stratosphere and across the PBL- tropopause.

transport time of trace species in tropics is lowest. It takes few days to months for complete vertical mixing in the tropical troposphere. However, the vertical mixing is very fast at ITCZ and it takes only few hours to transport the trace species from upper troposphere to lower stratosphere under strong convective activity (see *Figures 1.1* and 1.6).

Transport is widely recognized to be a significant source of air pollution worldwide. Among the continental transport, soil dust has been the principal species studied in long-range transport from Asia over the North Pacific Ocean in last two decades [Duce *et al.*, 1980; Tsunogai and Kondo, 1982]. Recently, the transport of chemically and radiatively active trace species produced due to increasing population and economic growth has acquired increasing importance in Asia [Ramanathan *et al.*, 1996]. Many international campaigns have

been conducted to study the long-range transport of trace species (GAMETAG, RITS, SAGA, PEM, SAFARI, NARE, APARE, INDOEX, BOBEX) in different regions and environments of the globe [Johnson *et al.*, 1990; Smit *et al.*, 1990; Thompson *et al.*, 1993; Singh *et al.*, 1996; Rhoads *et al.*, 1997; Lal *et al.*, 1998]. Among these, the most recent campaigns were the INDIan Ocean EXperiment (INDOEX) and Bay of Bengal Experiment (BOBEX). INDOEX was a multiplatform international program designed to characterize and quantify the air pollution transported from South and South-East Asia and to study the physical, chemical and optical properties of the atmosphere over the Indian Ocean and its implications on atmospheric composition and climate.

1.6 Objectives of this study

1.6.1 Indian scenario

So far Indian subcontinent is a data void region for the study of atmospheric trace gases. Only few measurements of ozone and its related gases are available in this region. Measurements of surface ozone were initiated in mid 1950s during pre-International Geophysical Year (IGY) using an Ehmert instrument [Ramanathan, 1956; Dave, 1957], but regular measurements of surface ozone were started by Indian Meteorological Department (IMD) during 1960-70s at Trivandrum, Kodaikanal, Pune, Nagpur, Delhi and Srinagar [e.g. Sreedharan and Tiwari, 1971]. During 1990s, measurements of ozone were started by groups at Jawaharlal Nehru University (JNU) in New Delhi and Indian Institute of Tropical Meteorology (IITM) in Pune [Varshney and Aggarawal, 1992; Khemani *et al.*, 1995]. First systematic measurements of ozone and other trace gases in the Indian subcontinent were started at Physical Research Laboratory (PRL), Ahmedabad in 1995 [Subbaraya *et al.*, 1995; Naja, 1997; Lal *et al.*, 1998] and this study is also an extension of these measurements [Chand *et al.*, 2001a; Chand *et al.*, 2001b; Nair *et al.*, 2001; Lal *et al.*, 2002; Chand *et al.*, 2002].

1.6.2 Focus of this thesis

This work is devoted to the study surface ozone and its related trace species in different environments of the tropical troposphere in the Indian subcontinent (see *Figure 1.8*). The study in marine environments includes the Arabian Sea, Bay of Bengal and Indian Ocean during INDOEX and BOBEX cruises (*Chapters 3, 4*). Over the continent, the studies of the trace species are made at urban (Ahmedabad; 23°N, 72.6°E, 50m), rural (Gadanki; 13.5°N,

79.2°E, 375m) and relatively cleaner elevated site in the free troposphere (Mt Abu; 24.6°N, 72.7°E, 1680 m) (*Chapters 5, 6*). Mobile lab experiments were also conducted over continental region to study the transport of the trace gases from the source regions to remote sites (*Chapter 6*).

The tropical region is of special significance to atmospheric and climatic studies because (a) it contributes almost half of the biogenic input of the trace gases, (b) it has abundant solar radiation throughout the year including the UVB* radiation, (c) it is associated with the convective activity which acts as a mass carrier of air from the troposphere to

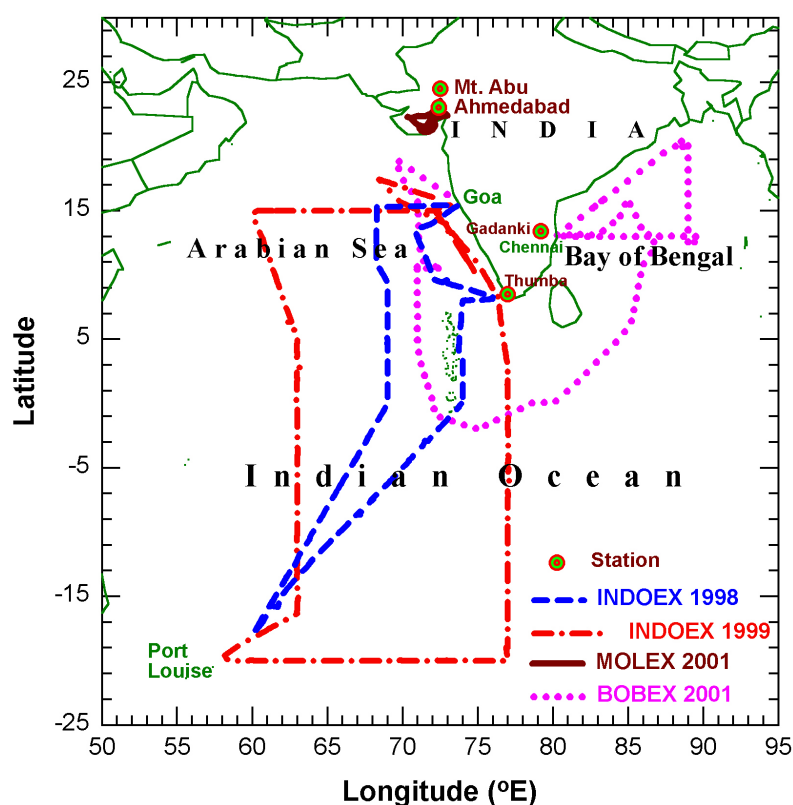


Figure 1.8 Cruise tracks of INDOEX 1998, 1999 and BOBEX 2001 along with mobile track of MOLEX-2001. Fixed observational sites (stations) are indicated by circles on the map.

stratosphere and thus affects the global stratosphere (d) it has higher tropopause level compared to the other regions of the globe, and (e) it has higher water vapor content and lower tropopause temperature. Intense convective activity and photochemistry make the tropical troposphere a unique natural laboratory to study atmospheric physics and chemistry.

In addition to all the above features, the tropical troposphere covering the Indian subcontinent has further implications for atmospheric studies. India is the second most populated country in the world. Its increasing population and economic growth have acquired greater

* UVB are the radiations in the wavelength range of 290-315 nm.

importance in Asia [*Ramanathan et al.*, 1996]. Since at present, the central, south and east Asia are the most developing regions on the globe, large increase in their energy consumption and emission of air pollutants are expected. The seasonally changing winds make this region a very good natural laboratory to study the transport and transformations of trace gases and their impacts on climate and composition of the atmosphere.

Chapter 2

Experimental techniques

Measurements form the basis on which our understanding of the atmosphere is built. New or improved capability of measurement and/or application of measurement techniques in new ways or situations have often resulted in a significant improvement in our understanding. Measurements provide the information for testing the models, validate the theoretical concepts and provide a unique opportunity to discover new physical processes. In atmospheric physics and chemistry, no measurement is more fundamental than the measurement of the composition of the atmosphere. Concentrations of the constituents vary from 78% (N_2) to less than ten parts per quadrillion (OH), as given in Chapter 1. At present, a real challenge in instrumentation requires the development of many types of instruments based on different physical, chemical and/or a combination of these properties of the gases to be measured.

The last two decades have played a significant role in mutations and improvements in the techniques for the measurement of ozone and its precursor gases. These techniques use optical (absorption of light and chemiluminescence) and chemical (reactions) interactions of gases with selected chemicals and radiation. The in-situ measurements of short-lived trace gases like O_3 , CO and NO have been made using optical and chemical methods. Analysis of the air samples for long-lived trace gases such as CH_4 and SF_6 are made using gas chromatographic (GC) methods. The detailed description of the measurement techniques used in this study are discussed in this chapter.

2.1 Ozone measurements

The discovery of ozone and its measurement technique pioneered by Schonbein in 1839, used a paper covered in a paste of starch and KI, which turned blue by exposure to ozone [Schonbein, 1840]. After 12 hours of exposure, the amount of O₃ was deduced by comparison with colors on a test chart. These ‘*Schonbein Papers*’ were also affected by other oxidants along with humidity and sunlight, but a quantitative revision of these data from many sites has been possible [Bojkov, 1986]. Another different method, iodine catalyzed oxidation of arsenite in aqueous solution, was developed at Montsouris observatory between 1876-1909 [AOMM, 1876-1910]. Other chemical techniques developed during the last century are chemiluminescent and electrochemical methods. The reaction of luminol or rhodamine-B dye (Rh-B) or olefines with ozone gives the chemiluminescence effect. But chemiluminescent substances may get affected by light and moisture and this method need further extra efforts in its use. Electro-chemical method makes use of the reaction of ozone with potassium iodide (KI) solution liberating iodine. Being based on oxidation and reduction processes, this method is also affected by interferences by other oxidizing and reducing agents like SO₂ and NO₂. This method needs regular and frequent calibrations [Regener, 1960; Komhyr, 1969]. However, electro-chemical cells (ECC) are frequently used for vertical profiles of ozone since the ECCs are light and compact and can be easily lifted by a small balloon [Logan, 1994; Beekmann *et al.*, 1995; Logan *et al.*, 1999].

Measurement of ozone in laboratory using ultraviolet (UV) light was started in 1912 [Fonrobot, 1916]. Since then this method has greatly improved with advancement of technology. The principle of this method is the absorption of UV light by ozone molecules at 253.7 nm. In the present study surface measurements are made in different environments (see Chapter 1) using ozone analyzers (Dasibi, USA, model 1008 and Environment S. A., France, model O₃ 31 M). All these analyzers are based on the same principle. The absorption of radiation by Beer Lambert’s law is expressed as below:

Intensity of radiation, I , in optical cell filled with air sample is given by

$$I = I_0 \exp \left[- \int_0^l (\sigma_{O_3} n_{O_3} + \sigma_r n_{air} + \sum \sigma_i' n_i') dl \right] \quad (2.1)$$

Where,

I = Attenuated intensity due to air sample (i.e. ozone and other species),

I_0	= Unattenuated intensity (intensity of the UV source)
σ_{O_3}	= Cross section of ozone in cm^2
n_{O_3}	= Ozone number density in cm^{-3}
σ_r	= Rayleigh scattering cross section of air in cm^2
n_{air}	= Air number density in cm^{-3}
σ'_i	= Absorption cross section of other (i th) species in cm^2
n'_i	= Number density of other (i th) species in cm^{-3}
l	= Length of the absorption cell in cm

Similar to equation 2.1, intensity I' of radiation in optical cell filled with zero air (without O_3) is given by

$$I' = I_0 \exp \left[- \int_0^l (\sigma_r n_{\text{air}} + \sum \sigma'_i n'_i) dl \right] \quad (2.2)$$

The ratio of these two signals from equations 2.1 and 2.2 is used to obtain the ozone number density, i.e.

$$\frac{I}{I'} = \exp \left[- \int_0^l (\sigma_{O_3} n_{O_3}) dl \right] \quad (2.3)$$

The ratio of the two signals, as defined by equation 2.3, is a function of ozone only. Except ozone number density, other parameters are known. In addition, the analyzer incorporates the correction due to changes in pressure and temperature in the absorption cell. The drift in the intensity of the UV lamp is also compensated in the analyzer.

Figure 2.1 shows the instrumental implementation of the Beer Lambert's law. The instrument samples the ambient air with ozone and ozone free air through three way solenoid valve. Ozone free air is produced by using a ozone scrubber (MnO_2). The switching time of the solenoid valve is 5 seconds in Dasibi and Environment S. A. (ESA) analyzers. Two complete cycles (10 seconds) of solenoid valves provide the resolution of the ozone measurements. The absorption cell, having optical path of 75 cm, is illuminated by a low pressure mercury vapor lamp to provide UV radiation at 253.7 nm which is the main emission line of mercury and the ozone absorption cross section (σ_{O_3}) is highest at this wavelength. By choosing a special combination of filter (vicor) and detector (Cesium Telluride), the bandwidth of the lines is minimized around 253.7 nm (see *Figure 2.2*).

Calibration of the systems is done regularly by using their inbuilt ozone generators. Zero setting of the instruments is also performed regularly. After calibration, all the ozone analyzers were inter-compared. *Figure 2.3* shows the inter-comparison plots of these analyzers. The Dasibi analyzer was calibrated at Research Center, Juelich, Germany in 1998. This analyzer was also inter-compared for a day on the Indian Oceanic Research Vessel

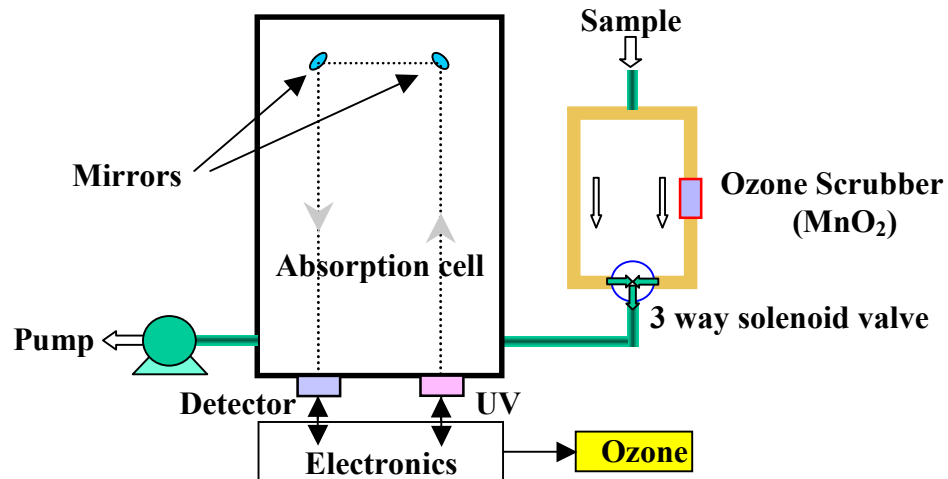


Figure 2.1 A simplified block diagram of the ozone analyzer showing the working principle and other key component of the system.

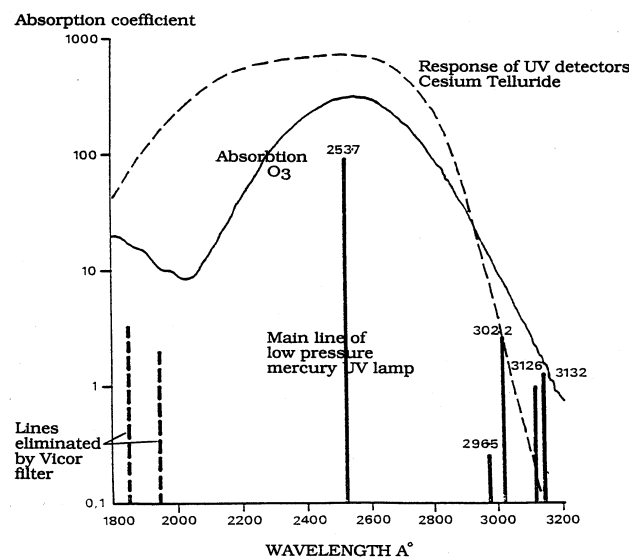


Figure 2.2 Absorption spectrum of ozone (solid thin line) and main emission lines of mercury at low pressure (continuous vertical lines). Dashed curve shows the response of the UV detector used in the ozone analyzer.

(ORV) *Sagar Kanya* along with the simultaneous measurements of ozone made on NOAA's ORV *Ron Brown* during the INDIAN Ocean EXperiment (INDOEX) campaign in March, 1999. The comparison showed a good agreement with a correlation coefficient (r^2) of better

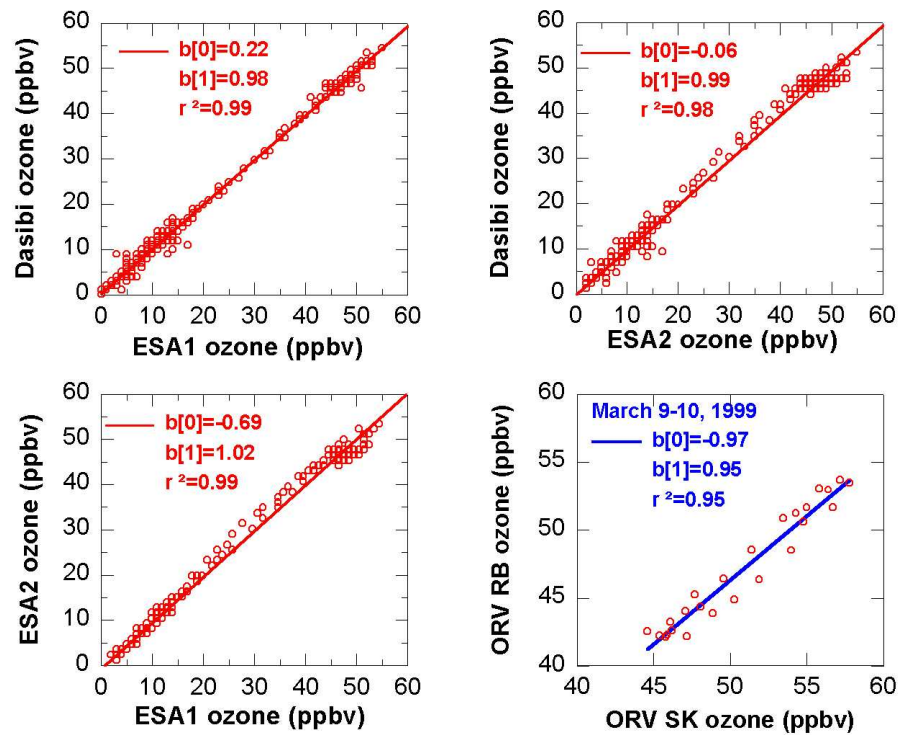


Figure 2.3 Inter-comparison of different ozone analyzers. ESA 1 and ESA 2 are two different Environment S A analyzers. Comparison is also shown between Dasibi ozone analyzer on ORV Sagar Kanya and NOAA's ozone analyzer on ORV Ronald Brown when both ships were moving parallel to each other during INDOEX 1999 over the Arabian Sea. The slope and intercept of the line fit are represented by $b(1)$ and $b(0)$ respectively.

than 0.95. Also, all the analyzers inter-compared with a correlation coefficient better than 0.98 and with a difference of less than 3% in the absolute values, as shown in *Figure 2.3*. The switching time of the solenoid valve in ozone analyzers determines the response time to be 10 seconds. However the data is averaged over 5 minutes and stored in data loggers and personal computers. The detection limit of the ozone analyzers is 1 ppbv, as shown in *Table 2.1*. The absolute accuracy of these instruments is above 95% [Kleinman *et al.*, 1994].

2.2 Carbon monoxide measurements

After rapid development of the electronic devices in 1940s and its combination with optical devices later, opto-electronics contraptions have given a new direction to the commercial instruments. Using such instruments, the first measurements of CO were made by *Migeotte and Neven* [1952]. Further advancement of technology have improved these instruments for better precision and accuracy. The latest review of the methods commonly used for measuring the atmospheric carbon monoxide is compiled by *Novelli* [1999]. The most

advanced CO, NO₂ and SO₂ instruments work on the principle of gas correlation spectroscopy (GCS). In gas correlation spectroscopy, a cell filled with the gas of interest is used instead of grating. Comparison of the attenuated signals from these cells filled with different gases reduce the absorption interference from other gases and separate the absorption signal of desired gas [Reichle *et al.*, 1986; Roscoe and Clemitshaw, 1997].

A commercial analyzer (Monitor Labs, USA, model ML 9830) based on GCS is used for CO measurements. *Figure 2.4* shows the simplified layout of this instrument. Two cells filled with CO and N₂ along with a dummy metallic (opaque) cell are used for getting the

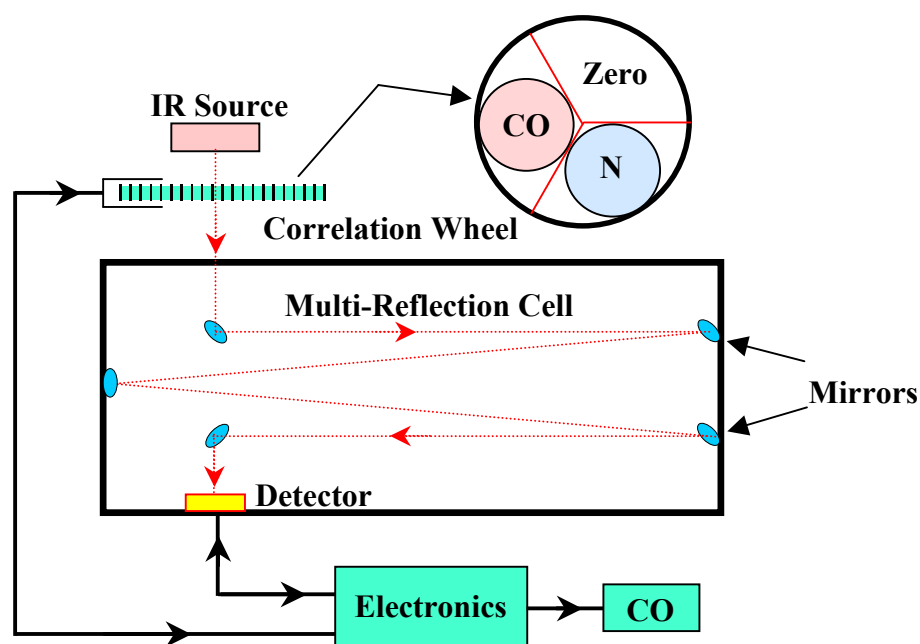


Figure 2.4 A simplified block diagram of the carbon monoxide analyzer showing the working principle and other important parts of the system.

correlated signals. These cells are filled at high pressure to achieve maximum optical attenuation in a small path of the cell. A heated resistor is used as IR source. It gives a broad band spectrum centered at 4.67 μm . Optical filter is used to narrow the spectrum band of the IR source. The IR signal is absorbed in a 5 meter long multi-reflection optical chamber as shown in *Figure 2.4*. Lead selenide IR detector chilled at -20°C is used for measuring the attenuated IR signal. Using similar calculation as used for ozone in equation 2.1 to 2.3, CO concentration can be deduced from the signals from these three cells. Zero setting of the instrument was done daily. The instrument was regularly calibrated with calibration mixtures (Linde, UK, 1000 ppbv; Matheson, USA, 2100 ppbv). *Figure 2.5* is a typical calibration plot of the CO analyzer. A good linearity was found over ranges of CO values. The minimum detection limit of the analyzer is 50 ppbv with 25 ppbv as noise level (see *Table 2.1*).

Table 2.1: Details of gas analyzers used for this study

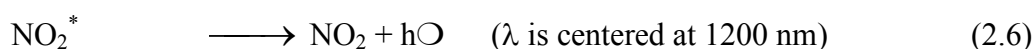
Gas	Method	Instrument and Model	MDL*	MRT [†]
Ozone	UV absorption	Dasibi, USA; Model 1008-RS	1 ppbv	10 sec
		Environmental S. A, France Model O ₃ 31 M	1 ppbv	10 sec
CO	Non-Dispersive IR (NDIR) gas filter correlation	Monitor Labs, USA; Model ML 9830	50 ppbv	60 sec
NO	Chemiluminescence	Eco Physics, Switzerland; Model CLD 780TR	5 pptv	62 sec

*MDL: Minimum Detection Limit

†MRT: Minimum Response Time

2.3 Nitric oxide measurements

Nitric oxide (NO) is measured using a high sensitivity chemiluminescent analyzer (Eco Physics CLD 780 TR). *Figure 2.6* shows simplified diagram of the nitric oxide analyzer. The chemiluminescence system uses photomultiplier detection of luminescence from the decay of excited nitrogen dioxide (NO₂^{*}) molecules produced by the reaction of NO with O₃, as follows:



NO₂^{*} denotes the excited nitrogen dioxide molecule, M for deactivating collision species such as N₂, O₂. The spontaneous deactivation of NO₂^{*} occurs with the emission of broadband radiations centered at 1200 nm wavelength (reaction 2.6). The light intensity generated by the chemiluminescent reaction is proportional to the mixing ratio of NO. The low light signal emitted by the chemiluminescence is amplified by a photo multiplier tube (PMT) and recorded.

Sensitivity of this instrument is very high for NO detection. It is important to recognize all the source of the signals detected by PMT. There are three different types of signals in the NO analyzer, as follows:

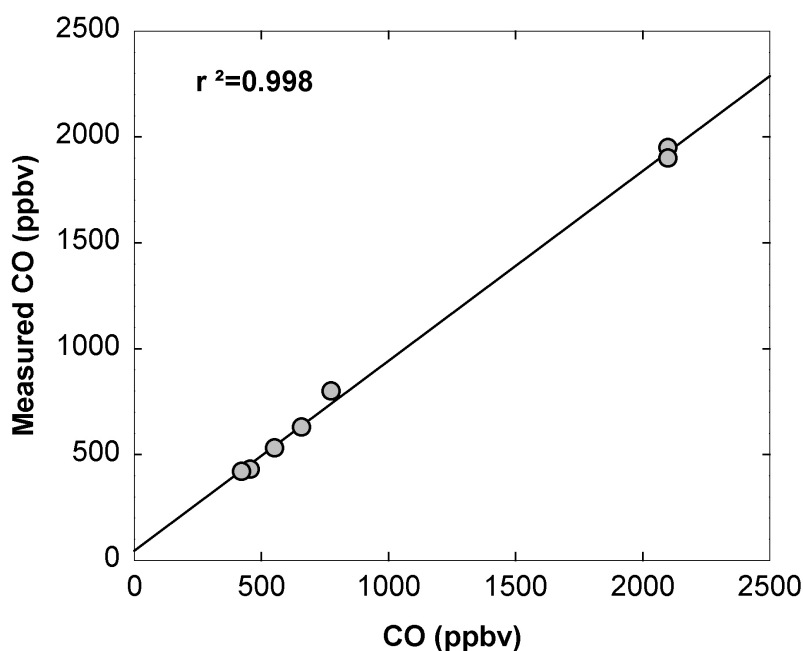


Figure 2.5 Calibration curve of CO analyzer (Monitors Lab, USA). X and Y axes represent calibrated and measured CO respectively.

- (i) Signal due to excited NO_2^* (S_{NO})
- (ii) Signal due to dark current (S_{D})
- (iii) Signal from other interfering reactions (S_{I})

The total signal S is such that,

$$S = S_{\text{NO}} + S_{\text{D}} + S_{\text{I}}$$

For the correct measurement of low levels of NO (pptv range), CLD 780 TR employs a pre-chamber where NO completely reacts with ozone (see *Figure 2.6*). If the residence time of the sample gas in the pre-chamber allows the complete deactivation of the excited NO_2^* , shown by reaction 2.5, the signal S_{NO} detected by the PMT in the main reaction chamber is the zero air signal. Alternating measurements with and without the pre-chamber allow the calculation of the correct NO concentration in the sample.

$$S_{\text{M}} = S_{\text{NO}} + S_{\text{D}} + S_{\text{I}} \quad (\text{Reaction in the main chamber})$$

$$S_{\text{P}} = S_{\text{D}} + S_{\text{I}} \quad (\text{Reaction in the pre-chamber})$$

$$S_{\text{NO}} = S_{\text{M}} - S_{\text{P}}$$

One measuring cycle consists of two steps, (i) measuring mode producing the signal S_M in the main chamber and (ii) zero mode producing the signal S_p in the pre chamber. In both modes, the sample is mixed with high-concentration ozone at lower pressure (~ 15 mb). Low pressure

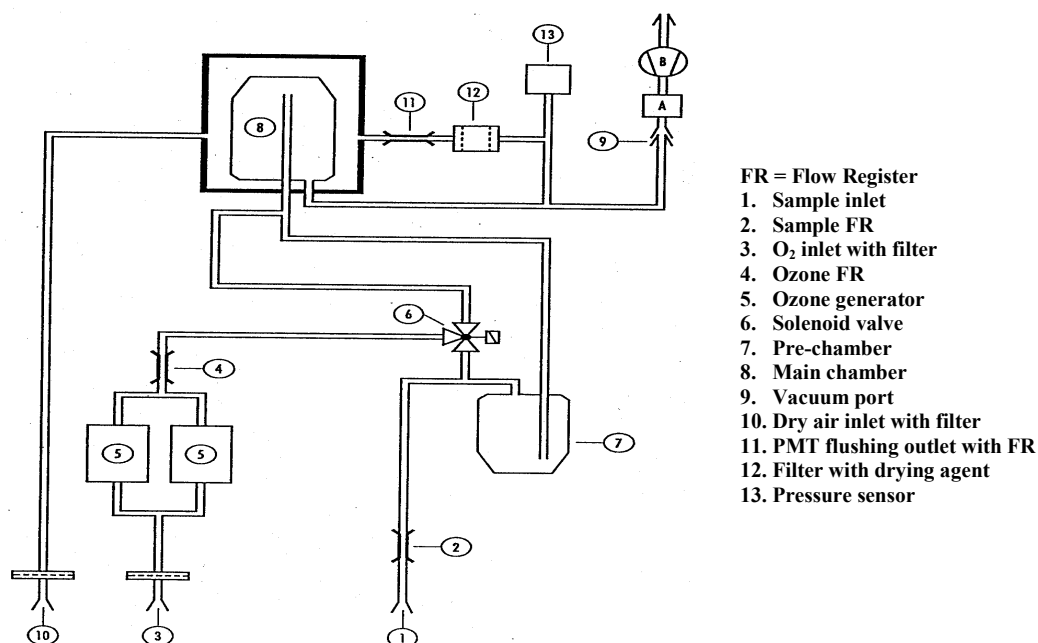


Figure 2.6 Block diagram of the NO analyzer. The major parts of the system are shown in the figure sequentially.

is to avoid the deactivation of NO_2^* by collisions. The PMT always measures the optical emission from the main chamber only. Thus the complete measurement is of two cycle

A general description of such a chemiluminescence analyzer can be seen in *Delnay et al.*, 1982; *Dickerson*, 1984; and *Wang et al.*, 2001. NO (in N₂) mixture of 0.8 ppbv from Matheson, USA is used for calibration. *Figure 2.7* shows the calibration graph of NO instrument. The concentration of NO mixture was varied from 20 pptv to 800 ppbv during the calibrations using a specially designed glass chamber. High purity nitrogen gas is used for diluting the NO concentration. A very good linearity is found with r^2 of 0.99 and a difference of less than 3% at all ranges of NO. The minimum detectable limit of the NO instrument is 5 pptv at about 60 second integration time (*Table 2.1*).

2.4 Measurements of trace gases using GC techniques

Study of short lived trace gases, as mentioned in earlier section, is based on the real time (online) measurements. But the trace gases like CH₄ and SF₆ have long lifetimes of the order of many years. Air samples for these gases can be collected in specially built air samplers and

can be later analyzed by different techniques like chromatography, mass spectrometry etc. Chromatography is one of the important analytical techniques to measure concentration of various trace compounds. In general, the term *chromatography* describes a wide range of techniques that separate mixtures of chemicals into their various components.

Because of its versatility and the nature of the medium to be analyzed, gas chromatography (GC) is the most widely used technique for separating and measuring the components of complex air mixtures (see *Figures 2.8 and 2.9*). Analysis of trace gases in ppbv or lower levels often involves the pre-concentration of these compounds from samples.

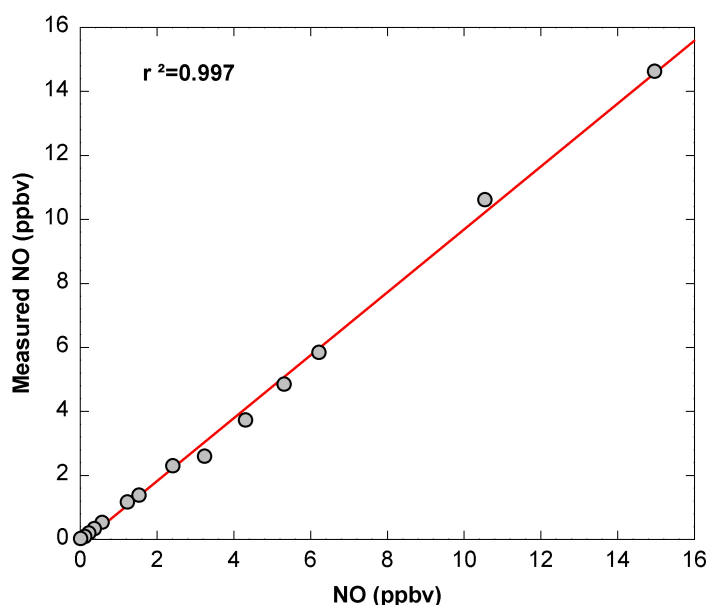


Figure 2.7 Calibration curve of Eco Physics NO analyzer (Eco Physics CLD 780 TR, Switzerland). *X* and *Y* axes represent calibrated and measured NO respectively.

Sensitivity of different detectors used in GC range 10^{-9} - 10^{-12} gram levels. To measure various compounds from ppmv to pptv ranges, the volume of the samples used ranges from few milliliter to liters. *Figure 2.8* shows a simplified diagram of the gas chromatography (GC) system. The principal of operation of a GC is based on differential migration of the components of a gas mixture in mobile phase (carrier gas) with respect to the stationary phase in the column. Separation and detection of a component is decided by specific selection of column, carrier gas and detector. The gases like CO (with methaniser) and CH_4 are detected using flame ionization detector (FID). Trace gases having electron affinity (like CFCs, SF_6 , N_2O etc) are measured using an electron capture detector (ECD). The detailed specifications of the columns, carrier flows for all these gases are given in *Table 2.2*. *Figure 2.9* shows typical chromatograms.

The reproducibility of the analyses for SF₆ and CH₄ are within 1% whereas for CO it is about 5-6 %. A good match is found in the measurements of CO made by an analyzer and GC. CH₄

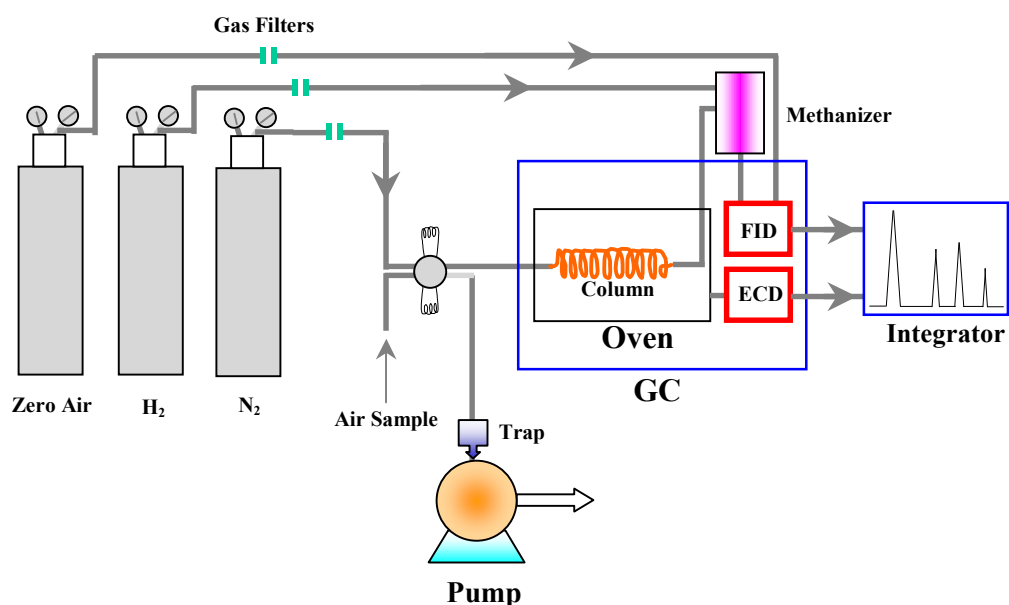


Figure 2.8 Schematic diagram of Gas Chromatograph system.

is calibrated with the NIST, USA and LINDE, UK calibration mixtures, whereas SF₆ is calibrated with respect to a gravimetrically prepared standard at the Institut für Umweltphysik, University of Heidelberg, Germany [Maiss et al., 1996].

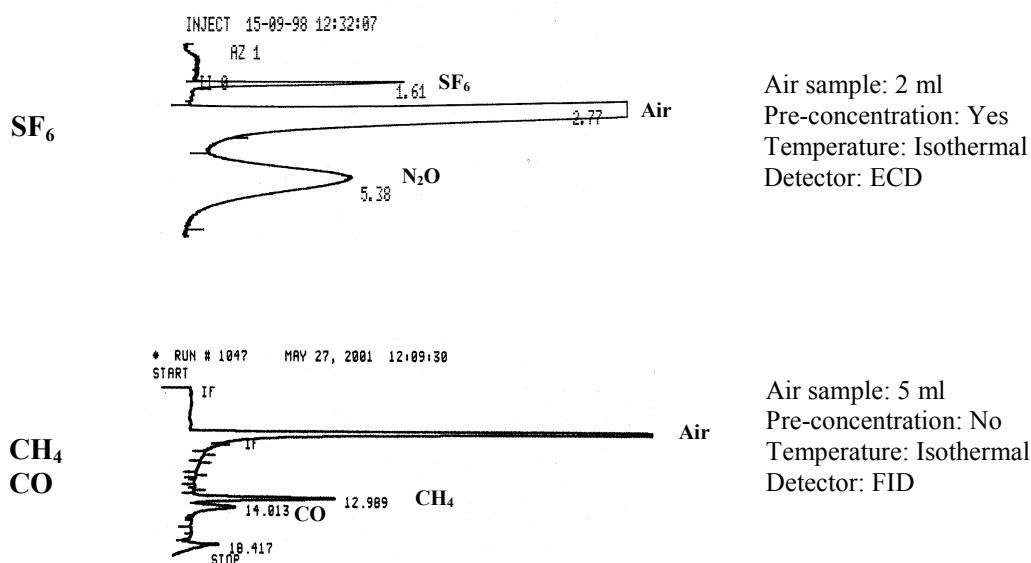


Figure 2.9 Gas chromatograms showing separation and detection of SF₆, CH₄ and CO.

Table 2.2: Experimental details of the GC system used for analysis of various trace gases.

Analyzed gas (direct/pre-trap)	Column used (length, OD, ID in mm)	Carrier gas used (flow rate ml min ⁻¹)	Detector used
CO (direct-injection)	Molecular Sieve 13X, (550, 3.2, 1.9)	N ₂ (~30)	Methaniser+FID
CH ₄ (direct-injection)	Molecular Sieve 13X, (550, 3.2, 1.9)	N ₂ (~30)	<i>FID</i>
SF ₆ (pre- concentrated)	Molecular Sieve 5A, (350, 3.2, 1.5)	N ₂ (~30)	<i>ECD</i>

Chapter 3

Ozone and other trace gases over the Indian Ocean and Arabian Sea

The Indian Ocean, bordered in the south by one of the most sparsely populated areas and north by the densely populated and rapidly developing subcontinent, is a unique environment to study the transport of air pollutants and their impact on atmospheric composition and climate. During the northern hemispheric winter, large-scale cooling of the Tibetan Plateau is associated with the development of a high pressure over the Asian continent. The north-easterly outflow from this high-pressure area transports polluted air masses from the Asian region to the Indian Ocean. The important question is to what extent the growing emission of pollutants from South Asian region can affect the composition, chemistry and climate of this relatively pristine atmosphere. The warm water of the Indian Ocean triggers the deep convective cirrus clouds in association with the Inter Tropical Convergence Zone (ITCZ) and contributes significantly to the vertical exchange of minor constituents (gases and particles) between the surface and the upper troposphere/lower stratosphere. Due to the intense and deep convective activity together with higher solar radiation flux along the ITCZ, there is a large production of OH radicals. The INDIan Ocean EXperiment (INDOEX) provided an excellent opportunity to study the transport of various trace gases from the Indian continent to the Indian Ocean and the role of ITCZ in the inter-hemispheric transport of trace gases, as shown in *Figure 3.1*.

3.1 Introduction

Long-range transports of ozone and other pollutants have been observed in different regions of the world [Kley *et al.*, 1997; Roelofs *et al.*, 1997a; Fujiwara *et al.*, 1999; Jacob *et al.*, 1999]. The Asian region (mainly China, India, East Asia) is the fastest developing region with increasing levels of pollution from industries and other man-made sources. It is well known now that ozone is mainly produced by the photo-oxidation of pollutants (like carbon

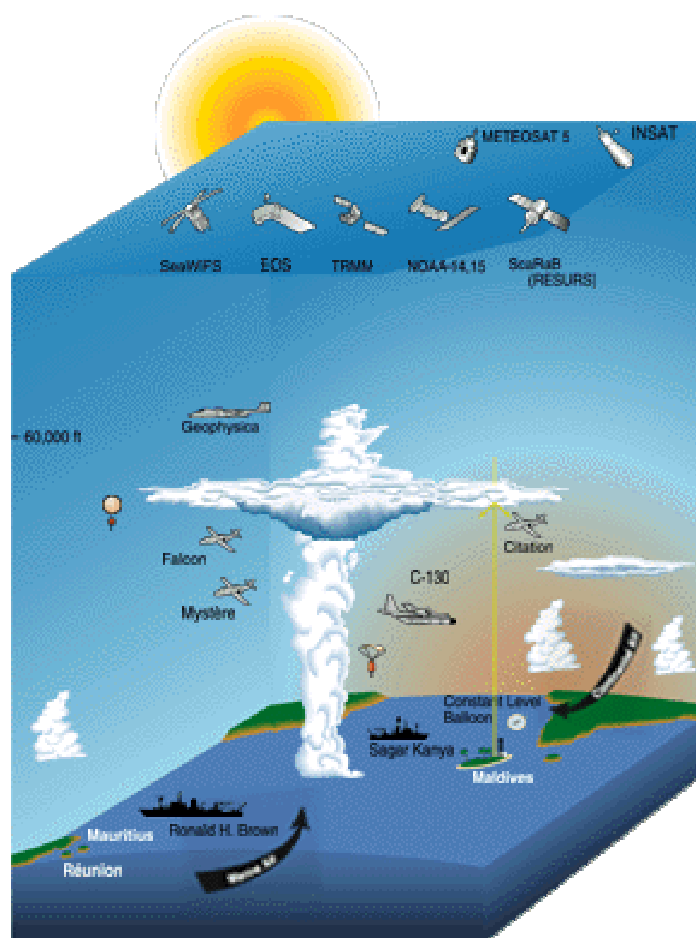


Figure 3.1 INDOEX cube showing the various observational platforms including satellites, aircrafts, ships, balloons, dropsondes and surface stations at Maldives and India. The oceanic research vessels Sagar Kanya (India) and Ronald H. Brown (USA) travelled between Goa, Male, Mauritius covering vast area over the Indian Ocean and Arabians Sea [Ramanathan *et al.*, 1996].

monoxide and hydrocarbons) in the presence of adequate amounts of nitrogen oxides (NO , NO_2) at lower altitudes [e.g. Lelieveld *et al.*, 1991; Crutzen *et al.*, 1999]. Once ozone is produced, it can get transported to distant places along with other pollutants.

The ITCZ controls the mixing of the northern hemispheric polluted air with the pristine air of the southern hemisphere over the Indian Ocean, as shown in Figure 3.1.

Among the international efforts to better understand the tropospheric ozone and its effects on climate change, many campaigns have been conducted over different marine regions like the Atlantic Ocean [e.g. *Smit et al.*, 1990], the Pacific Ocean [*Johnson et al.*, 1990; *Thompson et al.*, 1993; *Diab et al.*, 1996] and the Indian Ocean [*Johnson et al.*, 1990; *Ayers et al.*, 1997; *Rhoads et al.*, 1997; *Bremaud et al.*, 1998; *Lal et al.*, 1998]. However, there are limited observations to study the transport and en route transformation of ozone and its year-to-year variability particularly over the Indian Ocean. In this sense, INDOEX was designed to study the movement of pollutants from the Indian sub-continent to the Indian Ocean [*Ramanathan et al.*, 1996]. Detailed results of the measurements of surface ozone in the marine boundary layer over the Arabian Sea and the Indian Ocean adjoining the Indian peninsula during the ORV *Sagar Kanya* cruises in 1998 and 1999 as part of the international program, INDOEX, are presented in this chapter.

3.2 Meteorological conditions

The INDOEX was conducted in the northern hemispheric (NH) winter. During the period of this study, the general synoptic scale pattern at surface level is northeasterly/easterly winds so that the oceanic region covered by the cruises during both the years were on the downwind side of the continent [*Jha and Krishnamurti*, 1998 and 1999]. *Figure 3.2* shows the general surface wind flow during summer and winter over the Indian Ocean. In summer, the winds flow from the Arabian Sea and the Indian Ocean to the Indian sub continent and it is in the

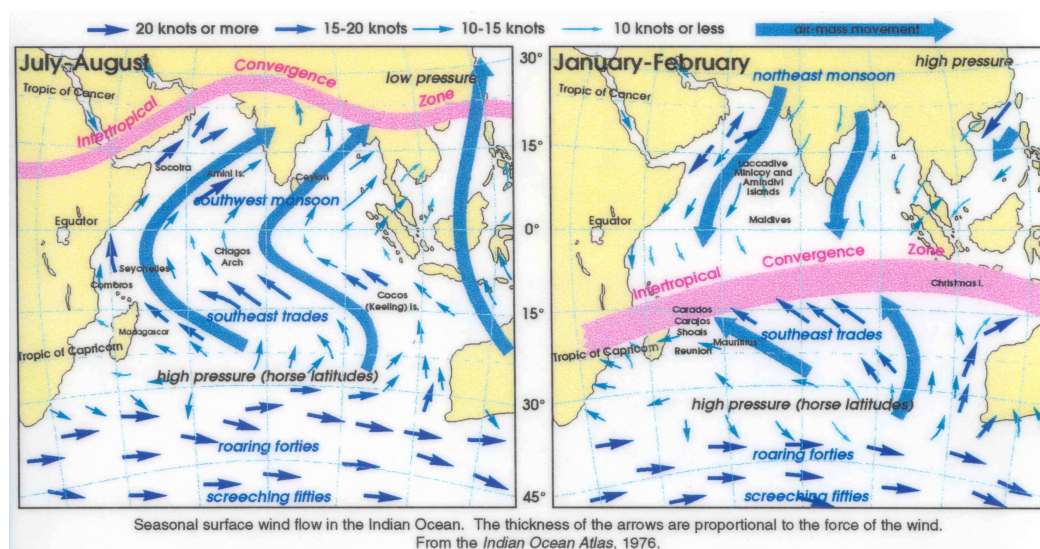


Figure 3.2 Seasonal surface winds along with the position of ITCZ over the Indian Ocean. The thickness of the wind field is proportional to the speed of the wind [*Indian Ocean Atlas*, 1976].

reverse direction in winter. The region where the air mixes and converges from the two hemispheres is called inter tropical convergence zone (ITCZ).

The years 1998 and 1999 were *El Nino* and *La Nina* years respectively [Zachariasse *et al.*, 2001]. The monsoonal flow from the Indian continent was stronger in February 1999 as compared to that in February 1998. The winter period of 1999 had many anti-cyclones and stronger inversions [Lelieveld *et al.*, 2001; Verver *et al.*, 2001]. The descent velocity of air was stronger in INDOEX 1999 compared to that in 1998 thereby leading to reduced venting of pollutants from boundary layer. The average wind speed over the entire area during INDOEX 1998 was $4.5 \pm 2.3 \text{ ms}^{-1}$ whereas during INDOEX 1999 it was $5.9 \pm 2.6 \text{ ms}^{-1}$. However, there were large variabilities in wind speeds during both the years. The wind speeds during the first half of the journey (henceforth first half of the cruise will be known as *onward journey* and the second half of the cruise as *return journey*) in both the campaigns were higher than the wind speed during the respective return journeys. The changes in wind speeds during onward and return journeys in both the cruises are attributed to the Madden-Julian oscillation (MJO), which has a period of 30-60 days [Madden and Julian, 1972; Rasch *et al.*, 2001]. MJO is due to the change in position and strengths of the low and high pressures centers over the Indian subcontinent arising out of differential heating. There were large fluctuations in the position of ITCZ during INDOEX 1999. However, the average movement of ITCZ was from 5°S to 1°S during INDOEX 1999, as shown in *Figure 3.3*.

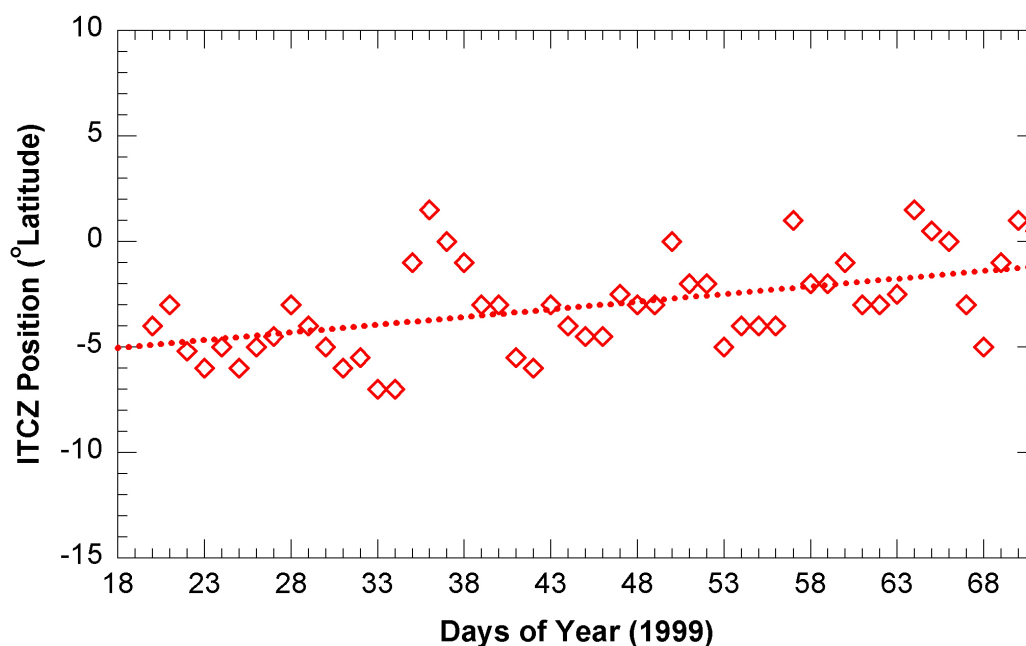


Figure 3.3 The scatter plot showing the latitudinal location of ITCZ over the Indian Ocean during INDOEX 1999. Dotted line is least square fit line for all the points.

The data from National Center for Environmental Prediction (NCEP) are used for wind fields. The back trajectories (BTs) are used to trace the transport of the air parcel. Hybrid Single Particle Lagrangian Integrated Trajectory (HySPLIT-4) Model, Version-4, was used for getting the BTs [Draxler and Hess 1997; 1998]. The NCEP data was downloaded from NOAA's site <http://www.cdc.noaa.gov/cdc/data.nmc.reanalysis.html> and the trajectories were downloaded from <http://www.arl.noaa.gov/ready/hysplit4.html>.

3.3 Experimental details

The First Field Phase (FFP) INDOEX 1998 and the Intensive Field Phase (IFP) INDOEX 1999 cruises were conducted during February 18 - March 30, 1998 and January 20 - March 12, 1999 respectively. The other cruise details are given in *Table 3.1*. For real time measurements of short lived trace gases ambient air was taken from the bow of the ship at an height of about 10 m from the sea level through an inlet line made up of teflon to minimize smoke-stack contamination. Ozone, CO and NO were measured onboard the ship and air samples were also collected for analysis of other long-lived trace gases from the front of the ship when it was cruising. These air samples were analyzed at PRL for other gases like CH₄, SF₆ etc.

Table 3.1: Details of INDOEX 1998 and INDOEX 1999 cruises over the Indian Ocean.

Cruise Details	INDOEX 1998		INDOEX 1999	
	Onward Journey	Return Journey	Onward Journey	Return Journey
Cruising period	Feb. 18 - Mar. 11	Mar. 16 - Mar. 30	Jan. 20 - Feb. 11	Feb. 19- Mar. 12
Latitudinal coverage	15°N - 20 °S	20 °S – 15 °N	15 °N - 20 °S	20 °S - 17 °N
Longitudinal coverage	76 °E - 59 °E	59 °E - 73 °E	77 °E - 59 °E	59 °E - 77 °E
ITCZ crossing time	Mar. 07-08	Mar. 20-21	Jan. 30-31	Feb. 23-26
ITCZ crossing latitude	10 °S - 11°S	08 °S- 05 °S	05 °S - 08 °S	06 °S - 03 °N

Ozone was measured by a Dasibi analyzer (RS-1008, USA) based on UV absorption at 253.7 nm, while CO was measured using a non-dispersive infrared (NDIR) gas filter correlation analyzer (Monitor Labs, USA, ML 9830) based on the principle of absorption of infrared radiation at 4.67 μ m in its vibrational-rotational bands. Further details of the O₃ and CO analyzers are given in Chapter 2. Air samples were collected during both the cruises in specially designed, pre-evacuated glass bottles at a pressure of about 1.5 bar using a metal

bellow compressor. These samples were analyzed at Physical Research Laboratory (PRL), Ahmedabad using gas chromatograph (GC-Varian Vista 6000, USA) coupled with flame ionization detector (FID) for CH₄ and electron capturing detector (ECD) for SF₆. Further details of the measurement techniques and calibration procedures for O₃, CO and CH₄ are also given in Chapter 2. The precision of analyses for CH₄ and SF₆ is less than 1%.

Ozone measurements were made simultaneously onboard the Indian Oceanic Research Vessel (ORV) *Sagar Kanya* and NOAA's ORV Ronald Brown for about a day for inter-comparison of the onboard instruments during the INDOEX 1999. The two vessels moved side by side during March 9 and 10 over the Arabian Sea for this purpose. The results of the inter-comparison between the two independent ozone measurements show very good agreement ($r^2 = 0.95$), as shown in *Figure 2.3* in *Chapter 2*.

The cruise tracks for INDOEX 1998 and INDOEX 1999 are shown in *Figure 3.4*. The

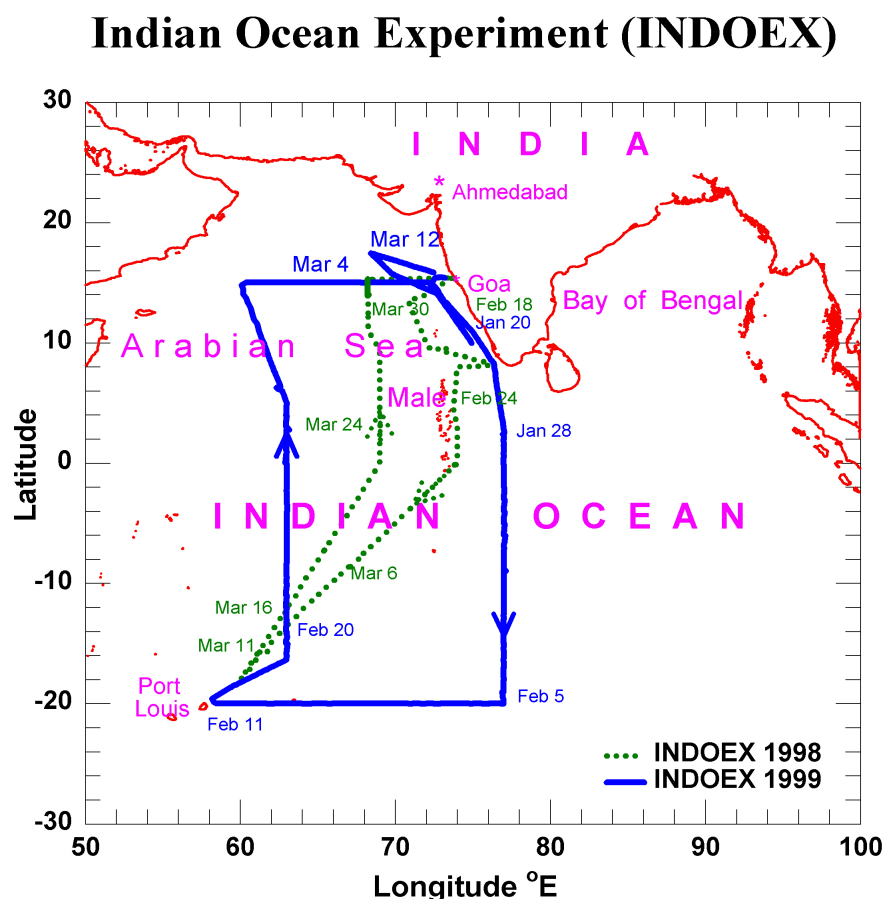


Figure 3.4 Cruise tracks of INDOEX 1998 and 1999 represented by dotted and continuous lines respectively. The position of the ship with dates is also given along with the cruise tracks during the two campaigns. The arrows show the direction of movement of the ship.

ship ORV *Sagar Kanya* sailed from Goa (15.3°N, 73.4°E) to Port Louis (20.2°S, 57.5°E) and returned back to Goa during both the cruises. However, the area covered during INDOEX

1999 was much broader than the area covered during INDOEX 1998 cruise. The ship crossed the ITCZ during each latitudinal transects (see *Table 3.1*). The ship also made two longitudinal transects, one each in the northern region and southern region in addition to the latitudinal coverage during INDOEX 1999.

3.4 Variations in ozone (O_3)

3.4.1 Ozone levels during INDOEX 1998

Figure 3.5 shows observed variation in hourly averaged surface ozone during the INDOEX 1998 cruise. Information on latitude and longitude are also shown. Average ozone value is found to be about 46 ppbv near the Goa coast and on the next day decreased to about 30 ppbv as the ship moved away towards south. For the next 2-3 days, ozone values showed some fluctuations as the ship further moved southward and parallel to the coast. Ozone values further decreased sharply from 35 ppbv on February 22 (day 53) to 13 ppbv on February 23

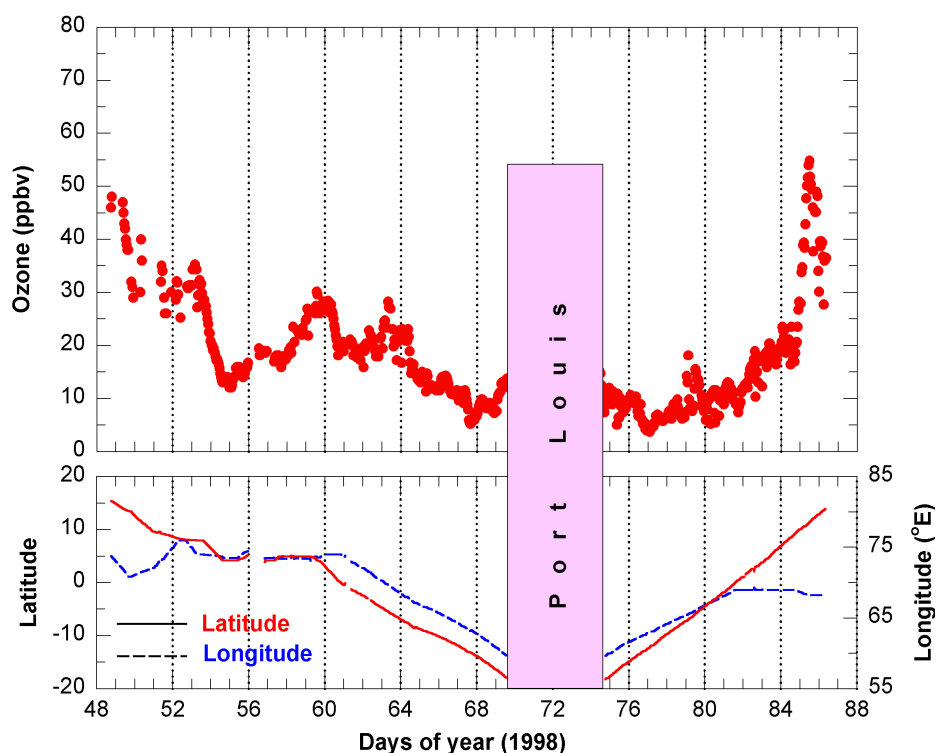


Figure 3.5 Hourly averaged surface ozone during INDOEX 1998 along with latitude and longitude. The vertical shaded area represents stationary status of the ship (at Port Louis). The continuous line represents latitude whereas the dashed line is for longitude. The ship was stationary from day 55-59 near Male.

(day 54) as observations were taken away from the Indian source region towards the cleaner Indian Ocean. The wind streamlines show that the ship experienced polluted air from India

on day 53, whereas on day 54 it experienced air mass from the northern Indian Ocean and southern Bay of Bengal (*Figures 3.6a, 3.6b*). The ship was stationary near Male during February 24-28. However, there is an increase again in ozone from the low level of 13 ppbv to 30 ppbv on day 60. This increase is attributed to the gradual change in the source of wind from the cleaner marine to the polluted continental air from Mumbai region (*Figure 3.6c*).

The ship crossed the ITCZ during day numbers 66 and 67 and minimum ozone level of about 5 ppbv was observed on day 67, when the air was coming from the clean southern

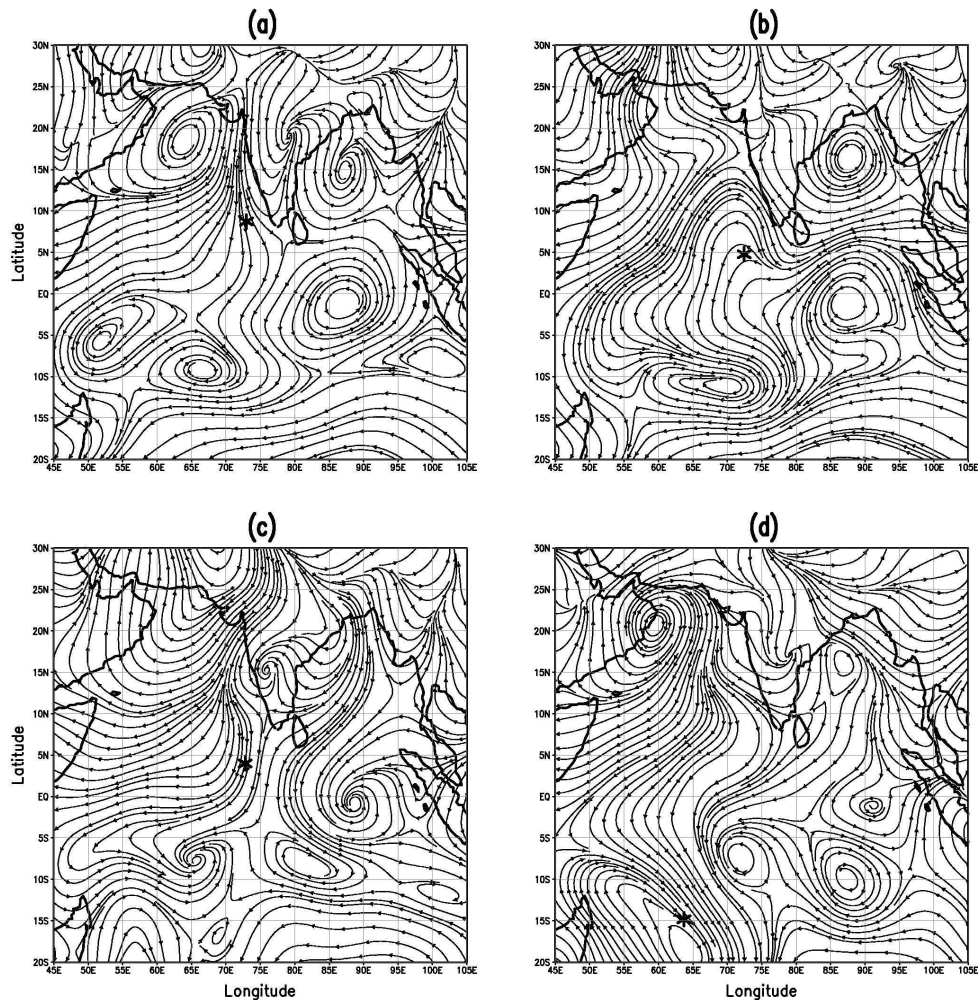


Figure 3.6 Average wind field lines at 925mb during INDOEX 1998 on (a) February 22, 1998 [day 53]; (b) February 23, 1998 [day 54]; (c) March 01, 1998 [day 60] and (d) March 08, 1998 [day 67]. The position of the ship is represented by asterisk. ITCZ is the region where the streamlines coming from NH combine with those coming from SH.

Indian Ocean (*Figure 3.6d*). It reached Port Louis on day 70 (March 11) and it started sailing from there on day 75 (March 16). After moving away from Port Louis, minimum ozone of about 4 ppbv was recorded on day 77, south of ITCZ and thereafter it started increasing as the ship moved towards India. The ITCZ was encountered on days 79 and 80 during the return leg. Lower aerosol optical depth and aerosol loading are also observed in the ITCZ region

[Rajeev *et al.*, 2001, Parameswaran *et al.*, 2001]. The lower levels of ozone and aerosol at ITCZ indicate that ITCZ acts as a sink for these species. Significant loss of ozone may be possible on the surface of cloud droplets in the convective region of the ITCZ [Lelieveld and Crutzen, 1990; Kley *et al.*, 1996]. Similar effects of ITCZ with low levels of ozone were observed over the Atlantic Ocean [Browell *et al.*, 1996] and Pacific Ocean [Kley *et al.*, 1996].

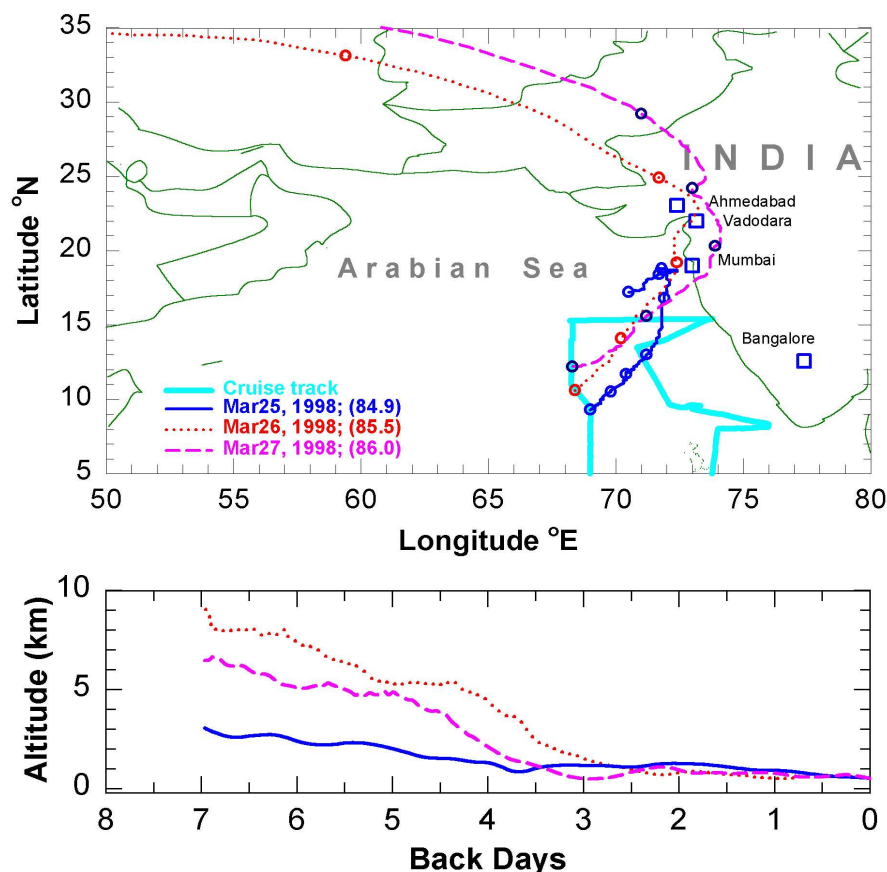


Figure 3.7. Three dimensional 7-days back trajectory of the air parcels transported from the continental region and arriving at the observation site on the mentioned dates and time during INDOEX 1998. The circles embedded on the lines are at each day interval. The squares represent the major cities of in western India

After crossing the ITCZ, ozone levels increased gradually from 8 ppbv to 19 ppbv and highest ozone of 55 ppbv was observed on day 85 (March 26) near 10-12°N. Back trajectory analysis shows that on day 85 the elevated ozone air mass arrived at the observational site in a short time of less than 3 days (Figure 3.7) from the industrial region of Gujarat.

3.4.2 Ozone levels during INDOEX 1999

Figure 3.8 shows variation in hourly averaged ozone values for the INDOEX 1999 cruise. The ozone values are in the range of 50 to 70 ppbv near the Indian coast during days 21 to 24.

Back trajectory and wind field analysis (not shown here) show that winds passed over the south Indian urban regions of Bangalore and Chennai, which are highly industrialized cities. In an earlier study, high levels of ozone of about 60-70 ppbv were also observed at a rural place, Gadanki [13.5°N, 79.2°E, 375m], nearer to these two cities, when the winds were coming from these sites in the month of March [Naja and Lal, 2002]. Such high ozone values were not observed during INDOEX 1998, possibly due to remoteness of the cruise track from the Indian coast and also due to the weaker winds during February 1998. After day 24, ozone mixing ratios kept on decreasing until day 31 (January 31) when the ship reached near 7°S. It

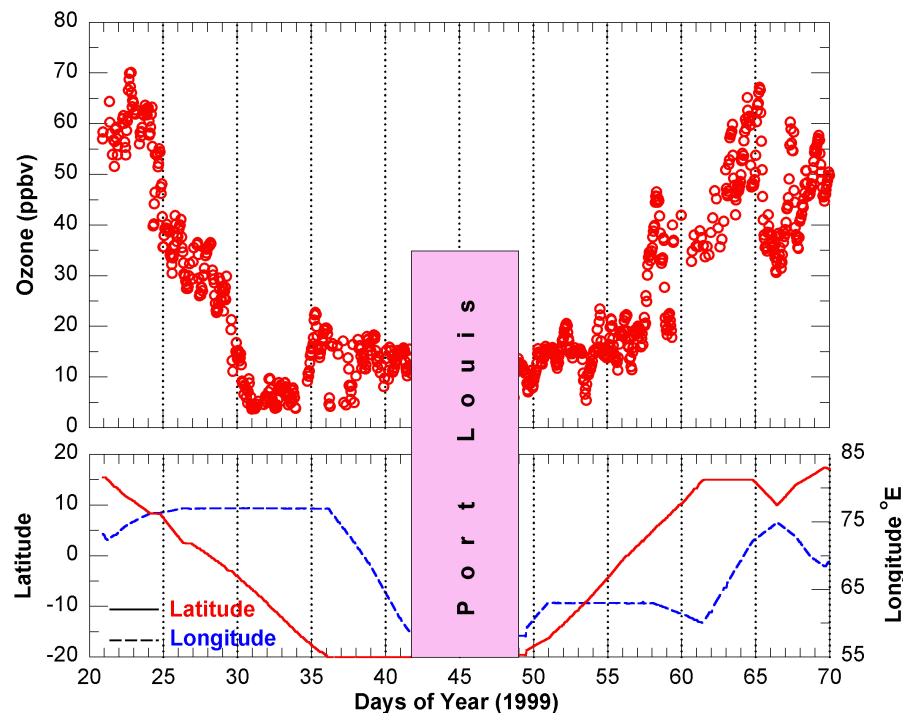


Figure 3.8 Same as Figure 3.5 except for INDOEX 1999.

encountered the ITCZ on days 30-31 and the lowest ozone levels of about 4-5 ppbv were observed in the same period. Aerosol optical depth and its loading are again observed to be lower in the ITCZ region during INDOEX 1999 [Jayaraman *et al.*, 2001; Parameswaran *et al.*, 2001]. This feature is similar to the observations during INDOEX 1998. Figures 3.9a and 3.9b show the surface streamlines for days 30 and 31 along with the position of the ship. It is clearly discernable from these figures that while on day 30, the air reaching the ship was coming from the Indian continent but on day 31 the air also started coming from southern Indian Ocean. The ozone levels increased dramatically on day 35 (February 4) from about 5 ppbv to about 20 ppbv and remained in the range of 10 to 15 ppbv when the ship was moving on the longitudinal transect until it reached Port Louis. This four fold increase in ozone from the minimum level of 5 ppbv to about 20 ppbv within 24 hours from day 34 (February 3) to day 35 (February 4) is due to sudden change in source of air from the ITCZ region to air

flowing from the southern Indian Ocean. The low levels of ozone during INDOEX 1999 in the ITCZ region again confirm the role of ITCZ as a sink of ozone over the Indian Ocean.

The ship reached Port Louis on day 42 (February 11) where it stayed till day 48 (February 17). The return leg started on day 49 (February 18) at around 0400 hrs local time. The ITCZ on this return leg was encountered between 6°S to 3°N during days 54 (February 23) to 56 (February 25) when the source of air changed from the southern Indian Ocean to the

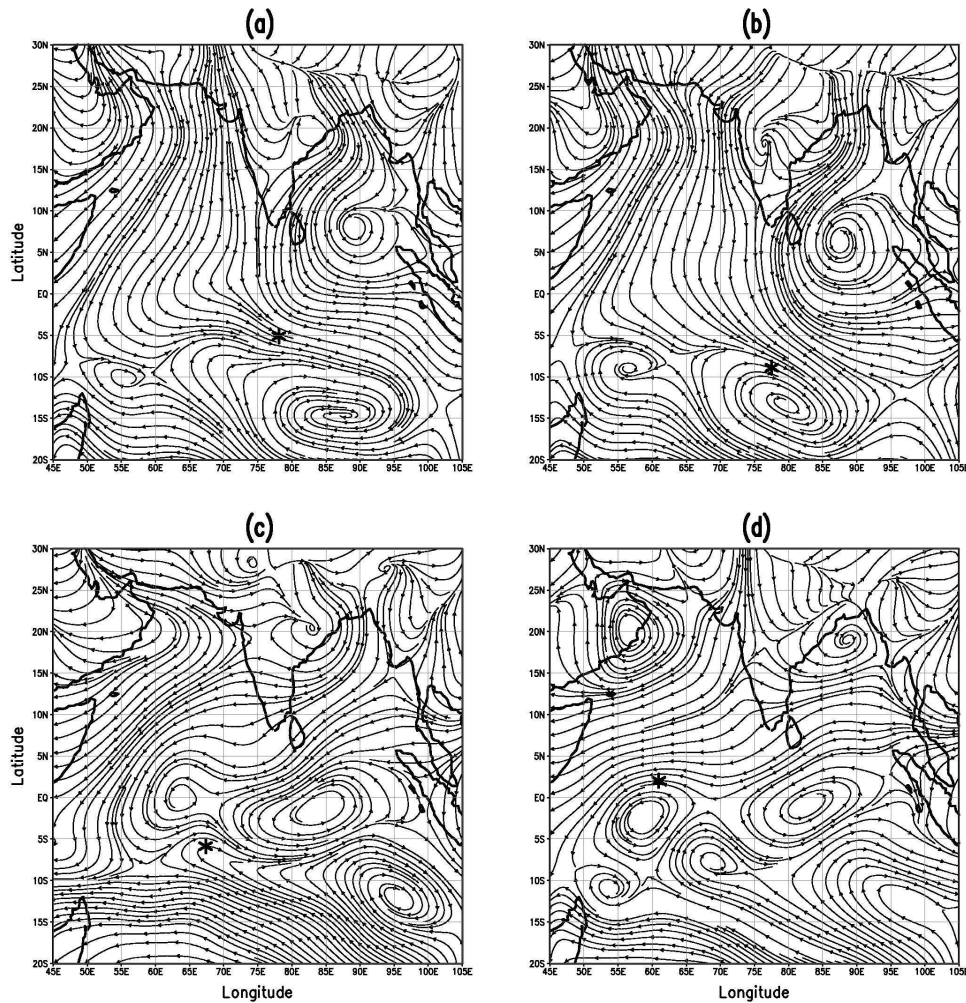


Figure 3.9 Same as Figure 3.6 except for INDOEX 1999 and (a) January 30, 1999 [day 30]; (b) January 31, 1999 [day 31]; (c) February 23, 1999 [day 54] and (d) February 25, 1999 [day 56].

northern Indian Ocean and the Bay of Bengal (*Figures 3.9c and 3.9d*). After coming out of the ITCZ, ozone increased to about 45 ppbv on day 58 (February 27) and further to about 67 ppbv on day 65 (March 6) when the ship approached the west Indian coast. These features of high levels of ozone near the Indian coast during INDOEX 1998 and INDOEX 1999 indicate that the coastal marine regions are much more affected by polluted continental air than the remote marine environments. On day 58 (February 27), the wind had passed from the polluted region around Mumbai and it reached the observational point in less than 4 days, as shown in the back trajectory (*Figure 3.10*). NCEP wind analysis indicates that the winds were

reaching the cruise track from the industrial regions of Gujarat during days 63-65 when the high ozone values were observed. Elevated ozone mixing ratios of 70-110 ppbv have been observed in the month of January in 2001 and also in 2002 near the northern coast (Khambhat, 22.2°N, 72.4°E, 5m) of the Arabian Sea in downwind of urban Gujarat. These elevated ozone levels over the coastal/rural areas could get transported over the Arabian Sea and the Indian Ocean as far as 3000 km from the source regions within 7 days [Chand *et al.*, 2002]. The decrease in ozone on days 66-67 (March 7-8) is due to the fact that the ship went away from

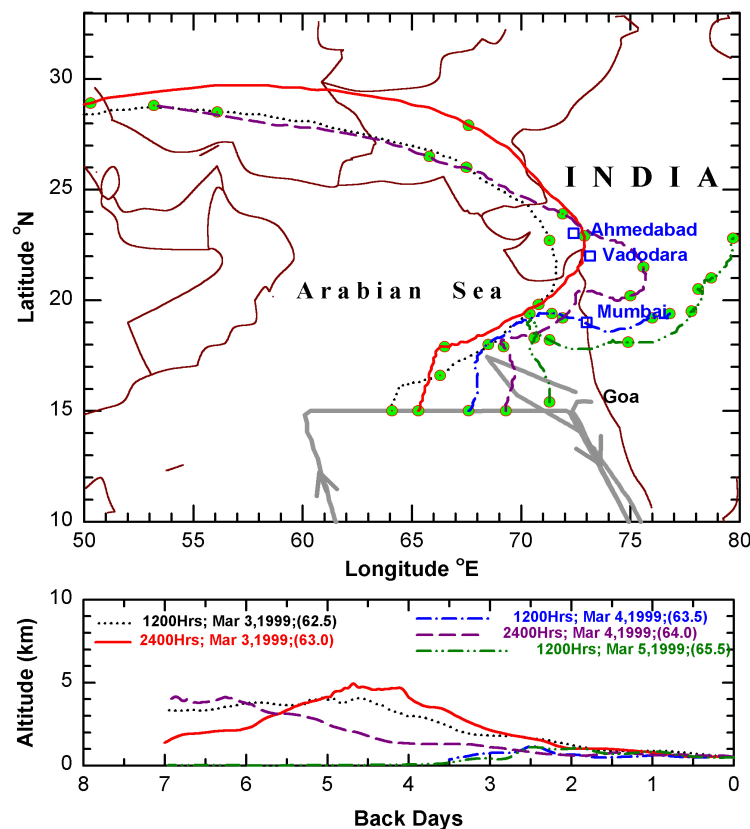


Figure 3.10 Three dimensional 7-days back trajectory of the air parcels transported from the continental region and arriving at the observation site on the mentioned dates and time during INDOEX 1999. The circles embedded on the lines are at each day interval. The squares represent the major cities of in western India.

source regions towards south from 15°N to 10°N to start an inter-comparison of the measurements on the two ships as mentioned earlier. The increase of ozone from about 30 ppbv to 55-60 ppbv from days 68-69 (March 9-10) to the next few days is due to the movement of the ship back from 10°N to 17°N. The lowest ozone levels observed in the MBL south of ITCZ during INDOEX 1998 and 1999 could be due to (i) loss of ozone on surface of cloud droplets in the convective active region of the ITCZ [Lelieveld and Crutzen, 1990; Kley *et al.*, 1996], and (ii) due to low concentration of NO (<15 pptv, not shown here), which leads to photochemical loss of ozone [Crutzen *et al.*, 1999].

3.4.3 Latitudinal variations in ozone during INDOEX 1998 and 1999

Figure 3.11 shows a latitudinal comparison of daily average ozone mixing ratios observed during INDOEX 1998 and INDOEX 1999 cruises. Ozone values are higher at north of 3°S with highest of 63 ppbv around 10°N during the onward leg of INDOEX 1999 compared to the corresponding ozone values during the return leg of INDOEX 1999 and both the legs of INDOEX 1998. These higher ozone levels, in general, are due to the transport of ozone rich air from the Indian region and the highest levels around 10°N are due to air coming from the downwind of urban regions of south India, as mentioned earlier in this section. However, ozone mixing ratios in the 15°S-5°S region are higher in the return leg than in the onward leg

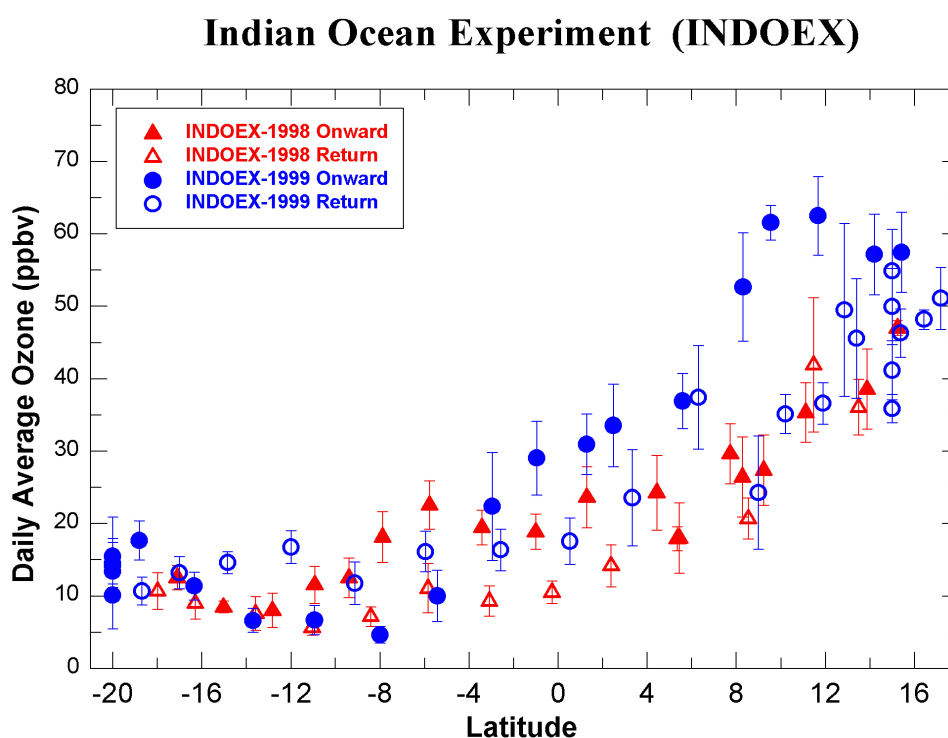


Figure 3.11 Latitudinal variations in O_3 during INDOEX 1998 and 1999 for onward and return journeys.

of INDOEX 1999. This could possibly be due to the return track being in the vicinity of the main African continent, Madagascar and other smaller islands. Minimum ozone is observed to be about 4-6 ppbv in the ITCZ region of the Indian Ocean during both the cruises. The observed ozone range (30-50 ppbv) at 5-15°N over the Arabian Sea/Indian Ocean during the INDOEX campaigns is much higher than the observed range (5-30 ppbv) at the same latitudes over the Pacific and the Atlantic Oceans [Routhier *et al.*, 1980; Piotrowicz *et al.*, 1986; Johnson *et al.*, 1990; Smit *et al.*, 1990 and Thompson *et al.*, 1993]. This indicates that

the Arabian Sea and the Indian Ocean are significantly affected by the anthropogenic activities from the surrounding regions.

Similar to the ozone variations, measurements of aerosols made on these cruises also show higher levels during INDOEX 1999 than during INDOEX 1998 [Jayaraman *et al.*, 2001; Moorthy *et al.*, 2001; Parameswaran *et al.*, 2001]. Higher levels of aerosols are also found by satellite observations as well as by model simulations over the Indian Ocean during INDOEX 1999 [Rajeev *et al.*, 2000; Rasch *et al.*, 2001]. In general, a direct correlation is seen in ozone and aerosols during INDOEX 1998 and 1999. Lal *et al.* [1998] have shown a positive correlation of ozone with CO and aerosols in an earlier study during INDOEX 1996. Here, it is inferred that higher levels of ozone as well as aerosols must have been transported from common anthropogenic source regions of the Indian sub-continent. The meteorological conditions were significantly different during INDOEX 1999 than in 1998 and might have, in part, contributed to ozone variabilities. It is observed that there were strong anti-cyclones and inversions over the Indian sub-continent during INDOEX 1999 as mentioned earlier. This kept the air pushing downward and thus the pollutants were trapped in the planetary boundary layer (PBL). The higher wind speed took the trapped pollutants from the PBL and spread them over the Arabian Sea and the Indian Ocean.

Figure 3.12 shows the latitudinal variation of average ozone observed during INDOEX 1998 and 1999 together at each degree. The latitudinal average is made up to 10°S, the mean position of ITCZ, where the lowest ozone was observed during both INDOEX 1998 and 1999 campaigns. It is assumed that ozone decreases exponentially when it gets transported from the source region of the Indian subcontinent towards the ITCZ. This decrease in ozone from the source region to the remote cleaner environments of the Indian Ocean is due to combination of mixing and photochemical loss in low NO_x environment. For this purpose, a simple exponential equation representing ozone loss as a function of distance from its northern region is proposed here,

$$O_3(D) = O_3(D_0) \text{Exp} \left(- \frac{D}{D_e} \right) \quad (3.1)$$

where $O_3(D)$ is the mixing ratio of ozone at a distance D , $O_3(D_0)$ is mixing ratio of ozone at $D=0$ (15°N) and D_e (e-fold distance) is the distance at which its concentration drops to $1/e$ of its original concentration (at 15°N). The corresponding time taken to transport over this distance is known as the e-fold time or lifetime of ozone. Here, only latitudinal data are used

for this study and it is assumed that the transport is mainly meridional from the Indian sub-continent to the Indian Ocean.

The exponential fitting of equation (3.1) in *Figure 3.12* is found to be very good ($r^2 = 0.98$) with an e-fold distance (D_e) of 1870 km. The average wind speed in the 15°N - 10°S latitudinal range for the INDOEX 1998 and 1999 campaigns is estimated to be $4.5 \pm 2.0 \text{ ms}^{-1}$. If this average wind speed of 4.5 ms^{-1} is used, the time taken to cover D_e distance is 4.8 days [Chand *et al.*, 2001b]. This is in good agreement with the estimated lifetime of ozone (less than a week) in the remote marine boundary layer [Liu *et al.*, 1983]. A very good exponential fit to these data indicates that ozone over the Indian Ocean is controlled by advection rather than entrainment. However, for aerosols an e-fold distance of 2700 km and an e-fold time of

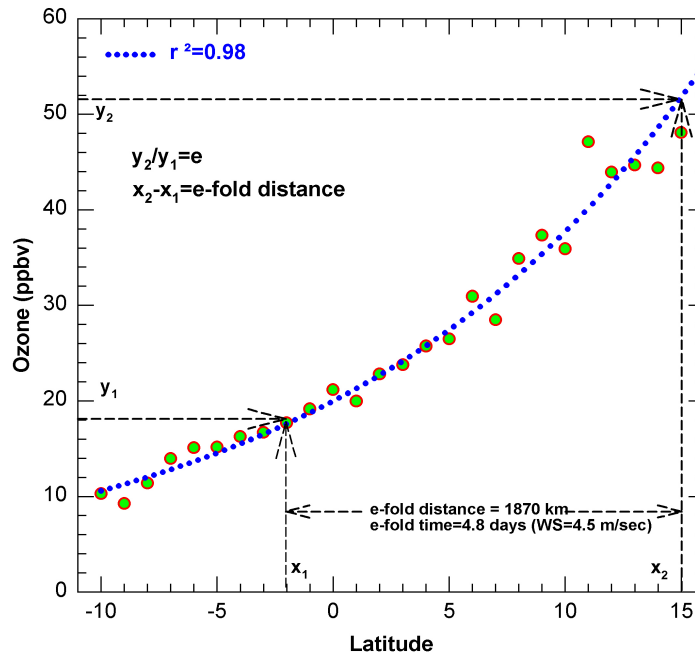


Figure 3.12 Mean ozone mixing ratios at each degree latitudinal bin averaged for INDOEX 1998 and 1999 for calculating its e-fold transportation distance and e-fold time over the Indian Ocean.

7 days are estimated over the Indian Ocean assuming this average wind speed [Satheesh *et al.*, 1998]. The lifetime of aerosols is also taken as 7 days in an aerosol assimilation over the Indian Ocean [Rasch *et al.*, 2001]. The lower e-fold distance for ozone compared to aerosols is due to the additional photochemical loss of ozone during the day in the marine environment assuming that ozone and aerosols get transported from the same source region of the continent and also other removal processes are same for aerosols and ozone. The common removal processes in ozone and aerosols are dilution or mixing of air and deposition. Since there are larger variations in ozone concentrations as well as winds, these derived parameters for ozone are of first order estimates only.

3.4.4 Latitudinal gradients in ozone during INDOEX 1998 and 1999

Gradients in ozone mixing ratios from north to south reflect how advection is transporting this gas away from its source. The observed gradients for the years 1998 and 1999 in 5° latitudinal bins from 10°N to 20°S are shown in *Figure 3.13* and are also given in *Table 3.2*. Gradients for the onward as well as for the return routes are estimated individually in the latitudinal bins for both the years using hourly averaged data. Positive values of the gradients

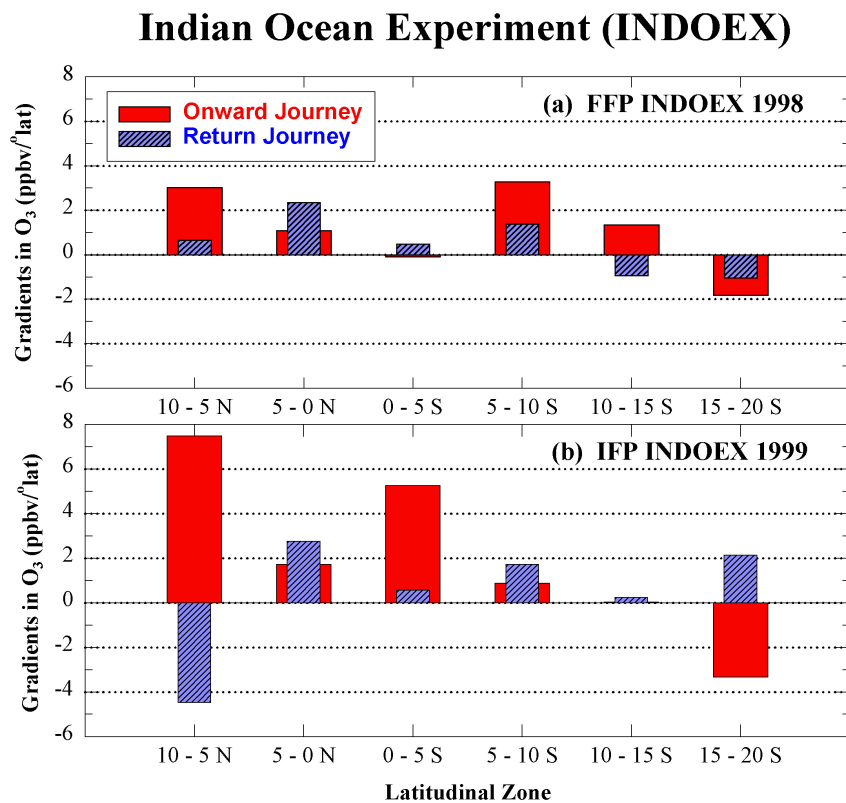


Figure 3.13 (a) A comparison of estimated gradients of ozone in 5° latitudinal bins for INDOEX 1998 over the Indian Ocean. Individual estimates were made for onward and return legs (b) same as (a) except for INDOEX 1999.

indicate decreasing mixing ratio when moving from the northern region to the southern region. This is generally an expected trend in ozone considering the northern region as more polluted than the southern region. However, opposite trends are also observed occasionally, which are shown by negative values. North of 10°N region is not considered due to presence of larger variabilities in ozone mixing ratios, which could be caused by changes in the wind pattern. In general, the observed gradients are higher during INDOEX 1999. The range in gradients during INDOEX 1998 is -1.8 to 3.3 ppbv lat⁻¹ whereas during 1999 the range is -4.5 to 7.5 ppbv lat⁻¹. Gradients are observed to be normal in the 10-5°N and 5-0°N regions during the onward journeys of both INDOEX cruises. Negative gradients are observed in the 15-20°S during both the cruises except during the return journey of INDOEX 1999.

In addition to the latitudinal transects, measurements of ozone have also been made in longitudinal transects during the INDOEX 1999 cruise at 20°S and 15°N. A substantial longitudinal gradient of 2.2 ppbv long⁻¹ with higher ozone level towards the Indian coast is observed at 15°N transect when the ship approached the Indian continent from 60°E to 72°E, as shown in *Figure 3.14b*. However, there is no significant longitudinal gradient (0.2 ppbv long⁻¹ only) at 20°S transect (*Figure 3.14a*). The recorded average ozone along the 20°S transect in the pristine Indian Ocean is 14.5 ± 3.5 ppbv. Similar low levels of ozone of about

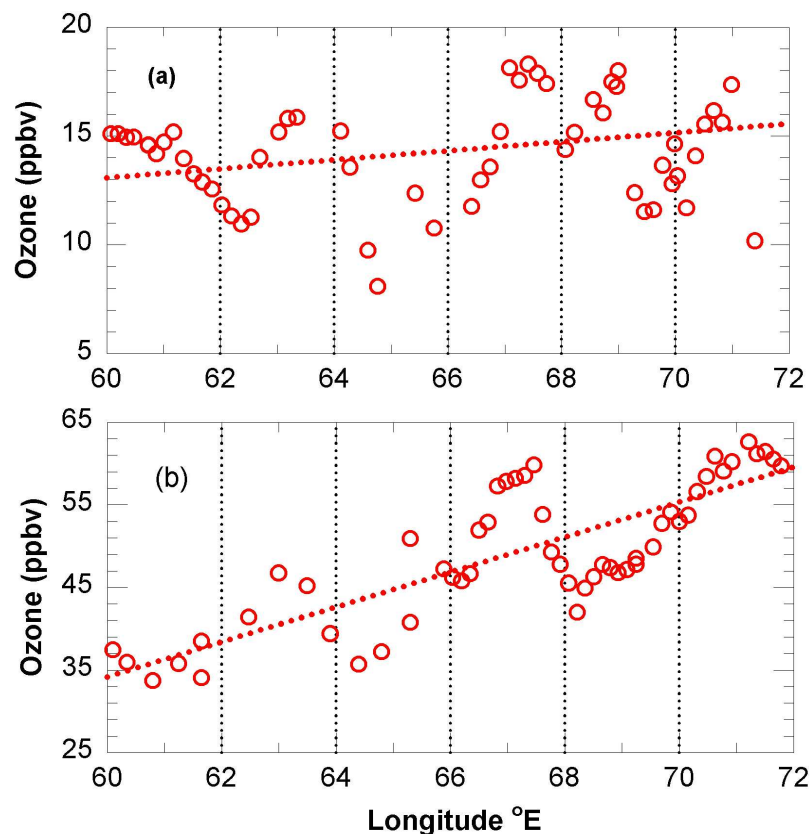


Figure 3.14 Latitudinal gradients in ozone (a) at 20°S longitudinal transect (b) on the 15°N longitudinal transects during INDOEX 1999.

15 ppbv were observed at 20°S during two different cruises in 1987 and 1995 over the Indian Ocean [Johnson *et al.*, 1990; Rhoads *et al.*, 1997]. Average surface ozone level at Reunion Island (21°S, 55°E) was also observed to be about 15 ppbv in the month of January during 1992-1997 [Taupin *et al.*, 1999]. In an extensive study of surface ozone at Amsterdam Island (37°S, 77°E) in the Indian Ocean during 1994-1996, Gros *et al.* [1998] observed ozone mixing ratio of about 14 ppbv in the months of January, February and March. Further, observations as well as model simulations show that ozone at Amsterdam island is least affected by biomass burning and other anthropogenic activities from Africa, Madagascar and other continents in this period. All these observations from island sites and ship cruises show that ozone levels over this region of the Indian Ocean is about 14 ppbv in the month of

January without much variability. This indicates that this region of Indian Ocean is free from anthropogenic perturbation during this period.

3.4.5 Diurnal variations in ozone during INDOEX 1998 and 1999

Surface ozone shows different types of diurnal variations in different environments. Observations of its diurnal variations can be used to study its photochemistry, role of transport and also in validating the photochemical models. The diurnal variations of ozone in the Indian Ocean marine boundary layer were observed and discussed in the earlier limited studies [Johnson *et al.*, 1990; Rhoads *et al.*, 1997; Lal *et al.*, 1998; Dickerson *et al.*, 1999]. The general feature of ozone mixing ratios in the MBL shows afternoon decrease and nighttime increase. The low daytime and high night time ozone levels over the oceanic region have been linked to many physical and chemical processes. These processes are as follow:

- (i) Chemistry of very low levels of NO [Liu *et al.*, 1983; Torres *et al.*, 1993; Thompson *et al.*, 1993; Ayers *et al.*, 1997].
- (ii) Loss of ozone due to HO_x and halogen chemistry in daytime [Vogt *et al.*, 1996; Dickerson *et al.*, 1999].
- (iii) Exchange between the ozone-rich free tropospheric air and ozone-poor boundary layer air, which dominates during night hours [Ayers *et al.*, 1997; Bremaud *et al.*, 1998].
- (iv) Recently, de Laat and Lelieveld [2000] have proposed a new theory based on the advection of the air parcel from source region to the remote marine environment.

The first two theories are based on the chemistry and the last two are based on the dynamics. Low levels of NO along with HO_x and halogen chemistry lead to daytime loss of ozone. On the other hand horizontal and vertical transport of air from source regions may lead to net ozone loss in daytime.

There have been several attempts to explain this diurnal variation using models incorporating chemistry [Kley *et al.*, 1996; Vogt *et al.*, 1996] and dynamical processes such as entrainment [Thompson and Lenschow, 1984; Bremaud *et al.*, 1998] and advection [de Laat and Lelieveld, 2000]. In daytime, major part of the ozone loss is due to its reaction with OH and HO₂ radicals in a cleaner environment. As it is well known that the only source of OH radical is photodissociation of ozone by UV radiation ($\lambda < 310$ nm) producing O(¹D) and its subsequent reaction with the water vapor [Duderstadt *et al.*, 1998]. One of the explanations

given for the nighttime increase is entrainment from the free troposphere [Thompson *et al.*, 1993; Bremaud *et al.*, 1998; Monks *et al.*, 2000; Suhre *et al.*, 2000]. However, Dickerson *et al.* [1999] could not explain the observed large amplitudes of diurnal variations up to 32% even by including Br chemistry in their model as suggested by Vogt *et al.* [1996] and Sander and Crutzen [1996]. But this additional chemistry could increase the amplitude up to 22%. de Laat and Lelieveld [2000] have tried to explain the diurnal variation in ozone over the oceanic region by photochemistry and advection and comparing mostly with our earlier limited observations from INDOEX 1996 reported in Lal *et al.* [1998]. Extensive measurements related to diurnal patterns and changes in their amplitudes for a larger range of latitude over the Arabian Sea and the Indian Ocean during INDOEX 1998 and INDOEX 1999 are presented here.

Figures 3.15 and 3.16 show diurnal patterns in ozone during INDOEX 1998 and 1999

FFP INDOEX 1998

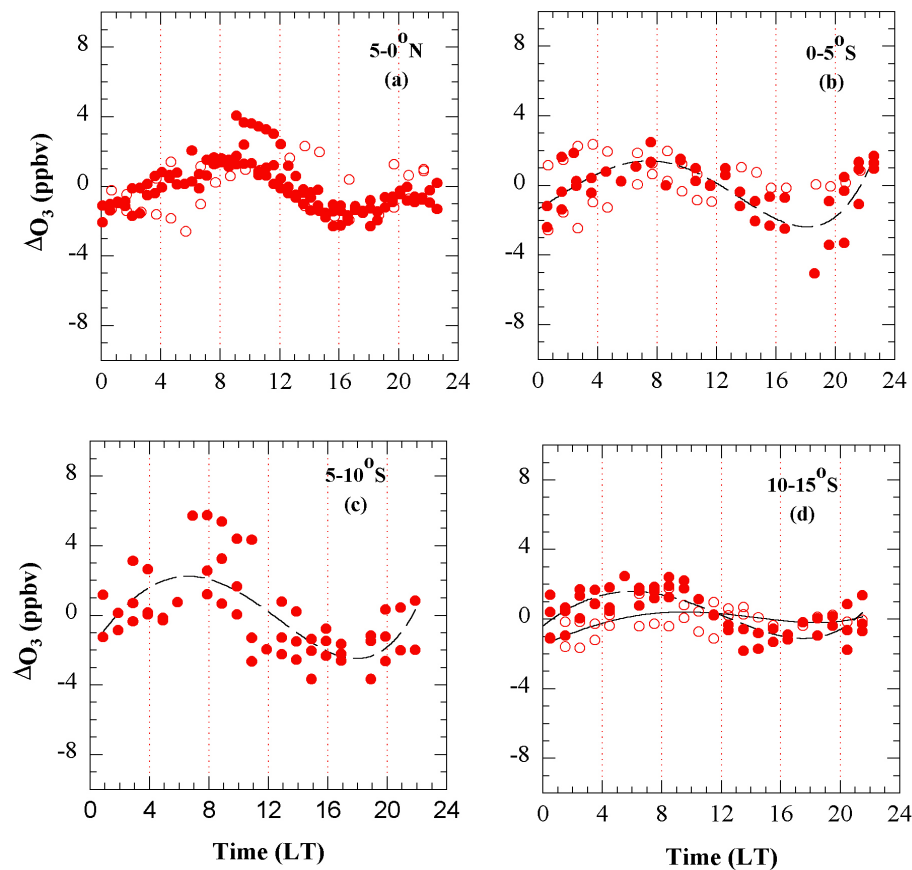


Figure 3.15 Amplitudes of diurnal variations in ozone (ΔO_3) representing (a) $5-0^\circ N$, (b) $0-5^\circ S$, (c) $5-10^\circ S$ and (d) $10-15^\circ S$ latitudinal regions during INDOEX 1998 at local time (LT). The solid symbols are for the onward journey whereas the open symbols are for the return journey of the cruise. Lines are the best fit to the diurnal variations.

respectively. Daily gradients in ozone are removed for individual days and then the data in each 5° latitudinal bins are used for calculating the diurnal variations (see Table 3.2).

Generally, diurnal patterns in ozone are not very clear near the coastal regions due to large variability within a day itself. Therefore, the data only south of 5°N have been chosen for this analysis. Henceforth, the diurnal variations and amplitudes will be considered in percentage of their mean ozone levels unless other units are specified.

During INDOEX 1998 the diurnal patterns are generally clearer and the amplitudes are almost double in onward journey than in the return journey (see *Table 3.2*). Higher wind speeds during onward journey have led to higher ozone levels, its gradients and amplitudes of

IFP INDOEX 1999

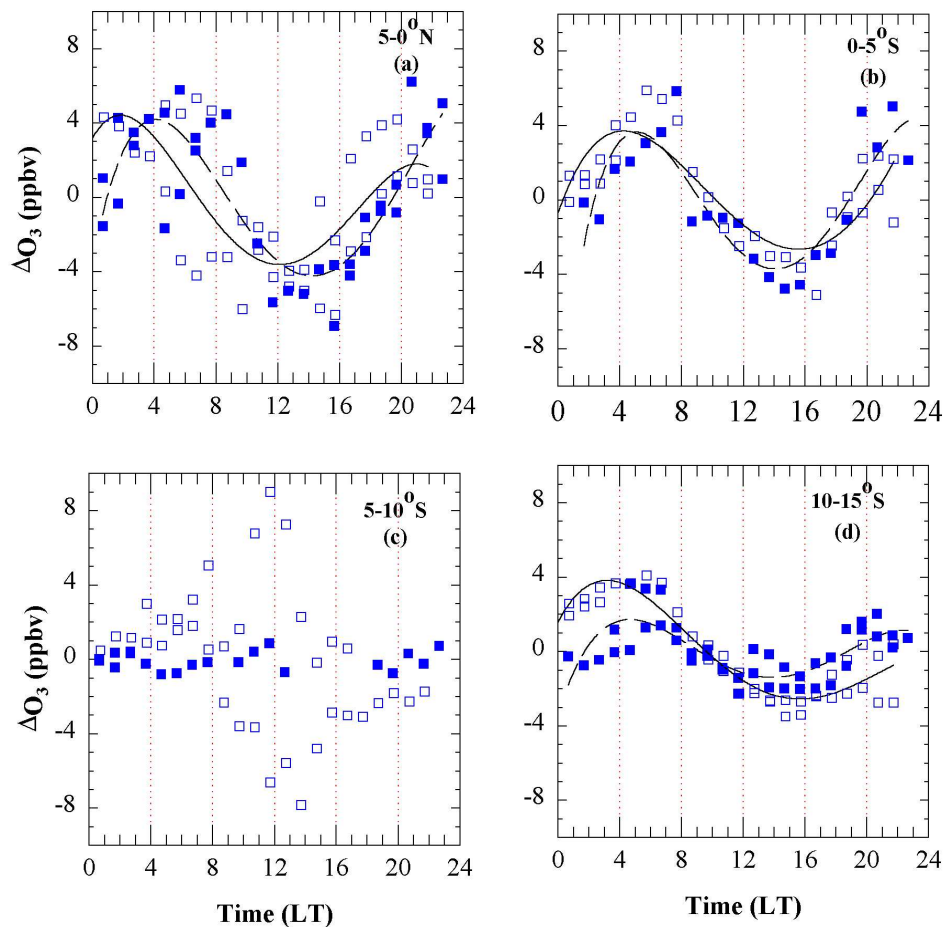


Figure 3.16 Same as figure 3.15 except for INDOEX 1999.

diurnal variations by transporting the pollutants faster. In the 5-0°N latitudinal belt, diurnal patterns are observed with relatively higher ozone levels in the morning hours (*Figure 3.15a*). The features are not so clear during the return route in the same latitudinal region. Diurnal patterns in ozone are observed to be of marine type with decrease in ozone during afternoon (amplitude of about 1.5 ppbv) in the 0-5°S belt. This pattern is relatively clearer again in the onward route (*Figure 3.15b*). The highest diurnal variation is observed to be 17% in the 10-15°S region during onward journey (*Figure 3.15d* and *Table 3.2*). During INDOEX 1999, the patterns of diurnal variations are of similar type but the amplitudes show large variability

from 7-54%. *Figures 3.16a and 3.16d* show highest diurnal variations of 54% and 21% occurring at 5-0°N and 10-15°S respectively during onward and return journey of INDOEX 1999. The range in amplitudes of diurnal variations is 6-17% during INDOEX 1998 where as it is 7-54% during INDOEX 1999 (*Figures 3.16a-3.16d*). *Figure 3.17a and 3.17b* shows the diurnal variations of 14% and 13% at 20°S and 15°N longitudinal transects respectively. There is large difference in sigma O₃ (ΔO_3) but the differences in diurnal variation are very less at these transects.

The amplitudes of diurnal variations are higher in INDOEX 1999 than in INDOEX 1998 as shown in *Table 3.2*. Like the latitudinal gradients, the maximum diurnal amplitude

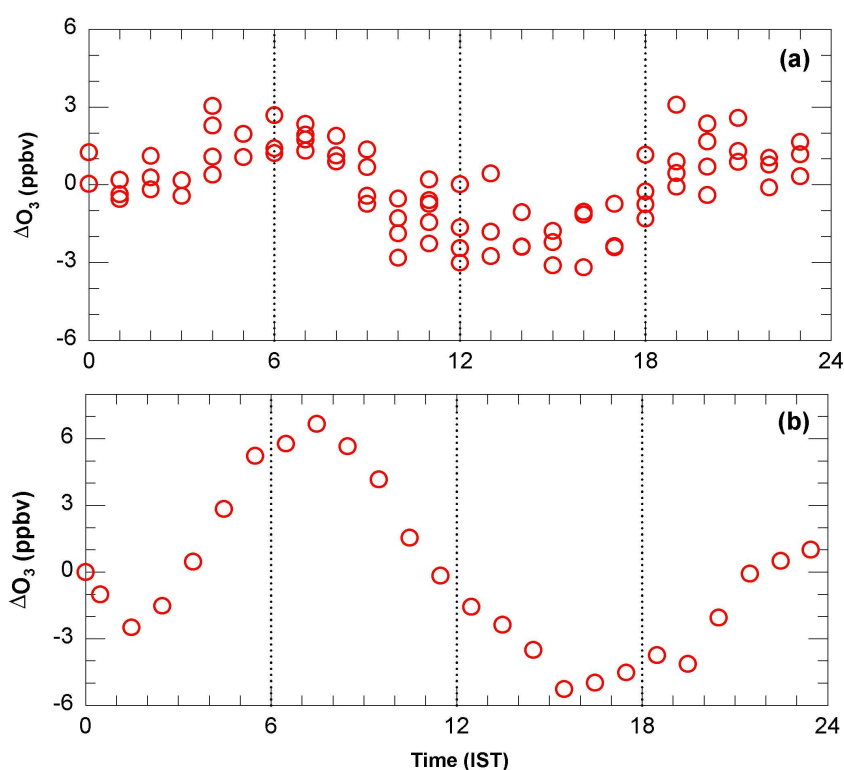


Figure 3.17 Amplitudes of diurnal variations in ozone (ΔO_3) (a) at 20°S longitudinal transect during INDOEX 1999. (b) on the 15°N longitudinal transect

during INDOEX 1999 is almost two times higher than in INDOEX 1998. But variabilities in ozone are very less during INDOEX 1998 compared to INDOEX 1999.

de Laat and Lelieveld [2000] suggested that the diurnal variations in the MBL are most pronounced in the downwind of O₃ sources and the nighttime increase is due to advection rather than entrainment. Further, they suggested that higher latitudinal gradients could result in higher amplitude of diurnal variation.

Table 3.2. Summary of average ozone mixing ratios, amplitude of its diurnal variations (ΔO_3), % of diurnal variations wrt its mean mixing ratio, latitudinal gradients and wind speed averaged at each 5 degree latitudinal bins along with 1σ values during onward and return journeys of INDOEX 1998 and 1999 cruises over the Indian Ocean.

Latitude	Average Wind Speed (ms^{-1})		Average Ozone (ppbv)		Average Gradient in Ozone (ppbv lat^{-1})		Diurnal Amplitude of Ozone (ΔO_3 (ppbv))		% ΔO_3 wrt. Average Ozone $\frac{1}{O_3} \Delta O_3 \times 100$		
	Onward	Return	Onward	Return	Onward	Return	Onward	Return	Onward	Return	
INDOEX 1998											
5° Interval											
10-05 °N	2.9±1.8	2.38±1.1	27.2±5.2	19.4±2.0	3.0	0.7	---	---	---	---	---
05-00 °N	3.6±1.8	2.9±1.8	18.8±4.8	14.9±3.4	1.1	2.3	1.5	---	8	---	---
00-05 °S	5.9±1.9	3.9±2.4	17.6±1.9	10.9±1.5	-0.1	0.5	1.5	---	9	---	---
05-10 °S	6.7±1.6	4.4±2.6	19.5±4.6	8.2±2.7	3.3	1.4	2.3	0.5	12	6	6
10-15 °S	5.8±2.6	2.8±1.9	10.1±2.7	7.4±1.7	1.3	-0.9	1.7	0.5	17	7	7
15-20 °S	4.2±2.4	7.9±1.9	11.9±2.5	11.5±1.6	-1.8	-1.0	---	---	---	---	---
INDOEX 1999											
10-05 °N	4.3±2.4	4.8±1.1	46.6±10.6	33.8±9.8	7.5	-4.5	---	---	---	---	---
05-00 °N	5.3±1.4	3.6±2.0	30.4±4.5	21.8±6.9	1.7	2.7	4.3	4.0	14	18	18
00-05 °S	6.3±2.0	3.6±0.8	23.8±7.0	17.9±2.8	5.3	0.6	3.7	3.7	16	21	21
05-10 °S	6.7±1.9	4.4±1.1	6.2±2.1	14.4±3.9	0.9	1.7	---	---	---	---	---
10-15 °S	5.6±1.4	6.5±1.0	6.7±2.2	15.4±2.2	~0	0.2	3.6	2.0	54	13	13
15-20 °S	10.3±1.9	7.6±1.8	16.3±4.1	14.4±2.7	-3.3	2.1	3.0	1.0	18	7	7

However, diurnal pattern in ozone during present extensive measurements, particularly where gradients are very low or even reverse (negative) (like at south of the ITCZ region where the wind generally comes from the southern Indian Ocean) indicate that the advection theory of diurnal variation is not sufficient to explain these variations. The diurnal variations with afternoon low values and nighttime and morning higher values are observed even south of 10-15°S (see *Figures 3.15* and *3.16*) where there is almost no latitudinal gradient during both onward as well as return journeys of INDOEX 1999. Similarly, pronounced diurnal variations in ozone are observed at the 20°S longitudinal transect without any longitudinal gradient. *Figures 3.15* and *3.16* show clear diurnal variations in ozone near the ITCZ region, where advection is supposed to be minimum. Also, there is no one to one correlation between gradients in ozone, wind speed and amplitudes of diurnal variation. These observations suggest that the advection theory cannot fully explain the diurnal variations in ozone over the marine environment of the Indian Ocean. It has been also found that the 7-days back trajectories are often descending from above the MBL indicating that the entrainment from the free troposphere cannot be ruled out [e.g. *Thompson and Lenschow* 1984; *Thompson et al.*, 1993; *Ayers et al.*, 1997; *Bremaud et al.*, 1998; *Monks et al.*, 2000].

3.5 Diurnal variations in nitric oxide (NO)

Figure 3.18 shows typical NO diurnal variation in the 0-5°S latitudinal region during INDOEX 1998. NO levels increase during daytime from the nighttime levels of about 12 pptv, peaking during noontime (about 28 pptv) and then decrease. The nighttime NO levels are assumed as background and are subtracted from the daytime NO levels to get its net diurnal variation. Similar low levels of NO are also observed during INDOEX 1999 (*Figure 3.19*). The observed amplitudes of diurnal variations in the remote Indian Ocean are in the range of about 5-20 pptv during both INDOEX 1998 and 1999 cruises. During the daytime NO is produced by the photodissociation of NO₂. Very few observations made over the Pacific and Atlantic Oceans show similar diurnal variations in NO from 5 to 15 pptv [*Thompson et al.*, 1993; *Torres et al.*, 1993]. The observed diurnal variation in NO over the Indian Ocean differs from a continental site where NO levels are low during the day and higher during the morning and evening hours due to local emission [*Lal et al.*, 2000]. In the remote marine boundary layer, NO concentrations are generally found to be lower so that the reaction 1.9 (see *Chapter 1*) dominates over the reaction (1.5) and loss of ozone takes place [*Crutzen et al.*, 1999; *Chameides et al.*, 1992]

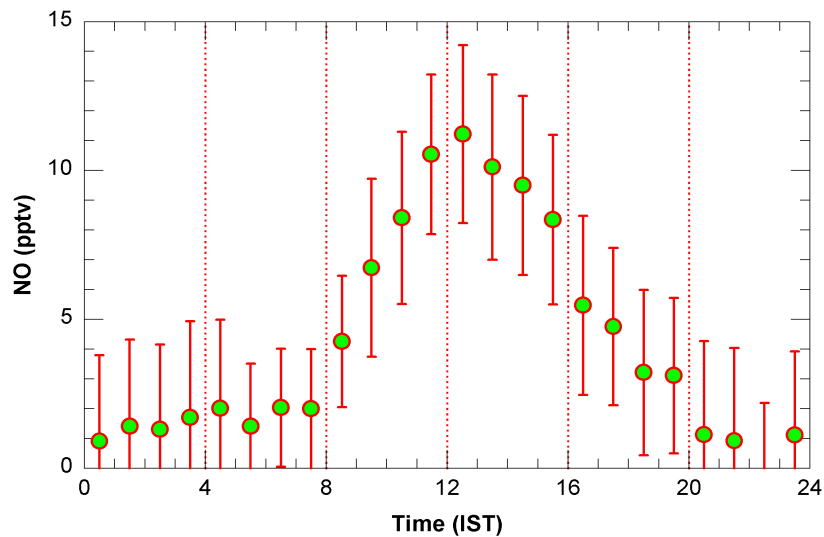


Figure 3.18 Hourly average diurnal variation of NO in the 0-5°S region during INDOEX 1998.

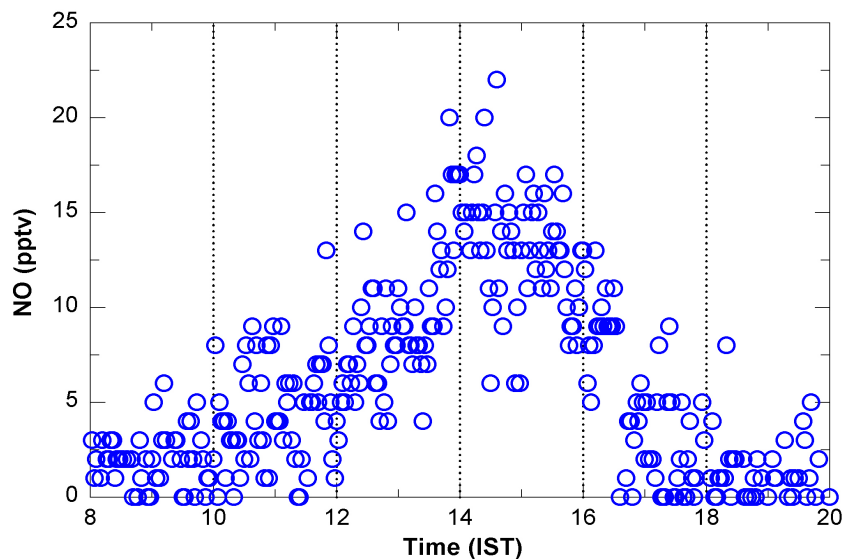


Figure 3.19 A typical diurnal variation of NO in remote Indian Ocean on February 4, 1999 near 18°S during INDOEX 1999.

3.6 Variations in carbon monoxide (CO)

The daily average carbon monoxide (CO) measured during the INDOEX 1999 cruise is shown in *Figure 3.20* along with results of the INDOEX 1998 for a comparison. Highest CO concentrations (about 300 ppbv) are observed in the 8-12°N during the onward journey. There is a gradual decrease in its mixing ratios towards the south. The CO variations are significantly affected by the presence of local source (islands etc.) and by changing meteorology. Winds can transport CO up to thousands of km since the lifetime of CO is much more than its horizontal transportation time. At Port Louis, CO concentration is observed in the range of 60-100 ppbv. There is no clear difference in the CO mixing ratios

during the two legs except north of 8°N, i.e. near the Indian continent and this could be due to longer lifetime (~ 2 -3 months) of CO than that of ozone. However, in the vicinity of the Indian continent, the differences in CO mixing ratios in the two legs are similar to those in ozone. The combined average latitudinal gradient for INDOEX 1998 and 1999 is about 3 ppbv °lat⁻¹. As observed during the previous cruises, there was a good correlation ($r^2 = 0.69$) of ozone with CO during INDOEX 1996 [Lal *et al.*, 1998]. However, in the clean region of the Indian Ocean where NO values are very low, ozone does not increase even if CO increases. Measurements made by Rhoads *et al.* [1997] during the 1995 ship cruise over the Indian ocean from Africa to Sri Lanka, revealed CO concentration of about 140 ppbv near

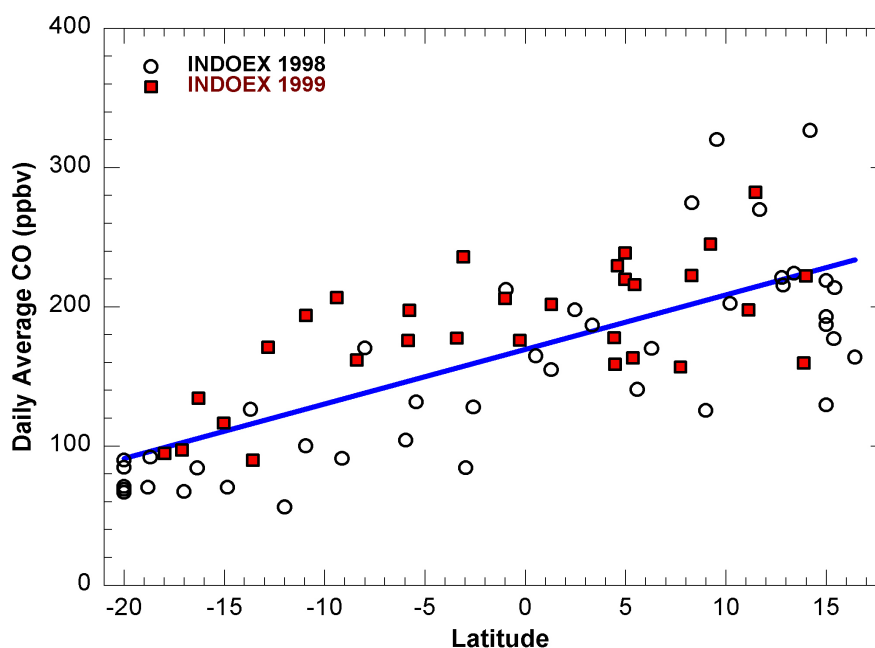


Figure 3.20 Latitudinal variation of daily average CO during the INDOEX 1998 and 1999 cruises. Line represents the average latitudinal gradient in CO for both the campaigns.

6°N which decreased to about 50 ppbv near 33°S. There are no systematic differences in CO mixing ratios observed in INDOEX 1999 and INDOEX 1998 cruises. Also the CO levels observed in winter during INDOEX 1998 and 1999 are higher than the other measurements made in spring to monsoon transition in 1995 [Rhoads *et al.*, 1997; de Laat *et al.*, 2000]

Positive correlations in O₃ and CO have been found in a set of data of near coastal region. Figures 3.21 and 3.22 show correlation plots between O₃ and CO during INDOEX 1998. These data are divided in three groups viz 15-5°N, 5°N-5°S and 5-20°S. When moving away from the source region, concentrations of O₃ and CO decrease due to dilution and loss by chemistry. Nonetheless, the loss due to chemistry is much more in ozone than CO. Thus the gradients in O₃ and CO vary with latitude. The slopes in O₃ and CO between the three regions during INDOEX 1998 are 0.07, 0.01 and 0.03 whereas during INDOEX 1999 are

0.09, 0.04 and are -0.07 respectively. However, the correlation coefficient r^2 is not very good. Large scattering in correlations of O_3 and CO and less correlation slope between these gases indicate that O_3 is not completely formed by CO oxidation. The region between 15°N is nearer to the source of the gases and shows high levels of CO and O_3 with a positive correlation between the two gases. Due to relatively shorter lifetime of O_3 than CO, the other two regions show lower ozone with almost nil or negative correlation between the two gases. Positive correlation between CO and O_3 indicates that both O_3 and CO have common continental sources and are transported from there in time scale shorter than the lifetime of ozone. Due to close proximity of the source regions, the variations in the two gases are

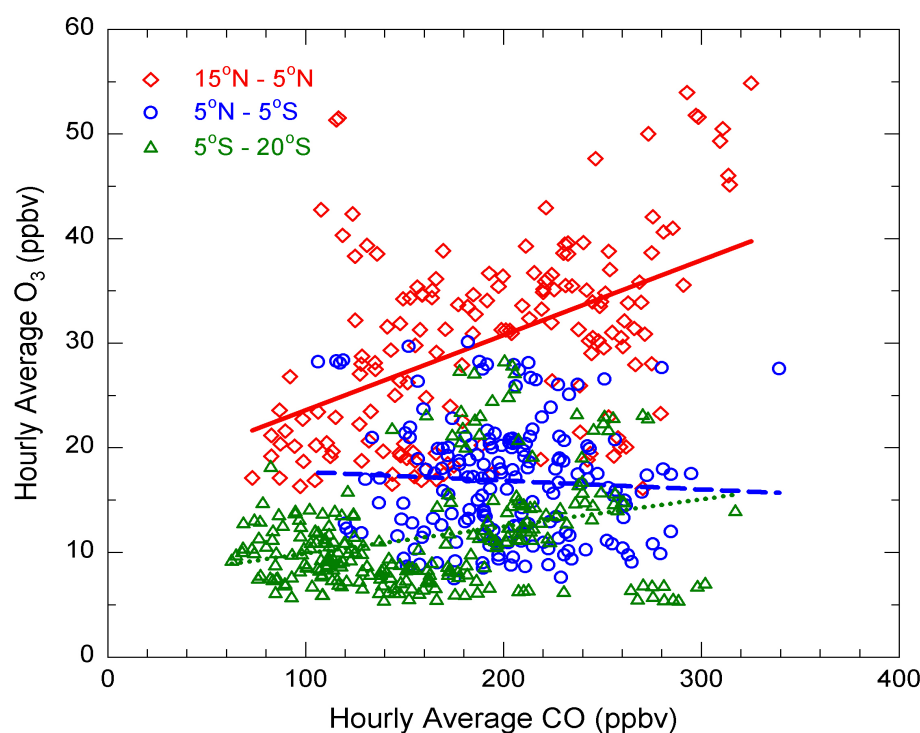


Figure 3.21 Scattered plot between O_3 and CO in three different marine regions during INDOEX 1998. Lines are least square fits for 15°N (continuous line), 5°N - 5°S (dashed line) and 5°S - 20°S (dotted line) latitudinal regions.

almost similar in the 15°N - 5°N during INDOEX 1998 and 1999. However, CO and O_3 show some differences in variation during INDOEX 1999 than INDOEX 1998 in 5°N - 5°S and 5°S - 20°S . These differences are possibly due to different meteorological conditions, higher wind speed, higher descent velocity and different position of ITCZ during INDOEX 1999, as mentioned in the earlier section. The negative correlation ratio in O_3 and CO south of ITCZ is due to opposite gradients between these gases.

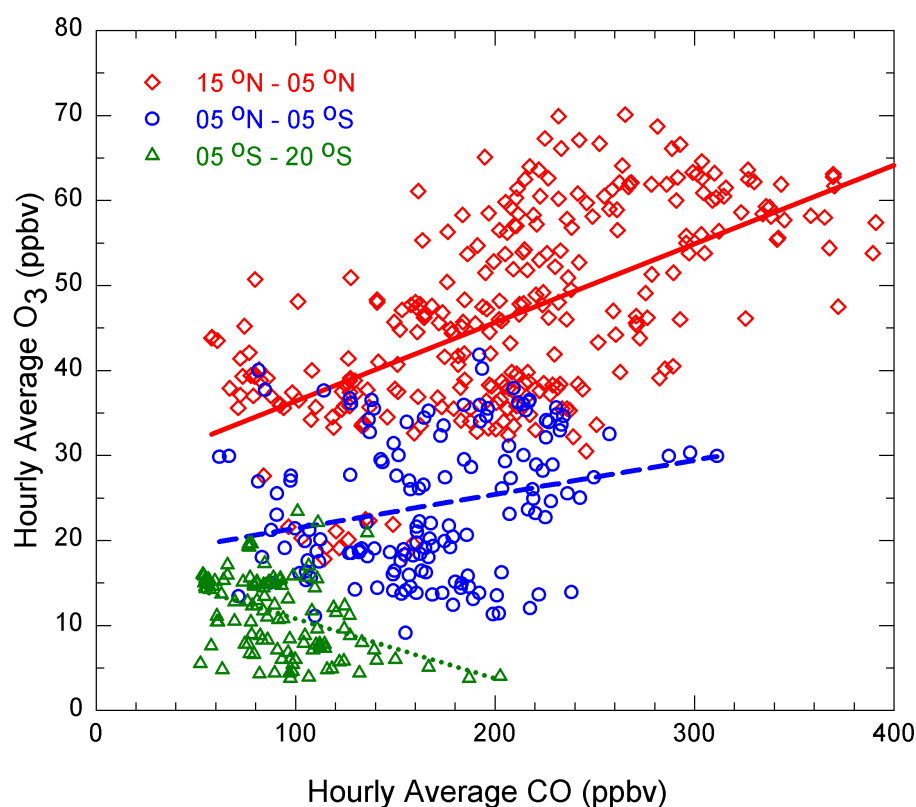


Figure 3.22 Same as Figure 3.21 except for INDOEX 1999.

3.7 Variations in methane (CH_4)

The latitudinal distributions of methane mixing ratios obtained from the air samples collected during INDOEX 1998 and INDOEX 1999 are shown in Figure 3.23. Its mixing ratio decreases from an average value of about 1.8 ppmv near the Indian coast to about 1.6 ppmv at 20°S. There is a scatter of about ± 0.1 ppmv about the mean values in all the data during both the legs. The gradient is observed to be smaller for this gas in comparison to the short lived trace gases like NO , O_3 and CO . Near the coastal region of Goa, CH_4 is observed to be higher during INDOEX 1998, compared to the INDOEX 1999. The latitude gradients observed during INDOEX 1998 and 1999 are 4.2 ppbv and 2.3 ppbv/lat respectively. The combined latitudinal gradient for both the cruises is 3.3 ppbv/lat. There is no appreciable difference in the average mixing ratios during the two years (Figure 3.23). The lower gradients and less difference in the mean concentrations of methane during INDOEX 1998 and 1999 indicate that the growth rate of methane is very low and it is trying to redistribute uniformly in the two hemispheres. Lower or almost no growth rate of CH_4 in the recent past has been a point of discussion [WMO, 1999; IPCC, 2001].

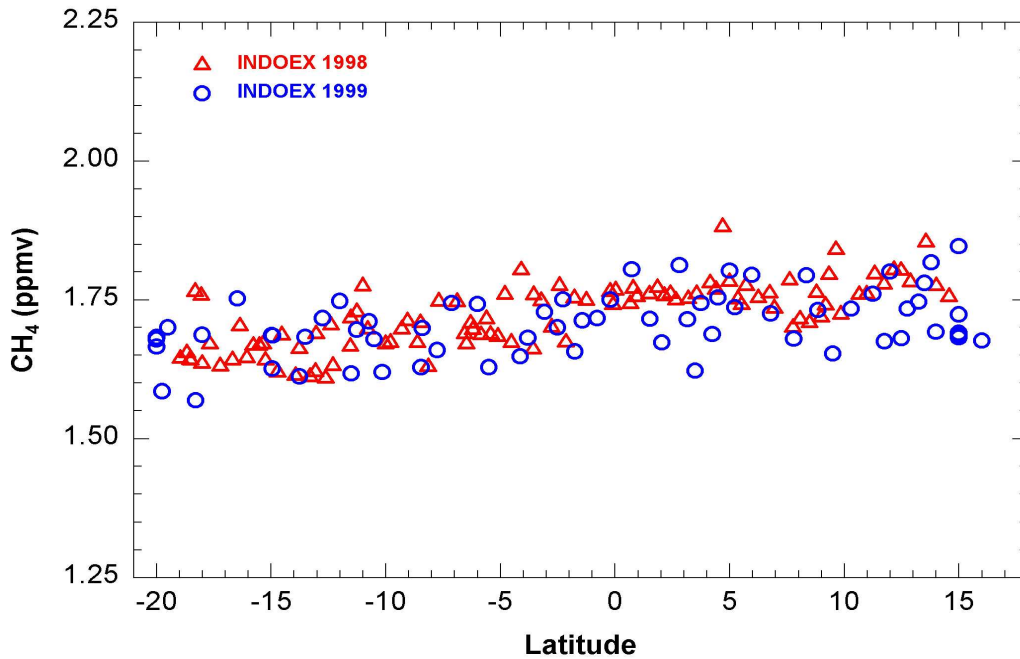


Figure 3.23 Latitudinal variation of CH_4 during the INDOEX 1998 and 1999 cruises.

3.8 Variations in sulfur hexafluoride (SF_6)

Sulfur hexafluoride (SF_6) is an extremely stable gas that has received considerable attention recently. Its unique physical and chemical properties make this gas ideally suited for many applications, predominantly in electrical insulation and switching. Due to its growing industrial production and long lifetime (2000 - 3000 years) SF_6 is rapidly accumulating in the atmosphere [Ravishankara *et al.*, 1993; Patra *et al.*, 1997]. The sink of SF_6 is mainly above the upper stratosphere. Atmospheric SF_6 concentration has increased by two orders of magnitude since 1970 [Maiss *et al.*, 1996; Maiss and Brenninkmeijer, 1998]. Though SF_6 is one of the strongest greenhouse gases, with its low ambient mixing ratio, its effect in climate forcing is insignificant at present [Ko *et al.*, 1993]. Greater stability and high growth rate make SF_6 a valuable atmospheric tracer.

Figure 3.24 shows a comparison of SF_6 measurements made during the INDOEX 1998 and 1999 with measurements made in the Pacific and Atlantic Oceans in January 1994 and October 1994 [Geller *et al.*, 1997]. Latter measurements are presented here only for the latitude range covered by the INDOEX cruises. SF_6 mixing ratios of about 4.4 pptv are observed in the northern region and relatively lower values in the southern region. However, the lowest levels (~ 3.9 pptv) are observed in the 5-15°S latitude region. SF_6 mixing ratios increased slightly near the Port Louis during the onward leg. There is a positive gradient from south to north like in other gases. The average gradient during INDOEX 1998 and 1999 are 6.99×10^{-3} and 8.96×10^{-3} pptv/lat⁻¹ respectively. The average latitudinal gradients of

SF_6 measured during the two INDOEX cruises is 8.33×10^{-3} pptv/lat⁻¹. The higher slope during INDOEX 1999 than in 1998 may be due to stronger wind fields during 1999 than in 1998 and/or increasing growth rate in SF_6 . The scatter in the mixing ratios is observed both during onward as well as during return journeys. However, the spread is beyond the measurement errors. Higher mixing ratios in the northern region have been observed in the earlier cruise data also. This is due to its dominant source in the northern hemisphere. Even though, the lifetime of SF_6 is much higher, the latitudinal gradient is mainly caused by the

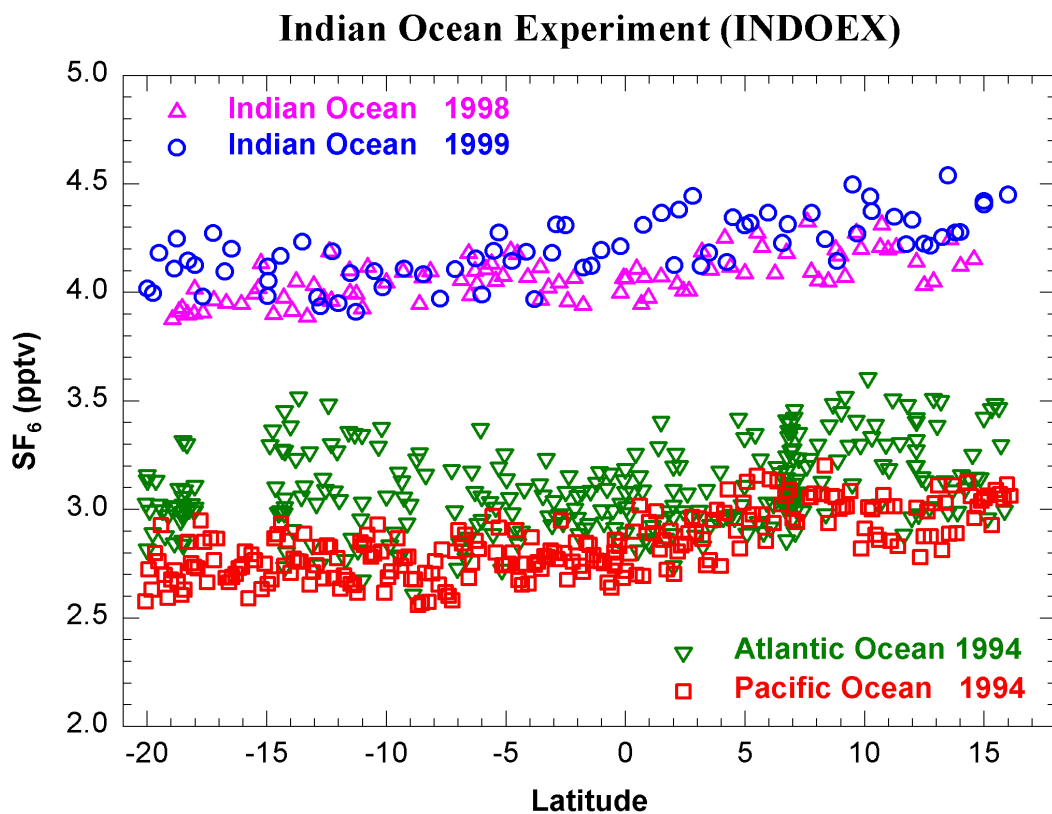


Figure 3.24 Latitudinal variation of SF_6 during INDOEX 1998 and INDOEX 1999 cruises compared with measurements from the Pacific Ocean and Atlantic Ocean cruises taken from Geller et al. [1997].

anthropogenic sources in the northern hemisphere with its high growth rate.

These observations show an increase in SF_6 mixing ratios from INDOEX 1998 to INDOEX 1999 by about $4\% \text{ yr}^{-1}$. However, there is small scale latitudinal variability in the SF_6 levels in both the years. Using the observations made in the Pacific Ocean and the INDOEX 1999 data, a linear growth rate of about $9\% \text{ yr}^{-1}$ is inferred during 1994-1999 period. The average global growth rate in SF_6 is reported to be $6.9\% \text{ yr}^{-1}$ [WMO, 1998; Levin and Hesshaimer, 1996; Maiss et al., 1996]. The INDOEX data show a slower growth rate. During winter the wind carried the air plume from Indian subcontinent to the surrounding marine environments. In this season the observed growth rate of SF_6 over the surrounding

marine environments represents the growth rate over the Indian subcontinent. These observations suggest that the growth of SF₆ over the Indian subcontinent is lower than the global growth rate.

Mixing of a trace gas between the two hemispheres depends on inter-hemispheric exchange time [Jacob *et al.*, 1987]. The inter-hemispheric exchange time varies with the season and further depends on the position of the ITCZ. The ITCZ oscillates with a time period of one year due to the earth's tilt on its axis and its orbital motion around the sun. Surface wind fields analysis given by Jha and Krishnamurty [1998, 1999] indicate that the ITCZ had moved from 5°S to 1°S, during INDOEX 1999, as shown in Figure 3.3. Due to this movement of ITCZ, the extent of transportation of pollutants from NH to SH during onward journey is relatively more than that during the return journey. Similar effect is observed on the other trace gases also.

Inter-hemispheric exchange time (τ_{ex}) is a very important parameter for models to characterize the global atmospheric transport. τ_{ex} expresses the strength of the ITCZ acting as a major resistance of air mass exchange between the two hemispheres [Bolin and Rodhe, 1973; Singh *et al.*, 1977]. The present measurements of SF₆ over the Indian Ocean are used to estimate τ_{ex} . The region of measurements is divided into two parts 0-15°N and 0-15°S. The following equation based on the two-box model of Singh *et al.*, [1977] is used to calculate τ_{ex} , as:

$$\tau_{ex} = \frac{\frac{C_{NH}}{C_{SH}} - 1}{b + \frac{1}{\tau_s}} \quad (3.2)$$

Where C_{NH} , and C_{SH} are the average mixing ratios of SF₆ in the NH and the SH respectively, τ_s is the SF₆ atmospheric residence time which is taken as 2000 - 3000 years [Ravishankara *et al.*, 1993; Patra *et al.*, 1997] and b is its growth rate. Using the INDOEX 1999 and 1998 cruises data and taking b as computed, 4% yr⁻¹, an inter-hemispheric exchange time (HET) of 1.5±0.1 year is calculated. The spatial coverage of these measurements in the NH and SH is limited in the tropics, and hence this result of HET is of rough estimate only. Jacob *et al.* [1987], Levin and Hesshaimer [1996] and Maiss *et al.* [1996] calculated τ_{ex} values of 1.7 years, 1.5 years and 1.3 years respectively using the global data sets. These results show that the inter-hemispheric exchange time over the Indian Ocean is in the range of the average global exchange time [Chand *et al.*, 2001a].

Chapter 4

Ozone and other trace gases over the Bay of Bengal

India has densely populated and industrial areas in its east and west sides. The prevailing winds in winter months can transport the pollutants from these areas to the surrounding marine environments of the Arabian Sea (AS), Bay of Bengal (BOB) and Indian Ocean (IO). The highly populated and industrial areas adjoining the marine environments of the Indian sub continent in eastern flank (Kolkata, Dhaka) are affecting the composition and chemistry of the atmosphere over BOB whereas the western flank (Karanchi, Ahmedabad, Vadodara, Surat, Mumbai,) is influencing the AS region. The downwind areas of these rapidly developing regions are unique environments to study the effects of transport of air pollutants on the marine tropospheric chemistry and its impact on composition, and climate. Trace gases over the Arabian Sea and Indian Ocean were studied extensively during INDOEX campaigns but Bay of Bengal is a data void region. The Bay of Bengal Experiment (BOBEX) offered an excellent opportunity to study the transport of various trace gases from the eastern and western Indian urban regions to the surrounding marine environments over Bay of Bengal, Arabian Sea and Indian Ocean.

4.1 Introduction

As a result of higher anthropogenic emissions in the Asian region [Akimoto and Narita, 1994; Streets and Waldhoff, 2000], tropospheric ozone mixing ratios may increase significantly in future in this part of the world [Brasseur *et al.*, 1998; Lelieveld *et al.*, 2001]. The results from a recently concluded Indian Ocean Experiment (INDOEX) show a plume of pollutants, known as the South Asian brown haze, transported from the continent to the Arabian Sea and the Indian Ocean [Lelieveld *et al.*, 2001, Ramanathan *et al.*, 2001]. Generally, there is no photochemical production of ozone due to lack of sufficient amount of precursor gases over the remote marine environments [Lal *et al.*, 1998; Dickerson *et al.*, 1999] except in the narrow shipping lanes where there can be ozone production [Lawrence and Crutzen, 1999]. However, high levels of ozone along with aerosols have been observed in the marine boundary layer and at lower tropospheric heights over this region [Lal *et al.*, 1998; Lal and Lawrence, 2001; Chand *et al.*, 2001b; Ramanathan *et al.*, 2001b]. These measurements were restricted to the marine regions of the south-western part of India covering the Arabian Sea and the Indian Ocean only. Model results show that Bay of Bengal region is more polluted than the Arabian Sea [Lelieveld *et al.*, 2001]. Also, in a recent study, Verver *et al.* [2001] have shown that the significant amount of air trajectories of pollutants transported over the Indian Ocean via Bay of Bengal. But so far no observations of trace gases have been made over the Bay of Bengal. Here, in this chapter, detailed measurements of O₃, CO, CH₄ and SF₆ mainly over this region and also over the Indian Ocean and the Arabian Sea, made as a part of the Bay of Bengal Experiment (BOBEX) conducted in February-March, 2001. The results during BOBEX over Bay of Bengal will be inter-compared with the results over Arabian Sea taken during INDOEX and BOBEX cruises.

4.2 Experimental details

The BOBEX was conducted from February 18 to March 23, 2001 onboard the ORV *Sagar Kanya*. In the first phase of the campaign, the ship started from Chennai (13°N, 80.2°E) on February 18 (day number 49) and returned to the same port on February 27 (58) covering the northern parts of the Bay of Bengal (see *Figure 4.1*). In the second phase, the ship again started from Chennai on March 2 (61) and returned to Goa (15.3°N, 73.4°E) on March 23. This phase covered central and southern part of the Bay of Bengal, and parts of the Indian Ocean and the Arabian Sea. Onboard measurements of ozone were made by a Dasibi (RS

1008) analyzer. Ozone, NO, solar fluxes (UVB and total) and meteorological data were averaged over 5 minutes interval. However, only hourly or longer period averaged data of these measurements are used in this study.

Air samples were also collected once in 8-10 hours a day throughout the cruise in 300 ml capacity glass bottles using a metal bellow pump. These samples were analyzed for CH₄, CO and SF₆ using gas chromatographic (GC) techniques. The repeatability of SF₆ and CH₄ analyses are within 1% and that for CO is about 5-6%. Continuous measurements of CO were

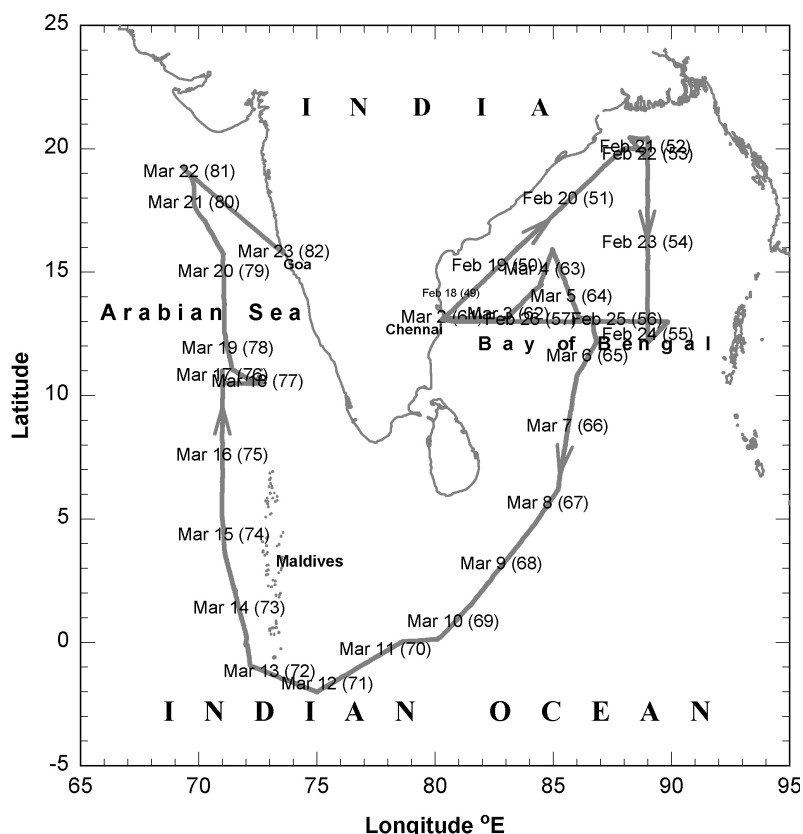


Figure 4.1 Cruise track during BOBEX 2001 over the Bay of Bengal, the Indian Ocean and the Arabian Sea. The dates and day numbers (in bracket) are marked at respective locations on the cruise track.

also made using a CO analyzer (Monitor Lab, USA) in the first 4 days of the cruise. However, the analyzer failed later due to hardware problem. A good match is found between the CO measurements using GC-FID and CO analyzer onboard during the overlapping period.

4.3 Meteorological conditions

The Indian winter season is characterized by lower tropospheric winds, which generally flow in two channels. One channel carries the continental outflow from the northern India to the

Bay of Bengal through the eastern side of India. The other channel of the flow passes from the northwest India to the Arabian Sea. Both these channels finally take the pollutants to the Indian Ocean as shown in *Lelieveld et al.* [2001]. Here, geographically, Bay of Bengal and Arabian Sea are defined as the marine regions north of 6°N. The marine region south of 6°N is taken as the Indian Ocean. Regional average wind speed and relative humidity parameters over the Bay of Bengal, Arabian Sea and Indian Ocean are shown in *Table 4.1*. The average wind field lines during the cruising period (Feb 18 – Mar 23, 2001) are shown in *Figure 4.2*.

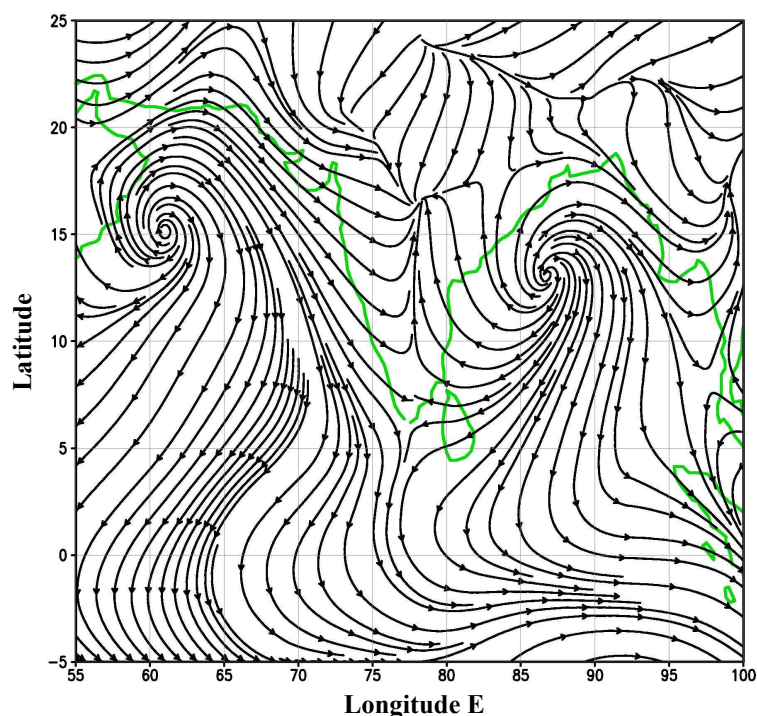


Figure 4. 2 Average NCEP wind field flow at 1000 mb during BOBEX (Feb18-Mar23, 2001) over Bay of Bengal, Indian Ocean and Arabian Sea.

Similar to average wind fields, wind field analysis on individual day indicate that the sampled air originated from relatively cleaner regions for most of the time except a few events when the air parcels were transported from polluted environments. The ITCZ on March 12, 2001 was located near 5°S.

4.4 Ozone and other trace gases

4.4.1 Variation in ozone

Figure 4.3a depicts the temporal and spatial variations of hourly averaged ozone mixing ratios observed during the entire cruise. Latitude and longitude information along with markings for the three marine regions are also given against days of the year (DOY) 2001.

Ozone mixing ratios were only about 25 ppbv near the Chennai coast on Feb. 18 (49). However, near the north most point on days 51-52 (Feb. 20-21) ozone values were lower,

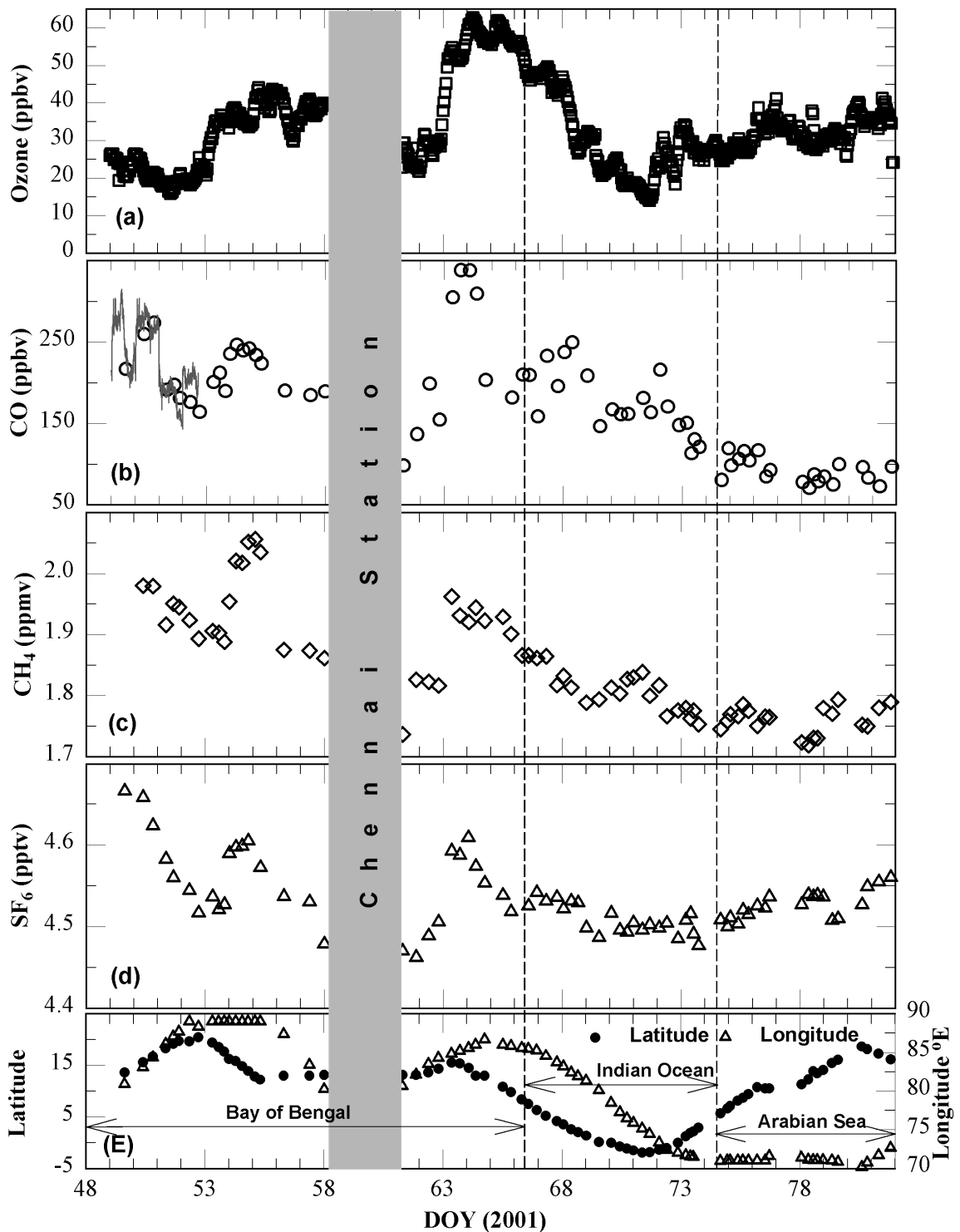


Figure 4. 3 Hourly averaged variation of ozone and other gases observed during the cruise along with latitude (filled circles) and longitude (open triangles) information.

about 16-18 ppbv. This is rather surprising assuming that northern region is the entry point of the continental pollutants. As the ship moved towards south, away from the Indian coastal region, ozone values again increased. Higher ozone values of about 44 ppbv were observed

on days 55 and 56 when the ship was almost in the middle of the Bay of Bengal ~ 1000 km off the Chennai coast. At the Chennai coast on day 57, ozone values (about 40 ppbv) were relatively higher than earlier values when the observations were taken in starting of the campaign.

Trajectory analysis for the day 51 (Feb. 20) shows that the air parcel originated over the marine region even before 7 days (*Figure 4.4a*). This could have diluted the air. However, on day 53 (Feb. 22), the air parcel came from the Indian region but spent 4-5 days in the marine region before reaching the measurement location, thereby showing a tendency for an increase in ozone. The back trajectory for day 56 (Feb. 26), when ozone levels are higher, passed through the north India before reaching the observational site. This trajectory also

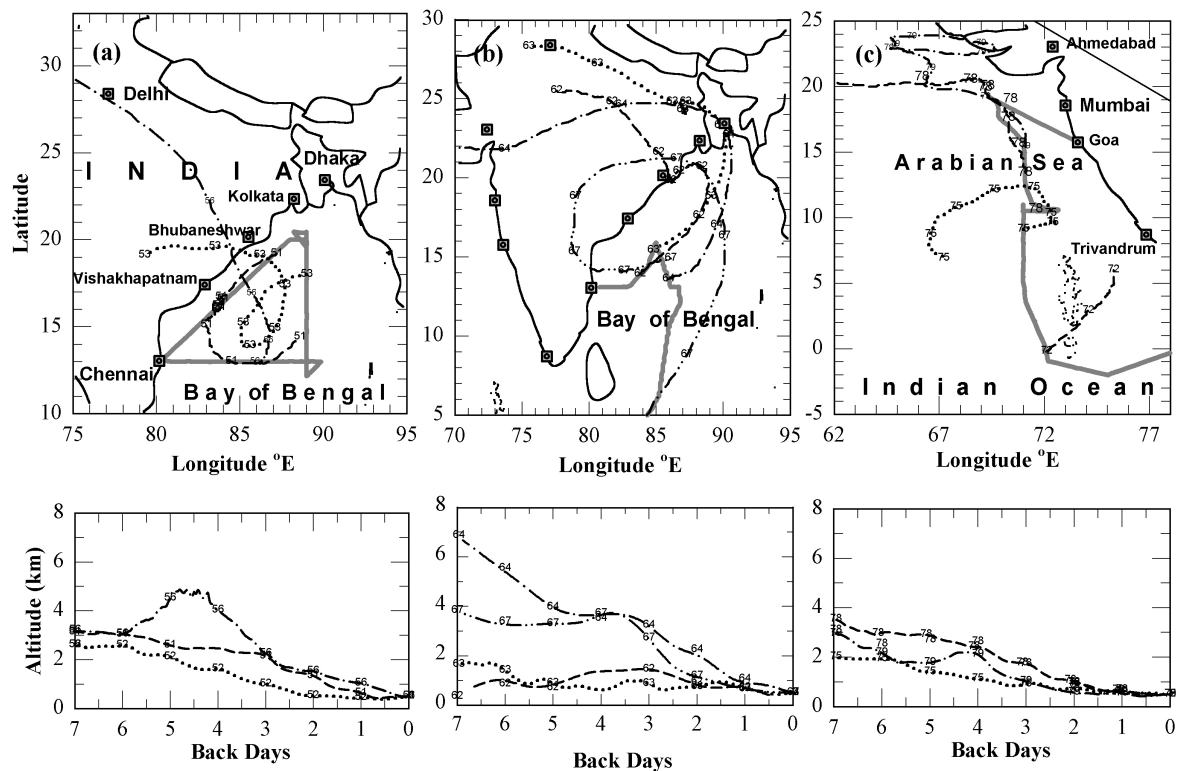


Figure 4.4 Three dimensional, 7-days back trajectories of air parcels arriving at the cruise track on the mentioned days in different marine regions.

indicates possibility of ozone coming from the free troposphere as it descended from a height of about 4.5 km within 4 days. Therefore, the higher ozone values around this area could be due to the polluted air parcels coming from the northern India and possibly due to transport from the free troposphere, where ozone concentration is generally higher.

The second phase of the cruise started again from Chennai on March 2 (61), when the ozone values were about 29 ppbv and it increased to as high as 62 ppbv on days 64 and 65 in the central Bay of Bengal. Thereafter these levels decreased gradually to a minimum of about 15 ppbv on days 71-72 when the ship was at the southern most point of the cruise at 2° S.

Seven days back trajectory analyses (*Figure 4.4b*) show that while on day 62 the air parcel came from the central-north Indian region and spent 3-4 days over the marine region, the air parcels on days 63 and 64 came from the northern and western industrial regions of India via Dhaka. Dhaka is a major city and entry point for the air to Bay of Bengal. The transported air parcel from Dhaka was relatively fresh as it spent only about 2 days over the marine region before reaching the cruise track on days 63 and 64. The later part of the cruise is also covered by this northerly wind (see trajectory for day 67) but the air was relatively aged and got diluted with the marine air on the way and that resulted in monotonous decrease in ozone levels with time and distance. The average latitudinal gradient of about 3 ppbv per degree latitude is observed from 13°N to 2°S in this region.

After the minimum in ozone on days 71-72 near the ITCZ, its level started increasing slowly as the ship turned north towards the Arabian Sea. There is a small increase in ozone on March 13-14 (days 72-73) and on March 17 (day 76) when the ship was in the vicinity of Male and Kavarrati (Lakshadweep) islands respectively. The highest ozone level in this region (Arabian Sea) was observed to be about 40 ppbv on days 77 and 80-82. Average wind pattern during these days shows that the wind came from the north-west Arabian Sea. Back trajectories for few days during 72-79 days are shown in *Figure 4.4c*. Some of these trajectories show that the air had moved over the marine region during the last 4-5 days and others show that the air had come from the Arabian countries.

These ozone levels over the Arabian Sea are lower than those observed during the INDOEX 1999 cruise when ozone was observed to be 40-70 ppbv near the Indian west coast. The wind patterns during that period showed that the air was coming directly from the Gujarat and Maharashtra states, which are considered to be highly industrialized regions in India.

4.4.2 Variation in other trace gases

Figures 4.3c-4.3d show variations in CO, CH₄ and SF₆ observed during the BOBEX cruise. These gases have longer lifetime than O₃ and the budgets of most of these gases are controlled by anthropogenic emissions. SF₆ is one among the best atmospheric tracers having longer lifetime and larger growth rate. These gases show distinctly higher levels in the first few days and lower values on day 53. On days 54 and 55 these gases again show higher values and a decrease thereafter. However, both ozone and CH₄ levels were higher during days 54-56 than those observed on earlier days but CO and SF₆ values were higher on days 50-51 than during days 54-56. The other difference is that while ozone peaks are broad, peaks

of other gases are relatively sharper and the decrease started earlier than in ozone. The broader peak in ozone than the other gases is observed in both the phases of the cruise. However, the broader peak is more pronounced in the second phase of the campaign during days 63-68. At the start of the second leg of the cruise, all the four gases (O_3 , CO, CH_4 and SF_6) show lower values on day 61 but their values increased and became high on days 63-64. Thereafter there is a gradual decrease in all these gases. When ozone is minimum on day 71, CO and CH_4 show secondary peaks. The total flux measurement shows that day 71 was a cloudy day. The ITCZ was located nearer this region at around $5^\circ S$. Over the western part of the cruise (west of $75^\circ E$ longitude and after day 71) covering part of the Indian Ocean and the Arabian Sea, there is a slow increase in ozone and SF_6 values while concentrations of CO and CH_4 continue to decrease except for CH_4 on the last few days from 79 to 82. Thus the broad features in ozone, like the two regions of higher ozone on days 54-56 and 64-68, are supported by similar changes in CO, CH_4 and SF_6 gases. It is also observed that while the starting periods of increase in ozone and other gases match well but ozone remains higher for extended periods when compared to other gases.

4.5 Correlations of ozone with other trace gases

CO and CH_4 are the precursors of ozone. In marine boundary layer, if ozone is produced by CO and/or CH_4 and then transported to the remote areas, there should be a positive correlation between these trace gases provided the air parcel is not older than a week. However, the observed correlations of ozone with CO, CH_4 and SF_6 are not significant during BOBEX except for few days when the air parcel was transported from the Dhaka region, as mentioned in the earlier section. This poor correlation is possible if the sampled air is relatively aged, more than 5 days. However, correlation of ozone with CO in the three different marine regions give interesting results even though the correlation coefficients are not very good (see *Figure 4.5*). In the eastern part (east of $75^\circ E$ longitude) of the cruise covering Bay of Bengal and part of the Indian Ocean, the correlation of CO with ozone shows a positive slope. On the contrary in the western part, which covers the Indian Ocean and the Arabian Sea, the slope is negative. This means that in the eastern part of the cruise, the air parcel has the signature of an urban air particularly on days 62 to 70. This has been already confirmed by back trajectories (*Figure 4.4b*). These positive correlations also imply that higher CO would lead to higher production of ozone in this region. However, over the western part, while ozone is showing an increase towards the Indian west coast, CO is decreasing. This is surprising since such opposite trends in the two gases are not observed

during all the INDOEX cruises over the Arabian Sea. But increase in ozone while CO and CH₄ decrease occur only during the daytime when oxidation of these gases produce ozone at polluted sites. Here, contrary to the INDOEX measurements where the air mostly came from

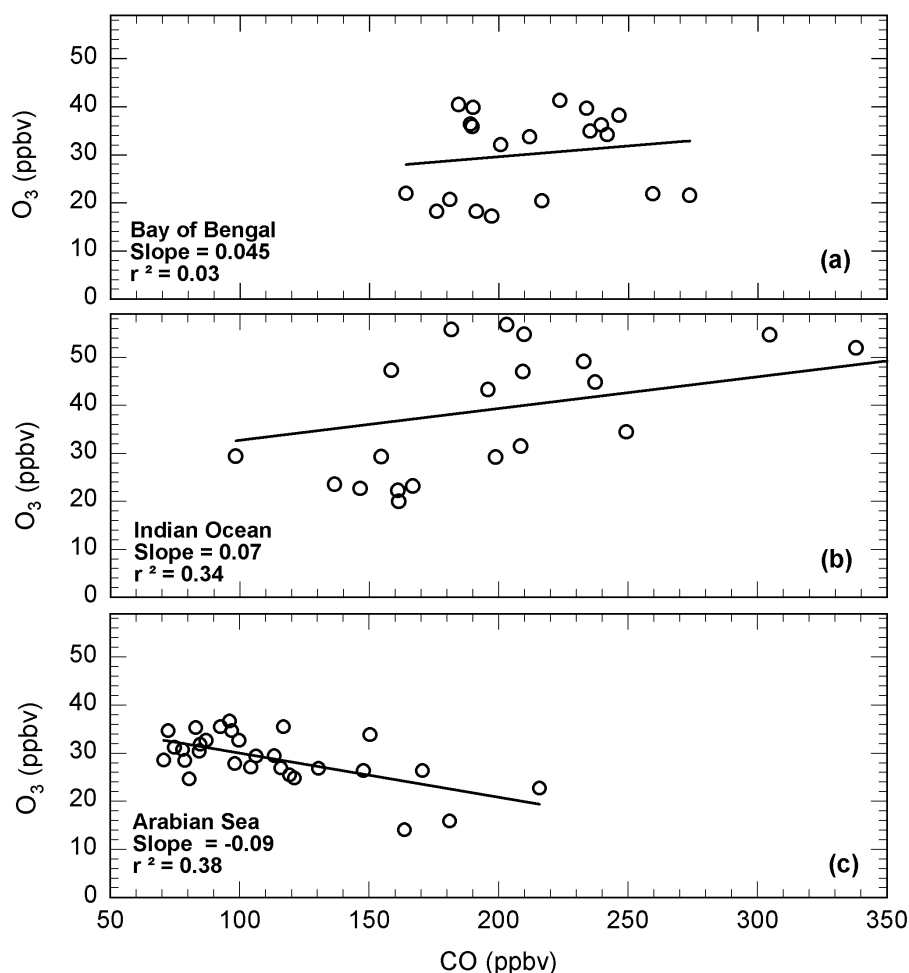


Figure 4.5 Correlations of O₃ and CO in three different marine environments during BOBEX 2001.

the west Indian region, the seven days back trajectories show that the air resided over the oceanic region for many days and on other occasions came from the Arabian countries (Figure 4.4c). From these limited observations it is not possible to identify the exact cause for such an opposite trend. However, observations over the cleaner Indian Oceanic region during INDOEX cruises showed even if CO increased there was no increase in ozone. This was attributed to the daytime ozone loss due to different mechanisms.

Methane and CO show better correlation throughout the cruise than correlations between other gases. This could be due to the fact that both CO and CH₄ have some common sources like biomass and fossil fuel burning etc whereas SF₆ is mostly used in high voltage electrical equipments and does not contribute to the tropospheric chemistry. It can also be seen that all these gases have higher concentrations over the Bay of Bengal and the Indian Ocean on the eastern side, where the wind is coming mostly from the land region. But

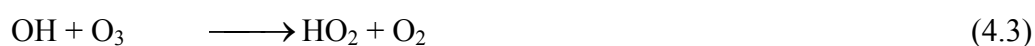
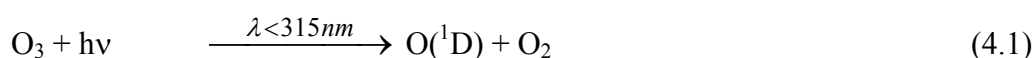
concentrations of these gases are much lower in the western region. This again implies that the air in this section is relatively cleaner. In the eastern region, observed CO is in the range of 150 and 300 ppbv whereas in the western region it varies between 75 and 200 ppbv. However, SF₆ is showing slow increase towards the north like in ozone over the Arabian Sea.

4.6 Variability in UVB and total solar flux

Ultraviolet B (295-315 nm) radiation along with atmospheric water vapor play important role in controlling the oxidation capacity of troposphere, shown by reactions 1.1-1.2 in *Chapter 1*. The tropical troposphere plays a major role in global hydroxyl (OH) radical budget, and thus this may have consequences for the oxidation capacity of the atmosphere. Major part of OH radicals is controlled by the UVB flux (photochemical reactions 1.1 and 1.2), as mentioned in *Chapter 1*.

UVB and total radiation flux are measured using UV Biometer (Solar Light Co, Model 5010) and Pyronometer (Kipp & Zonen, Model CM 3B/7B) respectively during BOBEX. These instruments inter-compared well with similar instruments onboard the *Sagar Kanya*. *Figure 4.6* shows the hourly average UVB and total flux in the marine environments of the Bay of Bengal, Indian Ocean and Arabian Sea. There is a time lag of about 30 minutes in flux peaks over the Bay of Bengal-Indian Ocean and Arabian Sea-Indian Ocean due to change in longitude. The UVB is lower over the Arabian Sea and the Bay of Bengal compared to the Indian Ocean where as the total flux is lower over the Indian Ocean compared to Arabian Sea and Bay of Bengal. This contrasting feature of maximum UVB over Indian Ocean (equatorial region) may be due to (a) lowest total atmospheric ozone which can lead to higher UVB at surface due to lower absorption, and (b) low attenuation of UVB by clouds and other air molecules/particles compared to the visible radiation. Similar features in UVB is found over a high altitude station at Mt Abu (see *Chapter 6* for details).

Higher UVB radiation due to lower total ozone can further reduce surface ozone in the presence of high water vapor and low NO. In the ITCZ region, higher water vapor can lead to ozone loss by the following OH-O₃-HO₂-OH cycle,



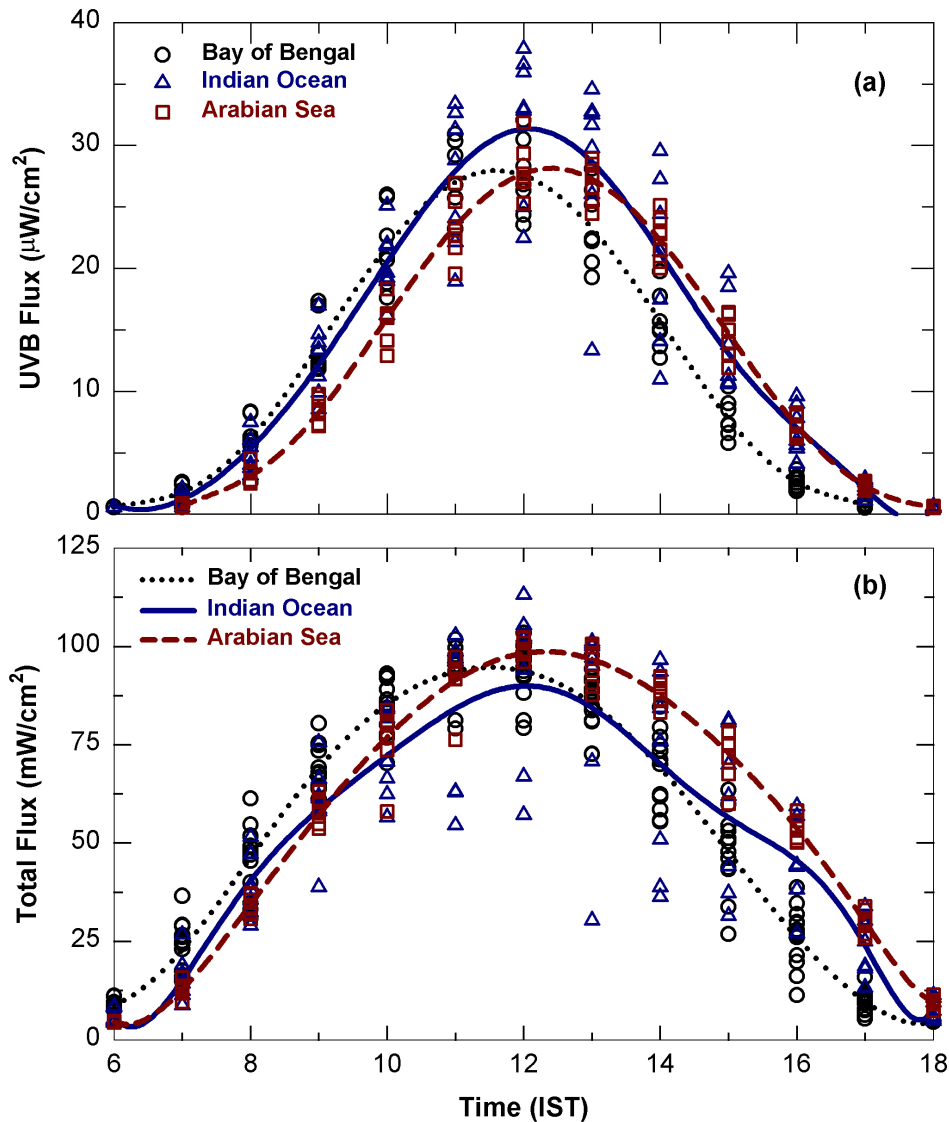


Figure 4.6 Diurnal variation of regional average (lines) UVB and total solar fluxes over the three different marine environments. Symbols represent the hourly averages of the flux over the respective marine environments during BOBEX-2001.

The lowest levels of ozone during BOBEX cruise near the ITCZ may be due to the above cycle [Vogt *et al.*, 1996; Dickerson *et al.*, 1999]. This loss cycle in daytime gives net loss of ozone resulting in marine type of diurnal variation. Such diurnal variations were also observed during INDOEX cruises.

4.7 Diurnal variations of NO and O₃.

Now it is well known that the photochemical oxidation of CO and CH₄, and other hydrocarbons in the atmosphere produce or destroy ozone if NO_x concentrations are above or below some critical limit [Liu *et al.*, 1983]. This critical limit of NO_x varies from 5 pptv to

about 50 pptv, depending on many factors including the background concentrations of ozone itself. Due to higher concentrations of NO_x above the threshold limit, most of the rural and urban environments show diurnal variation having net daytime ozone production [Crutzen, 1988, 1995; Lal *et al.*, 2000]. However, due to shorter lifetime of NO_x (few hours), the remote continental and marine environment may have NO_x below the critical levels and this may lead to ozone loss during daytime.

Figure 4.7 shows the average amplitude of diurnal variations of NO in the three different marine environments surrounding the Indian sub-continent. Average NO diurnal

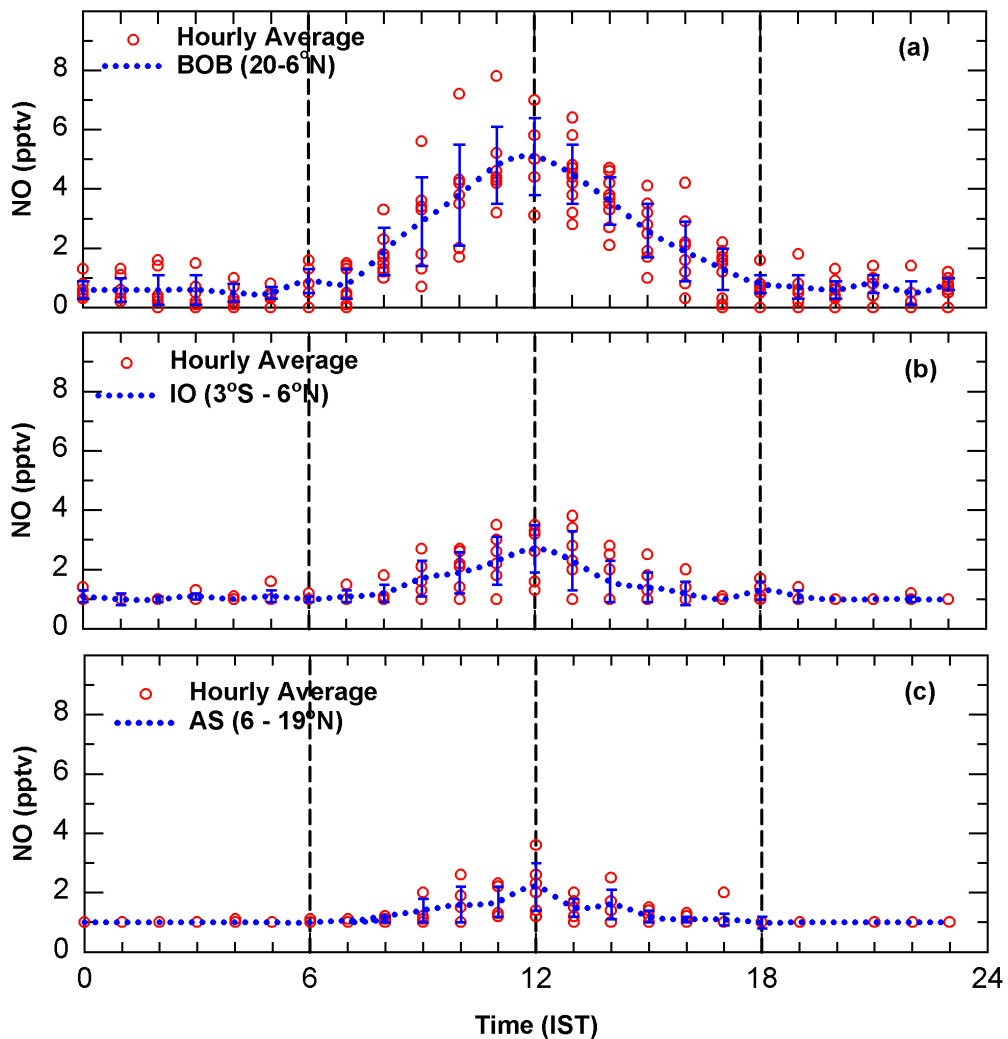


Figure 4.7 Diurnal variations in NO for three different marine environments over (a) Bay of Bengal (BOB), (b) Indian Ocean (IO) and (c) Arabian Sea (AS) during BOBEX 2001. Open circles are hourly average where as the dotted line is the regional average of NO over these marine environments.

amplitudes over the Bay of Bengal, Indian Ocean and Arabian Sea are 7 pptv, 3 pptv and 2 pptv respectively. These amplitudes are calculated by subtracting the nighttime NO background from its diurnal variation. All these levels of NO are below the threshold limit of ozone production since the observed diurnal variations in O_3 show net loss in sunlit hours, as

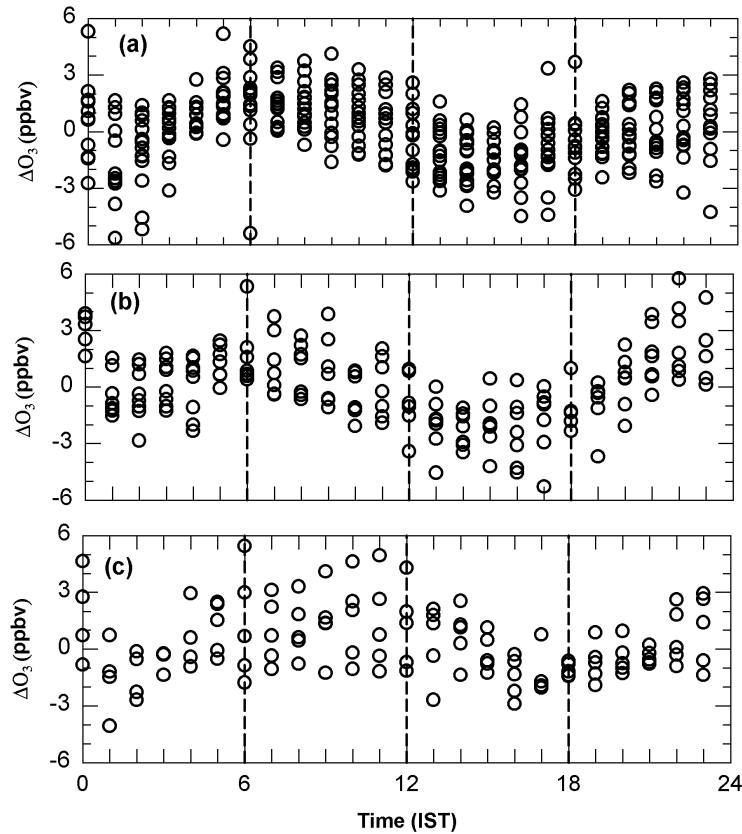


Figure 4.8 Amplitudes of diurnal variations (ΔO_3) of ozone in three different marine environments over (a) Bay of Bengal, (b) Indian Ocean and (c) Arabian Sea during BOBEX 2001.

shown in Figure 4.8. Due to lower concentrations of NO the relative diurnal variations* in ozone is about 5%, 3% and 3 % over Bay of Bengal, Indian Ocean and Arabian Sea respectively. These amplitudes in ozone are much lower than the INDOEX 1998 and 1999 levels as shown in Table 4.1.

4.8 Comparison with INDOEX results

Table 4.1 gives average mixing ratios of the measured gases during BOBEX 2001 in the three marine regions and INDOEX campaigns over the Arabian Sea and Indian Ocean. The average values are obtained by first calculating mean values at each degree latitude so as to have equidistant points. Figure 4.9 shows the comparison in average ozone values over Arabian Sea with that over the Bay of Bengal measured during the INDOEX 1996-1999 and BOBEX 2001. Each point in the plot represents average of all the data in each latitudinal bin. Average ozone levels of 42 ppbv are higher over the Bay of Bengal as compared to those over the Arabian Sea (31 ppbv) and the Indian Ocean (29 ppbv) during this cruise.

* The relative diurnal variation = $(\Delta O_3 / O_3) \times 100$

Concentrations of CO, CH₄ and SF₆ are also highest over the Bay of Bengal. However, the average ozone levels over the Bay of Bengal (6-20°N) in 2001 are not very different from those observed over the Arabian Sea during the INDOEX 1999. Also, the average ozone of 31 ppbv over the Arabian Sea is much lower than that observed (44 ppbv) during the INDOEX 1999 over the same region. SF₆ concentration is about 6.6% higher during BOBEX 2001 than during the INDOEX 1999. This growth rate is similar to the growth rate of SF₆ observed during INDOEX 1998-1999 campaigns [Chand *et al.*, 2001a]. The INDOEX 1998-

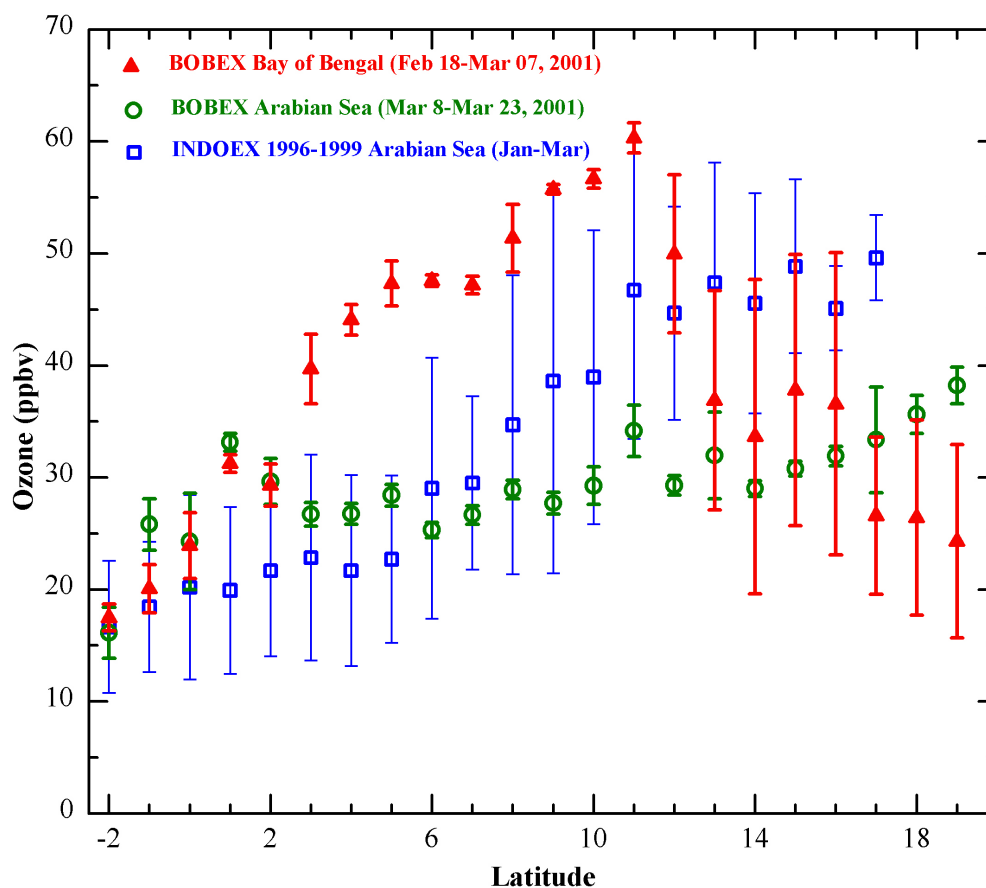


Figure 4.9 A comparison of average ozone at each degree latitude measured during BOBEX with the average ozone observed during all the four INDOEX cruises conducted in each winter from 1996 to 1999.

1999 and INDOEX-BOBEX SF₆ data confirm that the growth of SF₆ in the Indian region is lower than the global growth rate during winter season.

During days 64 to 72, the calculated e-fold time of ozone over the Bay of Bengal is 4.9 days (using exponential equation 3.1 mentioned in *Chapter 3*). During these days, the air plume was transported from source region to the remote marine environments of Bay of Bengal and the Indian Ocean. The Bay of Bengal is an ideal region for calculating the e-fold time using equation 3.1, as the cruise track and the wind flow are almost in the same direction.

Table 4.1: Regional average values of wind speed, relative humidity, O_3 , CO , CH_4 and SF_6 with their $\pm 1\sigma$ standard deviations during BOBEX 2001 and INDOEX 1999. Diurnal amplitude of O_3 , NO , UVB and total fluxes are also shown.

Parameters	BOBEX 2001			INDOEX 1999	
	Bay of Bengal (BOB)	Indian Ocean (IO)	Arabian Sea (AS)	Indian Ocean (IO)	Arabian Sea (AS)
Wind Speed ($m\ s^{-1}$)	6.4 ± 3.3	6.7 ± 3.3	5.5 ± 1.9	4.5 ± 2.2	4.3 ± 2.2
Relative Humidity (%)	75.5 ± 8.0	69.8 ± 4.6	72.0 ± 4.7	75.8 ± 6.4	73.9 ± 6.1
O_3 (ppbv)	42.2 ± 12.0	29.0 ± 7.1	30.9 ± 4.2	21.5 ± 3.5	43.9 ± 7.9
CO (ppbv)	217 ± 31	170 ± 12	91 ± 15	178 ± 22	217 ± 42
CH_4 (ppmv)	1.92 ± 0.05	1.80 ± 0.02	1.76 ± 0.02	1.72 ± 0.05	1.73 ± 0.05
SF_6 (pptv)	4.55 ± 0.03	4.51 ± 0.02	4.52 ± 0.02	4.06 ± 0.36	4.24 ± 0.32
ΔO_3 (ppbv)	3	1	1	0.5 - 6.0	0.5 - 5.0
ΔNO (pptv)	6	2	1	5-20	5-15
ΔUVB (μWcm^{-2})	27.91	31.3	28.01	--	--
$\Delta Total\ Flux$ ($mWcm^{-2}$)	94.75	90.00	98.29	--	--

The calculated e-fold time of ozone is almost equal as the e-fold time calculated during INDOEX 1998-1999 campaigns and it confirms our hypothesis (assumption of the Indian sub continent as source region of trace gases; advection and/or entrainment governs the transport as well as diurnal variation of ozone) leads as mentioned in *Chapter 3* [Chand *et al.*, 2001b]. However, the observed diurnal variations during BOBEX are lower compared to INDOEX campaigns.

Chapter 5

Surface ozone in downwind of urban Gujarat in India

The experimental evidence of high ozone concentrations (>80 ppbv) within urban plumes in India is very less and is limited to some seasons only. Unlike North America and Europe, in general, the limited observations in India show relatively lower ozone concentrations in the Indian subcontinent [Naja, 1997; Lal et al., 1998]. However, elevated ozone concentrations were observed in the remote marine boundary layer of the Arabian Sea during INDOEX 1999 campaign [Lal and Lawrence, 2001, Lal et al., 2002]. These ozone concentrations in the Indian subcontinent are based on the measurements at limited stations and during INDOEX cruises [Lal et al., 1998; Naja et al., 1999; Lal and Lawrence, 2001; Chand et al., 2001a, Chand et al., 2001b]. Lal and Lawrence [2001] suggested that the elevated ozone in the remote marine boundary layer of the Arabian Sea during INDOEX 1999 campaign could be either due to transport of ozone rich air from the free troposphere or advection of elevated ozone from the source regions of surrounding urban environments. To assimilate the transport (advection) and en route transformation of ozone, mobile lab experiments-advection (MOLEX-A) were conducted in the downwind and side winds of urban Gujarat in India in the month of January during 2001 and 2002.

5.1 Introduction

High levels of ozone concentration found in the boundary layer and lower troposphere have been a major problem in North America and Europe [White *et al.*, 1983; EEA, 1998; Aneja *et al.*, 1999; NARSTO, 2000]. Ozone, a secondary pollutant, is designated as a criteria pollutant under the clean air act amendment (CAAA) of 1990 [EPA, 1993]. A polluted environment, which is producing ozone more than 80 ppbv for more than 8 hours, is considered a violation of National Ambient Air Quality Standard (NAAQS) [EPA, 1993]. Health and crop have been adversely affected by high levels of ozone concentrations [NRC, 1991; EPA, 1996].

Recently considerable attention has been given to the production of ozone in the polluted regions of Asia and transport and transformations of pollutants from this region to its surrounding marine environments [Streets and Waldhoff, 2000; Ramanathan *et al.*, 1996]. The INDOEX results have shown a thick brown haze over the Arabian Sea and the Indian Ocean transported from the Indian subcontinent [Ramanathan *et al.*, 1996; Ramanathan *et al.*, 2001; Lelieveld *et al.*, 2001]. Transport of the pollutants from the Asian countries, particularly from China and India, are expected to make important changes in the atmospheric composition [Lelieveld *et al.*, 2001]. Elevated ozone levels (60-70 ppbv) were observed over the Arabian Sea during INDOEX 1999. Observations from limited continental stations in India at urban, rural and free tropospheric sites do not support the existence of such elevated ozone levels [Lal *et al.*, 2000; Lal and Lawrence, 2001; Nair *et al.*, 2002]. It was not discernable whether these elevated levels were transported from the free troposphere or were produced away from the source regions [Lal and Lawrence, 2001, Chand *et al.*, 2001b].

In order to understand the quantum of photochemical production of ozone away from the source regions, mobile lab experiments-advection (MOLEX-A) were conducted in downwind of major urban region of Gujarat in western India adjoining the Arabian Sea in January of 2001 and 2002. These results are discussed along with the supporting measurements made during the same season and year from an urban environment (Ahmedabad; 23°N, 72.6°E, 49m), a rural environment (Gadanki; 13.5°N, 79.2°E, 375m) and free troposphere (Mt. Abu; 24.6°N, 72.7°E, 1680m). Wind components (u and v) taken from NCEP are used for estimation of wind flow and HySPLIT-4 trajectories for tracing the air in backward and forward directions.

5.2 Experiment details

The mobile lab experiment was conducted in downwind of urban Gujarat using two vans each containing one ozone analyzer during January 22-27, 2001. The third ozone analyzer was kept at Ahmedabad, which is a major urban center in this region. *Figure 5.1* shows the mobile tracks of the region covered along with the average wind fields (faint arrow lines) during the campaign period. During mobile campaigns, isolated roads were used with almost no traffic to avoid the pollution due to vehicles in the vicinity of the observational sites

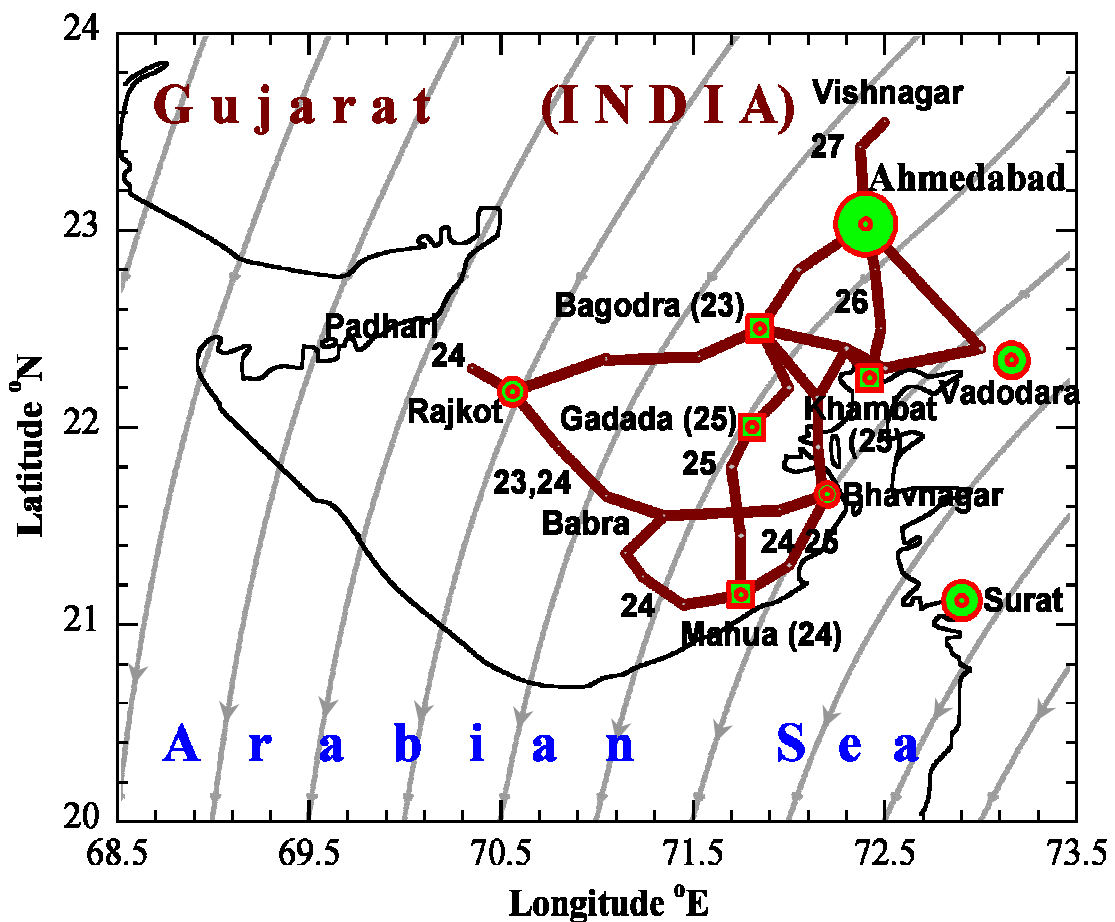


Figure 5.1 The observation tracks covered by the mobile labs in January 2001. Circles represent the urban regions, size of the circle is proportional to the population of the urban centers. Numbers on the track indicate the date of the observations. Square symbols represent observations in night taken at the fixed sites on the dates embedded in the brackets. Faint thin arrow lines show the average wind flow during the study period.

(tracks). The data from the national highways, such as Ahmedabad–Bagodra–Rajkot and Ahmedabad–Vadodara, are not used in this study. The circles in *Figure 5.1* are the main urban centers and the areas of the circles are proportional to the population of these urban centers. The numbers along the track indicate the date of observations in mobile phase during daytime. All the nighttime observations during the campaign were made at fixed sites.

Khambhat is a small town, about 100 km south of Ahmedabad, as shown in *Figure 5.1*. In winter, when the winds are northerly or north-easterly (see *Figure 5.1*), the polluted air from Ahmedabad and Vadodara regions passes over Khambhat on the way to the Arabian Sea. To assess the quantum of the pollutants transported, measurements were also taken at Khambhat for more than 20 hours on January 25-26, 2001. The observations at Khambhat and Ahmedabad were repeated during December 30, 2001 to January 6, 2002 to confirm the results from the first campaign.

Ozone measurements were made using Dasibi (Model 1008, USA) and Environmental S.A. (Model 41M, France) analyzers, working on the principle of UV absorption by ozone at 253.7 nm. All the analyzers are calibrated and they inter-compared well with a correlation coefficient better than 0.98 and a difference of less than 3% in the absolute values.

5.3 Ozone at urban and its surrounding regions

Figure 5.2a depicts the average diurnal variations of ozone observed at Ahmedabad from January 22-26, 2001 and at different tracks in its downwind sides observed in the MOLEX-A during January 24-26, 2001 (see *Figure 5.1* for track). The time mentioned in this study is in Indian Standard Time (IST), which is 5.5 hours ahead of UT. The average diurnal variation of ozone at Ahmedabad during January 22-26 shows distinct daytime production with maximum of about 52 ppbv at local noon. High ozone levels persisted for more than four hours from 1230 to 1700 hours. Low level of ozone (~12 ppbv) is observed just after sunrise. The observed net daytime photochemical production of ozone at Ahmedabad is about 40 ppbv. After sunrise, ozone is produced at the rate of about 6.7 ppbv hr⁻¹ and it takes about six hours to attain the peak level.

Ozone values observed in downwind of the urban center on January 24, 25 and 26 are significantly higher compared to the values at Ahmedabad (*Figure 5.2a*). The pronounced high photochemical production of ozone for these three consecutive days at Bagodra-Bhavnagar-Mahua and Mahua-Gadada tracks and at Khambhat lead to peak ozone levels of 78-86 ppbv. The net daytime production of ozone in downwind side is about 65 ppbv, which is about 60% higher than the net ozone production at Ahmedabad. The observed daytime net production rate of ozone is about 10 ppbv hr⁻¹. It takes 5-7 hours to attain the maximum ozone levels after sunrise. While O₃ levels are high on all the three consecutive days, there are some variations in their daytime and nighttime levels, perhaps due to changing observational regions on the mobile tracks.

The daytime peak amplitudes of ozone diurnal variations in the side and off wind directions of the urban area on Rajkot-Babra, Gadada-Bagodra and Ahmedabad-Vishnagar tracks are in the range of 50-60 ppbv (*Figure 5.2b*). The net observed average ozone production rate obtained from the slope of all the data in these regions is about 4.2 ppbv hr^{-1} . *Figure 5.2c* shows the average diurnal variation of ozone at Ahmedabad and its downwind direction at Khambhat during the second campaign from December 30, 2001 to January 6, 2002. The

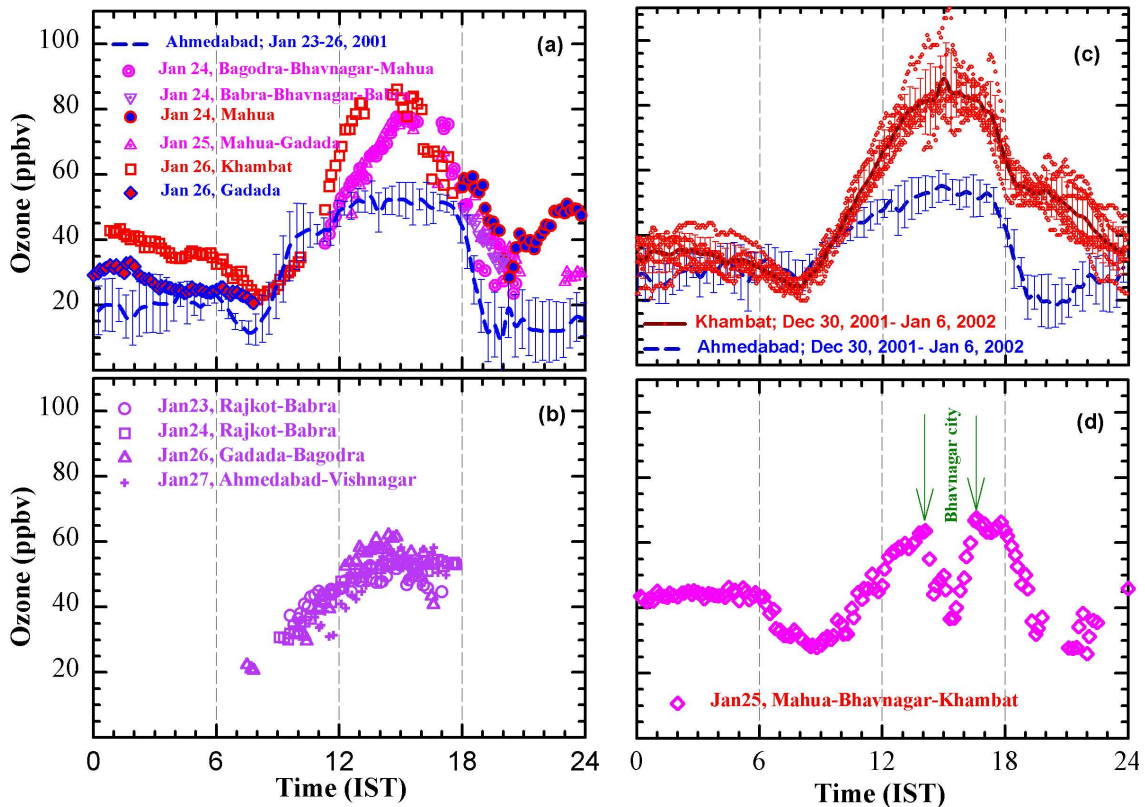


Figure 5.2 Ozone diurnal variations at urban center (Ahmedabad) and its surrounding regions during January 2001 and December-January 2002. Diurnal variations of ozone at (a) Ahmedabad and its downwind side, (b) in the side wind and off wind directions of Ahmedabad, (c) from December 30, 2001 to January 6, 2002 at Ahmedabad and Khambhat, a town at the downwind of urban Gujarat, (d) at Mahua-Bhavnagar-Khambhat mobile track on January 25, 2001 (The marked arrows show the limits of Bhavnagar city).

average peak ozone of about 55 ppbv is observed in the afternoon hours at Ahmedabad. The net ozone production rate at Ahmedabad is about 4.0 ppbv hr^{-1} producing 27 ppbv of ozone in daytime hours. There is a difference in ozone production rates due to change in the minimum O_3 after sunrise but the peak ozone levels at Ahmedabad are almost similar during both the campaigns (see *Table 5.1*).

High ozone is observed at Khambhat in the afternoon hours ranging from 70 to 110 ppbv during the observational period in 2001 and 2002. The mean of the elevated ozone during afternoon hours is about 85 ppbv and it lasted for more than three hours. The average ozone production rate from sunrise to afternoon hours is about 10 ppbv hr⁻¹ leading to high ozone production of about 58 ppbv. There is very less day-to-day ozone variability during 0800-1200 and 1700-1900 hours but the variability during the night and afternoon hours is considerable. The observed ozone levels are about 63% higher than at Ahmedabad. This is consistent with the observations during the first campaign in January 2001. In addition, there is no marked difference in the peak ozone levels and its production rates at Khambhat during both the campaigns.

Table 5.1: Summary ozone results observed at Ahmedabad (urban) and Khambhat (rural) during MOLEX-A 2001 and 2002. The minimum ozone is observed just after sunrise and maximum in the afternoon hours.

Campaign Period	Parameter	Ahmedabad (Urban)	Khambhat (Downwind)
Jan. 22-27, 2001	Maximum O ₃	52 ppbv	80 ppbv
	Minimum O ₃	12 ppbv	25 ppbv
	Net O ₃ production	40 ppbv	65 ppbv
	Ozone increase rate	6.7 ppbv hr ⁻¹	10.0 ppbv hr ⁻¹
Dec. 30, 2001- Jan. 6, 2002	Maximum O ₃	55 ppbv	88 ppbv
	Minimum O ₃	28 ppbv	25 ppbv
	Net O ₃ production	22 ppbv	58 ppbv
	Ozone increase rate	4.2 ppbv hr ⁻¹	9.9 ppbv hr ⁻¹

Figure 5.2d shows diurnal variation of ozone observed on January 25, 2001 along the northern coast of the Arabian Sea from Mahua to Khambhat via Bhavnagar on the mobile track. The ozone levels dropped drastically from 63 ppbv to about 37 ppbv and came back to its original level when the observations were taken across the city of Bhavnagar. The difference in the ozone values outside and inside the city was around 26 ppbv, which is about 70% higher than the ozone levels in the heart of the city. The difference in ozone inside and outside the Bhavnagar city is similar to the difference in ozone from urban center (Ahmedabad) to its downwind regions observed during both the mobile campaigns (Figures 5.2a-5.2c).

5.4 Ozone at other continental stations

Figure 5.3 shows a comparison of the diurnal variations of ozone observed at Ahmedabad, its downwind side, Mt. Abu and Gadanki in winter 2001. Being a free tropospheric and relatively cleaner site, Mt. Abu shows net photochemical ozone loss (4 ppbv) during daytime. The average ozone in the month of January is about 40 ppbv and there is no significant difference in ozone levels during January of 2000 and 2001. Ozone levels at Mt. Abu,

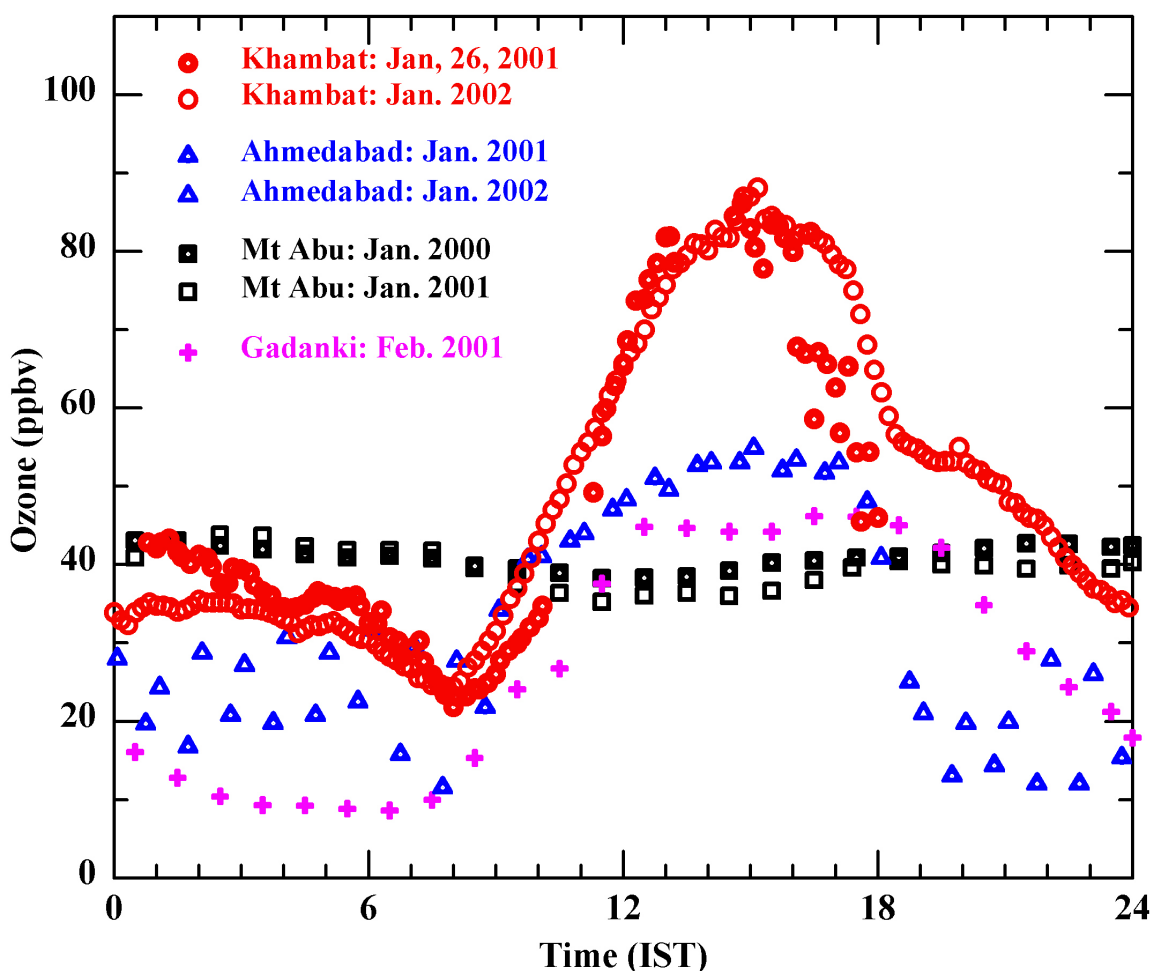


Figure 5.3 Comparison of the elevated ozone in downwind of the urban region with the observations taken at different sites in urban, rural and free tropospheric environments in India. The data at Mt Abu and Gadanki represent monthly averages at each hour.

Gadanki and the coastal environment at Thumba [Nair *et al.*, 2002] have rarely crossed 60 ppbv in the month of January. Gadanki is a typical rural environment in south India exhibiting diurnal variation similar to that at Ahmedabad with noontime maximum of 45 ppbv and a minimum of 8 ppbv just after sunrise. But at both the sites, ozone has rarely exceeded 60 ppbv during the winter of 2001.

In a detailed study of ozone at Ahmedabad, which is a major source of pollutants in the western India, the average maximum ozone at noontime was observed to be 41 ± 12 ppbv in the month of January during the period 1991-95 [Lal *et al.*, 2000]. The observed ozone levels at this site during the first and second campaigns of MOLEX-A in January of 2001 and 2002, as shown in the *Figures 5.2a and 5.2c*, are in general conformity of the earlier study. Back trajectory analyses at Mt Abu in January of 2000 (*Figure 5.4*) indicate that the air

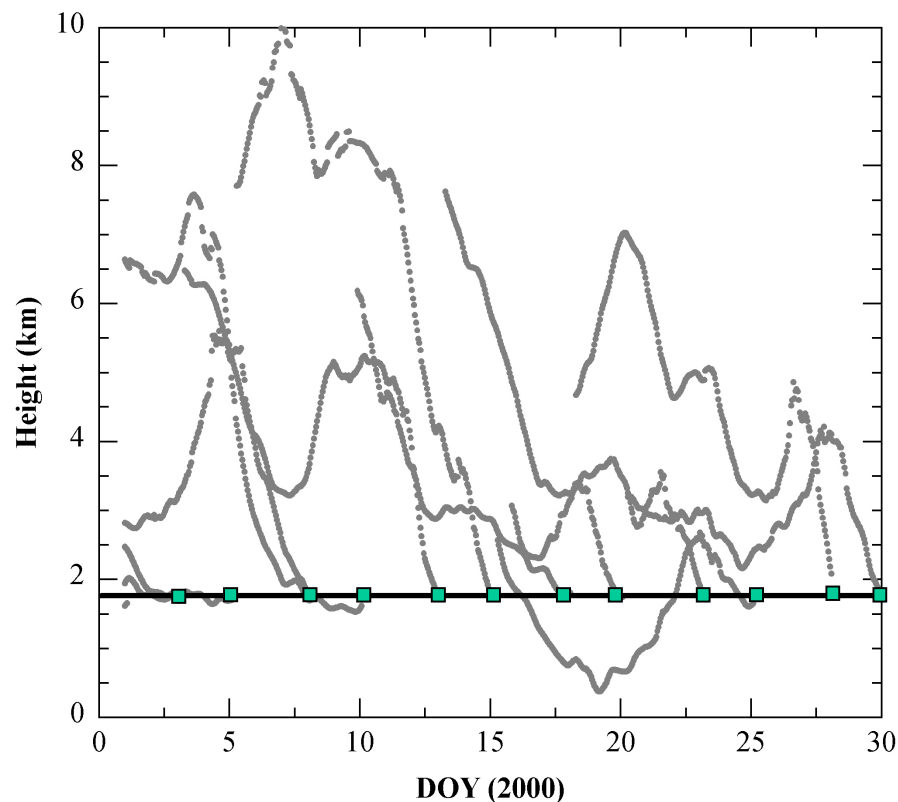


Figure 5.4 A set of 13 days, one-dimensional, 10 days back trajectories (BTs), descending from free troposphere to the observational site at Mt. Abu on different days of year (DOY) in 2000. Square symbols show the day of arrival of the BT at Mt. Abu. Horizontal line represents the height of Mt Abu observatory (1680 m), where observations were made.

descended from the free troposphere most of the times without showing any significant increase in the levels of ozone. Similar results are observed for the years 1999 and 2001 (not shown here). These observations suggest that the probability of transport of high ozone greater than 60 ppbv from free troposphere is very less in this region.

The down wind, side wind and up wind regions of Ahmedabad (*Figure 5.1*) are rural regions. Khambat, in the downwind of Ahmedabad, is also the entry point of pollutants to the Arabian Sea. The ozone levels at Khambat are much higher than the other rural regions and also higher than the urban region (Ahmedabad) itself. This is very clearly seen from the observations at Khambat during both the campaigns. Further, observations across the

Bhavnagar city confirm that net daytime photochemical production of ozone is relatively less in urban environment (*Figure 5.2d*). Being a rural region, high levels of ozone at Khambat are due to *in situ* production of ozone from the precursors transported in the downwind side of the urban regions.

Figure 5.5 shows an event of elevated ozone level along with SF₆ (over the Bay of Bengal), 1000 km downwind of Dhaka, during Bay of Bengal Experiment (BOBEX) in 2001. Details of BOBEX are given in *Lal et al.* [2002]. Here SF₆ is used as an atmospheric tracer. Increase of SF₆ and ozone together shows that the observed air had an urban signature. Seven

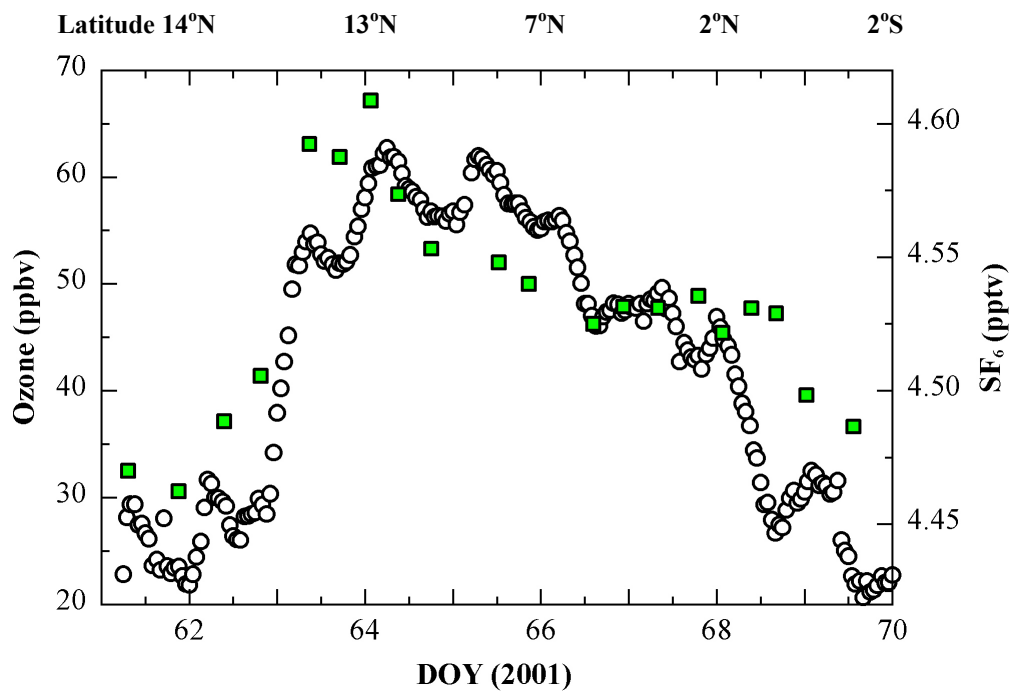


Figure 5.5 Spatial and temporal variations of ozone (open circles) and SF₆ (solid squares) downwind of Dhaka over the mid Bay of Bengal during BOBEX 2001. Approximate latitudes for the corresponding days are also given in the top of the x axis.

days back trajectory analysis derived from *HySPLIT* model further confirms that the air plume originated from the north India and it travelled through the boundary layer and passed through Dhaka before entering the Bay of Bengal (*Figure 3.5, Chapter 3*). On days 61-62, the air was coming from a relatively cleaner region and both ozone and SF₆ show lower values. Thereafter, both ozone and SF₆ continued increasing till day 64. When SF₆ started decreasing on day 64, the decrease rate of ozone is relatively less. Despite having very less lifetime compared to SF₆, ozone shows a broader peak than SF₆, which is possible only if there was an extra production of ozone on the way when the air parcel was moving away from Dhaka in its downwind side over Bay of Bengal. If an e-fold transport distance of ozone is taken as

1850 km over marine environment [Chand *et al.*, 2001b], ozone in downwind of Dhaka would have been about 97 ppbv.

Figure 5.6 shows three dimensional seven days forward trajectory originated at 500m above Ahmedabad. These forward trajectories indicate that the polluted air can get

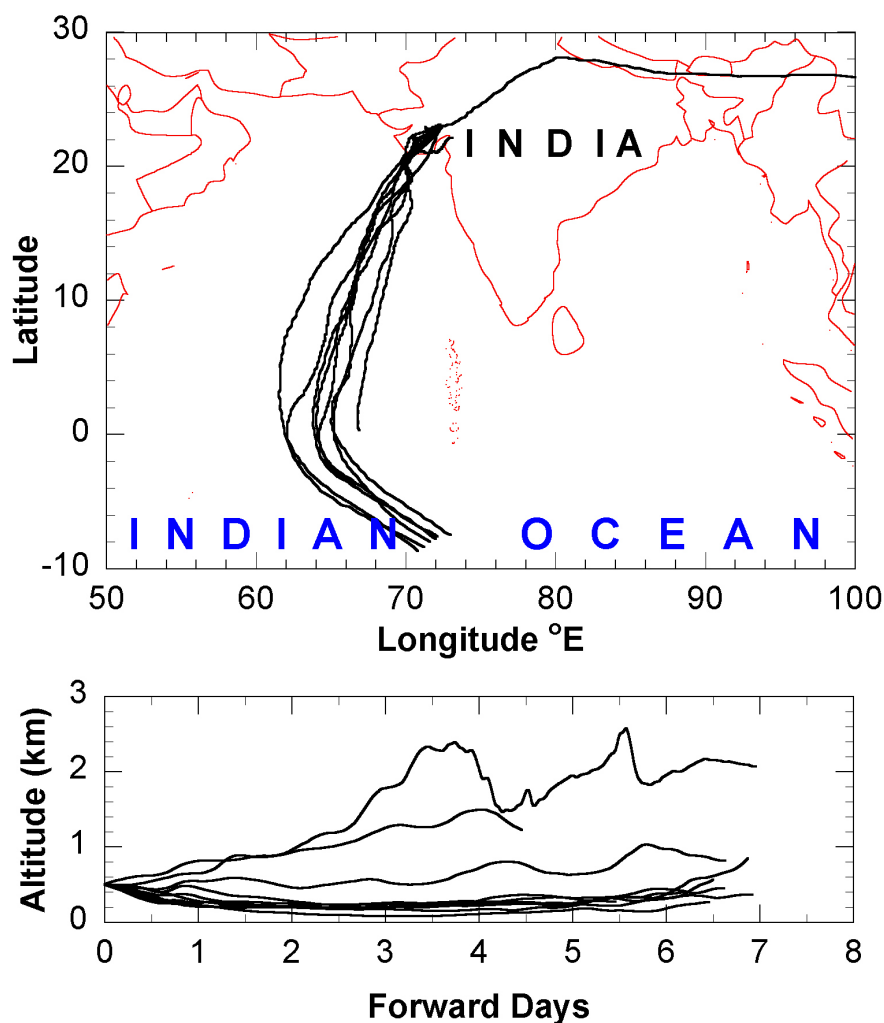


Figure 5.6 Three dimensional forward trajectories showing the air parcel flow from Ahmedabad to the Arabian Sea and Indian Ocean during January 23-27, 2000.

transported from Ahmedabad to more than 3000 km in its downwind side crossing the Arabian Sea to the Indian Ocean. The vertical motions of the trajectory show that most of the forward trajectory resided within the marine boundary layer. However, similar to the horizontal transport in downwind of urban centers, ozone and its precursors can also get transported to the free troposphere by convection and turbulent activities under suitable meteorological conditions in summer [Lehning *et al.*, 1998; Donnell *et al.*, 2001]. In the free troposphere ozone has longer lifetime and may have more climatic implications than in the atmospheric boundary layer. Since these are the first results of this kind from India, it is difficult to explain the quantum of the ozone production by other major urban centers. Apart from the climatic implications, the landlocked urban centers like Delhi, etc. may have

significant health and crop implications in the rural areas on its downwind side in the Indian subcontinent. Though the transport of pollutants from the urban region over long distances is an established fact in North America [*White et al.*, 1983; *Trainer et al.*, 1995; *Xiude et al.*, 1996; *Aneja et al.*, 1999], the present study suggests that the regions in the vicinity of the Indian urban regions will influence the composition of the relatively cleaner air in downwind sides at longer distance significantly.

Chapter 6

Trace gases at remote site: Mt Abu

Some of the chemical pollutants in the free troposphere have longer lifetimes, as there is reduced loss due to surface deposition. Longer lifetimes of the pollutants mean a greater chance of their long-range transport. The remote free troposphere is continually affected by these large-scale transports of anthropogenic and biogenic trace gases. In the background atmosphere, photochemistry and physical deposition combine to process a variety of trace gases. If the measurement site is elevated from surroundings and is also remote from the local sources, ozone related pollutants emitted at distant places may not reach there in enough quantity and chances of production of ozone by *in situ* photochemistry is very less. Ozone levels at such high altitude sites are mainly maintained by horizontal as well as vertical transport. These features of short and long-range transports with diurnal photochemistry and seasonal variations can be used to study ozone and other trace gases at local and regional scales.

6.1 Introduction

Impact of trace gases on the atmospheric chemistry and environment is being realized, particularly in the rapidly developing countries in the tropics and subtropics, which are also the regions (particularly in the Asian region) of very limited measurements. Among the trace gases, ozone plays an important role in composition and climate of the atmosphere. It is a secondary pollutant, a significant contributor in deciding the oxidizing capacity of the troposphere and an important greenhouse gas. There is a large variation in its growth rate in different regions of the world [e.g. *Logan et al.*, 1999 and references therein] leading to a large uncertainty in estimation of its contribution to global warming. It is known that there are two sources of tropospheric ozone, photochemical production [e.g. *Fishman and Crutzen*, 1978; *Lin et al.*, 1988] and downward transport of ozone rich air from the stratosphere [e.g. *Levy et al.*, 1985]. Details of the sources of ozone and its precursors and the different processes governing their budgets are given in *Chapter 1*.

Several studies have shown the impact of pollutants from Asia on the other parts of the world [e.g. *Jacob et al.*, 1999]. Importance of the tropical troposphere has been shown by *Portmann et al.* [1997] and *Martin et al.* [2000] highlighting the role of regional radiative forcing, biomass burning and lightning activities. Increase in anthropogenic sources together with natural features like higher solar radiation and water vapor leading to intense photochemistry, makes this region important to study the tropospheric chemistry. There are some studies of trace gases over the Pacific Ocean which were transported from the East Asia [e.g. *Akimoto et al.*, 1996; *Pochanart et al.*, 1999; *Mauzerall et al.*, 2000]. However, studies over the South Asia and its transport of O₃ over other regions including marine regions are very limited. Recently, measurements made over the Indian Ocean during INDOEX program have shown transport of plumes from the Indian subcontinent to the Arabian Sea and the Indian Ocean [*Lelieveld et al.*, 2001]. However, sources of such plumes are not well understood and this has been a topic of discussion [*Lal and Lawrence*, 2001; *Lelieveld et al.*, 2001]. In general, India is second after China for various emissions and energy consumption in Asia and first in the South Asia [*Akimoto and Narita*, 1994; *Aardenne et al.*, 1999]. Increasing ozone concentrations have already been observed in India [*Naja and Lal*, 1996].

Mt Abu (24.6°N, 72.7°E, 1680m) is situated in Western India, about 250 km from the Arabian coast, as shown by a asterisk in *Figure 6.1*. This station is in boundary layer during daytime and in free troposphere (FT) during nighttime. This temporal change in the BLH gives a good opportunity to understand the transport of trace gases from the boundary layer (BL) to the free troposphere. In addition, under seasonally changing wind patterns, this station being in the

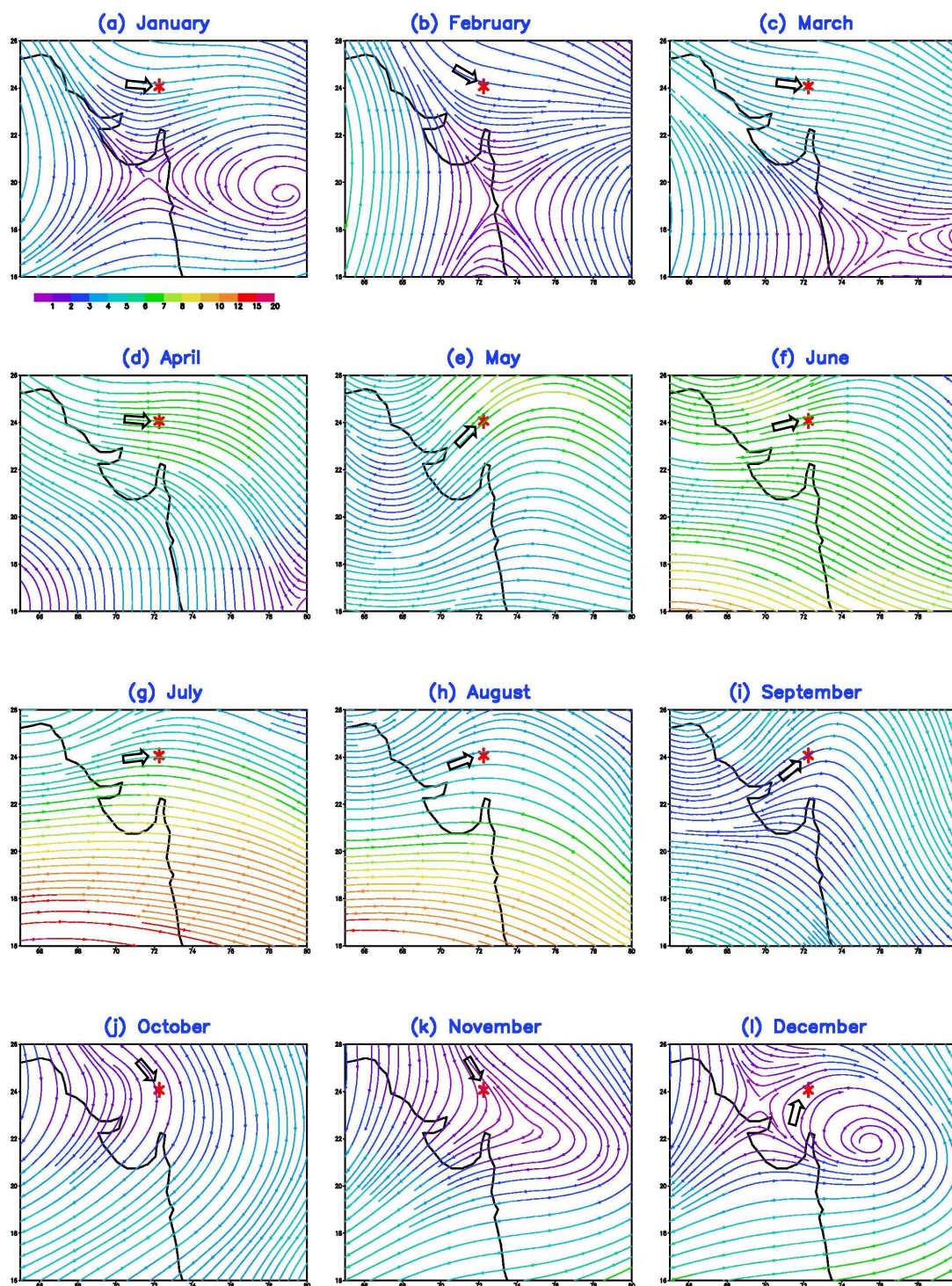


Figure 6.1 Monthly averaged NCEP wind field lines at 850 mb pressure level during different months of year 2000. The color bar represents the wind velocity. The position of Mt Abu is shown by asterisk. The bigger arrow shows the direction of wind flow arriving at Mt Abu.

FT during night, becomes very important for regional study of horizontal transport of trace gases in south Asia. So far, there has been no report of such systematic measurements of ozone and precursors at a high altitude site in this region.

This chapter presents continuous measurements of ozone, CO, NO and solar flux at an elevated remote site, Mt Abu in India during the year 2000. Some data collected during 1999 are also incorporated in this study. Mobile Lab Experiments-vertical (MOLEX-V) were conducted to measure O₃ from the bottom of the mountain to its top/peak to understand the boundary layer and free tropospheric processes.

6.2. Experimental site and general meteorology

Measurements were made at a remote mountaintop called Gurushikhar (24.6°N, 72.7°E, 1680 m) (henceforth, only Mt Abu will be mentioned) at Mt Abu in India. This elevated site is part of the *Aravalli* range of mountains and is the highest in entire western-central India. The main town, hill resort of Mt Abu, is situated at a height of 1220m with a population of about 20,000. But only 5-10 staff members stay at the measurement site. Nearest urban city Ahmedabad (23°N, 72.6°E, 49m), is about 180 km from Mt Abu. *Figure 6.1* shows the monthly wind field lines at 850hPa during 2000. These wind data are taken from the National Center for Environmental prediction (NCEP). In general, at Mt Abu, the northwest winds dominate in winter and southwest winds in summer. However, the meteorology over the Indian subcontinent is complex and different than the rest of the world [e.g. *Asnani*, 1993; *Lelieveld et al.*, 2001]. Measurements of wind direction, made at a nearby surface station, Ahmedabad, also show similar features of change in wind patterns as observed at Mt Abu [*Lal et al.*, 2000]. At Mt Abu, after September, wind pattern changes dramatically from southwesterly to northeasterly, which continues till February with some dominance of northerly winds. During early spring (March), wind pattern is northwesterly which changes gradually to southwesterly in late spring (May) and it dominates during entire summer period (June, July and August). This change in wind fields can also be seen by the monthly horizontal u (west to east) wind and v (south to north) wind components. The u wind is always positive showing net flow of wind from west to east. However, there are some seasonal variations in v winds. In summer/monsoon months the v wind is positive (south to north) whereas it is negative (north to south) in month of autumn and winter. The temperature difference in summer and winter seasons is about 14 °C, as shown in *Figure 6.2a*. The summer months shows large convective activity at Mt Abu, as shown by the w (vertical rate of change of air motion is called w or *omega*) component of wind in *Figure 6.2c*. The rate of ascent of air in summer is higher than the rate of descent in winter at Mt Abu. The months of June, July and August showing highest precipitable water content, are the monsoon months (*Figure 6.2b*). This is further confirmed by the total and UVB solar fluxes data taken at Mt Abu, as shown in *Figure 6.3*.

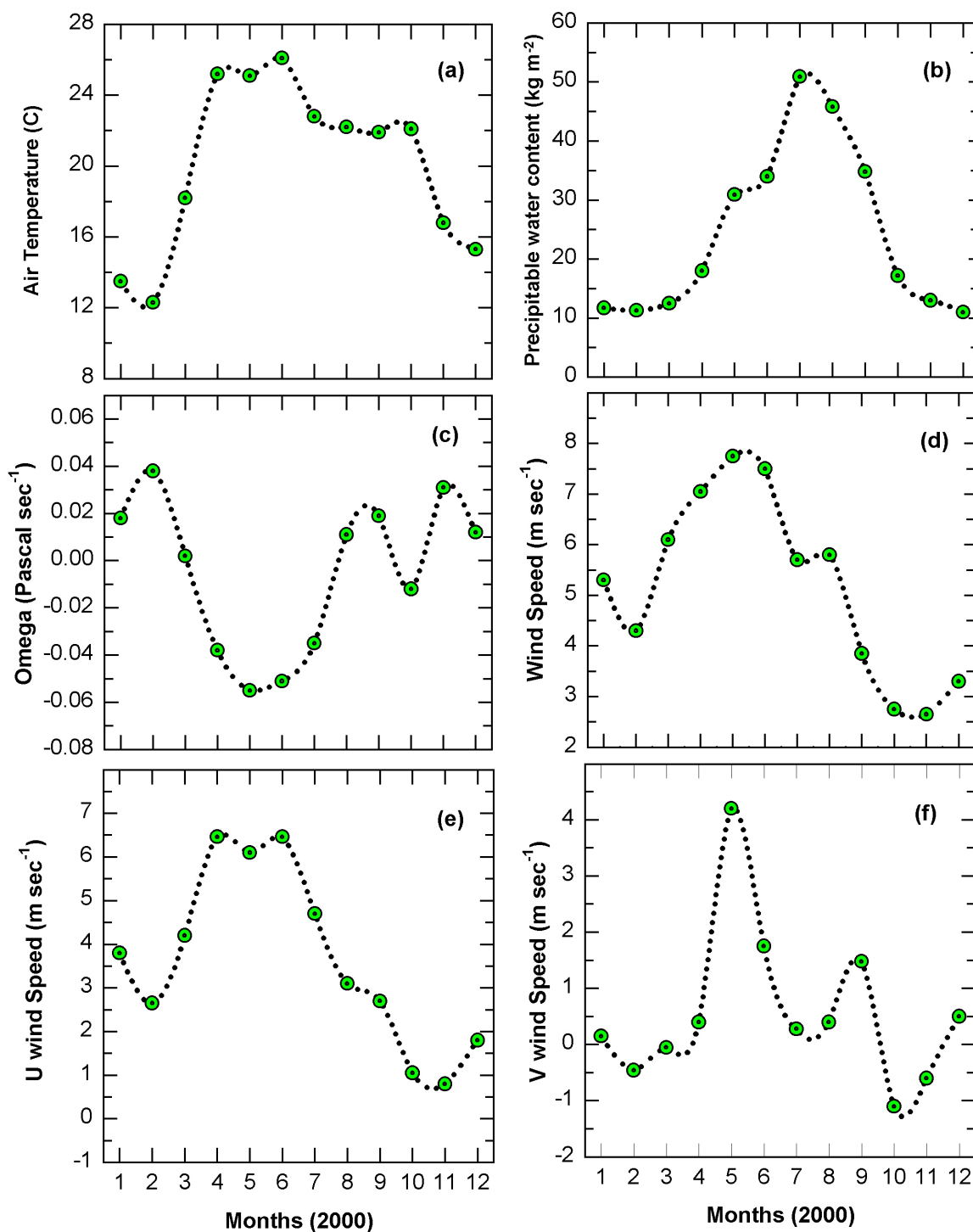


Figure 6.2 Monthly mean meteorological parameters at 850 mb pressure level during different months of year 2000.

Measurements of ozone were initiated in April 1993. Preliminary results on ozone and its precursors have been studied by *Naja* [1997]. However, detailed measurements along with solar flux, nitric oxide (NO) and carbon monoxide (CO) were taken only in year 2000. Ozone measurements at Mt Abu were made using ozone analyzer (Environmental S. A. Model 31M, France). Measurements of CO and NO were taken using analyzers from Monitor Labs and ECO-PHYSICS respectively. Details of these instruments and calibrations were given in *Chapter 2*.

6.3 Diurnal variations in ozone

Average diurnal variations of surface ozone during different months of 1999 and 2000 are shown in *Figures 6.4* and *6.5*. Daytime photochemical buildup in ozone, like that at urban or rural sites, is not observed throughout the year at this site. On the contrary, lower ozone mixing ratios are observed during daytime. However, the types of diurnal variations are different in different seasons. Three types of diurnal variations in ozone are observed in general. Type (i) is generally observed at cleaner remote elevated sites [e.g. *Oltmans and Komhyr, 1986; Kajii et al., 1998; Pochanart et al., 1999; Tsutsumi and Matsueda, 2000; Gallardo et al., 2000*]. This type of

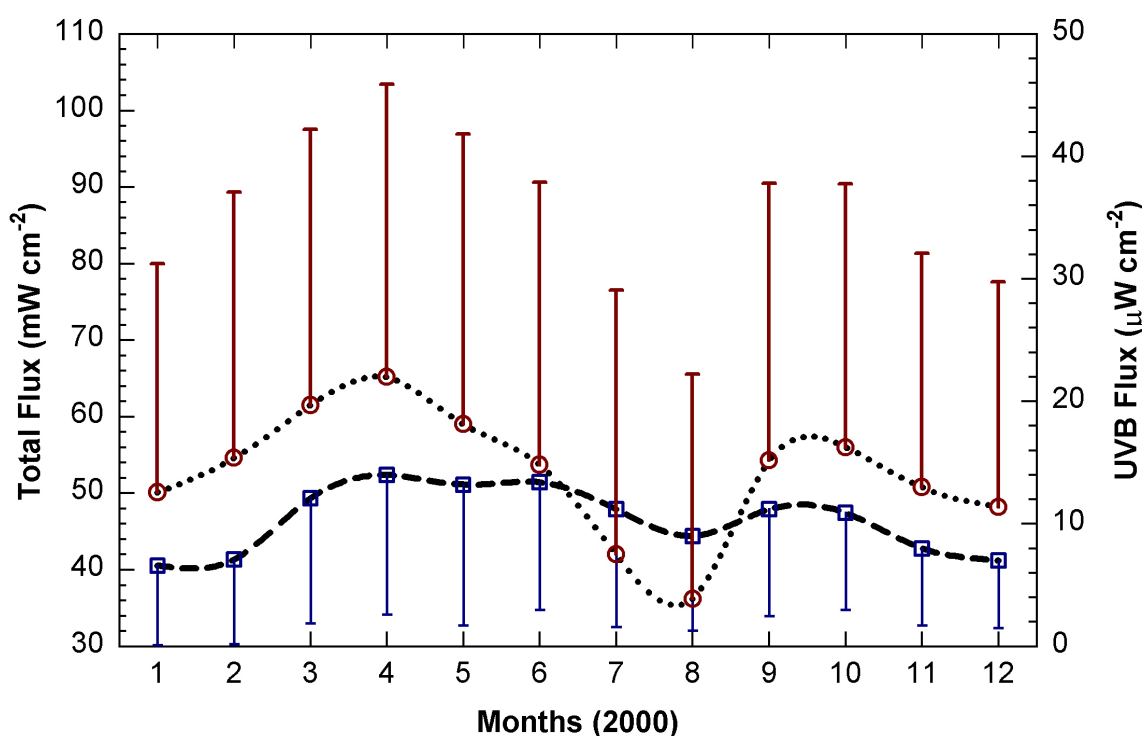


Figure 6.3 Monthly mean total flux (circles) and UVB flux (squares) in different months of year 2000. One side bar shows the 1σ variation.

diurnal variation at Mt Abu shows minimum ozone in local noon and maximum in night hours from September to February (see *Figure 6.5*). Ozone diurnal variation of type (ii) is a bimodal in nature and it shows two peaks and one dip during the day. This type of diurnal variation is observed from March to May. Such bimodal diurnal variation appears to be specific to Mt Abu. The daily change in wind pattern from cleaner and semi-rural sites can lead to this type of diurnal variation. Diurnal pattern of type (iii) are of semi-rural nature, showing daytime ozone production in afternoon/evening hours. Such diurnal variations are observed in summer months. In summer, the transport of pollutants from boundary layer to the free troposphere could play significant role in producing this type of diurnal variation. At nighttime, the presence of temperature inversion isolates ozone at the surface levels from that of upper levels, as there is no

or very little vertical mixing between the surface levels and the levels above nocturnal boundary layer (NBL). In daytime, when the inversion layer lifts up, the air starts mixing between the BL and FT. Since mixing is a function of height from surface, the type and magnitude of diurnal variation depends on the height from the surface of the BL. With increase in height, the

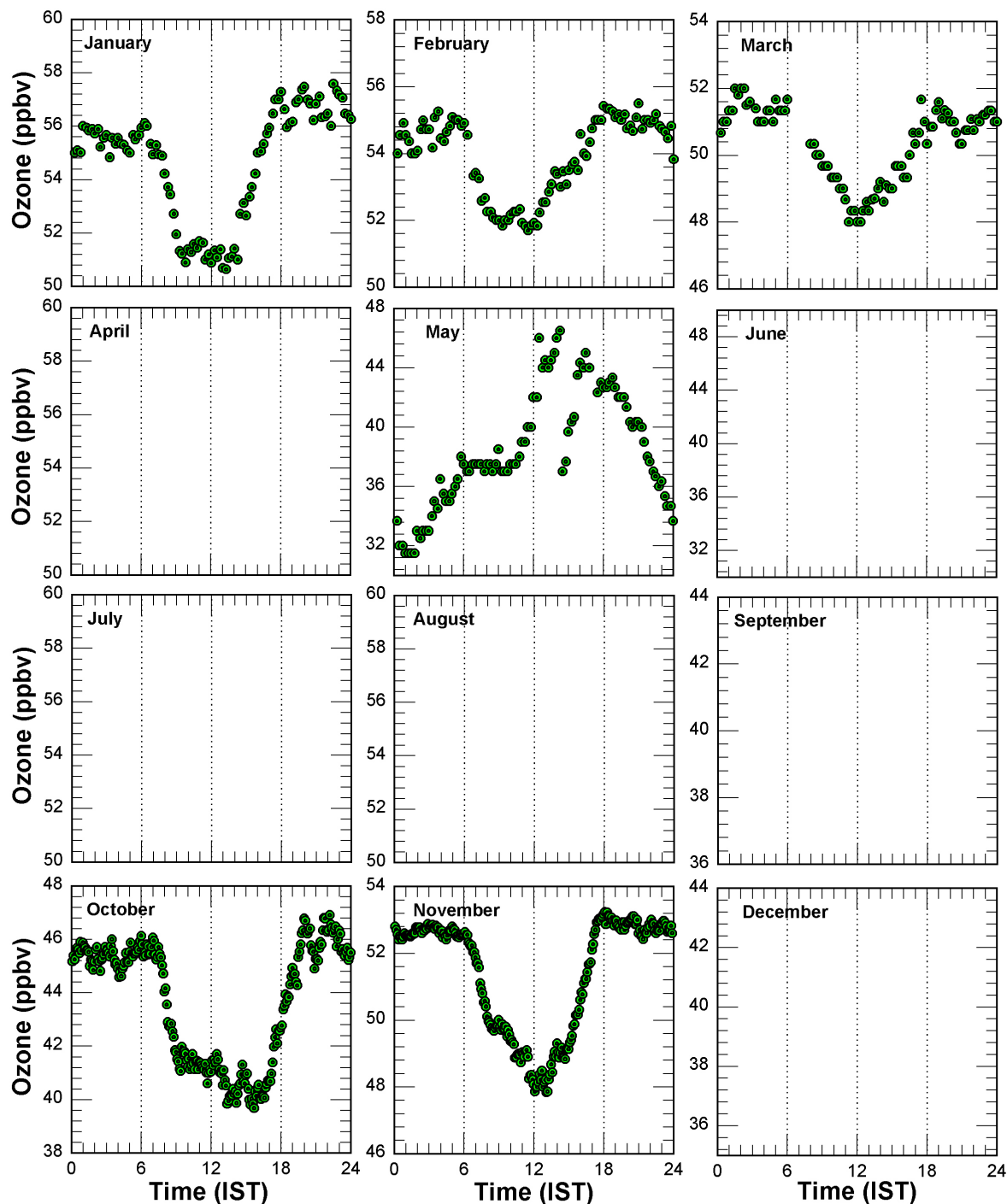


Figure 6.4 Monthly mean diurnal variations of ozone during 1999. The missing boxes represent no observation months.

amplitude of diurnal variation decreases and it seems that the morning minima at surface levels becomes the main noontime dip. In a detailed study of diurnal variations, *Aneja et al.* [2000] have shown similar results from the measurements taken at different heights of a tall tower.

However, there are some higher altitude sites showing ozone production in noon hours [e.g. *Oltmans and Levy, 1994*].

Here, the periods of December-January-February (DJF), March-April-May (MAM), June-July-August (JJA) and September-October-November (SON) are characterized as winter, spring,

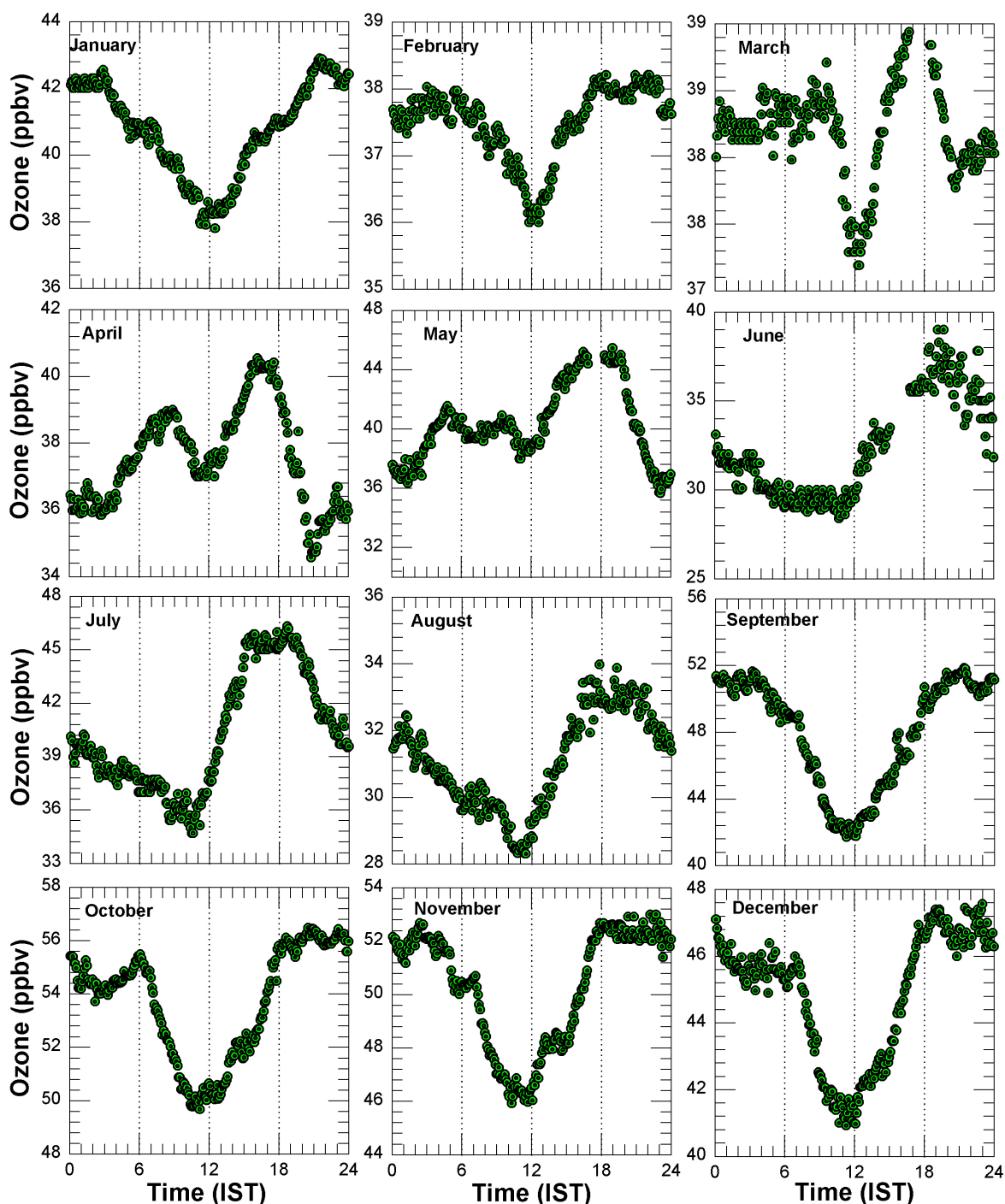


Figure 6.5 Same as Figure 6.4 except for year 2000.

summer/monsoon and autumn seasons respectively. Lowest amplitude (2 ppbv) of diurnal variation is observed in the month of March (Spring) whereas the highest amplitude (~11 ppbv) is observed in July (summer/monsoon). Thus, seasonal average diurnal amplitudes (peak-to-

Table 6.1: Monthly average ozone and solar fluxes with 1σ at Mt Abu during 1999-2000

Period of Study		Ozone (ppbv)			UVB Flux ($\mu\text{W cm}^{-2}$)		Total Flux (mW cm^{-2})		
Year	Month	Mean $\pm\sigma$	Mode	Data Points	Mean	SD	Mean	SD	Data Points
1999	January	54.7 \pm 9.9	48	1710	--	--	--	--	--
	February	53.8 \pm 4.9	52	1127	--	--	--	--	--
	March	50.3 \pm 3.7	46	284	--	--	--	--	--
	April	--	--	--	--	--	--	--	--
	May	38.7 \pm 5.4	37	228	--	--	--	--	--
	June	39.4 \pm 8.4	36	74	--	--	--	--	--
	July	--	--	--	--	--	--	--	--
	August	--	--	--	--	--	--	--	--
	September	--	--	--	--	--	--	--	--
	October	43.6 \pm 18.4	41	8796	10.3	8.5	48.2	34.3	8796
	November	51.4 \pm 4.8	50	8588	8.3	6.6	50.2	30.2	8588
	December	--	--	--	--	--	--	--	--
2000	January	40.8 \pm 5.5	40	8885	6.6	6.5	50.1	29.9	8885
	February	37.6 \pm 3.1	36	8303	7.1	6.9	54.6	34.7	8303
	March	38.3 \pm 4.9	37	8928	12.1	10.2	61.5	36.0	8928
	April	37.6 \pm 5.5	36	6997	14.0	11.4	65.2	38.2	6997
	May	40.5 \pm 7.3	37	5543	13.2	11.5	59.0	37.9	5543
	June	32.1 \pm 7.6	29	1156	13.4	10.4	53.7	36.9	1156
	July	36.3 \pm 10.3	32	4521	11.2	9.6	42.0	34.5	4521
	August	31.1 \pm 7.8	28	8755	9.0	7.7	36.2	29.3	8755
	September	48.5 \pm 9.7	47	4040	11.2	8.7	54.3	36.2	4040
	October	53.7 \pm 9.1	52	8860	10.9	7.9	56.0	34.4	8860
	November	50.3 \pm 8.0	48	8597	8.0	6.3	50.8	30.5	8597
	December	44.7 \pm 7.6	44	8833	7.0	5.5	48.2	29.4	8833
2001	January	41.2 \pm 5.3	39	4014	6.9	6.5	51.2	30.1	4234

peak) during different months are found to be 2-11 ppbv at Mt Abu. Rate of change in ozone mixing ratios before noon hours ($d[O_3]/dt$) varies in different months. The highest and lowest decrease rates ($d[O_3]/dt$) are observed in the months of September (2 ppbv hr^{-1}) and June (0.4 ppbv hr^{-1}) respectively. Detailed monthly averages of ozone and solar flux results are given in *Table 6.1*.

The boundary layer height over land in the tropics varies from 1000m to 3000m depending on the season and place [*Stull, 1994*]. BL touches the observational site at Mt Abu in daytime during some of the months in summer/monsoon. Therefore, air at this observational site is well mixed with the surface level air during daytime due to turbulent and convective mixing. This well mixed air may decide the diurnal variations in ozone and its levels at the observational site during daytime. The mixing height is very low (below about 200-500 m) and observation site remains well above the mixing height during evening and night hours. In this case the air at the mountaintop itself controls levels of ozone and its variations during evening and night hours at the observation site. The clean air, generally poor in ozone, arrives at the observation site at mountaintop mainly from the Arabian Sea and the Indian Ocean during summer/monsoon, hence lower ozone levels are observed during evening and nighttime in these seasons. However, polluted air, which is rich in ozone, reaches the observational site from the continental region during autumn and winter and thus show higher ozone levels during evening and nighttime in these seasons (*Figure 6.1*). A close analysis of monthly mean ozone diurnal patterns for different months reveal a clear change in diurnal patterns after September, when northeast wind pattern sets in and again a clear change in diurnal pattern after February, when southwest wind pattern begins (see *Figure 6.5*). Therefore, it appears that the boundary layer mixing and seasonal change in wind pattern over this region play important roles in changing diurnal patterns.

6.3.1 Low ozone levels in daytime

Basically, there are three main processes which can lead to low ozone in daytime at this mountain site, viz (i) diurnal variation in boundary layer height (ii) mountain-valley induced wind flow system, and (iii) chemical ozone loss in low NO environments [e.g. *Oltmans and Komhyr, 1986; Lin et. al., 1988, Donnell et al., 2001*]. Measurements show that convection is important in transport of pollutants from the boundary layer to the free troposphere [*Stohl and Trickl, 1999; Donnell et al., 2001*]. Once BLH crosses the observational site, there is change in signature of the air from free troposphere to the boundary layer or from boundary layer to the free troposphere. The diurnal variation at the observational site is decided by the concentration of ozone in the BL. If O_3 is higher in BL than in FT, the ozone levels will start increasing as soon as

the observational site is within the BL. Such patterns are more prominent in months of May to August (summer/monsoon) when the convective activity is intense (*Figure 6.5*). These convective activities in summer can prolong the BL air up to higher heights and this leads to higher amplitude of diurnal variation in ozone during these months. On the other hand, in winter, the observational site is in the FT most of the time of the day. It may encounter BL air only for short time (few hours) during noon hours. The mixing of the air from BL to the free troposphere is for a shorter time in winter, which leads to lower amplitude of diurnal variation.

The other mechanisms of daytime ozone losses are by surface deposition on upslope of mountain and *in situ* loss by chemistry in high OH and low NO levels. The air moves along the slopes of mountain due to warm upslope winds after the sunrise. Therefore, air reaching the observatory at the mountaintop may have had a long path of travel along the mountain slopes and thereby resulting in ozone loss during daytime due to surface deposition. Maximum effect of this process, leading to maximum ozone loss, should occur during noontime. Down-slope winds, resulting from radiative cooling of the mountain surfaces, bring down the ozone rich air in from aloft after the sunset. This may cause a gradual buildup in ozone during evening/night hours.

Similar to Mt Abu, transport of pollutants from BL to FT is also elaborated in previous works in Europe [*Forrer et al.*, 2000]. The tropical high altitude site, Mauna Loa (20°N, 3397m), is also reported to have strong effects of the mountain-valley induced wind flow patterns on the diurnal variations of ozone [*Oltmans and Komhyr*, 1986; *Oltmans and Levy*, 1994]. In winter, decrease in ozone continues until afternoon at Mauna Loa, similar to at Mt Abu (*Figure 6.5*). Minimum ozone mixing ratio is observed to be around 1400 hrs at Mauna Loa, which extends till about 1700 hrs. Lowest ozone mixing ratios are observed around 0900-1200 hours at Mt Abu, which start increasing afterwards (*Figures 6.4, 6.5*). Therefore, unlike at Mauna Loa, lowest ozone mixing ratio at or before 1200 hour (noontime) and its recovery after that suggests that contribution of upslope/downslope wind is not appearing to play an important role in explaining the diurnal variations in O₃ at Mt Abu.

It has been shown that the topography is favorable for mountain-valley induced wind flow patterns at Mauna Loa hence leading to ozone loss due to this process [*Oltmans and Levy*, 1994]. However, mountains near Mt Abu are not spread in a large region and do not form valleys. Therefore, it is not much favorable for longer mountain-valley induced wind flow pattern. A high altitude site in Japan, Mt Fuji (35.4°N, 3776 m), does not show very significant effect of upslope/downslope wind patterns [*Tsutsumi and Matsueda*, 2000]. Observation site at Cerro Tololo, Chile (30°S, 2200 m) is reported to have possible contribution of mountain-valley wind flow system only during spring and summer, with smaller diurnal amplitude [*Gallardo et al.*, 2000].

Chemical ozone loss in the environment of lower NO mixing ratio is the other possible reason for lower ozone values during daytime. *Figure 6.6* shows diurnal variations in NO mixing ratio at Mt Abu during the year 2000. The maximum levels in NO are observed much later (1300-1500 hours) than the minimum value in ozone (before 1200 hour). Also, ozone and NO do not show

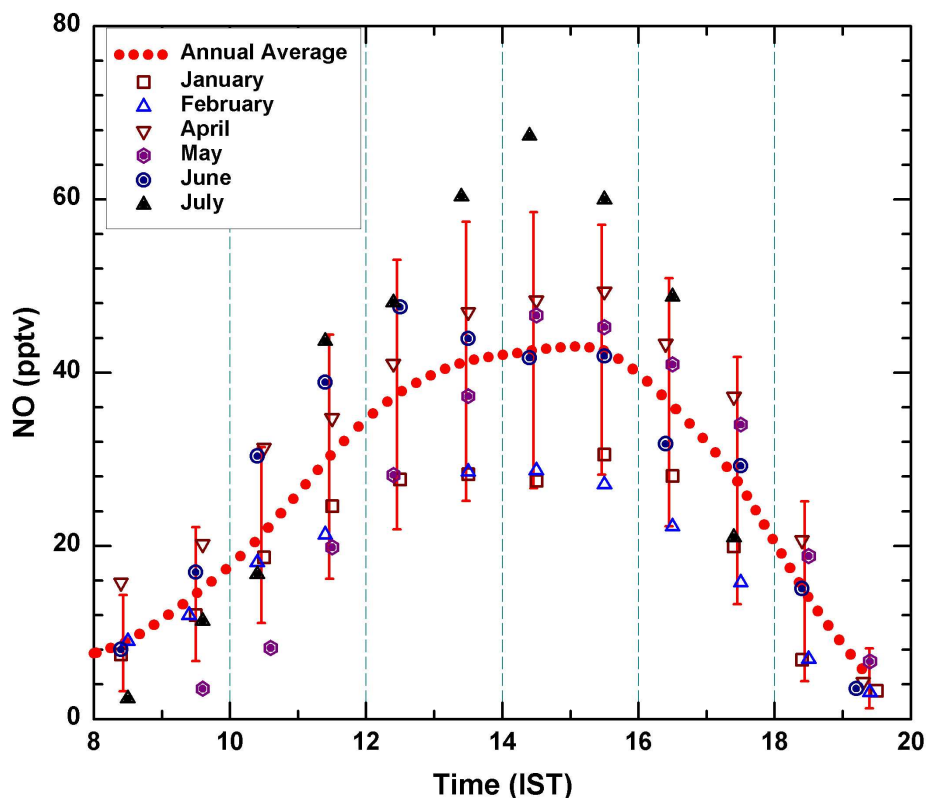


Figure 6.6 Monthly mean nitric oxide (NO) during different month of year 2000. At least 5 days data are averaged in each month. Dotted line is its mean annual diurnal variation. The bar shows the 1σ variation.

any relation between them (not shown here). These observations suggest that instead of chemistry, horizontal and vertical transport plays significant role in ozone loss in daytime at Mt Abu.

6.3.2 Background ozone level

It may be assumed that the nighttime ozone levels in the air near mountaintop of Mt Abu may be representative of the background ozone levels over this region, as convective mixing and photochemistry are not active during nighttime. Thus, during spring-summer seasons, the air mass coming from the Arabian Sea and the Indian Ocean (southwesterly wind) should represent the background ozone levels from these marine environments. Nonetheless the nighttime ozone levels during autumn-winter seasons, when air mass is generally coming from continental region (Indian Peninsula), (northwesterly wind, as shown in *Figure 6.1*) should represent the continental

ozone levels. Using these features, the background levels of ozone for the surrounding continental (northwest) and marine (Arabian Sea) environments can be calculated. The diurnal patterns are also clearly different for these two sets of seasons. This classification provides the background marine ozone level of 36.0 ± 14.6 ppbv and the background continental ozone level of 44.7 ± 9.1 ppbv. Similar or little higher ozone levels in background air mass (32-45 ppbv) and regional polluted air mass (44-57 ppbv) are estimated for the East Asia [Pochanart *et al.*, 1999]. Further, it can also be suggested that the difference between these two ozone levels from the present study, which is about 9 ppbv, would be the amount of ozone transported to Mt Abu from the continental region. However, these estimates of ozone levels could be considered as first order approximations only, as the wind pattern (northwest) during the respective three months period may not be uniform.

Seven days back vertical trajectory (BT) analysis shows that most of the time the observed air at Mt Abu descended from the free troposphere except during few months of summer (*Figure 6.7*). In summer, the air ascends from BL or gets advected from the southwest

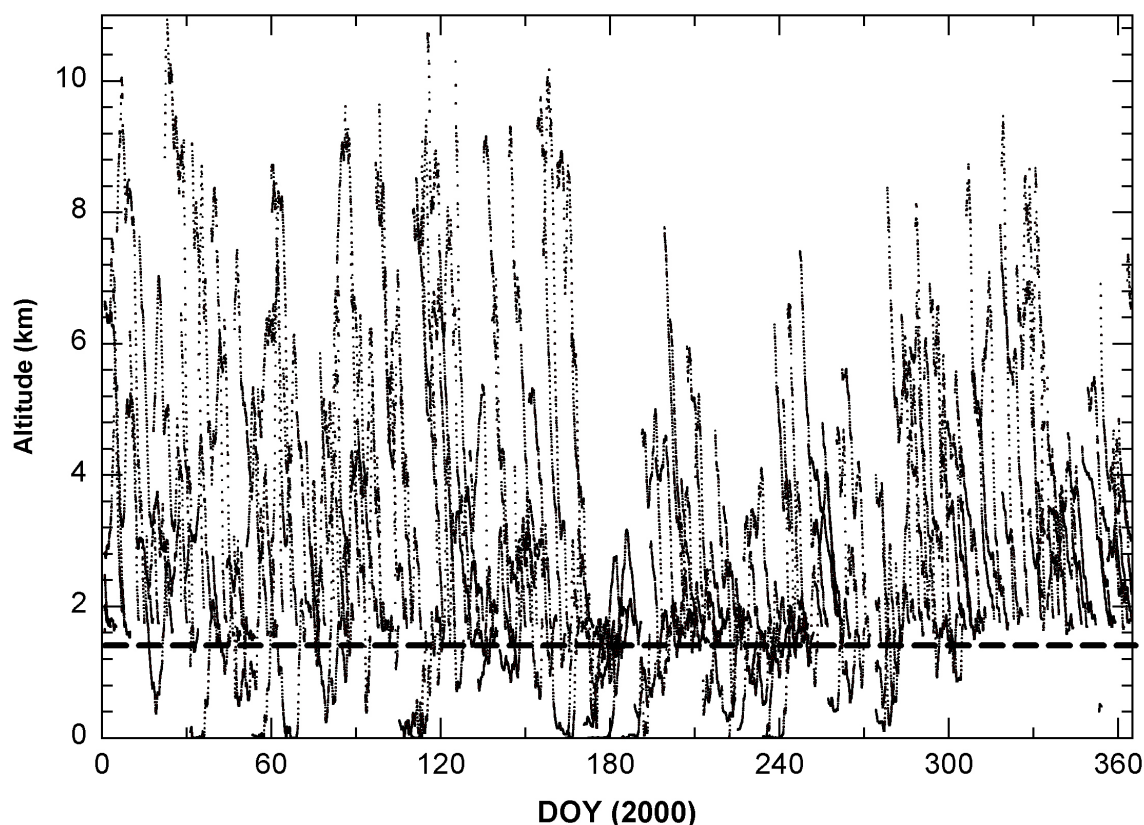


Figure 6.7 One dimensional 7 days back trajectories arriving at Mt Abu in each day at 1200 hours at local time. The dashed line marks the altitude of Mt Abu.

and reaches Mt Abu. This feature of ascending air in summer is also confirmed by its vertical motion (ω) at 850mb, as shown in *Figure 6.2c*. The vertical analysis of air parcels (using BTs) and rate of change of pressure (dP/dt , ω in Pascal sec^{-1} , using NCEP winds) show that Mt Abu is in the free troposphere most of the time of the year except in summer. Hence, these

BTs and omegas values confirm the nature of the wind flow assumed in last paragraph for calculating the regional background levels of ozone in winter and summer.

6.4 Seasonal variations in ozone

Monthly averaged ozone mixing ratios at Mt Abu show a systematic seasonal variation with maximum and minimum ozone levels of 53.7 ± 9.1 and 31.1 ± 7.8 ppbv in months of October and August respectively (Figure 6.8), resulting in a difference of about 23 ppbv. The maximum ozone is observed just after the wind pattern changes from southwest to north/northwest in month of September. The minimum monthly mean ozone mixing ratio is due to southwest wind flow from Arabian Sea during monsoon time (Figure 6.8). However, very low ozone levels as low as about 5 ppbv are also observed during rainy days. This ozone poor air might be due to clean air transported from the remote marine environments of equatorial Indian Ocean where such low levels of ozone were observed during INDOEX cruises [Chand *et al.*, 2001b]. In general,

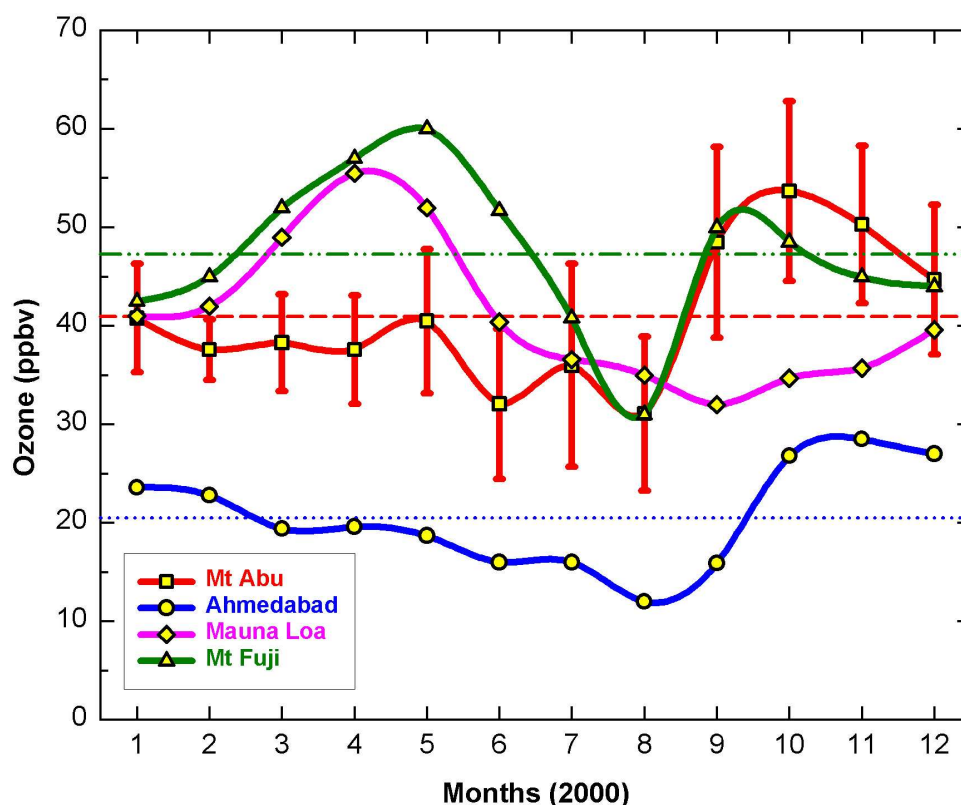


Figure 6.8 Monthly mean ozone mixing ratios at Mt Abu (24.6°N , 1680m asl) during 2000. Comparison is made with seasonal variations at Mt Fuji (35.4°N , 3776m asl), Mauna Loa (20°N , 3397m asl), and Ahmedabad (23°N , 49 m asl). The dashed line, dotted line and dotted-dashed line are annual averages at Mt Abu, Ahmedabad [Lal *et al.* 2000] and Mt Fuji [Tsutsumi and Matsueda, 2000] respectively. The Annual averages at Mt Abu and Mauna Loa are not significantly different. Mauna Loa seasonal variation is taken from Oltmans and Levy, [1994].

seasonal variation in average ozone at Mt Abu agrees well with the variability at Ahmedabad. Increase in ozone mixing ratio after the monsoon season is also clearly visible at both the sites. The important feature is that the amplitude of seasonal variation is more than two times higher the amplitude of diurnal variations at Mt Abu. This indicates that advection/convection (horizontal/vertical transport) predominates over photochemistry as well as vertical transport in ozone variability at Mt Abu.

The seasonal variation at Mt Abu is different than that observed at Mauna Loa (20°N, 3397 m asl) in Hawaii and Mt Fuji (35.4°N, 3776 m asl) due to the different roles of meteorology and topography of the mountains. The mixing ratios of ozone at Mt Abu are comparable or even higher during late autumn and winter than at these two other sites. Mt Fuji and Mauna Loa both show prominent maxima during spring, which are reported to be due to downward transport of ozone rich air from higher heights [Tsumi and Matsueda, 2000; Oltmans and Levy, 1994]. Other sites in the East Asia also show higher ozone levels during spring [Kajii *et al.*, 1998; Pochanart *et al.*, 1999; Mauzerall *et al.*, 2000].

6.5 Variations in O₃ and CO

Figure 6.9 shows a scatter plot of diurnal variation of CO and thick line is the best fit for all the data points observed during that year. CO shows a large diurnal variability in different months. However, there is not much change in the pattern of diurnal variations of CO for all these months. Nonetheless, the minimum and maximum levels of CO were observed after sunrise and afternoon hours respectively. The diurnal variation of CO and its lower concentration in nighttime and morning indicates FT nature of the site during these hours.

In a detailed study of trace gases at Ahmedabad, a strong daytime photochemical ozone buildup is shown due to photooxidation of precursor gases [Lal *et al.*, 2000]. But if we compare ozone levels at Mt Abu with Ahmedabad, noontime average ozone levels at Ahmedabad are lower than the average ozone values at Mt Abu during most of the times of the year. The difference in ozone at these two stations varies from 2 to 20 ppbv. Lowest difference is observed in winter whereas highest is observed in monsoon months. Therefore, the local/regional pollutants might not be contributing very significantly to the ozone amount at Mt Abu. The lower ozone levels at Ahmedabad indicate the lesser production of ozone by photochemistry at this site. At Mt Abu, it has also been observed that mixing ratio of ozone increases by more than two folds (23 ppbv to 56 ppbv) within 2-3 days on some occasions in spring and then gradually decreases. Therefore, higher ozone levels at Mt Abu, than those at Ahmedabad might be due to long-range transport of ozone rich air.

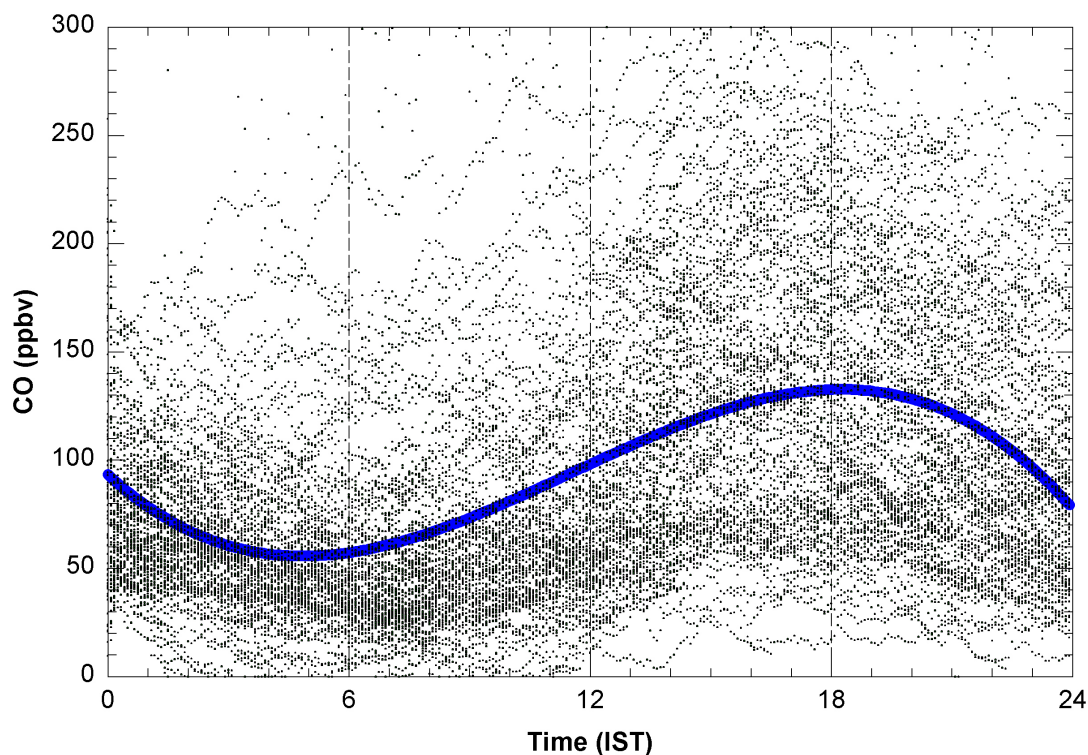


Figure 6.9 Diurnal variation in CO at Mt Abu during 2000. Each point represents average CO for 5 minutes. The thick line is best fit for its diurnal variation.

Figure 6.10 shows correlations in O_3 and CO for the available CO data at Mt Abu. The intercept is 45 ppbv and slope is 0.03 with very poor correlation coefficient ($r^2=0.04$). During INDOEX 1998 and 1999, this slope varied from -0.03 to 0.093 for different regions over the Arabian Sea and Indian Ocean. Table 6.2 provides a comparison of slopes and correlation

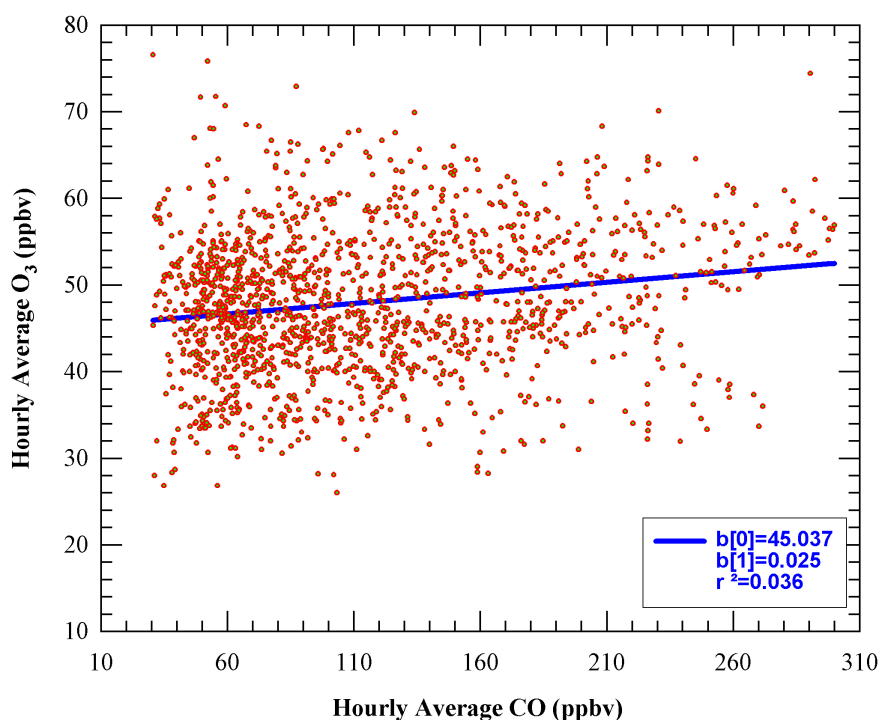


Figure 6.10 Correlation plot of hourly averaged CO and O_3 for the available data of CO during year the 2000 at Mt Abu.

coefficients with those at other observation sites in North America, Asia. *Chin et al.*, [1994] and *Parrish et al.*, [1998] suggested an average value of slope of about 0.3 for North America. However, studies made over the Asian region [*Kajii et al.*, 1998; *Pochanart et al.*, 1999; *Tsutsumi and Matsueda*, 2000], including this work, show rather lower values of slope (see *Table 6.2*). CO serves as a tracer for combustion and ozone is produced from it. Therefore, if air is processed sufficiently, the correlation between ozone and CO will be stronger and slope will provide the information of ozone production per molecules of CO. It has also been suggested that, larger scatter and relatively lower correlation are the indicators of incomplete photochemical process [e.g. *Parrish et al.*, 1998]. Therefore different measurements over the Asian sites indicate the possibilities of incomplete photochemical processes. It has been shown recently that the ratio of combined anthropogenic NO_x sources (S_N) and total CO and hydrocarbon sources (S_C), i.e. S_N/S_C, is more than four times lower in Asia than in North America [*Lelieveld et al.*, 2001]. This indicates that ozone photochemistry in Asia is strongly NO_x limited and regeneration of OH by NO is inefficient. Due to NO_x limited chemistry, O₃ and CO may have poor correlations.

Table 6.2: Details of ozone-CO correlations from observations in North America and Asia.

Site (Lat, Long)	Ozone (ppbv)	CO (ppbv)	Slope	Correlation Coefficient	References
Sable Island (43.9N, 60.0W)	33.3	114	0.3	0.68	<i>Chin et al.</i> , 1994; <i>Parrish et al.</i> , 1998
Seal Island (43.4N, 66.0W)	38.9	129	0.31	0.74	<i>Chin et al.</i> , 1994; <i>Parrish et al.</i> , 1998
Cape Race (46.7N, 53.2W)	30.3	124	0.33	0.47	<i>Chin et al.</i> , 1994; <i>Parrish et al.</i> , 1998
Bermuda (32N, 64W)	11–65	65–255	0.27	0.65	<i>Dickerson et al.</i> , 1995
Oki (36.3N, 133.2E)	29–55	105–248	0.01 – 0.23	0.18 – 0.66	<i>Pochanart et al.</i> , 1999
Happo (36.7N, 137.8E)	40–70	151–236	~ 0.1	~ 0.2	<i>Kajii et al.</i> , 1998
Mt Fuji (35.4N, 138.7E)	25–60	92–159	0.09 – 0.19	0.41 – 0.50	<i>Tsutsumi and Matsueda</i> , 2000
Mt Abu (24.6N, 72.7E)	42±7	112±60	0.03	0.04	This work

6.6 Mobile lab experiments: O₃ and CO in BL and FT

So far we have been discussing the variability of trace gases at a fixed station at an altitude of 1680m above mean sea level (amsl) at Mt Abu. In order to understand the boundary layer processes like ozone loss in boundary layer and transport of ozone from boundary layer to the

free troposphere etc, MOBILE Lab EXperiments-Vertical (MOLEX-V) from the foot of the mountain (998 mb) to its top (Mt Abu, 838 mb) were conducted during autumn/winter months. The instrumental setup and other technical details during MOLEX-V are similar to the experiments mentioned in MOLEX-A in *Chapter 5*. The only differences in MOLEX-V and *Chapter 5*, MOLEX-A (A is for advection) are the differences in the sites and the objectives of the studies. In *Chapter 5*, MOLEX-A was used to study the horizontal transport (advection) of pollutants away from the source region where as MOLEX-V is focused on the vertical transport of pollutants from BL to FT and other BL processes.

Figure 6.11 shows the mobile track, position of the Mt Abu observatory and Mt Abu town. Mt Abu town is a plateau of about 2 km diameter. These experiments were conducted in

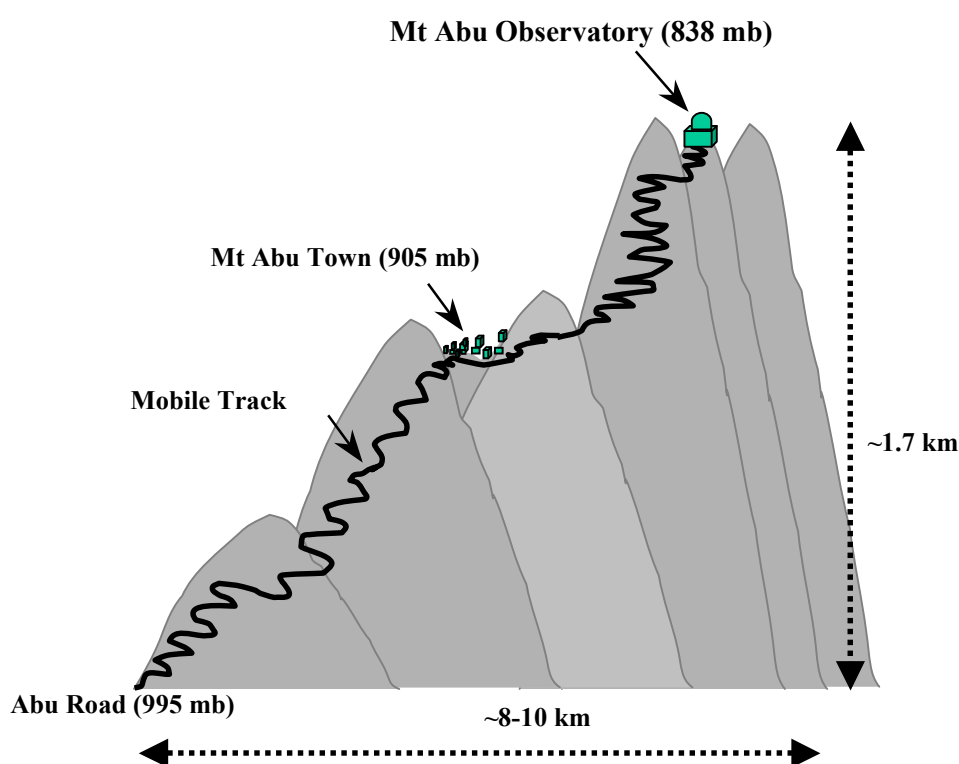


Figure 6.11 Track for the Mobile Lab Experiment-Vertical (MOLEX-V) conducted from the bottom of the Mt Abu to its top/peak in the months of October, November and December in 2000. In each month at least 28 up and down trips were made during day and night.

month of October, November and December in 2000. In each month the experiment was conducted for about a week. More than four vertical trips were made every night. Most of the trips/campaigns were conducted in the nights. However, some limited trips were also made in daytime in each month. Ozone, CO, atmospheric pressure and temperature data were observed at every 10 seconds and stored in a computer. Air temperature was measured using a thermistor. The atmospheric pressure was measured with a MKS, Baratron (221A) with an accuracy of 0.1mb. The pressure is used for deriving the height information.

Figure 6.12 shows the nighttime monthly average profiles during October, November and December in 2000. The temperature profile shows two boundary layer inversions, one at 960 mb and second was centered at 905 mb on the plateau at Mt Abu Town. A significant ozone loss of about 60-80% is found in both the boundary layers near the surface in all the three months of observations. To avoid the local effects due to moving vehicles, these mobile campaigns were conducted between 10 pm to 4 am (local times) when the traffic was almost nil. Due to this, the amount of NO would have been much lower and have chances of titration of ozone. The NO

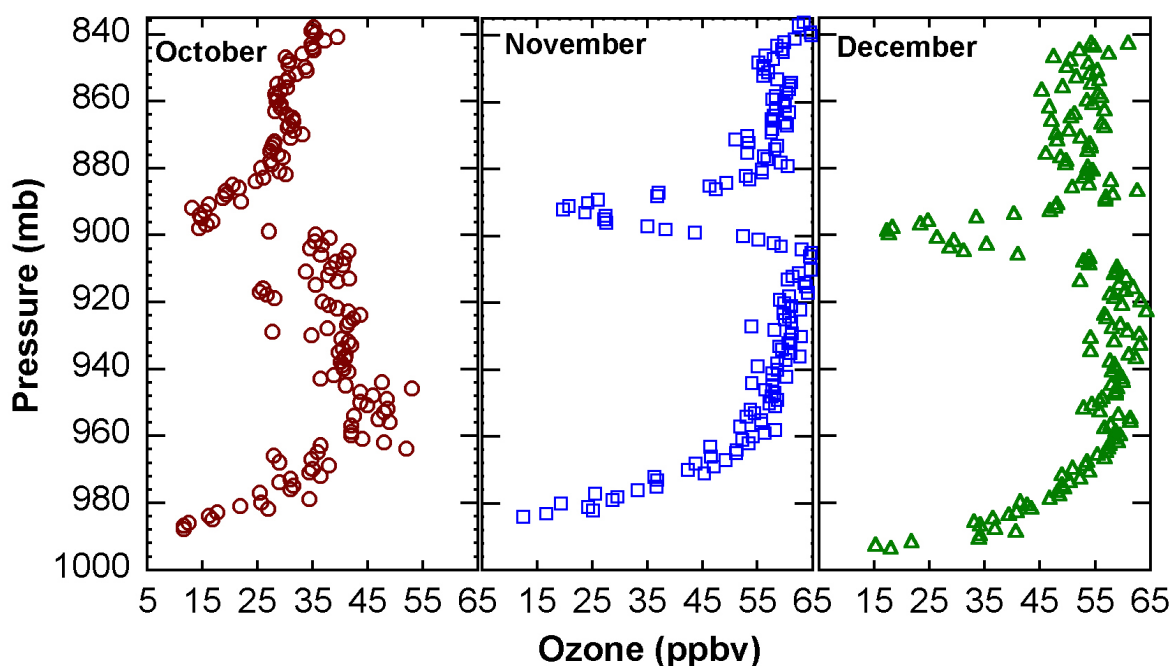


Figure 6.12 Average vertical profiles of ozone during night times for the October, November and December months of MOLEX-V observations. These observations were taken between 9 pm to 5 am local times. Each shown profile is a mean of at least 20 profiles. Standard deviations are not shown for the sake of clarity. All the data are within 95% confidence intervals.

observations taken at Mt Abu in different months vary between 20-70 pptv (see Figure 6.6). If we assume the highest levels of NO observed at Mt Abu to be present on the observational track, the maximum ozone loss by NO_x titration will be only upto 140 pptv which is very less compared to the observed ozone loss in the boundary layer. Hence, it is most probable that the ozone loss in the BL is only by surface deposition and not by the titration with NO_x and/or other chemical reactions. This assumption is confirmed by the observations of ozone during daytime hours. Figure 6.13 shows the ozone profiles for these three months in daytime hours. Here, it should be noted that some diesel vehicles (~15 vehicles and most of them were in light category) were encountered on the way and it may slightly affect the results. However, the NO_x emission by the diesel vehicles is very less compared to the petrol vehicles. All the daytime observations do not show ozone loss in the boundary layer. Also, the boundary layer inversion was almost zero or

very poor in daytime. Here, it is important to note that throughout the height regions, the ozone mixing ratios are lower in daytime (indicating daytime loss) compared to the nighttime levels on the mobile tracks. The average daytime ozone is lower by 5-10 ppbv (10-20 % of mean ozone) than the nighttime ozone profiles for all heights and months. This loss of ozone in daytime may be due to dilution/mixing of air having low ozone concentration within the boundary layer with the ozone rich air from the free troposphere when the air is mixed by turbulent and convective activities.

Figure 6.14 shows the profiles of ozone, CO and temperature for month of November. The two boundary layers are clearly reflected in these graphs. Here, it is interesting to note that

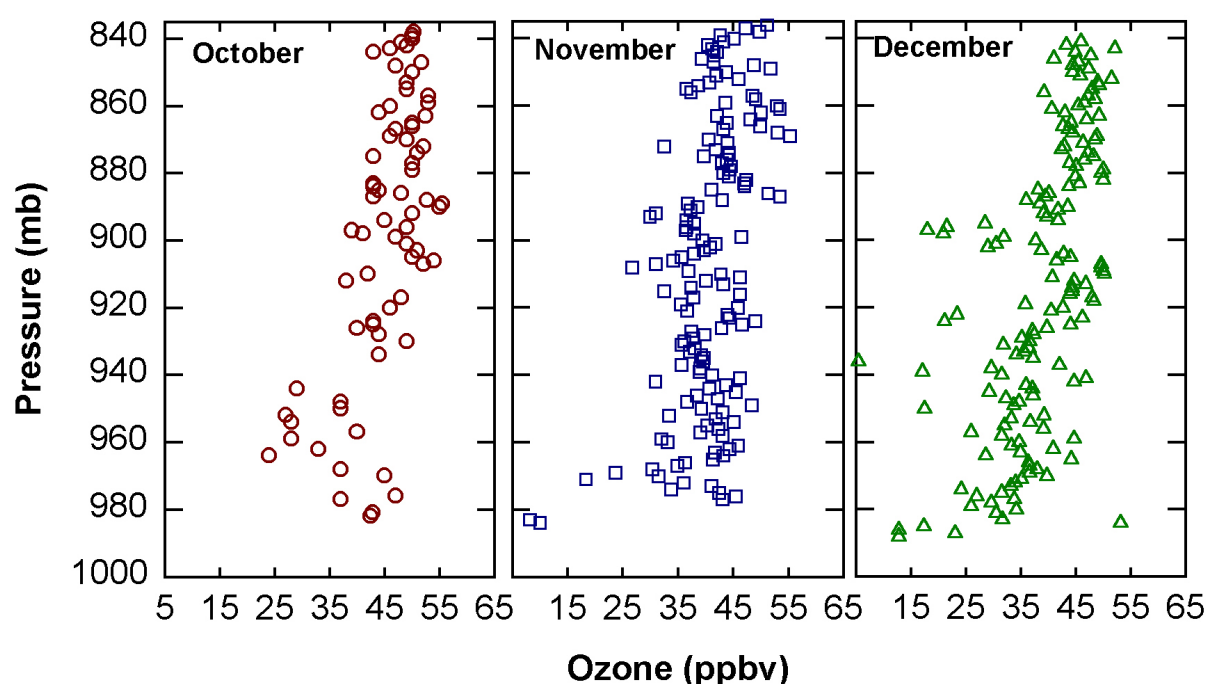


Figure 6.13 Average vertical profiles of ozone during day times observed in October, November and December months of MOLEX-V observations. These observations were taken between 10 am to 5 pm local times. Each profile is a mean of at least 8 profiles. Standard deviations are not shown for the sake of clarity. All the data are within 99% confidence intervals.

CO levels at Mt Abu are only in the range of 60-280 ppbv unlike at Ahmedabad [Naja, 1997; Lal et al., 2000] where the monthly CO levels are in the range of 400-1900 ppbv. Also, NO concentrations monitored in different months in 2000 are in the range of 20-70 pptv which is below the production limit of ozone.

All these factors viz (1) daytime ozone loss shown in its vertical profile, (2) noontime loss of ozone as shown in its diurnal variation at Mt Abu and (3) low concentrations of NO having no correlations with ozone and CO at Mt Abu suggest that NO and CO are not playing much role in ozone variations at Mt Abu in the months of October, November and December. These

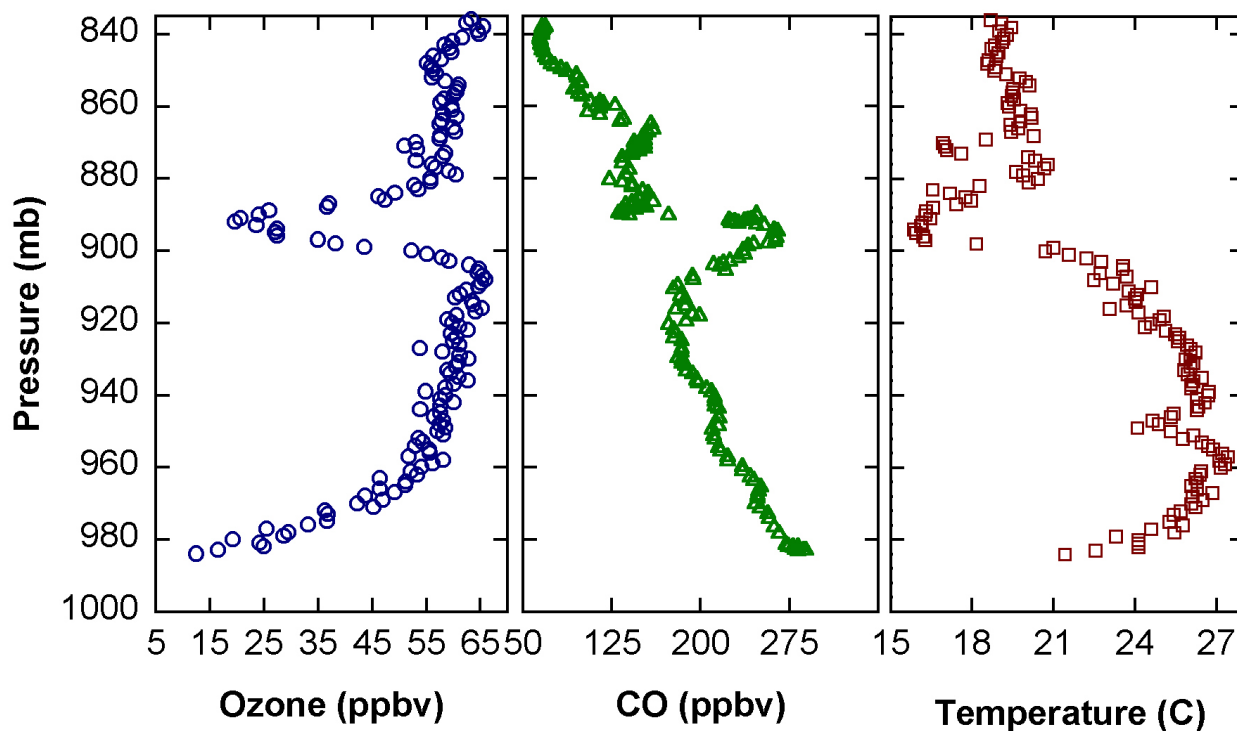


Figure 6.14 Average vertical profiles of ozone, CO and temperature observed during nights of November, 2000 at Mt Abu. These observations were taken between 9 pm to 5 am local times. Highest number of profiles (about 45) were taken in this month. All the data are within 95% confidence levels.

observations suggest that ozone is mainly controlled by boundary layer deposition at Mt Abu and chemistry plays a least role in its budget.

Chapter 7

Summary and future directions

This thesis is focused on the study of ozone and its related trace gases (CO, CH₄, NO, SF₆ etc) in different marine and continental environments of the tropical troposphere in the Indian subcontinent. The brief summary of this work is as follows:

7.1 Trace gases over the Indian Ocean and Arabian Sea

One of the main objectives of INDOEX was to understand the transport of trace species from the Indian subcontinent to the Indian Ocean across the ITCZ. Observations were made during the northern hemispheric (NH) winters of 1998 and 1999. The spatial coverage during INDOEX 1999 was from 15°N to 20°S and 77°E to 58°E.

Higher ozone is observed during INDOEX 1999 than INDOEX 1998 in the north of the equator due to anti-cyclonic conditions over the Indian continent. Maximum ozone of about 70 ppbv is observed near the Indian coastal region during INDOEX-1999, which is produced in downwind of the industrialized regions of south India and transported to the observation site. Similar elevated ozone levels (60-65 ppbv) are also transported over the Arabian Sea from the urban region of Gujarat. Lowest ozone of about 5 ppbv observed near ITCZ indicates that ITCZ acts as a sink of ozone. The observed ozone baseline in the pristine Indian Ocean is 14.5 ± 3.5 ppbv at 20°S. Earlier measurements made by other groups also

observed similar ozone levels, indicating that this part of the southern Indian Ocean is free from the effect of anthropogenic activities during NH winter. If we take 14 ppbv as baseline of O₃ over the remote Indian Ocean south of ITCZ, the anthropogenic O₃ transported over the Arabian Sea from its surrounding source regions is about four times the baseline. This shows the magnitude of the effect of anthropogenic activities in this region on the composition and chemistry of surrounding marine regions.

During the month of January, the wind flow over this region is more pronounced from the Bay of Bengal and it gets shifted to the Arabian Sea from late January to March within a time period of 30-60 days. Due to this change in wind flow, ozone levels during the onward journey of both the campaigns are found to be higher than the respective return journeys. The high ozone levels in onward journeys of both the campaigns could be due to two reasons (i) Wind flow from the Bay of Bengal channel is more polluted than the wind flow over the Arabian Sea (ii) The return transects are relatively at a greater distance from the coastal region. Ozone production near the coastal regions is more pronounced than the remote marine sites. Anti-cyclonic conditions prevailing over the Indian continent seem to be responsible for higher ozone during 1999 than in 1998. This difference is also observed in the aerosol optical depth (AOD) obtained from satellite measurements [Rajeev and Ramanathan, 2001]. Even the general patterns of AOD at 630 nm with latitude are matching with ozone variations for 1998 and 1999. Highest AOD and aerosol mass loading are observed around 10°N in January-March 1999 coinciding with the higher ozone in the same latitude region and for the same period [Jayaraman *et al.*, 2001; Moorthy *et al.*, 2001; Parameswaran *et al.*, 2001; Rajeev and Ramanathan, 2001]. All these observations suggest that ozone and aerosol over the marine region have common anthropogenic sources.

Higher latitudinal gradients in ozone are also observed during the INDOEX-1999 than INDOEX-1998. It seems that stronger winds are responsible for the higher gradients. The maximum gradient of 7.5 ppbv lat⁻¹ is observed during onward journey in 5-10°N latitudinal range. Higher variabilities in latitudinal gradients of ozone during INDOEX-1998 and 1999 indicate that the distribution of ozone over the Indian Ocean is highly transport dependent. Using observed ozone distributions during both the years, we have estimated the average e-fold distance of O₃ as 1870 km and the corresponding e-fold time as 4.8 days for the average wind speed of 4.5 ms⁻¹. The lower e-fold time of ozone than aerosols (7 days) shows the importance of photochemical loss of ozone as the air parcel moves away from the source region.

The amplitudes of observed diurnal variations during INDOEX-1999 are almost two times higher than those observed during INDOEX-1998. Diurnal variations in ozone up to

54% of its mean levels have been observed in INDOEX-1999. In a recent study over the Indian Ocean, *Dickerson et al.* [1999] have observed amplitude of diurnal variations up to 33% of the mean ozone. However, their model calculations, which included Br chemistry as well, could account up to 24% of the mean ozone levels in diurnal variations of O₃. We have also observed clear diurnal variations in ozone over the Indian Ocean when the winds were from the southern Indian Ocean without showing any significant gradient. These observations do not fully support the theory, which is only based on advection from polluted region for the nighttime increase of ozone in marine boundary layer. We feel that heterogeneous chemistry along with entrainment and advection may contribute significantly resulting in higher diurnal variations in ozone.

The levels of the short lived trace gases like O₃, CO and NO were lower during the INDOEX 1998 and other pre-INDOEX cruises in 1996 and 1997 [*Naja, 1997; Lal et al., 1998, Naja et al., 1999*] compared to INDOEX 1999 [*Lal et al., 2001; Chand et al., 2001a, Chand et al., 2001b*]. The concentrations of long lived trace gases like CH₄ and SF₆ are also found to be higher near the Indian coastal region during INDOEX 1999 than rest of the INDOEX cruises. Similar to O₃, CO is also more than five times higher (300 ppbv) over the northern Arabian Sea than over the Indian Ocean (50 ppbv) south of ITCZ.

A comparison of the gradients in methane distributions in the two INDOEX cruises reflects varying strength of transport of these gases over the Arabian Sea and the Indian Ocean. SF₆ levels from these two INDOEX cruises give a growth rate of about 4% yr⁻¹ from 1998 to 1999 period which is lower than the earlier global estimates of 6.9% yr⁻¹ [*WMO, 1999; Maiss et al., 1996; Geller et al., 1997*] for the 1994-1996 period. An inter-hemispheric exchange time of about 1.5 year is calculated using SF₆ data.

7.2 Trace gases over the Bay of Bengal

In winter, the pollutants are transported over the adjoining marine environments of the Indian sub-continent by two channels, one is via the Arabian Sea and other is via the Bay of Bengal [*Lelieveld et al., 2001*]. Extensive observations were made over the Arabian Sea and the Indian Ocean during the INDOEX campaigns. But, the Bay of Bengal is a data void region for such studies of atmospheric trace gases.

The model results show that pollutants (ozone and its precursors) from the north Indian region and from China may add together to make this region highly polluted [*Lelieveld et al., 2001*]. The first set of measurements of surface ozone and related gases over the Bay of Bengal (BOB) show that in the northern region, ozone values are not very high contrary to

the model simulations. The intriguing feature of these measurements is that the highest levels of ozone (60-64 ppbv) are observed over the central Bay of Bengal (10-15°N, 84-86°E) and not near the coastal regions. These ozone levels are higher than the average ozone levels measured during all the INDOEX cruises conducted during all the winters from 1996 to 1999 over the Arabian Sea, except north of 12°N. Elevated levels of CO, CH₄ and SF₆ have also been observed over the Bay of Bengal during BOBEX. These observations and seven days back trajectory analyses suggest that higher levels of ozone over the Bay of Bengal are due to the transport of pollutants from the continent and photochemical production on the way when the air parcel was moving away from the source regions. The back trajectory for the corresponding days show that the source of the air in this region was from north Indian and Dhaka region. However, ozone levels over the Arabian Sea during the BOBEX cruise are lower than the INDOEX levels. The broader peaks of ozone over the BOB compared to other gases also indicate additional photochemical production of ozone away from the source region.

7.3 Ozone in downwind of urban region

To understand the transport and en route transformation of ozone, mobile lab experiments-advection (MOLEX-A) were conducted in downwind and side winds of urban Gujarat during January 2001 and 2002.

The MOLEX-A observations in January of 2001 and 2002 indicate that the elevated ozone in the downwind of urban centers of Gujarat (India) is a regular process. Khambat, being an entry point to the Arabian Sea, is feeding high levels of ozone over this marine environment. Seven days forward trajectories for all the days during the first campaign show that the polluted air can get transported more than 3000 km from Ahmedabad over the Arabian Sea and Indian Ocean reaching up to ITCZ near 5°S. So, it is highly possible that the elevated ozone levels observed during INDOEX 1999 (*Lal and Lawrence, 2001*) were transported from the downwind of the urban regions of western India in a similar way as observed over the central Bay of Bengal in BOBEX 2001. Also, Mt. Abu observations suggest that the probability of elevated ozone transporting from the free troposphere is very rare.

The elevated ozone levels observed in downwind of urban region of Gujarat are in the range of 70-110 ppbv, about 60% higher than the ozone observed at urban center (Ahmedabad). The observations across the Bhavnagar city further confirms that ozone levels inside the urban center are much lower than its downwind side. The broader peak of ozone

over the Bay of Bengal suggest that ozone was produced away from the source region in a similar way as it has been observed over western region of Gujarat adjoining the Arabian Sea during both the mobile campaigns. In winter, when the wind flow prevails from north to south, these elevated ozone can get transported from the downwind of urban regions over the Arabian Sea and the Bay of Bengal and can significantly affect the composition of surrounding marine atmosphere.

Though the transport of pollutants from the urban regions over long distances is an established fact in North America (*White et al.*, 1983; *Trainer et al.*, 1995; *Xiude et al.*, 1996; *Aneja et al.*, 1999), the present study suggests that the regions in the vicinity of the Indian urban regions will influence significantly the composition of the relatively cleaner air in downwind sides up to large distance. To understand the budget of the tropospheric ozone better, the study of transport of pollutants in this region has to be supported by measurements from the downwind side of the urban regions in addition to the measurements at the urban regions.

Similar to the horizontal transport in downwind of urban centers, ozone and its precursors can also be transported to the free troposphere by convection and turbulent activities under suitable meteorological conditions in summer (*Lehning et al.*, 1998; *Donnell et al.*, 2001). In the free troposphere ozone has longer lifetime and may have more climatic implications than in the atmospheric boundary layer. Since these are the first results from India, it is difficult to explain the quantum of ozone production by other major urban centers. Apart from the climatic implications, the landlocked urban centers like Delhi, etc. may have significant health and crop implications in the rural areas on its downwind side in the Indian subcontinent.

7.4 Ozone and related gases over remote site: Mt Abu

Asia and particularly south Asia, is data void region for the study of surface and tropospheric ozone and its related trace gases. Mt Abu is situated in the Western India, about 250 km from the coast of the Arabian Sea. Under seasonally changing wind patterns, this station is very important for regional study of horizontal transports of trace gases in south Asia. Also the changing boundary layer (BL) height in summer is such that this site is in boundary layer during daytime and in the free troposphere (FT) during nighttime.

Continuous observations of ozone, UVB and total solar flux were taken at Mt Abu (24.6°N, 72.7°E, 1680m) from January 2000 to January 2001. Other trace gases like CO and NO are also monitored for some months. These measurements show daytime decrease in

ozone. Mountain-valley induced wind flow system is not appearing to play an important role in diurnal variations of ozone at this site, which is similar to that observed at Mt Fuji, Japan and Cerro Tololo, Chile. Among the three different types of diurnal variations in different seasons, bimodal diurnal variation at Mt Abu appears to be a special feature of this site. Seasonal variation shows maximum values during autumn and lowest during summer-monsoon. It is observed that boundary layer mixing and unique meteorology over this region play important roles in the diurnal and seasonal variations in ozone at Mt Abu.

Changes in BL height results to the distinct O₃ diurnal variations in different seasons. These changes in boundary layer height are reflected in diurnal variations of other trace gases also. In addition to boundary layer height, meteorology (winds) also plays a pivotal role in seasonal variation of ozone at this site. The diurnal amplitudes vary from 4 to 12 ppbv throughout the year but the monthly mean values exhibit a seasonal pattern with an amplitude of 22 ppbv. Higher amplitude of annual variation indicates that the regional meteorology plays a much more important role in ozone variations rather than the photochemistry. The daily average ozone value is minimum in August (31 ppbv) and maximum in October (53 ppbv). CO shows a large variability ranging from 50 ppbv to 250 ppbv. The diurnal amplitudes of NO vary from 25 pptv to 75 pptv at Mt Abu.

Ozone and CO correlation shows the ozone production efficiency (slope) of about 0.03, which is even lower than the studies over the Arabian Sea and the Indian Ocean during INDOEX campaigns (0.07 - 0.09). However, a value of about 0.3 which is an order higher, has been observed over North America. Lower ozone production efficiency and lower correlations are indications of incomplete photochemical processes over this region.

In addition to the continuous observations at Mt Abu, mobile lab experiments-vertical (MOLEX-V) were also conducted in the months of October, November and December in 2000. Measurements covered the height corresponding of 998 mb to 840 mb. Most of these experiments were conducted during the night hours. All the observations show a significant loss of ozone (60-80%) in the nocturnal boundary layer compared to the free troposphere. Also, in the free troposphere, the daytime ozone is lower by 10-20% than the nighttime ozone. This difference is due to loss of ozone by chemistry and by dilution of ozone poor air from the boundary layer with the air in the free troposphere during daytime. It is most likely that dilution plays more significant role rather than chemistry. Nighttime loss of ozone in all the campaigns indicates that surface deposition plays a very important role as a sink of ozone over this region.

7.5 Future directions

Despite important role of the tropical troposphere it is least probed for various physical and chemical processes. In the tropics, the Asian region (South Asia in particular) is a data void region for trace gases. Also the South Asian region is one of the fast developing regions, the biogenic and anthropogenic emissions of trace gases in tropics along with intense convective activity can perturb the atmosphere at local, regional and global scales. These pollutants can also get advected to longer distances and can affect remote cleaner atmosphere. There is a vast scope for expansion of this work. Following are some suggestions, which can be taken up to further improve our understanding of tropospheric ozone budget and its impact on the composition and climate in this region:

- Non-methane hydrocarbons (NMHCs), emitted by anthropogenic as well as natural processes, play important role in tropospheric chemistry. The ozone production efficiency is highest for NMHCs. However, there are no detailed measurements of these gases. Simultaneous measurements of NMHCs along with O₃, CH₄, CO, NO_x will form a better set for understanding of tropospheric chemistry and ozone budget.
- Ozone has long lifetime in the free troposphere. Once it is transported and/or produced in the free troposphere, it can impact the environment and climate. To better understand the budget of ozone in FT, *in-situ* as well as remote sensing techniques can be used. Differential absorption LIDAR (DIAL) and balloon sondes are some useful tools to monitor ozone profiles. The vertical measurements of ozone and its precursors can also be used to understand the transport and transformation of these gases between BL-FT and their troposphere-stratosphere exchange.
- The mobile lab experiment in urban Gujarat was at local scale. Similar experiments can be conducted at regional scale (India) using different platforms (like trains, aircrafts and ships). These campaigns will help in reducing the uncertainty in budget of ozone and its precursors.

There is a need for a detailed chemistry transport model (CTM) for understanding various physical, chemical and dynamical processes. In the initial stage, a box model with detailed atmospheric chemistry will be very helpful for understanding the local features of ozone variations in different environments. Such a model will also be useful to understand halogen chemistry through the hetrophase reaction. In the advanced stage both the chemistry and transport can be coupled in a 3D model. A combination of the measurements and model simulations can enhance our understanding of different features of tropospheric ozone and its related gases at the local, regional and global scales.

Bibliography

- Aardenne, J. A. Van, G. R. Carmichael, H. LevyII, D. Streets, L. Hordijk, Anthropogenic NO_x emissions in Asia in the period 1990-2020, *Atmos. Environ.*, 33, 633-646, 1999.
- Akimoto, H., and H. Narita, Distribution of SO₂, NO_x, and CO₂ emissions from fuel combustion and industrial activities in Asia with 1%1 resolution, *Atmos. Environ.*, 28, 213-225, 1994.
- Akimoto, H. and 12 others, Long-range transport of ozone in the East Asian Pacific rim region, *J. Geophys. Res.*, 101, 1999-2010, 1996.
- Annuaire de l'Observatoire Municipal de Montsouris (AOMM), Analyse de l' Air: Ozone, GalJthier-Villars, Paris, 1889-1910.
- Appenzeller, C., and R. J. Holton, Tracer lamination in the stratosphere: A global climatology, *J. Geophys. Res.*, 102, 13555-13569, 1996.
- Andreae, M.O. et al., Transport of biomass burning smoke to the upper troposphere by deep convection in the equatorial region, *Geophys. Res. Lett.*, 28, 951-954, 2001.
- Aneja, V. P., R.G. Oommen, A. J. Riordan, S.P. Arya, R.J. Wayland and G.C. Murray, Ozone patterns for three metropolitan statistical areas in North Carolina, USA, *Atmos. Environ.*, 33, 5081-5093, 1999.
- Aneja, V. P., S. P. Arya, and Y. Li; G. C. Murray, Jr. and T. L. Manuszak, Climatology of diurnal trends and vertical distribution of ozone in the atmospheric boundary layer in urban north Carolina, *Journal of the Air and Waste Management Association*, 50, 54-64, 2000.
- Asnani, G. C., Climatology of the tropics, in *Tropical Meteorology*, Vol. I, pp. 100-204, 1993.
- Ayers, G. P., H. Granek, and R. Boers, Ozone in the marine boundary layer at Cape Grim: Model Simulation, *J. Atmos. Chem.*, 27, 179-195, 1997.
- Baldy, S., G. Ancellet, M. Bessafi, A. Badr, and D. Lan Sun Luk, Field observations of the vertical distribution of tropospheric ozone at the island of Reunion (southern tropics), *J. Geophys. Res.*, 101, 23,835-23,849, 1996.
- Baray J. L., G. Ancellet, F. G. Taupin, M. Bessafi, and S. Baldy, Subtropical tropopause break as a possible stratospheric source of ozone in the tropical troposphere, *J. Atmos. Terr. Phys.*, 60, 27-36, 1998.
- Baray, J-L., G. Ancellet, T. Randriambelo, and S. Baldy, Tropical cyclone Marlene and stratosphere-troposphere exchange. *J. Geophys. Res.*, 104, 13,953-13,970, 1999.

- Bascom, R., et al., Health effects of out door air pollution, *Am. J. Respir. Crit. Care Med.*, 153 (1), 3-50, 1996.
- Beekmann, M., G. Ancellet, D. Martin, C. Abonnel, G. Duverneuil, F. Eideliman, P. Bessemoulin, N. Fritz, and E. Gizard, Intercomparison of tropospheric ozone profiles obtained by electrochemical sondes, a ground based Lidar and an airborne UV-photometer, *Atmos. Environ.*, 29, 1027-1042, 1995.
- Berntsen, T. K., and I. S. A. Isaksen, A global three dimensional transport model for the troposphere: 1 Model description and CO and O₃ results, *J. Geophys. Res.*, 102, 21239-21280, 1997.
- Bhugwant, C., H. Cachier, P. Brémaud, S. Roumeau and J. Leveau, Chemical effect of carbonaceous aerosols on the diurnal cycle of MBL ozone at a tropical site: Measurements and Simulations, *Tellus B*, 52B, 1232-1248, 2000.
- Bhugwant, C., M. Bessafi, E. Rivière, and J. Leveau, Diurnal and seasonal variation of carbonaceous aerosols at a remote MBL site of La Réunion island, *Atmos. Res.*, 57, 105-121, 2001a.
- Bhugwant, C., E. Rivière, P. Keckhut, and J. Leveau, Variability of carbonaceous aerosols, ozone and radon at Piton Textor, a mountain site on Réunion island (south-western Indian Ocean), *Tellus*, 53B, 546-563, 2001b.
- Bojkov, R. D., *J. Clim. Appl. Meteorol.*, 25, 343, 1986.
- Bolin, B., and H. Rodhe, A note on the concept of age distribution and transit time in natural reservoirs, *Tellus*, 25, 58-62, 1973.
- Brasseur, G.P., J. T. Kiehl, J. F. Muller, T. Schneider, C. Granier, X. Tie and D. Hauglustaine, Past and future changes in global tropospheric ozone: Impact on radiative forcing, *Geophys. Res. Lett.*, 23, 3807-3810, 1998.
- Brasseur, G. P., J. J. Orlando, G. S. Tyndall (editors), *Atmospheric Chemistry and Global Change*, Chapter 13, Oxford University Press, 1999.
- Bremaud, P. J., and F. Taupin, Ozone nighttime recovery in the marine boundary layer: measurements and simulation of the ozone diurnal cycle at Reunion Island, *J. Geophys. Res.*, 103, 3463-3473, 1998.
- Brewer, A. W., Evidence for a world circulation provided by the measurements of Helium and water vapor distribution in the stratosphere, *Quart. J. Roy. Meteor. Soc.*, 75, 351, 1949.

- Browell, E. V., M. A. Fenn, C. F. Butler, W. B. Grant, M. B. Clayton, J. Fishman, et al., Ozone and aerosol distributions and air mass characteristics over the South Atlantic basin during the burning season, *J. Geophys. Res.*, 101, 24,043-24,069, 1996.
- Bull, K. R., The critical loads/levels approach to the gaseous pollutant emission control, *Environmental pollution*, 69, 105-123, 1991.
- Carney, T. A., and J. A. Fishman, One dimensional photochemical model of the troposphere with a trade-wind boundary-layer parameterization, *Tellus*, 38B, 127-143, 1986.
- Charney, J. G., and P. G. Drazin, Propagating of planetary-scale disturbances from the lower into the upper atmosphere, *J. Geophys. Res.*, 66, 83-103, 1961.
- Chameides, W. L., and J. C. G. Walker, A time dependent photochemical model for ozone near the ground, *J. Geophys. Res.*, 81, 413-420, 1976.
- Chameides, W. L., F. Fehsenfeld, M. O. Rodgers, C. Cardelino, J. Martienz, D. Parrish, W. Lonneman, D. R. Lawson, R. A. Rasmussen, P. Zimmerman, J. Greenberg, P. Middleton and T. Wang, Ozone precursor relationship in the ambient atmosphere, *J. Geophys. Res.*, 97, 6037-6055, 1992.
- Chameides, W. L., L. Xingsheng, T. Xiaoyan, Z. Xiuji, L. Chao, C. S. Kiang, J. St. John, R. D. Saylor, S. C. Liu, K. S. Lam, T. Wang, F. Giorgi, Is Ozone Pollution Affecting Crop Yields in China?, *Geophys. Res., Lett.*, 26, 867-870, 1999.
- Chalita, S., D.A., Hauglustaine, H. Le Treut and J. F. Müller, Radiative forcing due to increased tropospheric ozone concentrations, *Atmos. Environ.*, 30, 1641-1646, 1996.
- Chand, D., K. S. Modh, M. Naja, S. Venkatramani and S. Lal, Latitudinal trends in O₃, CO, CH₄ and SF₆ over the Indian Ocean during the INDOEX IFP-1999 cruise, *Current Science*, 80, 100-104, 2001a.
- Chand, D., S. Lal and M. Naja, Variations of ozone in the marine boundary layer over the Arabian Sea and the Indian Ocean during the 1998 and 1999 INDOEX campaigns, *J. Geophys. Res.*, (submitted in Dec. 2001b).
- Chand, D., S. Lal and S. Venkataramani, High ozone at downwind of urban region in India, *Atmos. Environ.*, (submitted in April 2002).
- Chatfield, R., and H. Harrison, Ozone in the remote troposphere: mixing versus photochemistry, *J. Geophys. Res.*, 81, 421-423, 1976.
- Chin, M., D. J. Jacob, J. W. Munger, D. D. Parrish, B. G. Doddridge, Relationship of ozone and carbon monoxide over North America, *J. Geophys. Res.*, 99, 14565-14573, 1994.

- Crutzen, P. J., A discussion of the chemistry of some minor constituents in the stratosphere and troposphere, *Pure Appl. Geophys.*, 106-108, 1385-1399, 1973.
- Crutzen, P. J., Photochemical reactions initiated by influencing ozone in unpolluted tropospheric air, *Tellus*, 26,47-57,1974.
- Crutzen, P. J., A. C. Delany, J. Greenberg, P. Haagenson, L. Heidt, R. Lueb, W. Pollock, W. Seiler, A. Wartburg, and P. Zimmerman, Tropospheric chemical composition measurements in Brazil during the dry season, *J. Atmos. Chem.*, 2, 233-256, 1985.
- Crutzen, P. J., Tropospheric ozone: *An overview in the Tropospheric Ozone Regional and Global Scale Interactions*, Edited by I.S.A. Isaksen, pp 3-32, NATO ASI Ser. C, 227, 3-32, 1988.
- Crutzen, P. J., Ozone in the troposphere: *composition, chemistry, and climate of the atmosphere*, edited by H. B. Singh, pp. 349-393, 1995.
- Crutzen, P. J., M. G. Lawrence and U. Poschl, On the background photochemistry of tropospheric ozone, *Tellus*, 51 A-B, 123-146, 1999.
- Dave, J. V., Studies on twilight and atmospheric ozone, *Ph.D. Thesis*, pp. III.1-III.29, Gujarat University at Ahmedabad, India, Sep. 1957.
- Davis, D.D., G. Grodzinsky, P. Kasibhatla, J. Crawford, G. Chen, S. Liu, A. Bandy. D. Thronton, H. Guan, and S. Sandholm, Impact of Ship Emissions on marine Boundary Layer NO_x and SO₂ Distributions over the Pacific Basin, *Geophys. Res. Lett.*, 28, 235-238, 2001.
- de Laat, A. T. J., and J. Lelieveld, Diurnal ozone cycle in the tropical and subtropical marine boundary layer, *J. Geophys. Res.*, 105, 11547-11559, 2000.
- Delnay, A. C., R. R. Dickerson, F. L. Melchior and A. F. Wartburg, Modification of a commercial NO_x detector for high sensitivity, *Rev. Sci. Instrum.* 53, 1899-1902, 1982.
- Diab, R., A.M. Thompson, M. Zunckel, G. J. R. Coetzee, J. Combrink, G. E. Bodeker, J. Fishman, F. Sokolic, D. P. McNamara, C. B. Archer, and D. Nganga, Vertical ozone distribution over southern Africa and adjacent oceans during SAFARI-92, *J. Geophys. Res.*, 101, 23,823-23,833, 1996.
- Dickerson, R. R., Measurements of reactive nitrogen compounds in the free troposphere, *Atmos. Environ.*, 18, 2585-2593, 1984.
- Dickerson, R. R., G. J. Huffman, W. T. Luke, L. J. Nunnmermacker, K. E. Pickering, A. C. D. Leslie, C. G. Lindsey, W. G. N. Slinn, T. J. Kelly, P. H. Daum, A. C. Delany, J. P. Greenberg, P. R. Zimmerman, J. F. Boatman, J. D. Ray, and D. H. Stedman, Thunderstorm: An important mechanism in the transport of air pollutants, *Science*, 235, 460-465, 1987.

- Dickerson, R. R., K. P. Rhoads, T. P. Carsey, S. J. Oltmans, J. P. Burrows and P. J. Crutzen, Ozone in the remote marine boundary layer: A possible role of halogens, *J. Geophys. Res.*, 104, 21385-21395, 1999.
- Dlugokencky, E. J., K. A. Masarie, P. M. Lang, and P. P. Tans, Continuing declining of the growth rate of atmospheric methane, *Nature*, 393, 447-450, 1998.
- Dobson, G. M. B., Origin and distribution of the polyatomic molecules in the atmosphere, *Proc. Roy. Soc. London*, A236, 187, 1956.
- Donnell, E.A. D.J. Fish, Ed M. Dicks, and A.J. Thorpe, Mechanisms for pollutants transport between the boundary layer and the free troposphere, *J. Geophys. Res.*, 106, 7847-7856, 2001.
- Draxler, R.R., and G.D. Hess, Description of HySPLIT-4 modeling system, *NOAA Technical Memorandum ERL ARL-224*, 24p, 1997.
- Draxler, R.R., and G.D. Hess, An overview of the HySPLIT-4 modeling system for trajectory, dispersion and deposition, *Aust. Met. Mag.*, 47, 295-308, 1998.
- Duce, R. A., C. K. Unni, B. J. Ray, J. M. Prospero, and J. T. Merrill, Long-range atmospheric transport of soil dust to the tropical North Pacific: Temporal variability, *Science*, 209, 1522-1524, 1980.
- Duderstadt, K. A., M. A. Carroll, S. Sillman, T. Wang, C. M. Albercook, L. Geng, D. D. Parrish, J. S. Holloway, F. C. Fehsenfeld, D. R. Balke, N. J. Balke, and G. Forbes, Photochemical production and loss rates of ozone at Sable Island, Nova Scotia during the North Atlantic Regional Experiment (NARE) 1993 summer intensive, *J. Geophys. Res.*, 103, 13531-13555, 1998.
- European Environmental Agency (EEA)*, European topic center on air quality, summary based on the information reported in the framework of the Council Directive 92/72/EEC on air pollution by ozone, Sep 30, 1998.
- Environmental Protection Agency (EPA)*, The plain English Guide to the clean air act, EPA, 400-K-93-001, 1993.
- Environmental Protection Agency (EPA)*, 1996. National air quality & emission trends report, 1995, 454/R-96-005, p. 21.
- Fabian, P., and P. G. Pruchniewicz, Meridional distribution of ozone in the troposphere and its seasonal variations, *J. Geophys. Res.*, 82, 2063-2073, 1977.

- Fehsenfeld, F. C., and S. C. Liu, Tropospheric ozone: *Distribution and sources*, in *Global Atmospheric Chemical Change*, Edited by C. N. Hewitt and W. T. Sturges, pp. 169-228, Elsevier Sci., New York, 1993.
- Finlayson-Pitts B., and J. N. Pitts Jr., *Chemistry of the Upper and Lower Atmosphere, Theory, Experiments and Applications*, Ed. B. Finlayson-Pitts & J. N. Pitts Jr., Academic Press, 1999.
- Finnan, J. M., and J. I. Burke, An evaluation of the Indices that describe the impact of ozone on the yield of spring wheat, *Atmos. Environ.*, 31, 2685-2693, 1997.
- Fishman, J. and P. J. Crutzen, The origin of ozone in the troposphere, *Nature*, 274, 855, 1978.
- Fishman, J., S. Solomon, and P. J. Crutzen, Observation and theoretical evidence in support of a significant in situ photochemical source of tropospheric ozone, *Tellus*, 31, 432-446, 1979.
- Fonrobert, E., *In chemie in Einzeldarstellungen*, Ferdinand Enke, Germany, 16, 1916.
- Forrer, J., R. Ruttimann, D. Schneiter, A. Fischer, B. Buchmann, and P. Hofer, Variability of the trace gases at the high-Alpine site Junghfraujoch caused by meteorological transport process, *J. Geophys. Res.*, 105, 12241-12251, 2000.
- Fujiwara, M., K. Kita, S. Kawakami, T. Ogawa, N. Komala, S. Saraspriya, and A. Suropto, Tropospheric ozone enhancements during the Indonesian forest fire events in 1994 and in 1997 as revealed by ground-based observations, *Geophys. Res. Lett.*, 16, 2417-2420, 1999.
- Fuhrer, J., L. Skarby, and M. Ashmore, Critical levels of ozone effects in Europe, *Environmental Pollution*, 97, 91-106, 1997.
- Galanter, M., H. Levy II, and G. R. Carmichael, Impact of biomass burning on tropospheric CO, NO_x, and O₃, *J. Geophys. Res.*, 105, 6633-6653, 2000.
- Gallardo, L., J. Carrasco, and G. Olivares, An analysis of ozone measurements at Cerro Tololo (30°S, 70°W, 2000 m. a.s.l.) in Chile, *Tellus*, 52B, 50-59, 2000.
- Geller, J.W. Elkins, J.M. Lobert, A.D. Clarke, D.F. Hurst, J.H. Butler, and R.C. Myers, Tropospheric SF₆: Observed latitudinal distribution and trends, derived emissions and inter-hemisphere exchange time, *Geophys. Res. Lett.*, 24, 675-678, 1997.
- Ganzeveld, L., and J. Lelieveld, Dry deposition parameterization in a general circulation model and its influence on the distribution of reactive trace gases, *J. Geophys. Res.*, 100, 20999-21012, 1995.
- Gouget, H., Case study of a tropopause fold and of subsequent mixing in the subtropics of the Southern Hemisphere, *Atmos. Environ.*, 34, 2653-2658, 2000.

- Gros, V., N. Poisson, D. Martin, M. Kanakidou and B. Bonsang, Observations and modeling of the seasonal variation of surface ozone at Amsterdam island: 1994-1996, *J. Geophys. Res.*, 103, 28,103-28,109, 1998.
- Guenther, A., C. N. Hewitt, D. Erickson, R. Fall, C. Geron, T. Graedel, P. Harley, L. Klinger, M. Lerdau, W. A. McKay, T. Pierce, B. Scholes, R. Steinbrecher, R. Tallamraju, J. Taylor, and P. Zimmerman, A Global model of natural volatile organic compounds emissions, *J. Geophys. Res.*, 100, 8873-8892, 1995.
- Harnisch, J., and R. Brochers, Tropospheric trends for CF₄ and C₂F₆ since 1982 derived from SF₆ dated stratospheric air, *Geophys. Res. Lett.*, 23, 1099-1102, 1996.
- Hastenrath, S., Climate dynamics of the tropics, Updated from Climate and circulation of the tropics, Ed. Kluwer Academic Publishers, London, 1991.
- Hann, D., P. Martinerie, and D. Raynaud, Ice core data of the atmospheric carbon monoxide over Antarctica and Greenland during the last 200 years, *Geophys. Res. Lett.*, 23, 2235-2238, 1996.
- Hauglustaine, D. A., G. P. Brasseur, S. Walters, P. J. Rash, J. F. Muller, L. K. Emmons, and M. A. Carroll, MOZART, a global chemical transport model for ozone and related chemical tracers 2. Model results and evaluation, *J. Geophys. Res.*, 103, 28291-28335, 1998.
- Holton, J. R., P. H. Haynes, M. E. McIntyre, A. R. Douglass, R. B. Rood, and L. Pfister, Stratospheric-Tropospheric exchange, *Rev. Geophys.*, 33, 403, 1995.
- Houweling, S., F. Dentener, and J. Lelieveld, The impact of non-methane hydrocarbons compounds on the tropospheric photochemistry, *J. Geophys. Res.*, 103, 10673-10696, 1998.
- Haagen-Smit, A. J., and M. M. Fox, Ozone formation in photochemical oxidation of organic substances, *Ind. Eng. Chem. Res.*, 48, 1484-1487, 1956.
- Ian, E. Galbally, T. B. Simon C.P (Mick) Meyer, Mid-latitude marine boundary-layer ozone destruction at visible sunrise observed at Cape Grim, Tasmania, 41 °S, *Geophys. Res. Lett.*, 27, 3841-3844, 2000.
- Indian Ocean Atlas, Central Intelligence Agency, Washington DC, 1976.
- Intergovernmental Panel on Climate Change (IPCC), *Climate Change: The IPCC Scientific Assessment*, WMO/UNEP, edited by J. T. Houghton, G. T. Jenkins, and J. J. Ephraums, Cambridge University press, New York, 1990.

- Intergovernmental Panel on Climate Change (IPCC), *Climate Change 1992, IPCC scientific assessment*, edited by J. T. Houghton, B. A. Callander, and S. K. Varney, Cambridge university press, New York, 1992.
- Intergovernmental Panel on Climate Change (IPCC), *Climate Change 1995: The Science of Climate Change*, edited by J. T. Houghton, L. G. Meira, B. A. Callander, N. Harris, A. Kattenberg, and K. Maskell, Cambridge university press, New York, 1996.
- Intergovernmental Panel on Climate Change (IPCC), *Climate Change 2001: The Scientific basis*, edited by J. T. Houghton, Y. Ding, D. J. Driggs, M. Noguer, P. J. van der Linden, X. Dai, K. Maskell, and C. A. Johnson, Cambridge university press, New York, 2001.
- Jacob, D.J., M.J. Prather, S.C. Wofsy and M.B. McElroy, Atmospheric distributions of ^{85}Kr simulated with a general circulation model, *J. Geophys. Res.*, 92, 6614-6626, 1987.
- Jacob, D. J., J. A. Logan and P. P. Murti, Effect of rising Asian emissions on surface ozone in the United States, *Geophys. Res. Lett.*, 26, 2175-2178, 1999.
- Jacob, D.J, Heterogeneous chemistry and tropospheric ozone, *Atmos. Environ.*, 34, 2131-2159, 2000.
- Jayaraman, A., S. K. Satheesh, A. P. Mitra, and V. Ramanathan, Latitudinal gradient in aerosol properties across the Inter Tropical Convergence Zone: Results from the Joint Indo-US study onboard Sagar Kanya, *Current Science*, 80, 128-137, 2001.
- Jha, B., and T. N. Krishnamurti, Real-Time Meteorological Atlas During the INDOEX-1998, *FSU Report # 98-08*, Department of Meteorology, Florida State University, Tallahassee, FL 32306-4520, USA, August 1998.
- Jha, B., and T. N. Krishnamurti, Real-Time Meteorological Atlas During the INDOEX-1999, *FSU Report # 99-09*, Department of Meteorology, Florida State University, Tallahassee, FL 32306-4520, USA, August 1999.
- J. Geophys. Res.*, special issue, TRACE-A, SAFARI, vol. 101, 19, 1996. Ogren J. A., P. J. Groblicki, and R. J. Charlson, Measurement of the removal rate of elemental carbon from the *Atmosphere, Sci. Tot. Environ.*, 36, 329-338, 1984.
- Johnston, H., and D. Kinnison, Methane photooxidation in the atmosphere: Contrast between two methods of analysis, *J. Geophys. Res.*, 103, 21967, 21984, 1998.
- Johnson, J. E., R. H. Gammon J. Larsen, T. S. Bates, S. J. Oltmans, and J. C. Farmer, Ozone in the marine boundary layer over the Pacific and Indian Ocean: Latitudinal gradients and diurnal cycles, *J. Geophys. Res.*, 95, 11847-11856, 1990.

- Junge, C. E., Global ozone budget and exchange between stratosphere and troposphere, *Tellus*, 14, 363-377, 1962.
- Kajii, Y., K. Someno, H. Tanimoto, J. Hirokawa, H. Akimoto, T. Katsuno, J. Kawara, Evidence for the seasonal variation of photochemical activities of tropospheric ozone: Long term observation of ozone and CO at Mt. Happo, Japan, *Geophys. Res. Lett.*, 25, 3505-3508, 1998.
- Kaneyasu, N., Koji Takeuchi, Masayasu Hayashi, Chin-ichi Fujita, Itsushi Uno, and Hidetaka Sasaki, Outflow pattern of pollutants from East Asia to the North Pacific in the winter monsoon, *J. Geophys. Res.* 105, 17361-17377, 2000.
- Khalil, M. A. K., and R. A. Rasmussen, Carbon monoxide in the Earth's atmosphere: Indications of global increase, *Nature*, 332, 242-245, 1988.
- Khalil, M. A. K., and R. A. Rasmussen, Global decrease in the atmospheric carbon monoxide, *Nature*, 370, 639-641, 1994.
- Khemani, L., T., G. A. Momin, P. S. P. Rao, R. Vijayakumar, and P. D. Safai, Study of surface ozone behavior at urban and forested sites in India, *Atmos. Environ.*, 29, 2021-2024, 1995.
- Kleinman, L., Y. Lee, S. T. Springston, L. Nunnermacker, X. Zhou, R. Brown, K. Hallock, P. Klotz, D. Leahy, J. H. Lee, and L. Newman, Ozone formation at a rural site in the southern United States, *J. Geophys. Res.*, 99, 3469-3482, 1994.
- Kley, D., P. J. Crutzen, H. G. Smit, H. Vomal, S. J. Oltmans, H. Grassl and V. Ramanathan, Observations of near-zero ozone concentrations over the convective pacific: Effects on air chemistry, *Science*, 274, 230-233, 1996.
- Kley, D., Tropospheric chemistry and transport, *Science*, 276, 1043-1045, 1997.
- Ko, M.K.W., N.D. Sze, W.C. Wang, G. Shia, A. Goldman, F.J. Murcray, D.G. Murcray, and C.T. Rinsland, Atmospheric sulfur hexafluoride: Sources, sinks and greenhouse warming, *J. Geophys. Res.*, 98, 10499-10507, 1993.
- Komhyr, W. D., Electrochemical concentration cells for gas analysis, *Ann. Geophys.*, 25, 203-210, 1969.
- Knutson, T. R., and K. L. Weickmann, 30-60 days atmospheric oscillations: Composite life cycles of convection and circulation anomalies, *Mon. Weather Rev.*, 115, 1407-1435, 1987.
- Lal, S., M. Naja, and A. Jayaraman, Ozone in the marine boundary layer over the tropical Indian Ocean, *J. Geophys. Res.*, 103, 18907-18917, 1998.

- Lal, S., M. Naja, and B. H. Subbaraya, Seasonal variations in surface ozone and its precursors over an urban site in India, *Atmos. Environ.*, 34, 2713-2724, 2000.
- Lal, S., and M. G. Lawrence, Elevated mixing ratios of surface ozone over the Arabian Sea, *Geophys. Res. Lett.*, 28, 1487-90, 2001.
- Lal, S., D. Chand, L.K. Sahu and S. Venkataramani, Transport of ozone and related gases over the Bay of Bengal, *Geophys. Res. Lett.*, (to be submitted 2002).
- Lawrence, M. G., and P. J. Crutzen, Influence of NO_x emissions from ships on tropospheric photochemistry and climate, *Nature*, 402, 167-170, 1999.
- Lawrimore, J. H., M. Das, and V. P. Aneja, Vertical sampling and analysis of nonmethane hydrocarbons for ozone control in urban North Carolina, *J. Geophys. Res.*, 100, 22785-22793, 1995.
- Lehning, M., H. Richner G.L. Kok and B. Neininger, Vertical exchanges and regional budgets of air pollutants over densely populated areas, *Atmos. Environ.*, 32, 1353-1363, 1998.
- Leighton, P.A., *Photochemistry of air pollution*, Academic San Diego, California, 1961.
- Lelieveld, J., and P. J. Crutzen, Influences of cloud photochemical processes on tropospheric ozone, *Nature*, 343, 227-233, 1990.
- Lelieveld, J., and P.J. Crutzen, The role of the clouds in the tropospheric photochemistry, *J. Atmos. Chem.* 12, 229-267, 1991.
- Lelieveld, J., and F. Dentener, What controls tropospheric ozone? *J. Geophys. Res.*, 105, 3531-3551, 2000.
- Lelieveld, J., P. J. Crutzen, V. Ramanathan, M. O. Andreae, C. A. M. Brenninkmeijer, T. Campos, G. R. Cass, R. R. Dickerson, H. Fischer, J. A. de Gouw, A. Hansel, A. Jefferson, D. Kley, A. T. J. de Laat, S. Lal, M. G. Lawrence, J. M. Lobert, O. L. Mayol-Bracero, A. P. Mitra, T. Novakov, S. J. Oltmans, K. A. Prather, T. Reiner, H. Rodhe, H. A. Scheeren, D. Sikka, J. Williams, The Indian Ocean Experiment: Widespread Air Pollution from South and Southeast Asia, *Science*, 291, 1031-1036, 2001.
- Levin, I., and V. Hesshaimer, Refining of the atmospheric transport model entries by the globally observed passive tracer distributions of ⁸⁵Kr and SF₆, *J. Geophys. Res.*, 101, 16745-16755, 1996.
- Levy, H. II, Normal Atmosphere, large radical and formaldehyde concentrations predicted, *Science*, 173, 141-143, 1971.

- Levy, H. II, J. D. Mahlman, W. L. Moxim, and S. C. Liu, Tropospheric ozone: the role of transport, *J. Geophys. Res.*, 90, 3753-3771, 1985.
- Levy, H. II, P. S. Kasibhatla, W. J. Moxim, A. A. Klonecki, A. I. Hirsch, S. J. Oltmans, and W. L. Chameides, The global impact of human activity on tropospheric ozone, *Geophys. Res. Lett.*, 24, 791-794, 1997.
- Lin, X., M. Trainer, and S. C. Liu, On the non-linearity of the tropospheric ozone production, *J. Geophys. Res.*, 93, 15879-15888, 1988.
- Liu, S. C., M. MacFarland, D. Kley, O. Zafiriou and B. Huebert, Tropospheric NO_x and O₃ Budgets in the Equatorial Pacific, *J. Geophys. Res.*, 88, 1360-1368, 1983.
- Lobert, J., M., D. H. Scharffe, W. M. Hao, T. A. Kuhlbusch, R. Sewen, P. Warneck, and P. J. Crutzen, Experimental evaluation of biomass burning emissions: Nitrogen and carbon containing compounds, in global biomass burning: *Atmospheric Climate and Biospheric Implications*, edited by J. S. Levine, pp 289-304, MIT Press, Cambridge Mass, 1991.
- Logan, J. A., M. Prather, S.C. Wofsy, and M. B. McElroy, Tropospheric chemistry: A global perspective, *J. Geophys. Res.*, 86, 7210-7254, 1981.
- Logan, J. A., Trends in the vertical distributions of ozone: An analysis of ozonesonde data, *J. Geophys. Res.*, 99, 25553-25585, 1994.
- Logan, J. A. and 19 others, Trends in the vertical distribution of ozone: A comparison of two analyses of ozonesonde data, *J. Geophys. Res.*, 104, 26373-26399, 1999.
- Lovelock, J.E., Atmospheric fluorine compounds as indicator of air movements, *Nature*, 230, 379, 1971.
- Madden, R., and P. Julian, Description of global-scale circulation cells in the tropics with a 40-50 days period, *J. Atmos. Sci.*, 28, 1109-1123, 1972.
- Mahieu, E., R. Zander, L. Delbouille, P. Demoulin, G. Roland, and C. Servais, Observed Trends in total vertical column abundance of atmospheric gases from IR solar spectra recorded at the Jungfraujoch, *J. Atmos. Chem.*, 28, 227-243, 1997.
- Maiss, M., L.P. Steele, R. J. Francey, P. J. Fraser, R. L. Langenfelds, N. B. A. Trivett, and I. Levin, Sulfur hexafluoride: A powerful new atmospheric tracer, *Atmos. Environ.*, 30, 1621-1629, 1996.
- Maiss, M. and C. A. M. Brenninkmeijer, Atmospheric SF₆: trends sources and prospects, *Eni. Sci. Tech.*, 32, 3077-3086, 1998.

- Marenco, A., H. Gouget, P. Nedelec, J. P. Pages, and F. Karcher, Evidence of a long term increase in tropospheric ozone from Pic du Midi data series: Consequences: Positive radiative forcing, *J. Geophys. Res.*, 99, 16617-16632, 1994.
- Marion, T., *Mesures aeroportees des oxides d'azote: application a l'etude des processus de production d'ozone dans l'atmosphere tropicale*, Thesis, University of Creteil, France, 1998.
- Martin, R. V., D. J. Jacob, J. A. Logan, J. M. Ziemke, and R. Washington, Detection of a lightning influence on tropical tropospheric ozone, *Geophys. Res. Lett.*, 27, 1639-1642, 2000.
- Matseuda, H., and H. Y. Inoue, Measurements of atmospheric CO₂ and CH₄ using commercial airlines from 1993 to 1994, *Atmos. Environ.*, 30, 1647-1655, 1996.
- Matseuda, H., H. Y. Inoue, M. Ishii, and Y. Nogi, Atmospheric methane over the north the Pacific from 1987 to 1993, *Geochem. J.*, 30, 1-15, 1996.
- Mauzerall, D. L., D. Narita, H. Akimoto, L. Horowitz, S. Walters, D. A. Hauglustaine, G. Brasseur, Seasonal characteristics of tropospheric ozone production and mixing ratios over East Asia: A global three-dimensional chemical transport model analysis, *J. Geophys. Res.*, 105, 17895-17910, 2000.
- Mickley, L. J., P. P. Murthi, D. J. Jacob, J. A. Logan, D. M. Koch, and D. Rind, Radiative forcing from tropospheric ozone calculated with a unified chemistry-climate model, *J. Geophys. Res.*, 104, 30153-30172, 1999.
- Migeotte, M., and L. Neven, Recents progres dans l' observation du spectra solaire a la station scientific du Jungfraujoeh, *Soc. Sci. Liege*, 12, 165-169, 1952.
- Moorthy, K. K. and A. Saha, Aerosol Study during INDOEX: observation of enhanced aerosol activity over the Mid Arabian Sea during the northern winter, *J. Sol. and Terr. Phys.*, 62, 65-72, 2000.
- Moorthy, K. K., A. Saha and K. Niranjana, Spatial variation of aerosol spectral optical depth columnar water vapor content over the Arabian Sea and Indian Ocean during the IFP of INDOEX, *Current Science*, 80, 145-150, 2001.
- Monks, P. S., L. J. Carpenter, S. A. Penkett, G. P. Ayers, R. W. Gillett, I. E. Galbally and C. P. Meyer (Mick), Fundamental ozone photochemistry in the remote marine boundary layer: The SOAPEX experiment, measurements and theory, *Atmos. Environ.*, 32, 3647-3664, 1998.

- Monks, P. S., G. Salisbury, G. Holland, S. A. Penkett, and G. P. Ayers. A seasonal comparison of ozone photochemistry in the remote marine boundary layer, *Atmos. Environ.*, 34, 2000, 2547- 2561, 2000.
- Moorthy, K. K., A. Saha and K. Niranjana, Spatial variations of aerosol spectral optical depth and columnar water vapor content over the Arabian Sea and Indian Ocean during the IFP of INDOEX, *Current Science*, 80, 145-150, 2001.
- Monks, P. S., G. Salisbury, G. Holland, S. A. Penkett and G. P. Ayers. A seasonal comparison of ozone photochemistry in the remote marine boundary layer, *Atmos. Environ.*, 34, 2000, 2547- 2561, 2000.
- Müller, J. -F., and G. P. Brasseur, IMAGES: A three dimensional chemical transport model of the global troposphere, *J. Geophys. Res.*, 100,16445-16490, 1995.
- Myhre, G, A. Myhre, F. Stordal, Historical evolution of radiative forcing of climate, *Atmos. Environ.*, 35, 2361-2373, 2001.
- Nagao, I., K. Matsumoto and H. Tanaka, Characteristics of dimethylsulfide, ozone, aerosols and cloud condensation nuclei in air masses over the northwestern Pacific Ocean, *J. Geophys. Res.*, 104, 11675-11693, 1999.
- Nair, P. R., D. Chand, S. Lal , K. S. Modh, M. Naja, K. Parameswaran, S. Ravindran and S. Venkataramani, Temporal variations in surface ozone at Thumba (8.6°N, 77°E)-a tropical coastal site in India, *Atmos. Environ.*, 36, 603-610, 2002.
- Naja, M. and S. Lal, Changes in surface ozone amount and its diurnal and seasonal patterns, from 1954-55 to 1991-93, measured at Ahmedabad (23°N), India, *Geophys. Res. Lett.*, 23, 81-84, 1996.
- Naja, M., Tropospheric Chemistry in tropics, *Ph.D. Thesis*, submitted in Gujarat University, Oct. 1997.
- Naja, M., S. Lal, S.Venkataramani, K.S. Modh, and D. Chand, Variabilities in O₃, NO, CO, and CH₄ over the Indian Ocean during winter season, *Current Science*, 76, pp 931-937, 1999.
- Naja, M., and S. Lal, Surface ozone and precursor gases at Gadanki (13.5°N, 79.2°E, 375m), a tropical rural site in India, *J. Geophys. Res.*, 2002 (in press).
- North American Research Strategy for Tropospheric Ozone (NARSTO), An Assessment of Tropospheric Ozone Pollution, July 2000.
- Novelli, P. C., CO in the atmosphere: measurement techniques and related issues, *Chemosphere-Global Change Science*, 1, 115-126, 1999.

- National Research Council (NRC), 1991. Rethinking the ozone problem in urban and regional air pollution. National Academy Press, Washington, DC.
- Oltmans, S. J. and W. D. Komhyr, Surface ozone distribution and variations from 1973-1984 measurements at NOAA geophysical monitoring for climate change baseline observations, *J. Geophys. Res.*, 91, 5229-5236, 1986.
- Oltmans, S. J. and H. Levy II, Surface ozone measurements from a global network, *Atmospheric Environment*, 28, 9-24, 1994.
- Paluch, I., R., S. McKeen, D. H. Lenschow, R. D. Schillawski and G. L., Kok, Evolution of the Subtropical Marine Boundary Layer: Photochemical ozone loss, *J. of the Atmos. Scien.*, 52, 2967-2976, 1995.
- Parrish, D. D., M. Trainer, J. S. Holloway, J. E. Yee, M. S. Warshawsky, and F. C. Fehsenfeld, Relationships between ozone and carbon monoxide at surface sites in the North Atlantic region, *J. Geophys. Res.*, 103, 13357-13376, 1998.
- Patra, P. K., S. Lal, B.H. Subbaraya, C.H. Jackman, and P. Rajaratnam, Observed vertical profile of SF₆ and its atmospheric applications, *J. Geophys. Res.*, 102, 8855-8859, 1997.
- Parameswaran, K., R. P. Nair, R. Rananjana, and D. Balasubrahmanyam, Spatial distribution of aerosol concentrations over the Arabian Sea and the Indian Ocean During IFP of INDOEX, *Current Science*, 80, 161-165, 2001.
- Piotrowicz, S. R., D. A. Boran and C. J. Fischer, Ozone in the boundary layer of the equatorial Pacific Ocean, *J. Geophys. Res.*, 91, 13113-13119, 1986.
- Piotrowicz, S., R., R. A. Rasmussen, K. J. Hanson and C. J. Fischer, Ozone in the boundary layer of the equatorial Atlantic Ocean, *Tellus*, 41B, 314-322, 1989.
- Piotrowicz, S. R., H. F. Bezdek, G. R. Harvey and M. S. Young, On the ozone minimum over the equatorial Pacific Ocean, *J. Geophys. Res.*, 96, 18679-18687, 1991.
- Pochanart, P., J. Hirokawa, Y. Kajii, H. Akimoto, and M. Nakao, The influence of regional scale anthropogenic activity in northeast Asia on seasonal variations of surface ozone and carbon monoxide observed at Oki, Japan, *J. Geophys. Res.*, 104, 3621-3631, 1999.
- Pochanart, P., J. Kreasuwun, P. Sukasem, W. Geeratithadaniyom, M. S. Tabucanon, J. Hirokawa, Y. Kajii, and H. Akimoto, Tropical tropospheric ozone observed in Thailand, *Atmospheric Environment*, 35, 2657-2668, 2001.
- Poppe D., R. Koppmann, J. Rudolph, Ozone formation in biomass burning plums: Influence of atmospheric dilution, *Geophys. Res. Lett.*, 25, 3823-3826, 1998.

- Pont, V. and J. Fontan, Correlation between continental air mass and ozone concentrations, *J. Geophys. Res.*, 105, 17699-17707, 2000.
- Portmann, R. W., S. Solomon, J. Fishman, J. R. Olson, J. T. Kiehl, and B. Briegleb, Radiative forcing of the earth's climate system due to tropical tropospheric ozone production, *J. Geophys. Res.*, 102, 9409-9417, 1997.
- Prinn, R. G., R. F. Weiss, B. R. Miller, J. Huang, F. N. Alyea, D. M. Cunnold, P. J. Fraser, D. E. Hartley, and P. G. Simmonds, Atmospheric trend and lifetime of CH₃CCH₃ and global OH concentration, *Science*, 269, 187-192, 1995.
- Prinn, R. G., J. Huang, R. F. Weiss, D. M. Cunnold, P. J. Fraser, P. G. Simmonds, A. McCulloch, C. Harth, P. Salameh, S. O'Doherty, R. H. J. Wang, L. Porter and B. K. Miller, Evidence for substantial variation of atmospheric hydroxyl radicals in the past two decades, *Science*, 292, 1882-1888, 2001.
- Rajeev, K. and V. Ramanathan, Direct observations of clear-sky aerosol radiative forcing from space during the Indian Ocean Experiment, *J. Geophys. Res.*, 106, 17221-17235, 2001.
- Ramanathan, K. R., Atmospheric ozone and the general circulation of the atmosphere, *Sci. Proc. International Association of Meteorology*, IUGG 10th General Assembly, Rome, 1954, 3-24, 1956.
- Ramanathan, V., R. J. Cicerone, H. B. Singh, and J. T. Kiehl, Trace gas trends and their potential role in climate change, *J. Geophys. Res.*, 90, 5547-5566, 1985.
- Ramanathan, V. et al., *Indian Ocean Experiment (INDOEX)*, A multi-agency proposal for a field experiment in the Indian Ocean, C4, Scripps Inst. of Oceanography, University of California, San Diego, 1996.
- Ramanathan, V., P. J. Crutzen, J. T. Kiehl, and D. Rosenfeld, Aerosols, climate, and the hydrological cycle, *Science*, 294, 2119-2124, 2001.
- Randriambelo, T., J.-L. Baray, S. Baldy, P. Brémaud, and S. Cautenet, A case study of extreme tropospheric ozone contamination in the tropics using in-situ, satellite and meteorological data, *Geophys. Res. Lett.*, 26, 9, 1287-1290, 1999.
- Rasch, P. J., W. D. Collin and B. E. Eaton, Understanding the Indian Ocean Experiment (INDOEX) aerosol distribution with an aerosol assimilation, *J. Geophys. Res.*, 106, 7337-7355, 2001.
- Ravishankara, A. R., S. Solomon, A. A. Turnipseed, and R.F. Warren, Atmospheric life-times of long-lived halogenated species, *Science*, 259, 194-199, 1993.

- Regener, V. H., Vertical flux of atmospheric ozone, *J. Geophys. Res.*, 62, 221-228, 1957.
- Regener, V. H., On a sensitive method for recording atmospheric ozone, *J. Geophys. Res.*, 65, 3975-3977, 1960.
- Reginald, E. Newell and Mathew J. Evans, Seasonal changes in pollutant transport to the North Pacific: the relative importance of the Asian and European Sources, *Geophys. Res. Lett.*, 27, 2509-2512, 2000.
- Reichle, H. G. Jr., and H. A. Wallio, Gas filter radiometer for carbon monoxide measurements during the 1979 summer monsoon experiment (MONEX), *J. Geophys. Res.*, 91, 9841-9848, 1986.
- Reich, P. B., and R. G. Amundson, Ambient levels of ozone reduce net photosynthesis in tree and crop species, *Science*, 230, 566-570, 1985.
- Ridley, B. A., S. Madronich, R. B. Chatfield, J. G. Walega, R. E. Shetter, M. A. Carroll, and D. D. Montzka, Measurements and model simulations of the photochemistry state during the Mauna Loa Observatory Photochemistry Experiment: Implications for radical concentrations and ozone production and loss rate, *J. Geophys. Res.*, 97, 10375-10388, 1992.
- Rhoads, K. P., P. Kelley, R. R. Dickerson, T. P. Carsey, M. Sarmer, D. L. Savoie, and J. M. Prospero, Composition of the troposphere over the Indian Ocean during the monsoonal transition, *J. Geophys. Res.*, 102, 18981-18995, 1997.
- Roelofs, G. J., J. Lelieveld, G. J. Smit and D. Kley, Ozone production and transport in the tropical Atlantic region during the biomass burning season, *J. Geophys. Res.*, 102, 10637-10651, 1997a.
- Roelofs, G. J., J. Lelieveld, R. van Dorland, A three dimensional chemistry general circulation model simulations of anthropogenically derived ozone in the troposphere and its radiative climate forcing, *J. Geophys. Res.*, 102, 23389-23401, 1997b.
- Roscoe, H. K., and K. C. Clemitshaw, Measurement techniques in the Gas-Phase tropospheric chemistry: A selective view of the past, present, and future, *Science*, 276, 1065-1072, 1997.
- Routhier, F., R. Dennett, D. D. Davis, A. Wartrubg, P. Haagenson, and A. C. Delany, Free tropospheric and boundary-layer airborne measurements of ozone over the latitude range of 58°S to 70°N, *J. Geophys. Res.*, 85, 7307-7321, 1980.
- Sander, R., and P. J. Crutzen, Model study indicating halogen activation and ozone destruction in polluted air masses transported to the sea, *J. Geophys. Res.*, 101D, 9121-9138, 1996.

- Sander, R., R. Vogt, G. W. Harris & P. J. Crutzen Modeling the chemistry of ozone, halogen compounds, and hydrocarbons in the arctic troposphere during spring, *Tellus*, 49B, 522-532, 1997.
- Sasi, M. N., and Sen Gupta, K., A reference atmosphere for Indian Equatorial zone from surface to 80 km, *scientific report, SPL:SR:006:85*, Space Physical Laboratory, Vikram Sarabhai Space Center, Trivandrum, 1986.
- Satheesh, S., K. K. Moorthy, and B. V. K. Murthy, Spatial gradients in aerosol characteristics over the Arabian Sea and Indian Ocean, *J. Geophys. Res.*, 103, 26183-26192, 1998.
- Schiff, H. I., D. Pepper, and B. A. Ridley, Tropospheric NO measurements up to 7 km, *J. Geophys. Res.*, 84, 7895-7897, 1979.
- Schmidt, M., Evidence of a 50-year increase in tropospheric ozone in upper Bavaria, *Ann. Geophys.*, 12, 1197-1206, 1994.
- Schwarzkopf, M. D., and V. Ramaswamy, Radiative forcing due to ozone in the 1980s: Dependence on altitude of ozone change, *Geophys. Res. Lett.*, 20, 205-208, 1993.
- Seinfeld, J. H., and S. N. Pandis, Atmospheric Chemistry and Physics: From Air Pollution to Climate Change, Chapter 5, John Wiley and Sons Incorporation, 1998.
- Schonbein, C., Recherche sur la nature de l'odeur qui se manifeste dans certaines actions chimiques, *C. R. Acad. Sci.*, 15, 706-708, 1840.
- Scientific Assessment of Ozone Depletion (SAOD): 1998, Report N0. 44, Chapter 8.*
- Sillman, S., P. J. Samson, and J. M. Masters, Ozone production in urban plums transported over water: Photochemical model and case studies in the northeastern and Midwestern United States, *J. Geophys. Res.*, 98, 12687-12699, 1993.
- Singh, H. B., G. L. Gregory, B. Anderson, E. Browell, G. W. Sachse, D. D. Davis, J. Crawford, J. D. Bradshaw, R. Talbot, D. R. Blake, D. Thornton, R. Newell and J. Merrill, Low ozone in the marine boundary layer of the tropical Pacific ocean: Photochemical loss, chlorine atoms, and entrainment, *J. Geophys. Res.*, 101, 1907-1917, 1996.
- Singh, H.B., Atmospheric Halocarbons: Evidence in favor of reduced average hydroxyl radical concentration in the troposphere, *Geophys. Res. Lett.*, 4, 453-456, 1977.
- Smit, H. G. J., S. Gilge, and D. Kley, The meridional distribution of ozone and water vapor over the Atlantic Ocean between 30°S and 52°N in September/October 1988, G. Restelli, G. Angeletti (eds.), Physico-chemical behavior of the atmospheric pollutants, CEC., *Air pollution Report 23*, 630-637, Kuwar Acad. Publ., 1990.

- Solberg, S., C. Dye, S. Reimann, N.S. Schmidbauer, A. Herzog, R. Gehrig, Carbonyls and non-methane hydrocarbons at rural European sites from Mediterranean to the Arctic. *J. Atmos. Chem.*, 25, 33-66, 1996.
- Sreedharan, C. R., and V. S. Tiwari, The use of a Brewer 'bubbler' as a continuous surface ozone sensor, *J. Phys. E. Sci. Inst.*, 4, 706-707, 1971.
- Stohl, A., and Trickl, A textbook example of long-range transport: simultaneous observation of ozone maxima of stratospheric and North American origin in the free troposphere over Europe, *J. Geophys. Res.*, 104, 30445-30462, 1999.S
- Streets, D. G., and S. T. Waldhoff, Present and future emissions of air pollutants in China: SO₂, NO_x and CO, *Atmos. Environ.*, 34, 363-374, 2000.
- Stull, Ronald B., *An introduction to Boundary Layer Meteorology*, Kluwer Academic Publishers, 1994.
- Subbaraya, B. H., S. Lal, and M. Naja, Ozone and precursor gases in the Indian tropical region, proceedings of the *WMO IGAC* conference on the measurements and assessment of atmospheric composition change, pp. 167, Beijing, China, 1995.
- Suhre, K., V. Crassier, C. Mari, R. Rosset, D. W. Johnson, S. Osborne, R. Wood, M. O. Andreae, B. Bandy, T. S. Bates et al., Chemistry and aerosols in the marine boundary layer: 1-D modelling of the three ACE-2 Lagrangian experiments, *Atmos. Environ.* 34, 5079-5094, 2000.
- Syri, S., M. Amann, W. Schöpp, and C. Heyes, Estimating long-term population exposure to ozone in urban areas of Europe, *Environ. Pollution*, 113, 59-69, 2001.
- Taupin, F. G., M. Bessafi, S. Baldy, and P. J. Bernaud, Tropospheric ozone above the southern Indian Ocean is strongly linked to dynamical conditions prevailing in the tropics, *J. Geophys. Res.*, 104, 8057-8066, 1999.
- Thompson, A. M., and D. H. Lenschow, Mean profile of trace reactive species in the unpolluted marine surface layer, *J. Geophys. Res.*, 89, 4788-4796, 1984.
- Thompson, A. M., and O. C. Zafiriou, Air-sea fluxes of transient atmospheric species, *J. Geophys. Res.*, 92, 6696-6708, 1987.
- Thompson, A. M., J. E. Johnson, A. L. Torres, T. S. Bates, K. C. Kelly, E. Atlas, J. P. Greenberg, N. M. Donahue, S. A. Yvon, E. S. Saltzman, B.G. Heikes, B. W. Mosher, A. A. Shashkov, and V. I. Yegorov, Ozone observations and a model of marine boundary photochemistry during SAGA 3, *J. Geophys. Res.*, 98, 16995-16968, 1993.

- Thompson, A. M., R. D. Diab, G. E. Bodeker, M. Zunckel, G. J.R. Coetzee, C. B. Archer, D. P. McNamara, K.E. Pickering, J. Combrink, J. Fishman and D. Nganga, Ozone over southern Africa during SAFARI-92/TRACE-A, *J. Geophys. Res.*, 101, 19, 23,793-23,807, 1996.
- Thompson, A. M., W. K. Tao, K. E. Pickering, J. R. Scala, and J. Simpson, Tropical deep convection and ozone formation, *Bull. Am. Meteorol. Soc.*, 78, 1043-1054, 1997.
- Thompson, A., J. C. Witte, R. D. Hudson, H. Guo, J. R. Herman, M. Fujiwara, Tropical tropospheric ozone and biomass burning, *Science*, 291, 2128-2132, 2001.
- Torres, A. L., and A. M. Thompson, Nitric oxide in the equatorial Pacific boundary layer: SAGA 3 measurements, *J. Geophys. Res.*, 98, 16949-16954, 1993.
- Trainer, M., B.A. Ridley, M.P. Buhr, G. Kok, J. Walega, G. Hubler, D.D. Parrish, and F.C. Fehsenfeld, Regional ozone and urban plumes in the southeastern United States: Birmingham, a case study, *J. Geophys. Res.*, 100, 18823-18834, 1995.
- Tsunogai, S., T. Kondo, Sporadic transport and deposition of continental aerosols in the Pacific Ocean, *J. Geophys. Res.*, 87, 8870-8874, 1982.
- Tsutsumi, Y., and H. Matsueda, Relationship of ozone and CO at the summit of Mt. Fuji (35.35°N, 138.73°E, 3776 m above sea level) in summer 1997, *Atmos. Environ.*, 34, 553-561, 2000.
- Varshney, C. R., and M. Aggarawal, Ozone pollution in the urban atmosphere of Delhi, *Atmos. Environ.*, 26, 291-294, 1992.
- Verver, G. H. L., D. R. Sikka, J. M. Lobert, G. Stossmeister, and M. Zachariasse, Overview of the meteorological conditions and anthropogenic transport processes during INDOEX 1999, *J. Geophys. Res.*, 206, 28399-28414, 2001.
- Vogelmann, H. W., *Nat. Hist.*, 91, 8, 1982.
- Volz, A, and D. Kley, Evaluation of the Montsouris series of ozone measurements made in the nineteenth century, *Nature*, 332,240-242, 1988.
- Vogt, R., P. J. Crutzen, and R. Sander, A mechanism for halogen release from sea-salt aerosol in the remote marine boundary layer, *Nature*, 383, 327-330, 1996.
- Wang, Y. H., D. J. Jacob, and J. A. Logan, Global simulation of tropospheric O₃-NO_x-Hydrocarbon chemistry: 1, Model formulation, *J. Geophys. Res.*, 103, 10717-10726, 1998.
- Wang, T., T. F. C. Vincent, K. S. Lam, G. L. Kok and J. M. Harris, The characteristics of ozone and related compounds in the boundary layer of the south China coast: temporal and vertical variations during autumn season, *Atmos. Environ.*, 35, 2735-2746, 2001.

- Warneck, P., *Chemistry of the natural atmosphere*, pp-757, Academic, San Diego, California, 1998.
- White, H. W., D. E. Patterson, and W. E. Wilson Jr., Urban exports to the non-urban troposphere: Results from project MISTT, *J. Geophys. Res.*, 88, 10745-10752, 1983.
- WMO, *Scientific Assessment of Ozone Depletion: 1998*, Report No. 44, Chapter 1, 2.
- Xiude, Lin, P. R. Roussel, Steven Laszlo, Ron Taylor, and O. T. Meto; and P. B., Shepson, D. R. Hastie, and H. Niki, Impact of Toronto urban emission on ozone levels downwind, *Atmos. Environ.*, 30, 2177-2193, 1996.
- Zachariasse, M., H. G. J., Smit, P. F. J. van Velthoven, and H. Kelder, Cross-tropopause and interhemispheric transport into the tropical free troposphere over the Indian Ocean, *J. Geophys. Res.*, 106, 28441-28452, 2001.

List of abbreviations

APARE	Asian Pacific Regional Experiment
BL	Boundary Layer
BOBEX	Bay of Bengal Experiment
CBL	Continental Boundary Layer
GAMTAG	Global Atmospheric Measurements Experiments of Atmospheric Aerosols and Gases.
HET	Hemispheric Exchange Time of air
HySPLIT	Hybrid Single Particle Lagrangian Integrated Trajectory
ITCZ	Inter Tropical Convergence Zone
INDOEX	Indian Ocean Experiment
MOLEX-A	Mobile Lab Experiment-Advection
MOLEX-V	Mobile Lab Experiment-Vertical
MBL	Marine Boundary Layer
NARE	North American Regional Experiment
NCEP	National Center for Environmental Prediction
NH	Northern Hemisphere
NMHC	Non-Methane Hydrocarbons
NOAA	National Oceanic and Atmospheric Administration
ORV	Oceanic Research Vessel
PEM	Pacific Exploratory Mission
PEM-E	Pacific Exploratory Mission-Equatorial
ppbv	parts per billion by volume
ppmv	parts per million by volume
pptv	parts per trillion by volume
PRL	Physical Research Laboratory
RITS	Radiatively Important Trace Species
SAFARI	South African Fire Atmospheric Research Initiative.
SAGA	Soviet-American Gas and Aerosols experiment
SH	Southern Hemisphere
SK	ORV Sagar Kanya
UV	Ultra Violet

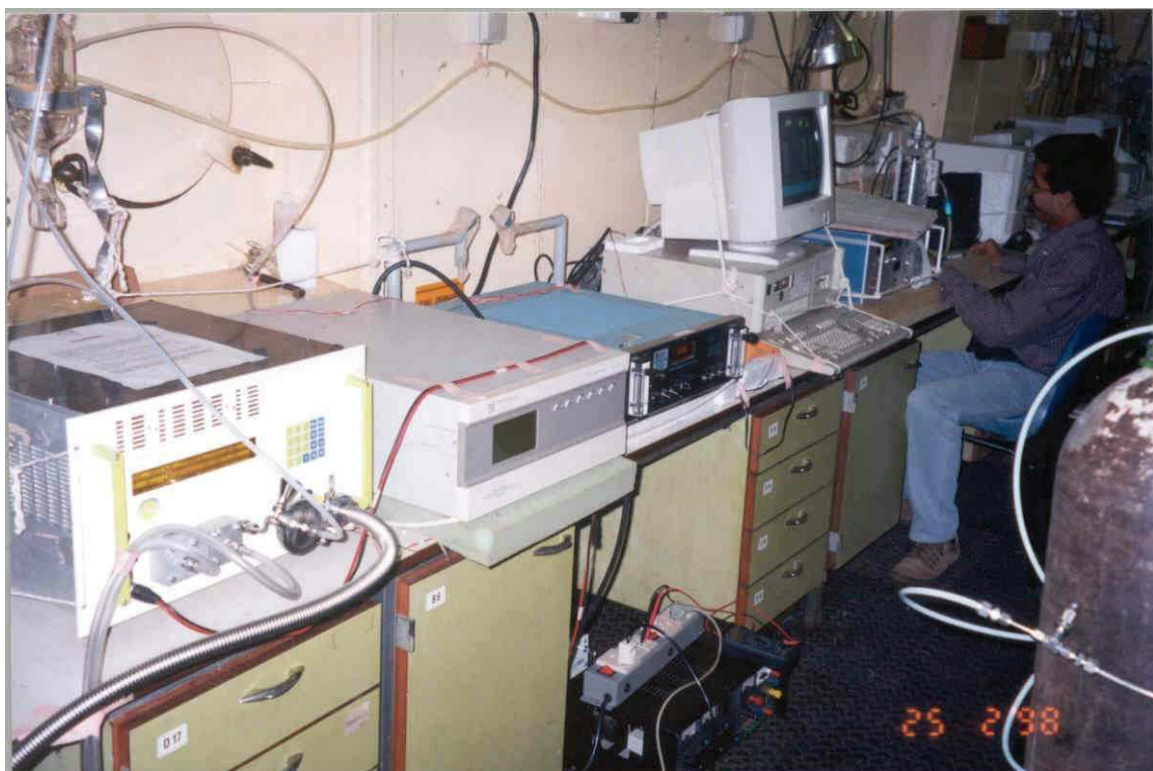
APPENDIX

Geographical locations of stations referred in this Thesis

Site	Latitude	Longitude	Elevation (amsl [*]) m
Ahmedabad	23.0°N	72.6°E	49
Amsaterdram Island	37.0°S	77.0°E	350
Bombay/Mumbai	18.6°N	73.0°E	100
Calcutta/Kolkota	23.3°N	88.2°E	100
Delhi	28.4°N	77.1°E	350
Mt Fuji	35.4°N	138.3°E	3776
Gadanki	13.5°N	79.2°E	375
Goa	15.8°N	73.6°E	200
Khambat	22.3°N	72.4°E	15
Madras/Chennai	13.0°N	80.2°E	20
Mauna Loa	20.0°N	155.6°W	3397
Mt Abu	24.6°N	72.7°E	1680
Port Louise	20.0°N	58.5°E	20
Reunion	21.20°S	55.7°E	2600
Surat	21.1°N	72.9°E	60
Trivandrum	8.7°N	76.8°E	15
Vadodara/Baroda	22.3°N	73.2°E	60

* amsl: above mean sea level

Onboard ORV Sagar Kanya



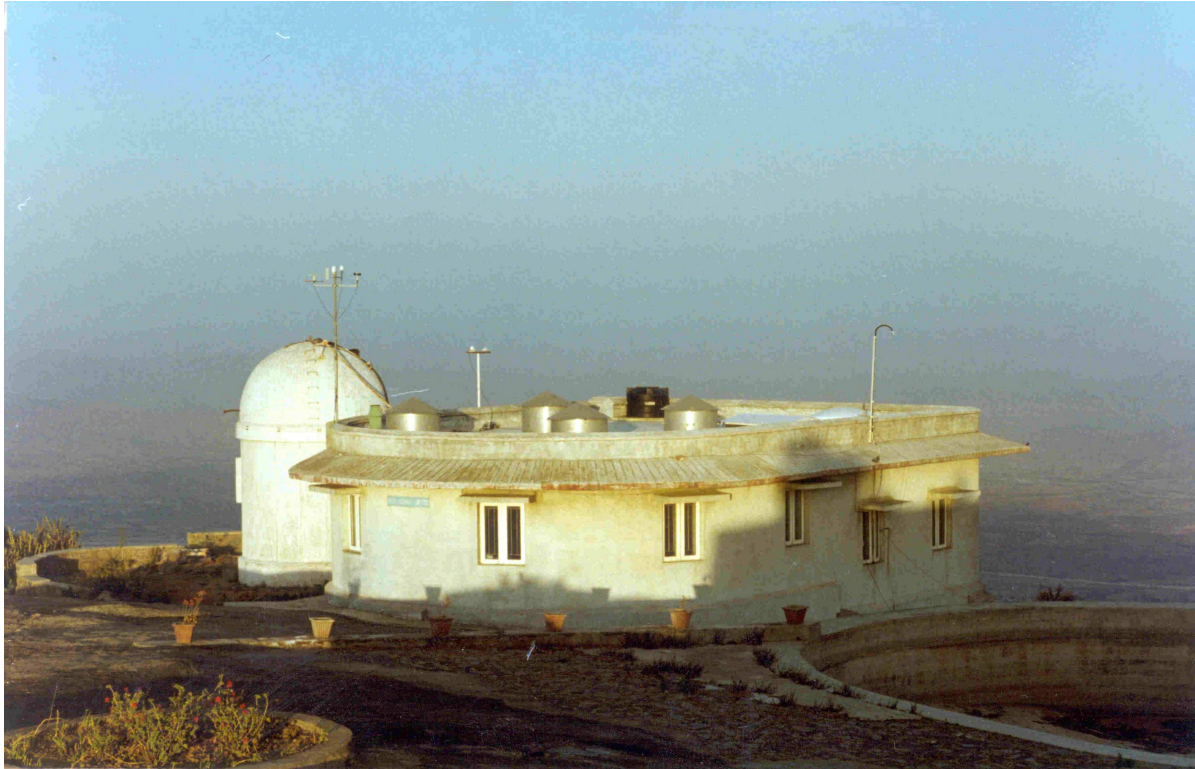
Onboard ORV Sagar Kanya



Mobile Lab Experiment



Mt Abu Observatory



Publications

- ✎1. Variabilities in O₃, NO, CO, and CH₄ over the Indian Ocean during winter season,, Manish Naja, Shyam Lal, S. Venkatramani, K.S. Modh, and **Duli Chand**, *Current Science*, 76, pp 931-937, 1998.
- ✎2. Change in the Vertical Distributions of Trace Gases over Hyderabad, Shyam. Lal, Y.B. Acharya, **Duli Chand**, P.Rajartnam and B.H. Subbaraya.. *Proc. LTAC*, 1999.
- ✎3. Latitudinal trends in O₃, CO, CH₄ and SF₆ over the Indian Ocean during the IFP INDOEX-1999 ship cruise, **Duli Chand**, K.S. Modh, M. Naja, S. Venkataramani and Shyam Lal *Current Science*, 80, 100-104, 2001.
- ✎4. Variations of ozone in the marine boundary layer over the Arabian Sea and the Indian Ocean during the 1998 and 1999 INDOEX campaigns, **Duli Chand**, Shyam Lal and Manish Naja, *Journal of Geophysical Research*, communicated.
- ✎5. Temporal variations in surface ozone at Thumba (8.6°N, 77°E)-a tropical coastal site in India, P. R. Nair, **Duli Chand**, Shyam Lal , K. S. Modh, M. Naja, K. Parameswaran, S. Ravindran and S. Venkataramani, *Atmospheric Environment*, 36, 603-610, 2002.
- ✎6. Transport of ozone and related gases over the Bay of Bengal, Shyam Lal, **Duli Chand**, L.K. Sahu and S. Venkataramani, *Geophysical Research Letters* (to be submitted).
- ✎7. HALOE and balloon-born measurements of methane in the stratosphere and their relations to QBO, P. K. Patra, Shyam Lal, **Duli Chand**, and S. Venkataramani, *Journal of Atmospheric Sciences*, communicated.
- ✎8. High ozone at downwind of urban region in India, **Duli Chand**, Shyam Lal and S. Venkataramani, *Atmospheric Environment*, communicated.
- ✎9. Trends in CH₄ and SF₆ at tropical coastal site Thumba in India, Shyam Lal, K. S. Appu, **Duli Chand**, M. Naja, P. K. Patra and S. Venkataramani, *Atmospheric Research* (to be submitted).
- ✎10. Diurnal and seasonal variabilities in the surface ozone at a high altitude station Mt Abu (24.6°N, 72.7°E, 1680m), India, *Journal of Geophysical Research* (under preparation)

Papers presented in national and international symposia

- ☞1. Distribution of SF₆, CH₄, CO and O₃ over the Indian Ocean during 1998 and 1999 and Inter-hemispheric exchange time, **Duli Chand**, Manish Naja, K.S. Modh and Shyam Lal, *National Workshop on Atmospheric Chemistry*, 1999.
- ☞2. Distribution of Halogenated trace gases over Indian Ocean during INDOEX-1999, **Duli Chand** and Shyam Lal, *National Space Science Symposium, Puri, March 1-4*, 2000.
- ☞3. Latitudinal Distribution of ozone and other trace gases over the Indian Ocean during INDOEX cruises, **Duli Chand**, K.S. Modh, Manish Naja, Shyam Lal and S. Venkataramani, *Conference on "CHEMISTRY-CLIMATE INTERACTIONS"*, International Centre for Theoretical Physics, ICTP, Trieste, Italy, June 12 - 14, 2000.
- ☞4. Ozone and other trace gases over the tropical troposphere, Shyam Lal, **Duli Chand**, S. Venkataramani and K.S. Modh, Indian Space Research Organisation, Geosphere Biosphere programme (IGBP), *Proc. of the working group on Atmospheric chemistry, Aerosols and Global Change*, Trivandrum, December, 2001.
- ☞5. Elevated ozone in downwind of urban environment in Indian sub-continent and its Implications, **Duli Chand**, Shyam Lal, K. S. Modh and S. Venkataramani, *National Space Science Symposium Bhopal*, January 25-28, 2002.
- ☞6. Study of ozone and other trace gases over the Arabian Sea, Bay of Bengal and Indian Sea during INDOEX and BOBEX cruises, **Duli Chand**, Shyam Lal, K. S. Modh, L. K. Sahu and S. Venkataramani, *National Space Science Symposium Bhopal*, January 25-28, 2002.
- ☞7. Ozone and its precursors at an elevated site Mt. Abu (24.6N, 72.7E, 1680 m) in India during 2000. **Duli Chand**, Shyam Lal and S. Venkataramani, (submitted for IGBP conference '*Atmospheric Chemistry in the Earth System: From Regional Pollution to Global Climate Change*' which will held on 18-25 September at Crete, Greece).
- ☞8. Transport of trace gases over the Arabian Sea, Bay of Bengal and Indian Ocean during winter, Shyam Lal, **Duli Chand** and S. Venkataramani, (submitted for IGBP conference '*Atmospheric Chemistry in the Earth System: From Regional Pollution to Global Climate Change*' which will held on 18-25 September at Crete, Greece)